Presentations e-Book

Workshop

Ground Improvement and Soil Stabilisation

September 4th 2016 - School of Engineering - University of Minho

Workshop of
3rd International Conference on Transportation Geotechnics
September 2016 | Guimarães | Portugal

Workshop 4

Ground Improvement and Soil Stabilisation

September 4th 2016
School of Engineering, University of Minho
Guimarães

Sponsored by

Ground Improvement and Soil Stabilisation
Workshop of
3rd International Conference on Transportation Geotechnics
September 4th 2016 | Guimarães | Portugal

Venue:
University of Minho, School of Engineering, Guimarães, Portugal

Website:
http://civil.uminho.pt/3rd-ICTG2016/WorkshopsThemes.php

Editors:
Serge Varaksin | Apageo, TC211
António Alberto S. Correia | CIEPQPF - University of Coimbra, TC211
Miguel Azenha | ISISE - University of Minho

Organized by
University of Minho (UM)
Portuguese Geotechnical Society (SPG)
International Society for Soil Mechanics and Geotechnical Engineering (ISSMGE)

Ground Improvement and Soil Stabilisation

Workshop of
3rd International Conference on Transportation Geotechnics
September 4th 2016 | Guimarães | Portugal

PRESENTATIONS e-BOOK

ISBN: 978-989-20-7008-7
Universidade do Minho
Departamento de Engenharia Civil, Azurém, P-4800-058 Guimarães
Email: secretaria@civil.uminho.pt
DOI: 10.5281/zenodo.154668

Credits for photo of the eBook cover: Serge Varaksin

Ground Improvement and Soil Stabilisation

Workshop of
3rd International Conference on Transportation Geotechnics
September 4th 2016 | Guimarães | Portugal

PREFACE

The Portuguese Geotechnical Society (SPG), the University of Minho and the International Society for Soil Mechanics and Geotechnical Engineering (ISSMGE) organized the international Workshop “Ground improvement and soil stabilization”, that took place in the School of Engineering of the University of Minho in the 4th September 2016, with support of the technical committee TC211 ‘Ground improvement’. This workshop is part of the 3rd International Conference on Transportation Geotechnics (3rd ICTG).

Soil improvement and transportation infrastructures are intimately connected, as the necessities of transportation infrastructures have motivated many advances and innovations in the scope of soil improvement, thus bringing economic feasibility to such projects. The main objective of this Workshop was to gather international experts connected to research and teaching or to the industry that are involved in the several types of improvement and soil stabilization. This brought about interesting opportunities for networking and discussion about ongoing works in the domain of transportation geotechnics. The Workshop was also an opportunity for presentation of the most recent research works, new technological developments and new applications in the scope of soil improvement and stabilization. The topics of analysis include dynamic compaction, vertical drains, chemical stabilization, alkaline activation, non-isothermal modelling, vacuum consolidation, reinforced embankments and load transfer platform.

The Editors: **Serge Varaksin** | **António Alberto S. Correia** | **Miguel Azenha**

Ground Improvement and Soil Stabilisation
Workshop of
3rd International Conference on Transportation Geotechnics
September 4th 2016 | Guimarães | Portugal

CONTENTS

Ground Improvement and Soil Stabilisation

Workshop of
3rd International Conference on Transportation Geotechnics
September 4th 2016 | Guimarães | Portugal

CONTENTS

Controlled Modulus Columns (CMC) Ground Improvement under the Future Embankment of the New Turcot Interchange

Jérôme Racinais[1], Adrien Viateau[2] , Hubert Guimont[2]

1. *Menard, France*
2. *Geopac, Canada*

Presentation of the project

- Location
- Project description
- Technical specifications

Soil conditions

CMC Ground Reinforcement solution

Design principles

- Analytical approach - Global Bearing Capacity and Settlement
- Finite Element Modelling to fine-tune the design
- Specific verification due to high lateral loads

Execution and controls

Conclusions

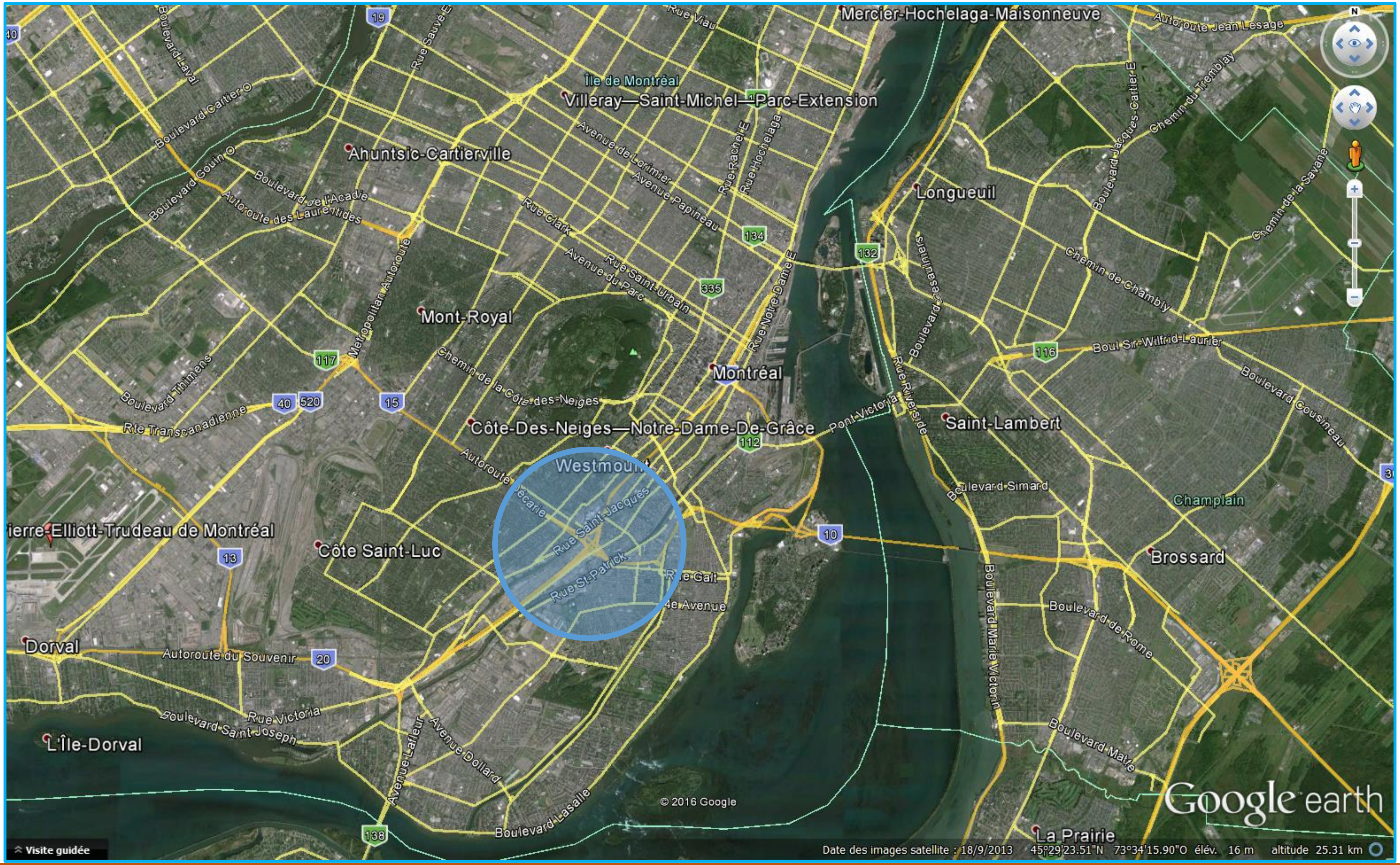
Mercier-Hochelaga-Maisonneuve
Autoroute Jean Lesage
Île de Montréal
Villeray—Saint-Michel—Parc-Extension
Ahuntsic-Cartierville
Boulevard Laval
Boulevard Cartier O
Boulevard Gouin O
Boulevard de l'Acadie
Autoroute des Laurentides
Rue Sauvé E
Rue Viau
Avenue de Lorimier
Avenue Papineau
Rue Clark
Avenue du Parc
Rue Saint-Urbain
Rue Hochelaga
Rue Notre-Dame E
Longueuil
Chemin du Tremblay
Boulevard Jacques-Cartier E
Chemin de la Savane
Chemin de Chambly
Boul Sir-Wilfrid-Laurier
Mont-Royal
Metropolitan Autoroute
Chemin de la Côte-des-Neiges
Montréal
Côte-Des-Neiges—Notre-Dame-De-Grâce
Pont Victoria
Rue Riverside
Saint-Lambert
Boulevard Cousineau
Boulevard Thimens
Rte Transcanadienne
Westmount
Décarie
Rue Saint-Jacques
Rue St-Patrick
Rue Galt
4e Avenue
Boulevard Simard
Champlain
Brossard
Pierre-Elliott-Trudeau de Montréal
Côte Saint-Luc
Boulevard Marie-Victorin
Boulevard de Rome
Dorval
Autoroute du Souvenir
Rue Victoria
Boulevard Saint-Joseph
L'Île-Dorval
Avenue Lafleur
Avenue Dollard
Boulevard Lasalle
© 2016 Google
Boulevard Marie
La Prairie
Google earth
Visite guidée
Date des images satellite : 18/9/2013 45°29'23.51"N 73°34'15.90"O élév. 16 m altitude 25.31 km

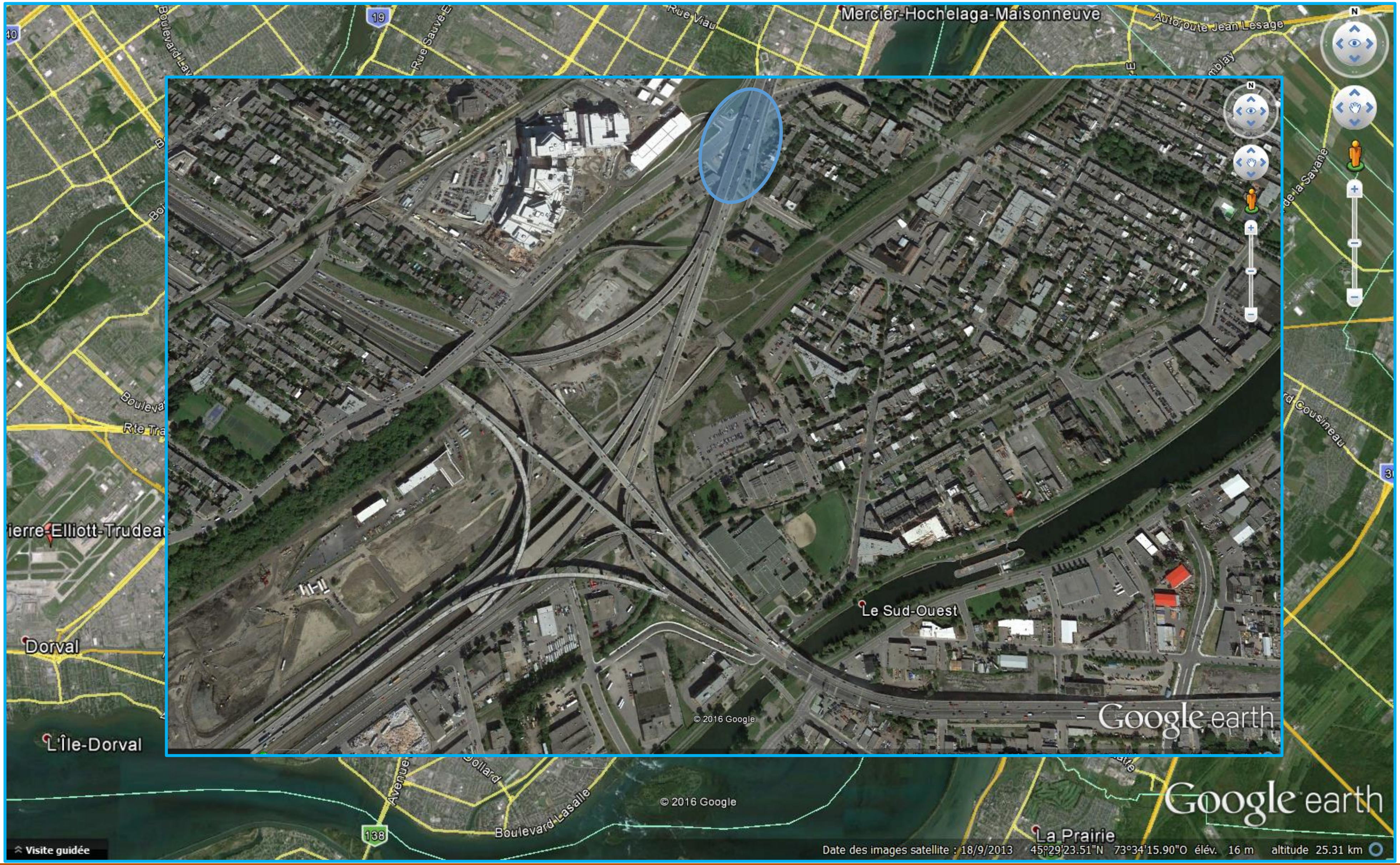
Mercier-Hochelaga-Maisonneuve
Autoroute Jean Lesage
Rue Viau
Le Sud-Ouest
Dorval
L'Île-Dorval
Boulevard Lasalle
La Prairie
© 2016 Google
Google earth
Visite guidée
Date des images satellite : 18/9/2013 45°29'23.51"N 73°34'15.90"O élév. 16 m altitude 25.31 km


Year 2013
Saint Jacques Street
Pullman Street
Saint Rémi Street
© 2016 Google
Google earth


27/10/2015
AB9
Year 2015
≈ 8000 m²
Saint Jacques Street
MSE Walls
Design cross-section
D3N1
Bridge on piles
Pullman Street
Saint Rémi Street
Image © 2016 DigitalGlobe
Google earth

$H_{fill/NGL}$ = 8,0 m

Client requirements:
- Bearing capacity
- Residual settlement over service life (35 years) ≤ **35 mm**
- Existing foundations to be demolished **at later stage -> low headroom area**

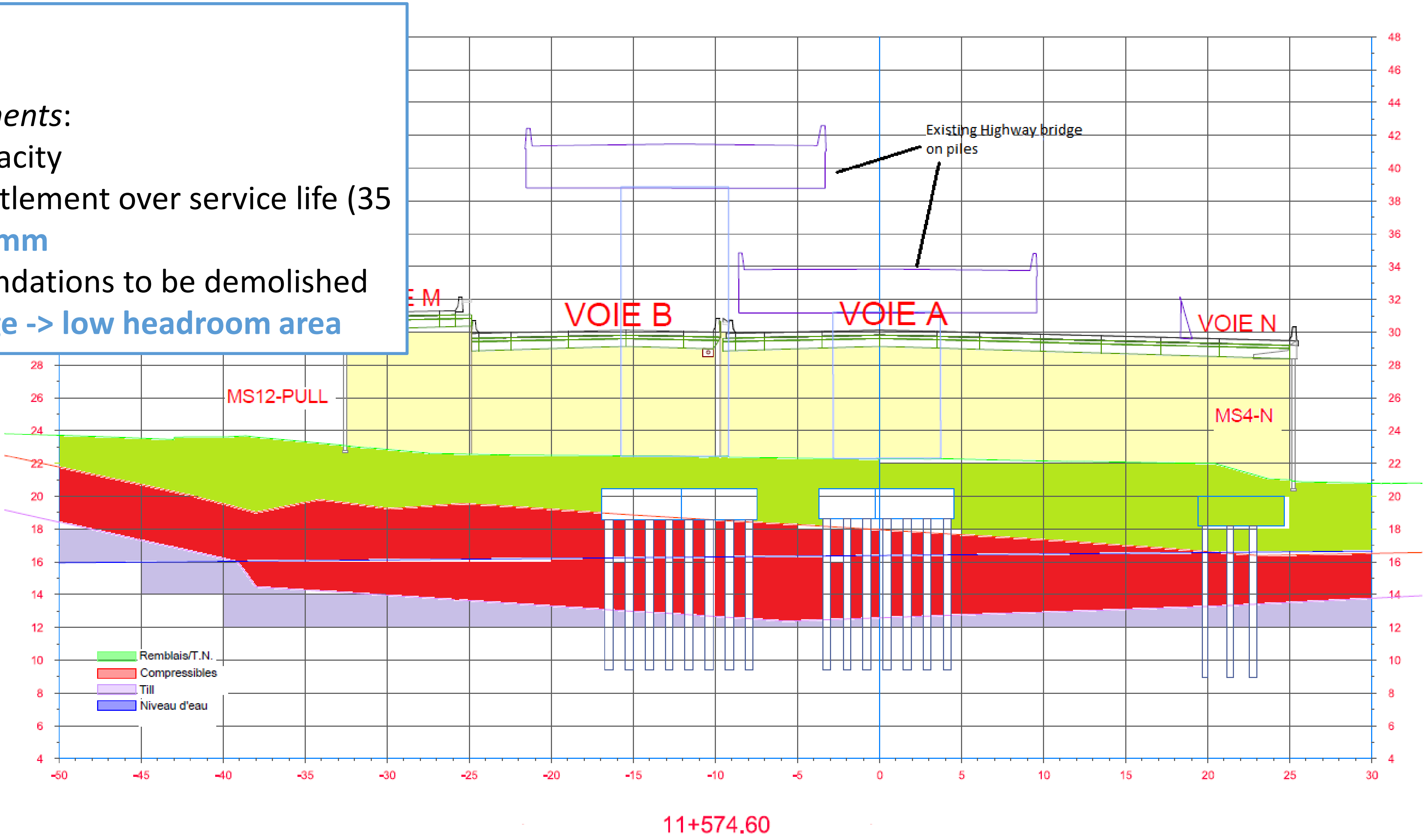

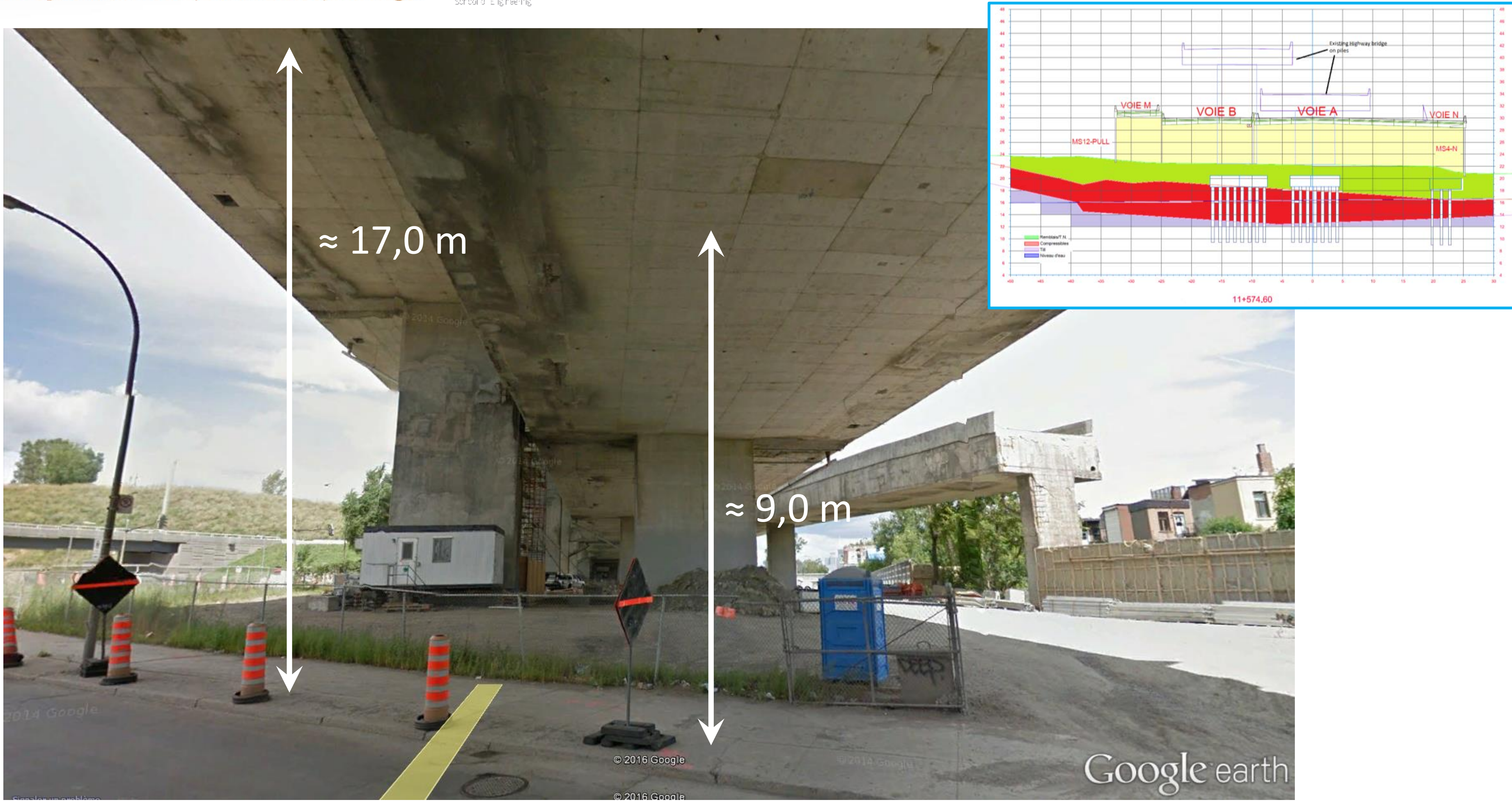
≈ 17,0 m
≈ 9,0 m
© 2016 Google
Google earth
VOIE M
VOIE B
VOIE A
VOIE N
MS12-PULL
MS4-N
11+574,60

Presentation of the project

- Location
- Project description
- Technical specifications

Soil conditions

CMC Ground Reinforcement solution

Design principles

- Analytical approach - Global Bearing Capacity and Settlement
- Finite Element Modelling to fine-tune the design
- Specific verification due to high lateral loads

Execution and controls

Conclusions

Boreholes, Standard Penetration Tests (SPT), Cone Penetration Tests (CPT) and Pressure Meter Tests (PMT) have highlighted **heterogeneous soil conditions** in terms of **thickness** and **compacity**.

Typical soil profile

Description	N_{SPT}	Thickness (m)
Existing fill	2-20	1,5 to 4,0
Sandy silt to silty sand	1-3	2,0 to 3,0
Peat / Marl / Clay	1-5	3,0 to 6,0
Med. dense to dense sand	15-30	3,0 to 6,0
Calcareous rock	>50	-

Water Level : approx. **6,0 m** below ground surface

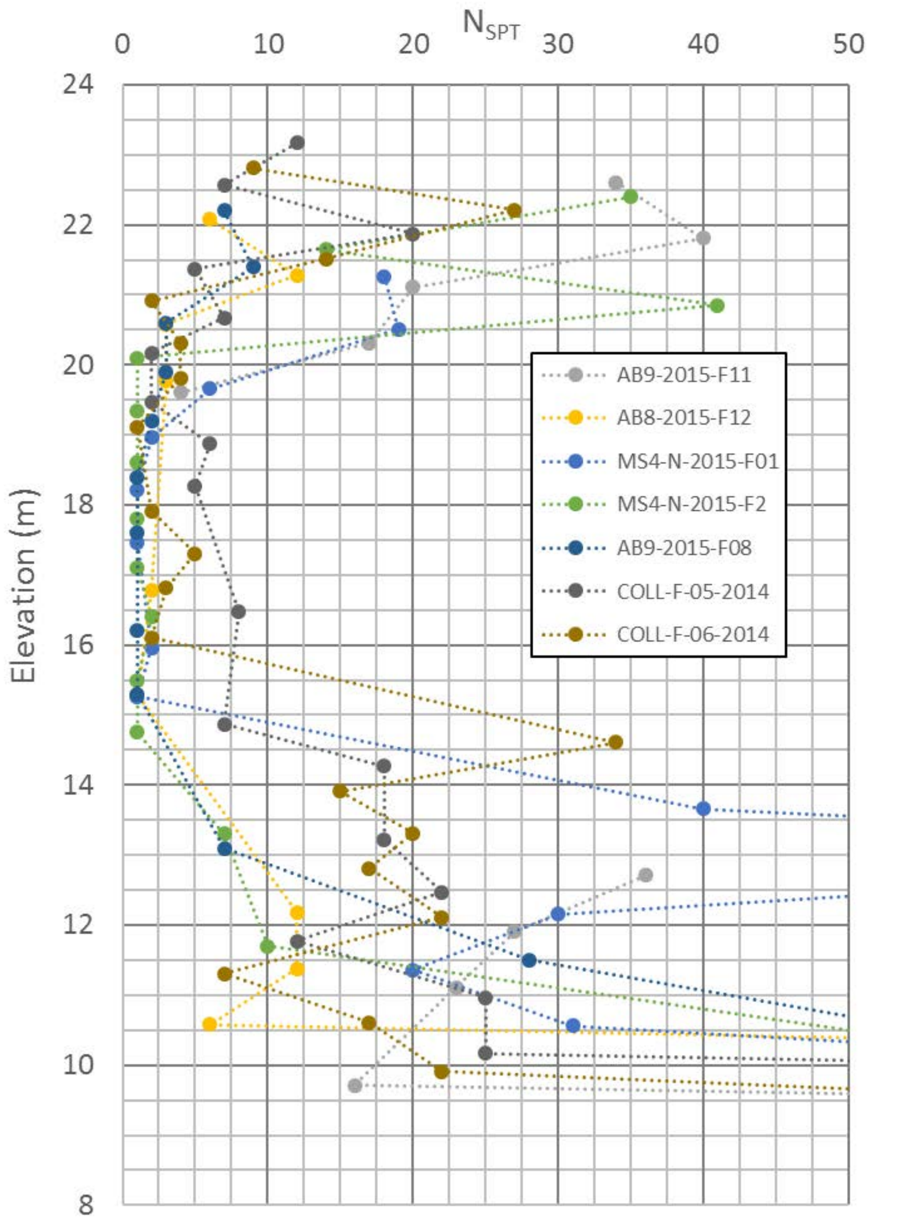

Soil properties

	γ (kN/m³)	E_Y (MPa)	ν (-)	c' (kPa)	φ' (°)	k (m/s)
Existing Fill	20	10	0,3	0	30	10^{-4}
Sandy Silt	12	8,4	0,3	0	30	10^{-7}
Dense Sand	20	30	0,3	0	30	$4{,}8\ 10^{-7}$
Calcareous Rock	20	500	0,3	5	38	$1{,}4\ 10^{-4}$

Linear Elastic Perfectly Plastic Model (also known as Mohr-Coulomb)

	γ (kN/m³)	C_c (-)	C_s (-)	e_0 (-)	$C_{\alpha e}$ (-)*	c' (kPa)	φ' (°)	k (m/s)
Peat	10	6,00	1,20	9,1	0,35	0	30	$6{,}3\ 10^{-7}$
Marl	12	1,44	0,33	4,4	0,10	0	30	$1{,}5\ 10^{-7}$
Clay	17	1,09	0,05	2,2	0,05	0	30	10^{-9}

Soft Soil Creep Model

$C_{\alpha e}$: creep index for secondary compression

Presentation of the project

- Location
- Project description
- Technical specifications

Soil conditions

CMC Ground Reinforcement solution

Design principles

- Analytical approach - Global Bearing Capacity and Settlement
- Finite Element Modelling to fine-tune the design
- Specific verification due to high lateral loads

Execution and controls

Conclusions

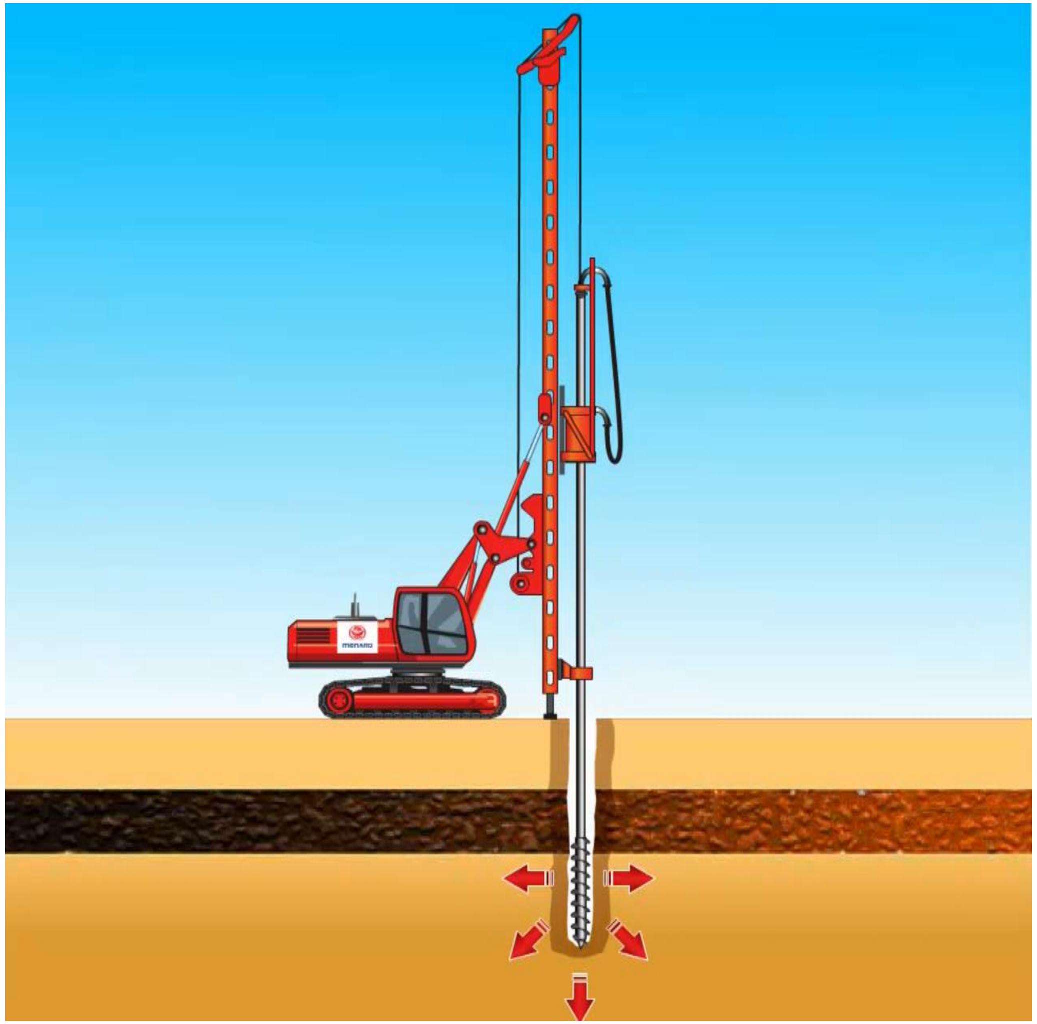

CMC Execution

- Soil-displacement column
- High static down thrust, large torque capacity
- No soil extraction, no vibration

Main CMC characteristics

- Diameter = 300 mm to 450 mm
- Unit cell area = 1 m^2 to 9 m^2
- Coverage area ratio = 1% to 10%
- Mortar / Concrete: UCS = 6 MPa to 25 MPa
- SLS Bearing Capacity = 300 kN to 700 kN
- Depth: up to 45 m
- Production rate = 450 lm to 800 lm / shift / day


SOILMEC

Data Recording

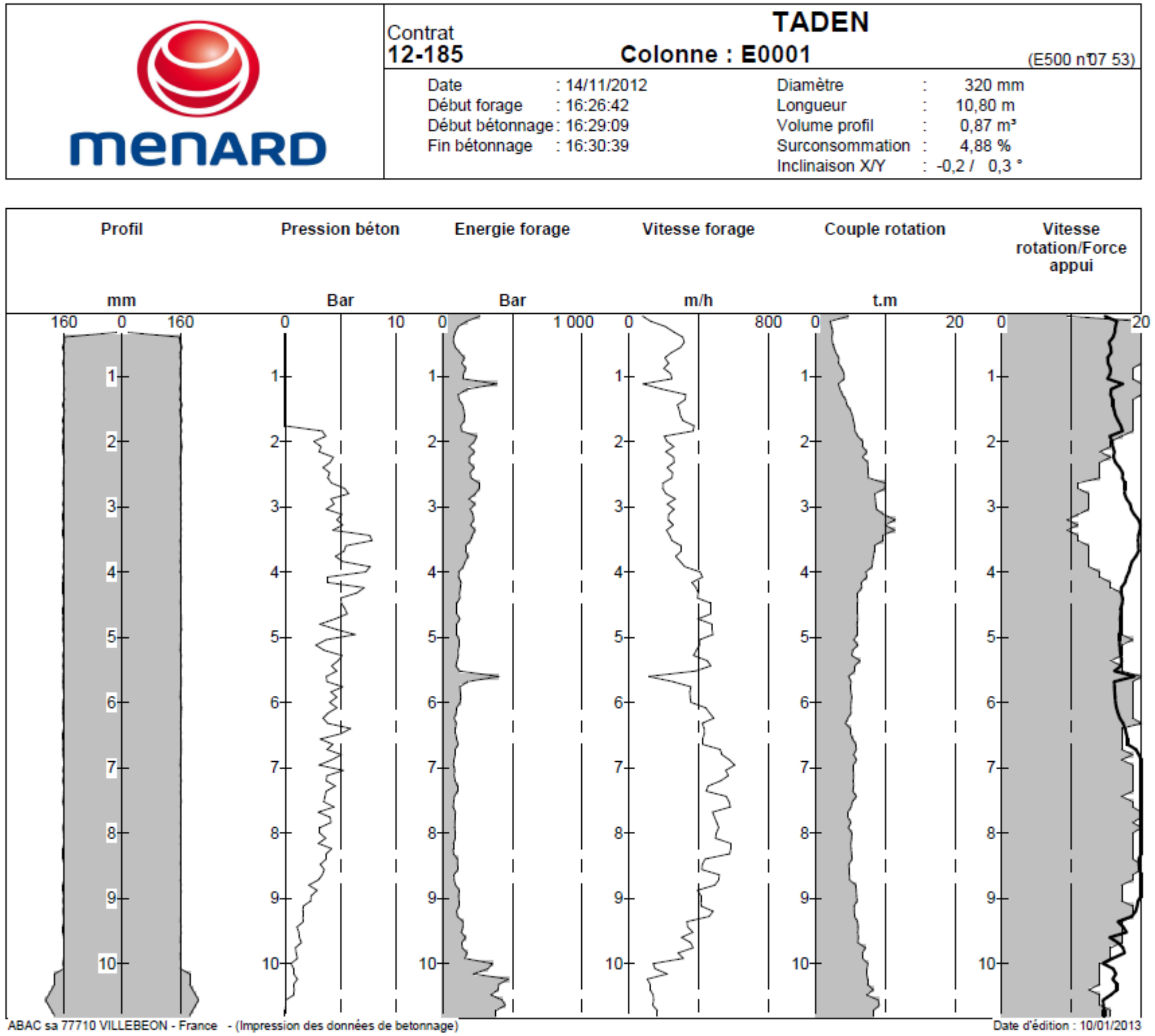
MENARD

Contrat
12-185

TADEN
Colonne : E0001
(E500 n°07 53)

Date	: 14/11/2012	Diamètre	: 320 mm
Début forage	: 16:26:42	Longueur	: 10,80 m
Début bétonnage	: 16:29:09	Volume profil	: 0,87 m³
Fin bétonnage	: 16:30:39	Surconsommation	: 4,88 %
		Inclinaison X/Y	: -0,2 / 0,3 °

ABAC sa 77710 VILLEBEON - France - (Impression des données de betonnage)
Date d'édition : 10/01/2013

How to classify Rigid Inclusions ?

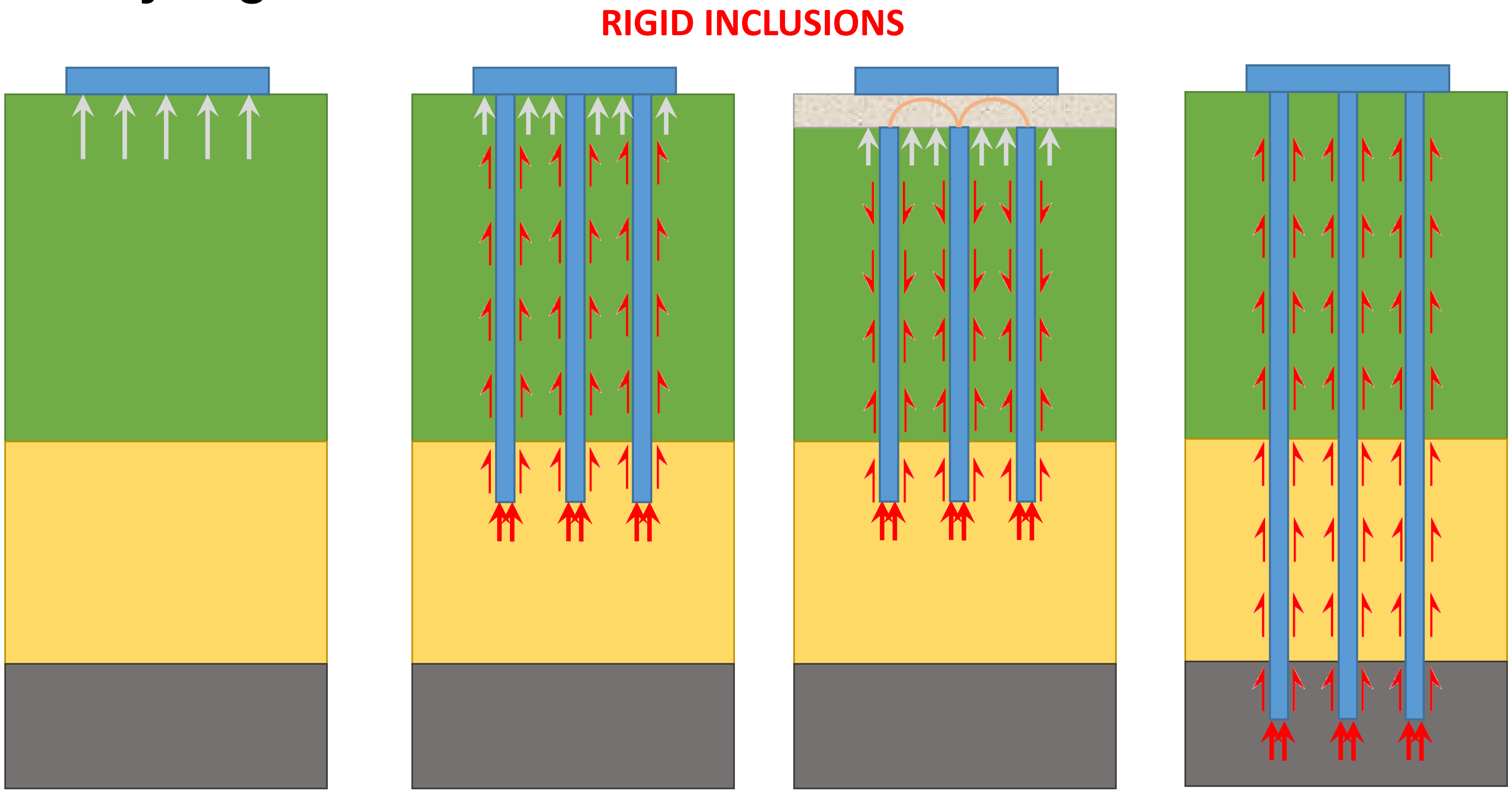

Shallow Foundation

Piled raft / Mixed foundation

Classical Rigid Inclusions foundation

Deep Foundation

General behaviour

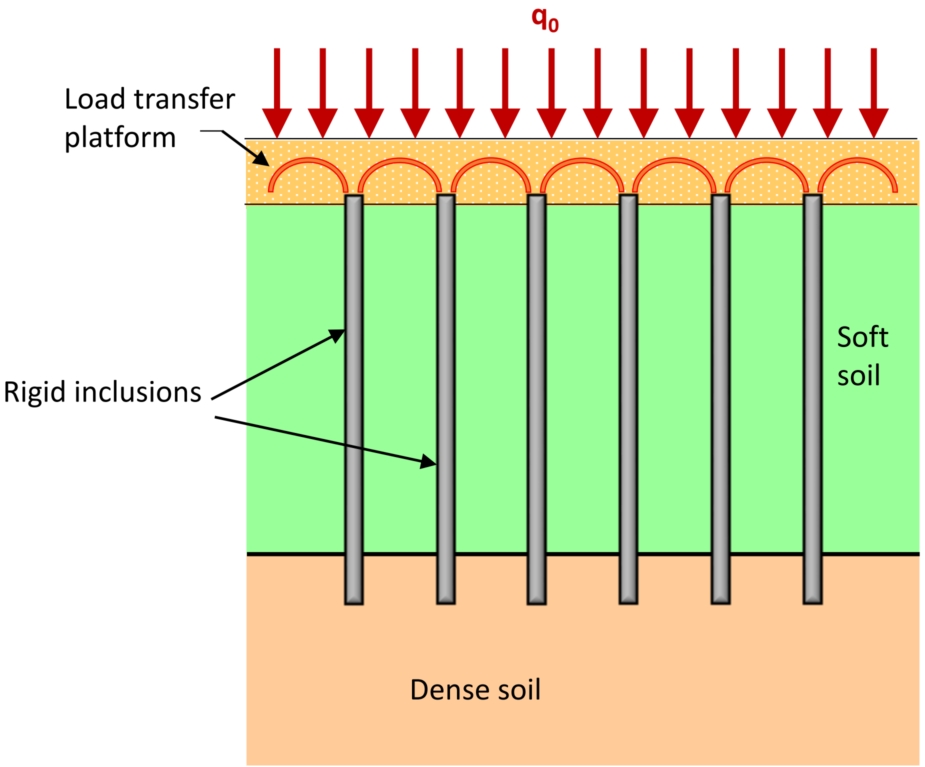

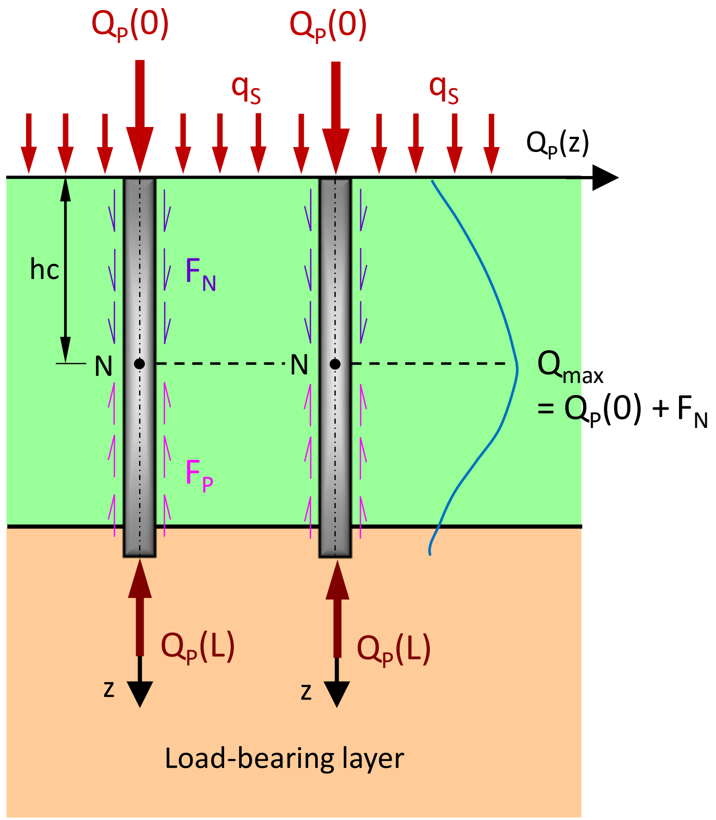

$$Q_P(0) + F_N = Q_{max} = F_P + Q_P(L)$$

ASIRI Guideline: 383 pages written by 40 partners between 2005 and 2012. Edited in 2013
Reference Document regarding rigid inclusions design

Presentation of the project

- Location
- Project description
- Technical specifications

Soil conditions

CMC Ground Reinforcement solution

Design principles

- Analytical approach - Global Bearing Capacity and Settlement
- Finite Element Modelling to fine-tune the design
- Specific verification due to high lateral loads

Execution and controls

Conclusions

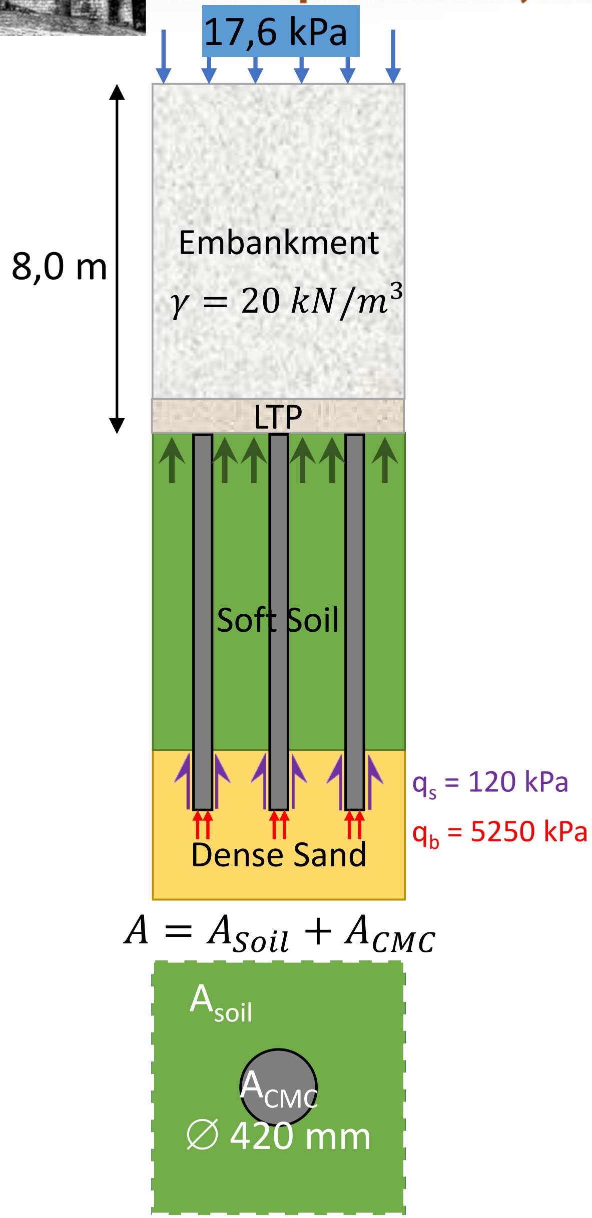

E_d (Design Actions Effects) $\leq$ R_d (Design Resistance)

SLS Numerical Application at the Unit Cell scale (more unfavourable than ULS)

LTP + Embankment + Live Load

$$Q_{SLS} = A \times \Delta\sigma$$

$$Q_{SLS} = A \times (\gamma_{emb} H_{emb} + q)$$

$$Q_{SLS} = 177{,}6 \times A \text{ (kN)}$$

Limit resistance of the Soil

$$Q_{Soil} = q_{soil} . A_{soil}$$

$$q_{soil} = k_p p_{le} + q'_0 = 250\ kPa$$

$$Q_{Soil} = 250 \times (A - A_{CMC}) \text{ (kN)}$$

Limit resistance of the CMC

$$Q_{CMC} = Q_S + Q_b$$

$$Q_{CMC} = 2\pi R \sum_i h_i . q_{s,i} + \pi R^2 . q_b$$

$$Q_{CMC} = 806{,}5\ kN$$

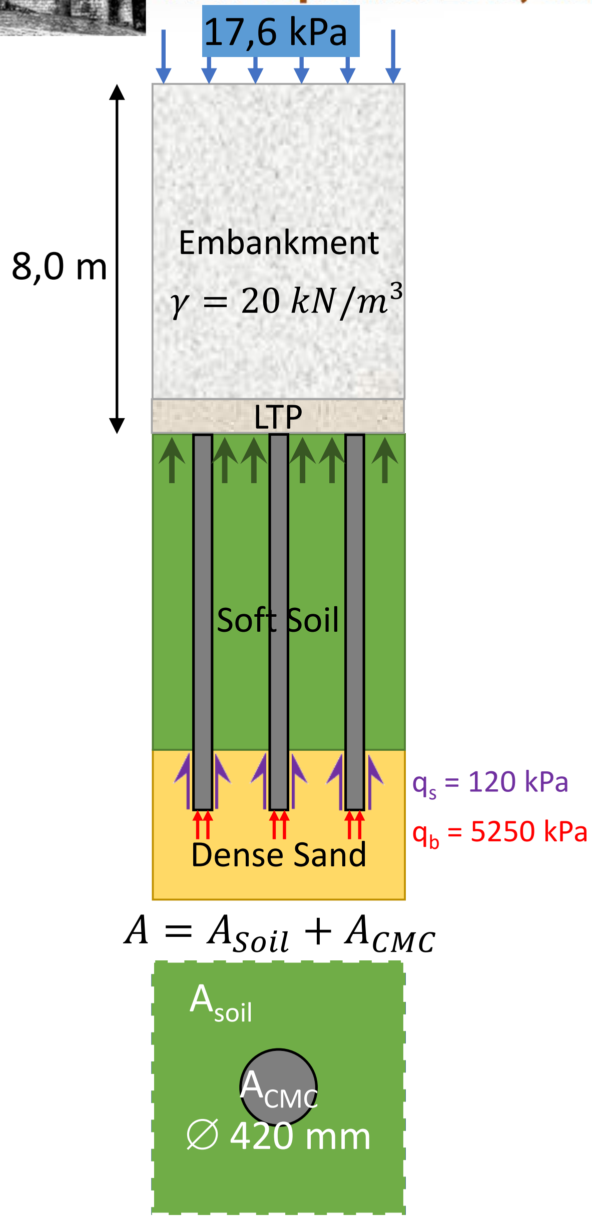

$$E_d \leq R_d$$

(Design Actions Effects) ≤ **(Design Resistance)**

SLS Numerical Application at the Unit Cell scale (more unfavourable than ULS)

$$Q_{SLS} = 177{,}6 \times A \text{ (kN)}$$

$$Q_{Soil} = 250 \times (A - A_{CMC})$$

$$Q_{CMC} = 806{,}5\ kN$$

$$Q_{SLS} \leq \frac{Q_{SOIL}}{\gamma_{soil}} + \frac{Q_{CMC}}{\gamma_{CMC}}$$

γ_{soil}: SLS partial factor for soil resistance (=2,76 according to French Appendix NF P 94-261 to EC7)

γ_{CMC}: SLS partial factor for CMC resistance (=1,96 according to French Appendix NF P 94-262 to EC7)

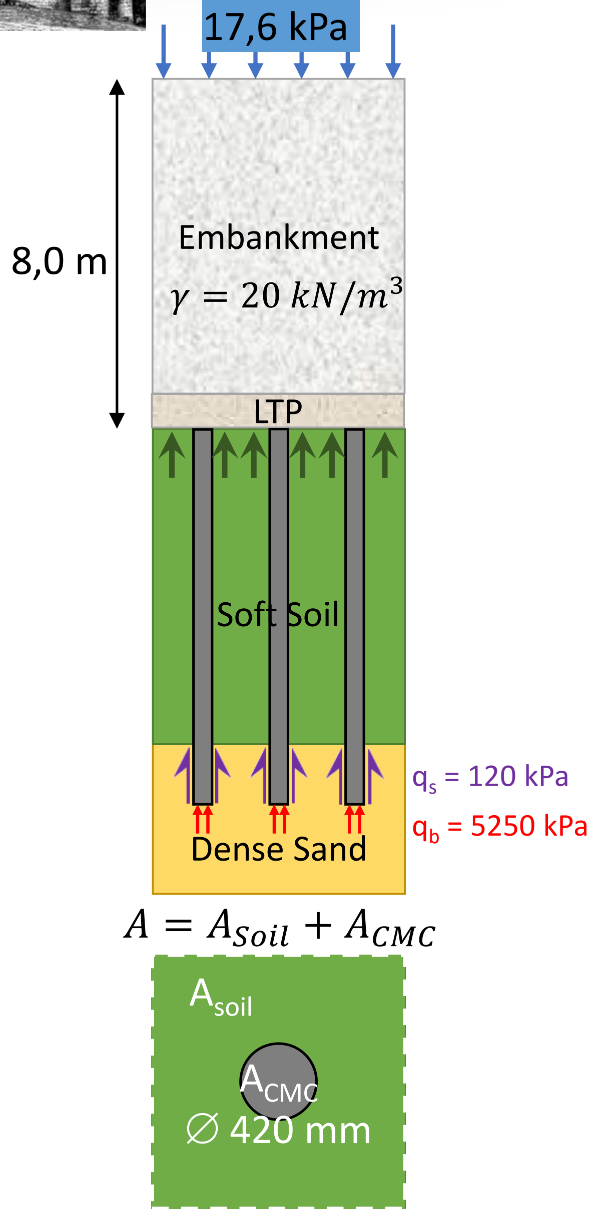

E_d (Design Actions Effects) $\leq$ R_d (Design Resistance)

SLS Numerical Application at the Unit Cell scale (more unfavourable than ULS)

$$Q_{SLS} = 177{,}6 \times A \text{ (kN)}$$

$$Q_{Soil} = 250 \times (A - A_{CMC})$$

$$Q_{CMC} = 806{,}5\ kN$$

$$Q_{SLS} \leq \frac{Q_{SOIL}}{2{,}76} + \frac{Q_{CMC}}{1{,}96}$$

γ_{soil}: SLS partial factor for soil resistance (=2,76 according to French Appendix NF P 94-261 to EC7)
γ_{CMC}: SLS partial factor for CMC resistance (=1,96 according to French Appendix NF P 94-262 to EC7)

$$A \leq 4{,}5\ m^2 (Square\ Grid = 2{,}1\ m\ x\ 2{,}1\ m)$$

Settlement

- Settlement Reduction Factor (SRF) obtained with rigid inclusions ranges typically from 2 to 10 for coverage area ratio from 1% to 10%. SRF depends also on the soil compressibility.
- A rough assessment of the settlement after ground reinforcement can be easily established as follows:
  - (i) Step 1: Calculation of the settlement without considering ground reinforcement
  - (ii) Step 2: Estimation of SRF value estimated from the coverage area ratio (1% -> SRF = 2 / 10% -> SRF = 10)
  - (iii) Step 3: Application of SRF value to assess the settlement after ground reinforcement
- This analysis should be systematic before running any Finite Element Model to get orders of magnitude and to avoid meaningless results.

Settlement

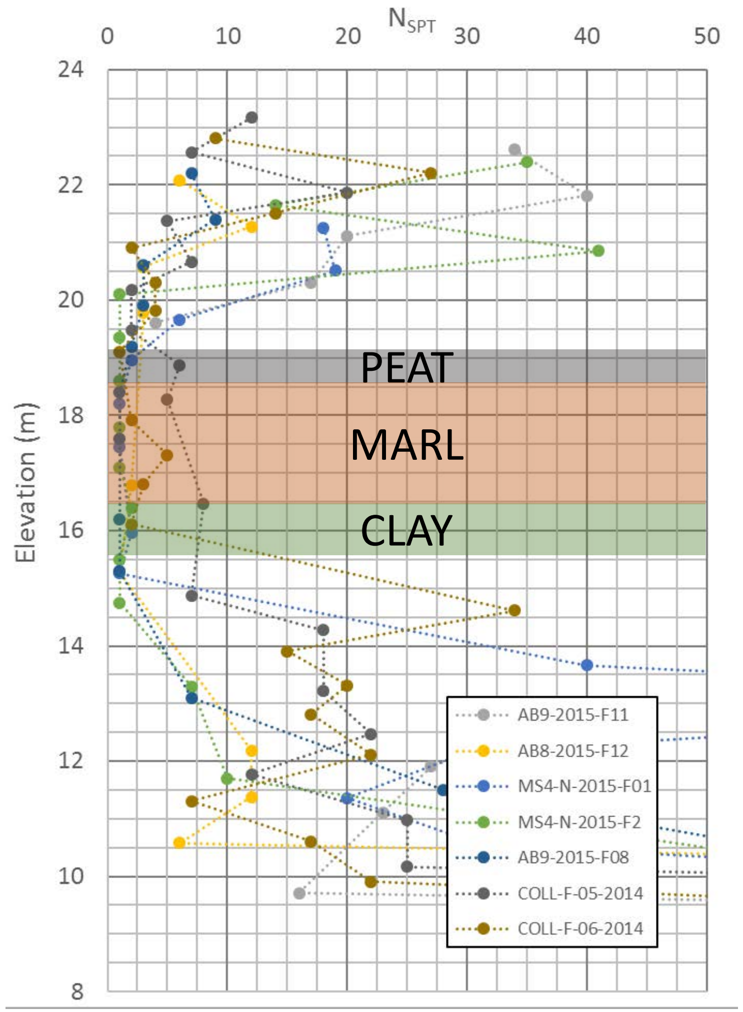

Primary compression

$$\Delta h_p = h \frac{C_c}{1+e_0} \log\left(\frac{\sigma'_{v_0} + \Delta\sigma}{\sigma'_{v_0}}\right)$$

	h (m)	$\frac{C_c}{1+e_0}$	σ'_{v_0} (kPa)	Δh_p (m)
Peat	0,60	0,59	100,6	0,16
Marl	2,15	0,27	108,8	0,24
Clay	0,90	0,34	114,1	0,12
				0,52

Secondary compression

$$\Delta h_s = h \frac{C_{\alpha e}}{1+e_0} \log\left(\frac{t}{t_0}\right)$$

t = 35 ans
t_0 = 1 day

	h (m)	$\frac{C_{\alpha e}}{1+e_0}$	Δh_p (m)
Peat	0,60	0,035	0,08
Marl	2,15	0,018	0,16
Clay	0,90	0,016	0,06
			0,30

Settlement

__Step 1__: Total settlement without ground reinforcement = 0,82 m

__Step2__: Coverage area ratio: $\frac{\pi R^2_{CMC}}{A} = \frac{0{,}138}{2{,}1^2} = 3{,}1\%$

Settlement Reduction Factor = 4

__Step 3__: Absolute settlement with CMC ground reinforcement = **0,20 m**

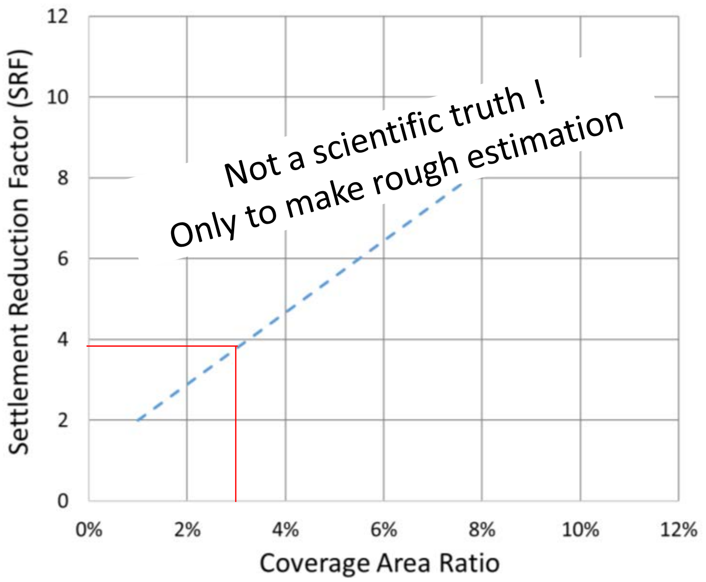

Finite Element Modelling becomes necessary at this stage because:

- The client technical specification is expressed in terms of post-construction (residual) settlement and not in terms of absolute settlement => curve settlement vs time is required;
- Peat, Marl and Clay on this site have high potential of creep. Advanced behaviour law is required.

Presentation of the project

- Location
- Project description
- Technical specifications

Soil conditions

CMC Ground Reinforcement solution

Design principles

- Analytical approach - Global Bearing Capacity and Settlement
- Finite Element Modelling to fine-tune the design
- Specific verification due to high lateral loads

Execution and controls

Conclusions

2D Axial-Symmetrical Model

- Analyse the behaviour of the Unit Cell Area (CMC + Surrounding Soil) at the centre of the treated area.
- Take into account **consolidation phenomenon** and **creep effect** in this "simple" model. Therefore, *Consolidation analysis* is activated in Plaxis and Soft Soil Creep Model is used for soft layers (Peat / Marl / Clay).
- Check **residual settlement requirement** and determine required concrete UCS from compressive stress.
- Deduce from *settlement vs time* curve the equivalent Young modulus $E_Y(t)$ at time *t* for the soft layers. Young Modulus will then be implemented in a simplified 2D Plane-Strain Model.

2D Plane-Strain Model

- Analyse the behaviour of the Ground Reinforcement on the boundary of the treated area, under the **MSE Wall**. Take into account lateral loads created by the **active earth pressure**.
- *Plastic analysis* is activated and Linear Elastic Perfectly Plastic Model (Mohr-Coulomb) is chosen for soft layers. **Consolidation and creep effects are "integrated" in the equivalent Young modulus $E_Y(t)$** deduced from the axial-symmetrical model.
- 2D plane-strain models are carried out for *t = End of Works*, *t = 1 year (after Road Opening)* and *t = 35 years*

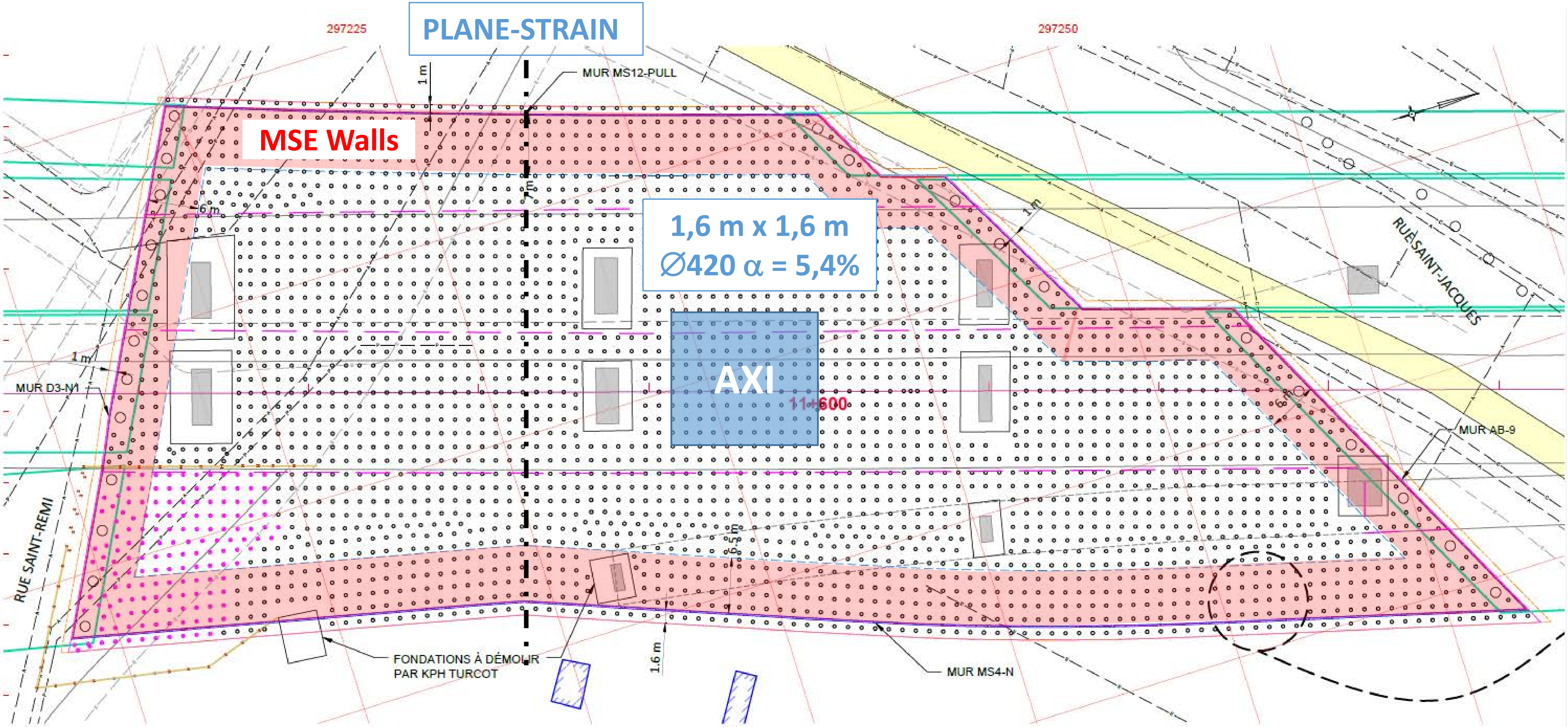
PLANE-STRAIN
297225
297250
MUR MS12-PULL
1 m
MSE Walls
1,6 m x 1,6 m
∅420 α = 5,4%
RUE SAINT-JACQUES
AXI
11+600
1 m
MUR D3-N1
MUR AB-9
RUE SAINT-REMI
FONDATIONS À DÉMOLIR
PAR KPH TURCOT
1.6 m
MUR MS4-N

Phase a – **Duration = 5,5 months**
CMC + Embankment + Pavement
Load = 8,0 m x 20 kN/m3 = 160 kPa

Phase b – **Duration = 35 years**
Road in Service
Live Load = 17,6 kPa

Road Opening

2D Axial-Symmetrical model

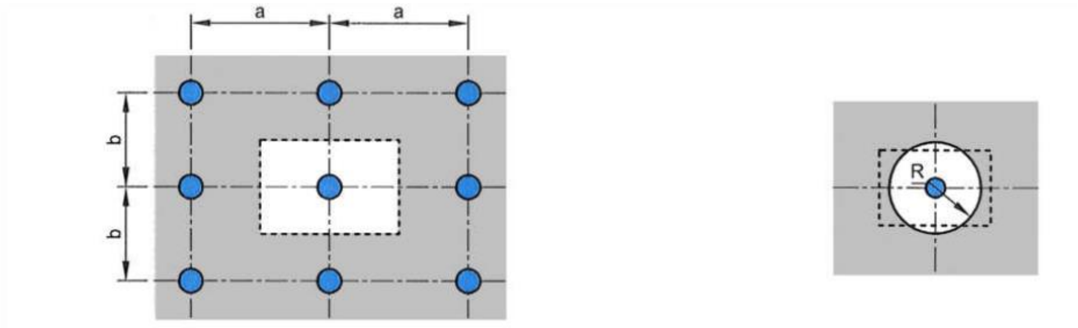

$$a \times b = \pi \times R_{model}^2$$

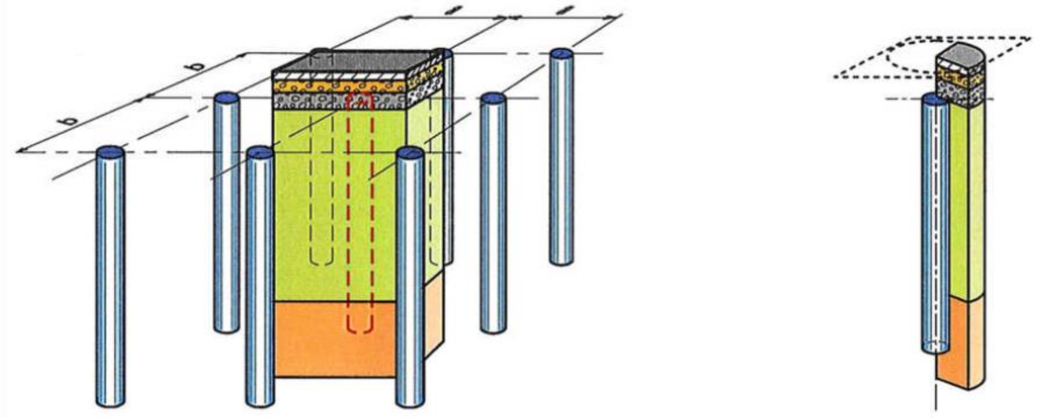

From ASIRI (2012)

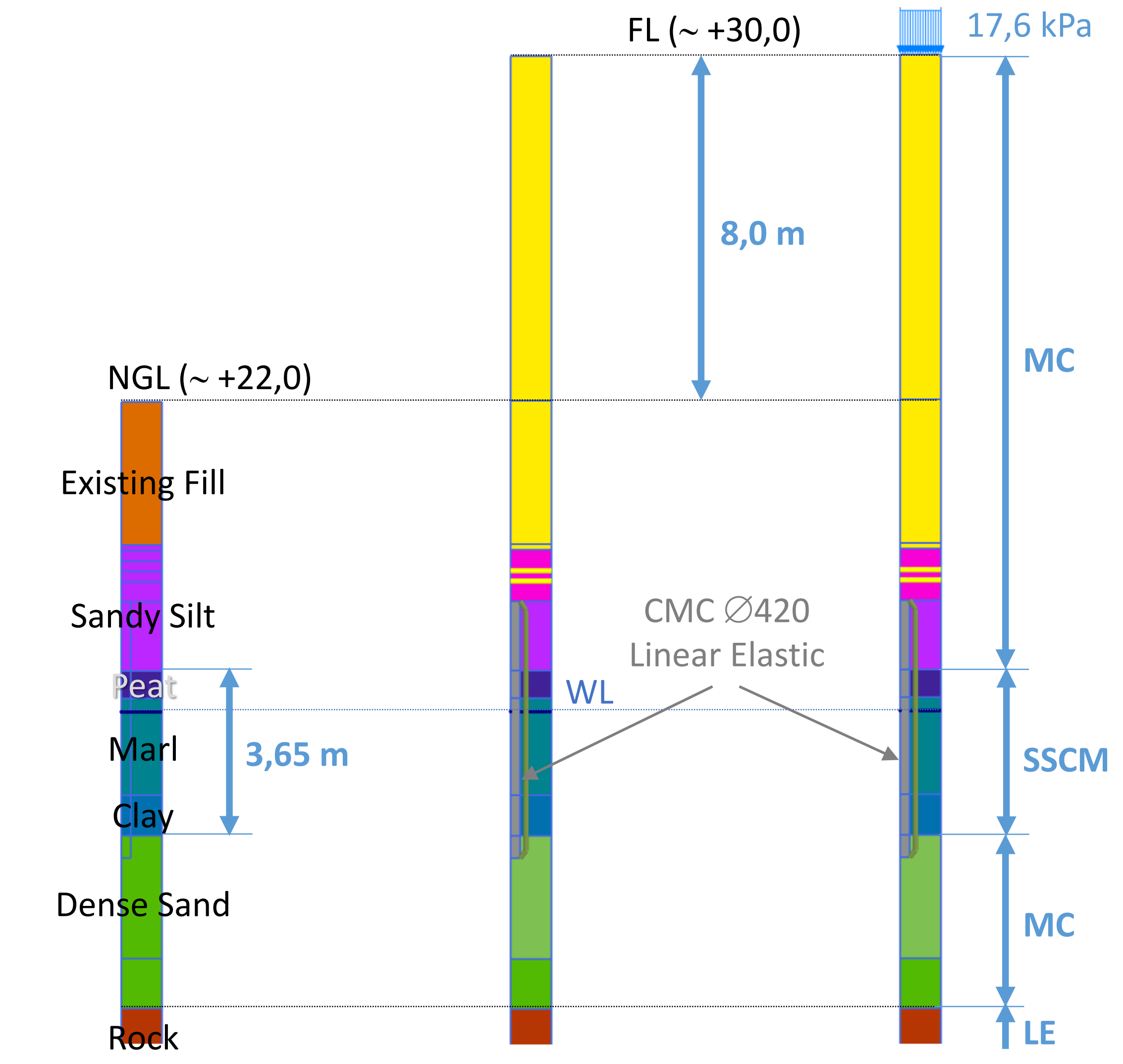

Initial Conditions *Phase a* *Phase b*

MC = Mohr-Coulomb / SSCM=Soft Soil Creep Model / LE = Linear Elastic

Phase a – **Duration = 5,5 months**
CMC + Embankment + Pavement
Load = 8,0 m x 20 kN/m3 = 160 kPa

Phase b – **Duration = 35 years**
Road in Service
Live Load = 17,6 kPa

Road Opening

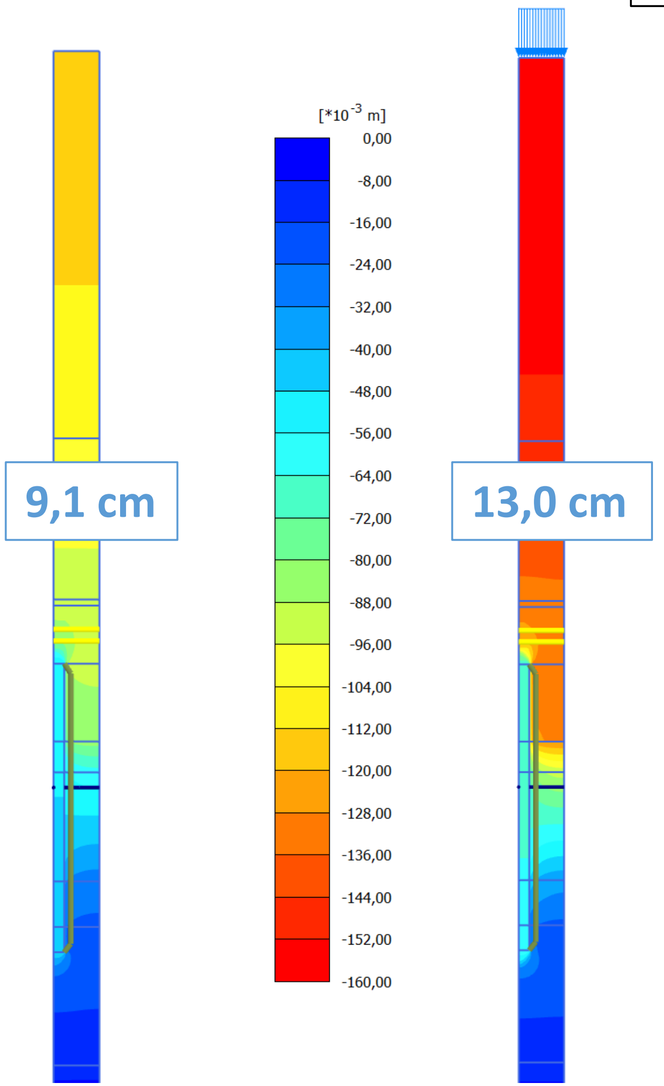

Phase a *Phase b*

Residual settlement (from Road opening to 35 years)

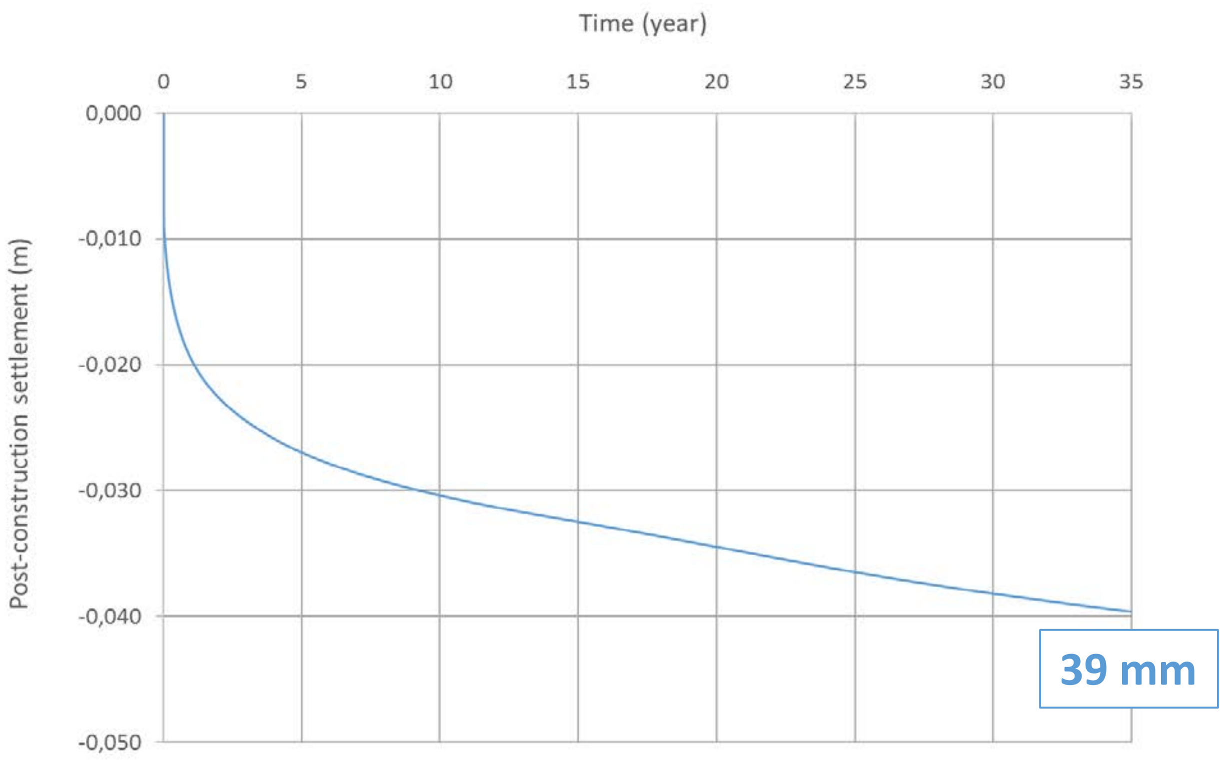

Phase a – **Duration = 5,5 months**
CMC + Embankment + PRELOADING + Pavement
Load = 8,0 m x 20 kN/m3 = 160 kPa

Phase b – **Duration = 35 years**
Road in Service
Live Load = 17,6 kPa

Road Opening

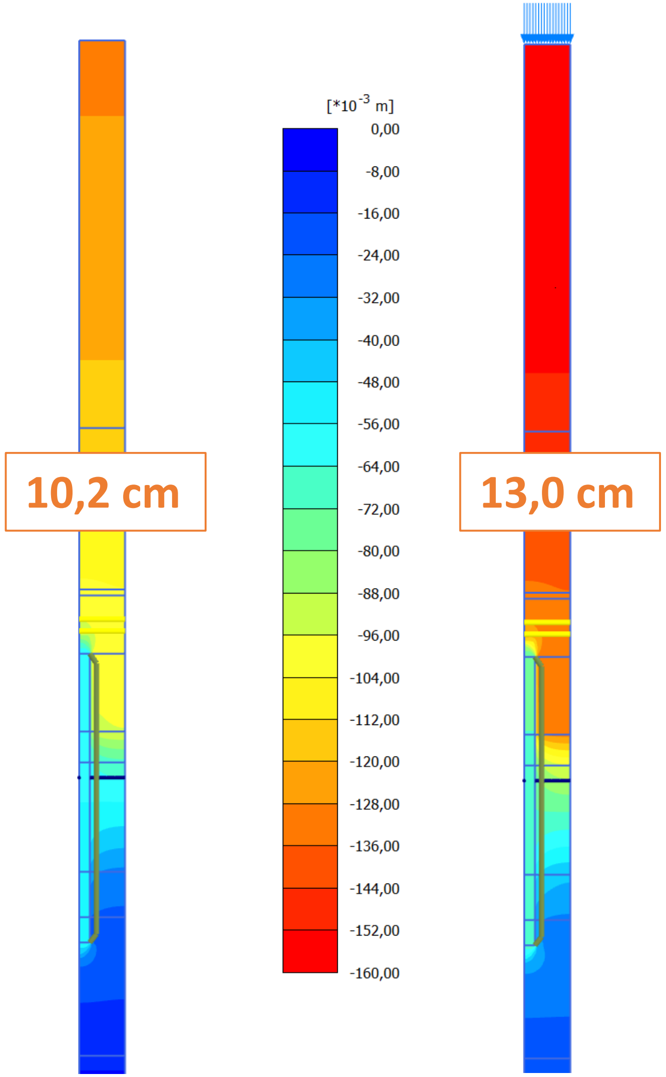

Phase a *Phase b*

Residual settlement (from Road opening to 35 years)

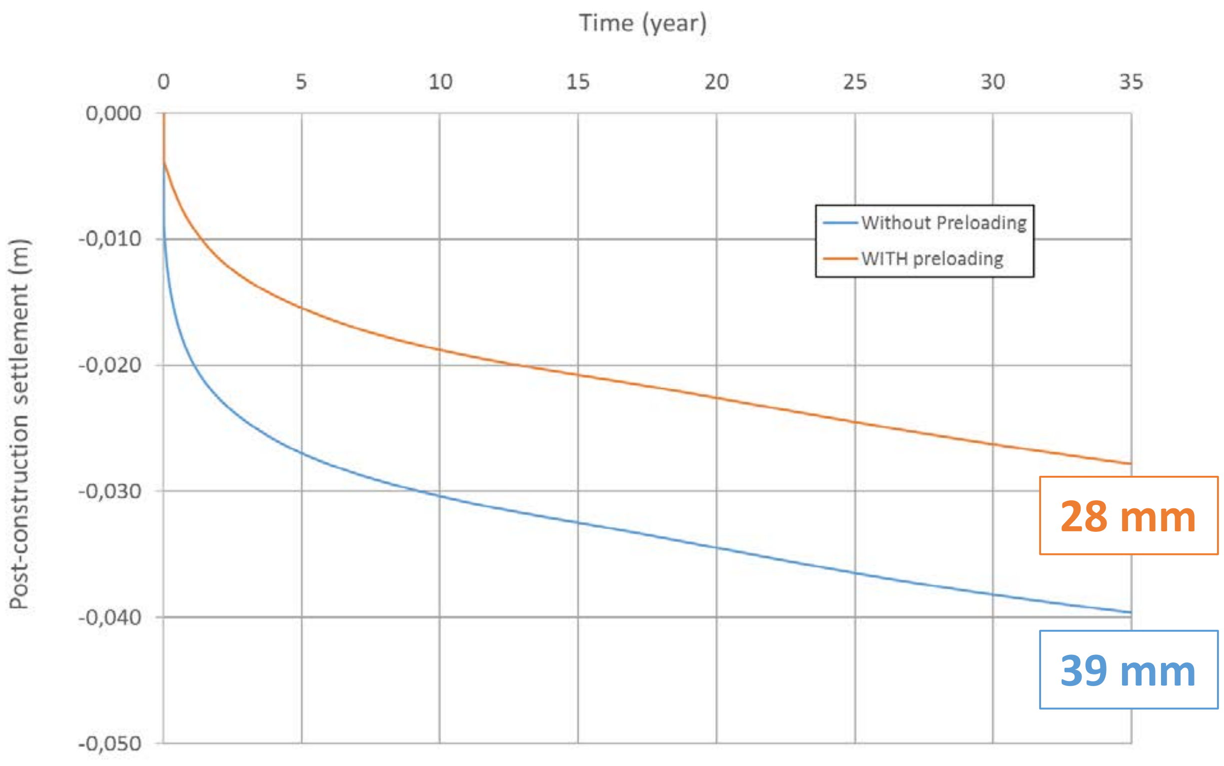

Phase a – **Duration = 5,5 months**
CMC + Embankment + **PRELOADING** + Pavement
Load = 8,0 m x 20 kN/m3 = 160 kPa

Phase b – **Duration = 35 years**
Road in Service
Live Load = 17,6 kPa

Road Opening

Compressive Stress

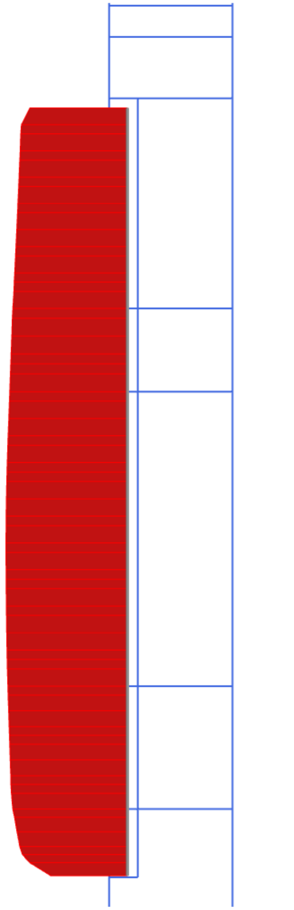

$$\sigma'_{yy_{max}} = 4{,}4\ MPa$$

Concrete C20/25
fc_{28} = UCS (28 days) = 20 MPa

Equivalent stiffness of soft soils with time

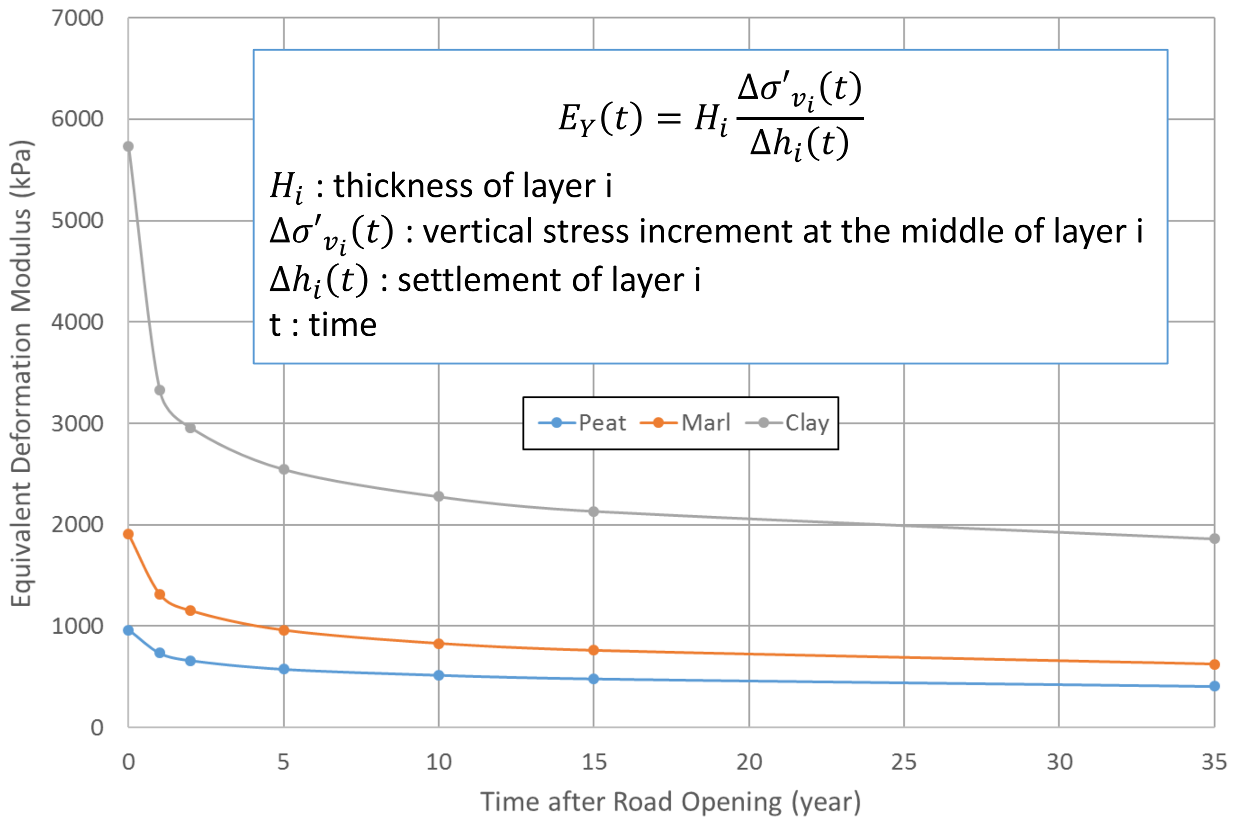

$$E_Y(t) = H_i \frac{\Delta\sigma'_{v_i}(t)}{\Delta h_i(t)}$$

H_i : thickness of layer i
$\Delta\sigma'_{v_i}(t)$: vertical stress increment at the middle of layer i
$\Delta h_i(t)$: settlement of layer i
t : time

Phase 1 - Road N construction CMC + Fill + PRELOADING + Pavement	1 year Road N in service	Phase 2 - Roads A, B, M construction CMC + Fill + PRELOADING + Pavement	35 years All Roads in Service

2D Plane-Strain model

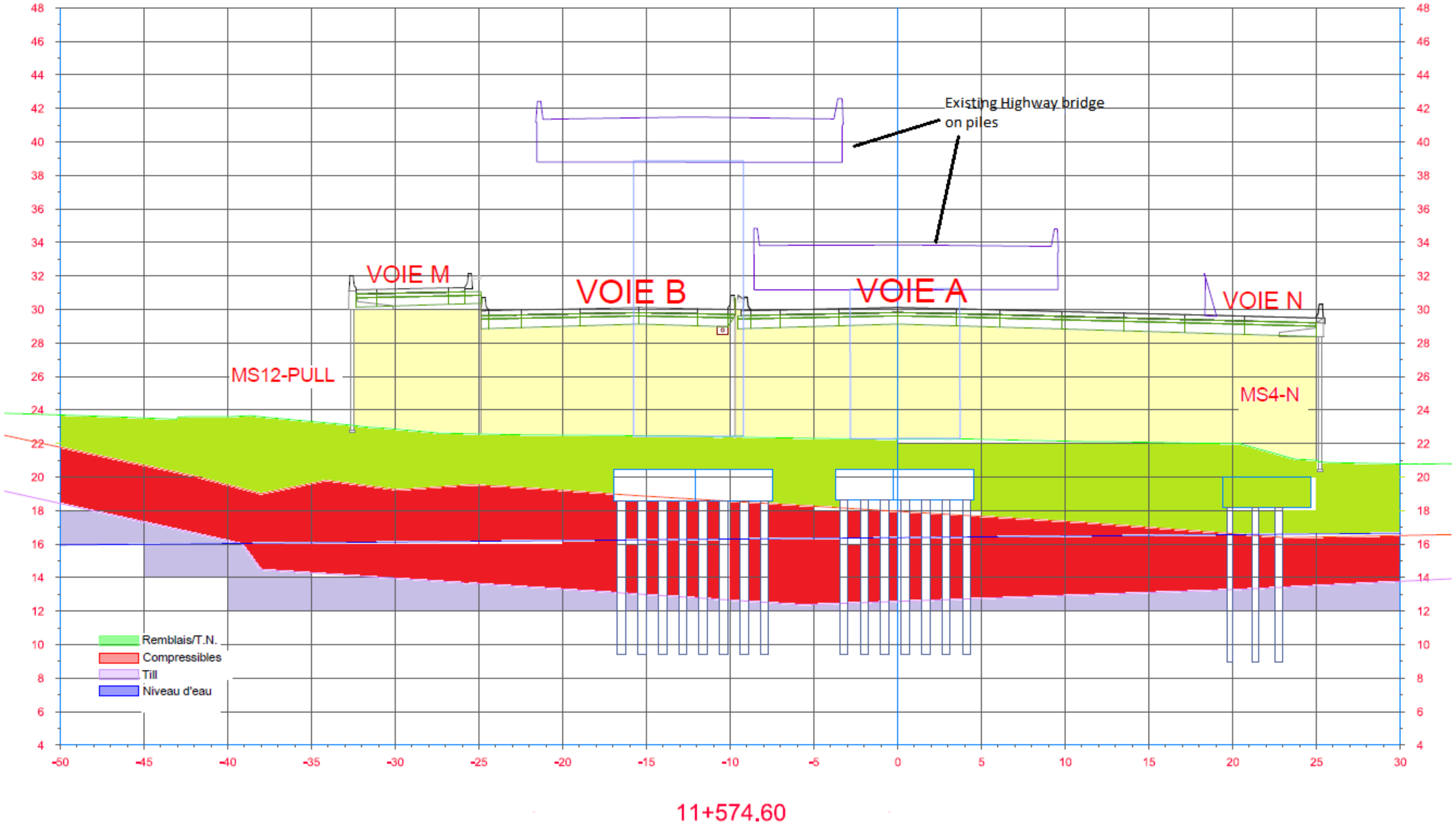

Phase 1 - Road N construction	**1 year**	**Phase 2** - Roads A, B, M construction	**35 years**
CMC + Fill + **PRELOADING** + Pavement	Road N in service	CMC + Fill + **PRELOADING** + Pavement	All Roads in Service

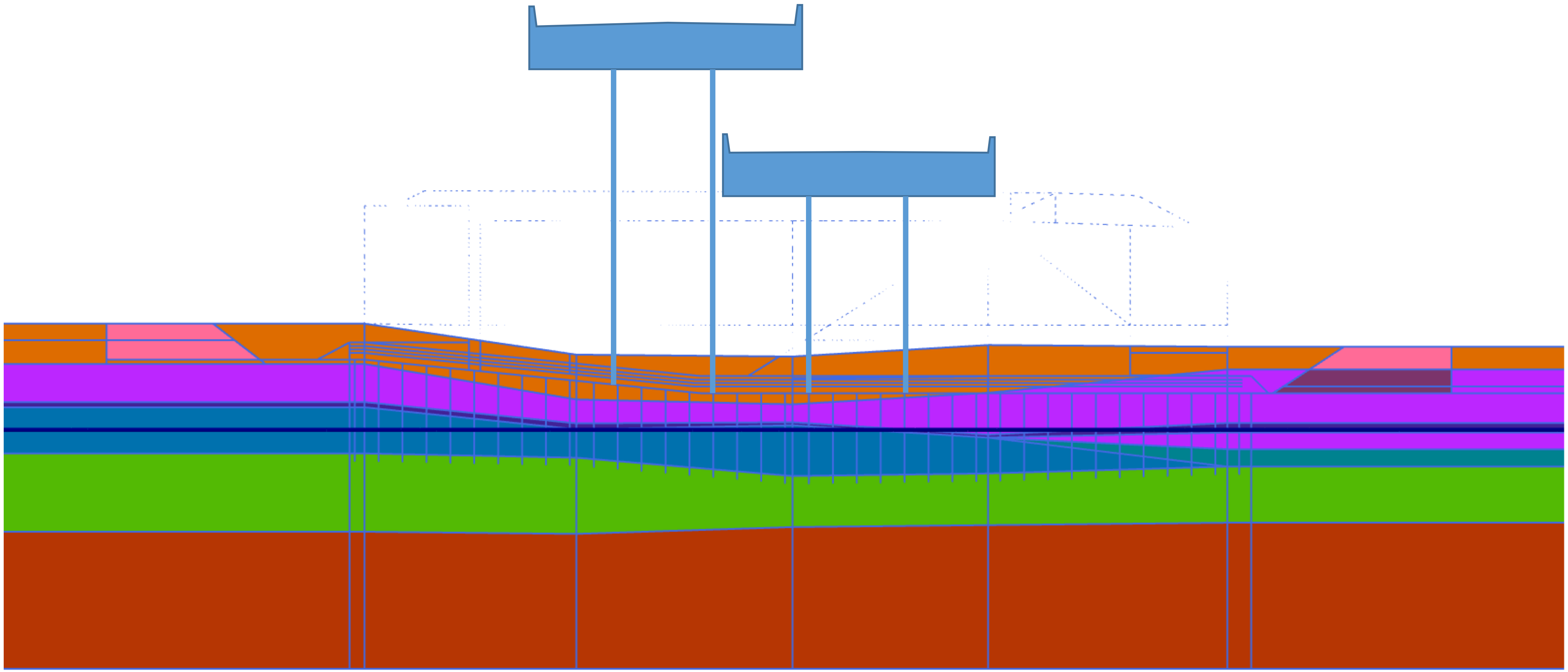

Initial conditions

Phase 1 - Road N construction
CMC + Fill + **PRELOADING** + Pavement

1 year
Road N in service

Phase 2 - Roads A, B, M construction
CMC + Fill + **PRELOADING** + Pavement

35 years
All Roads in Service

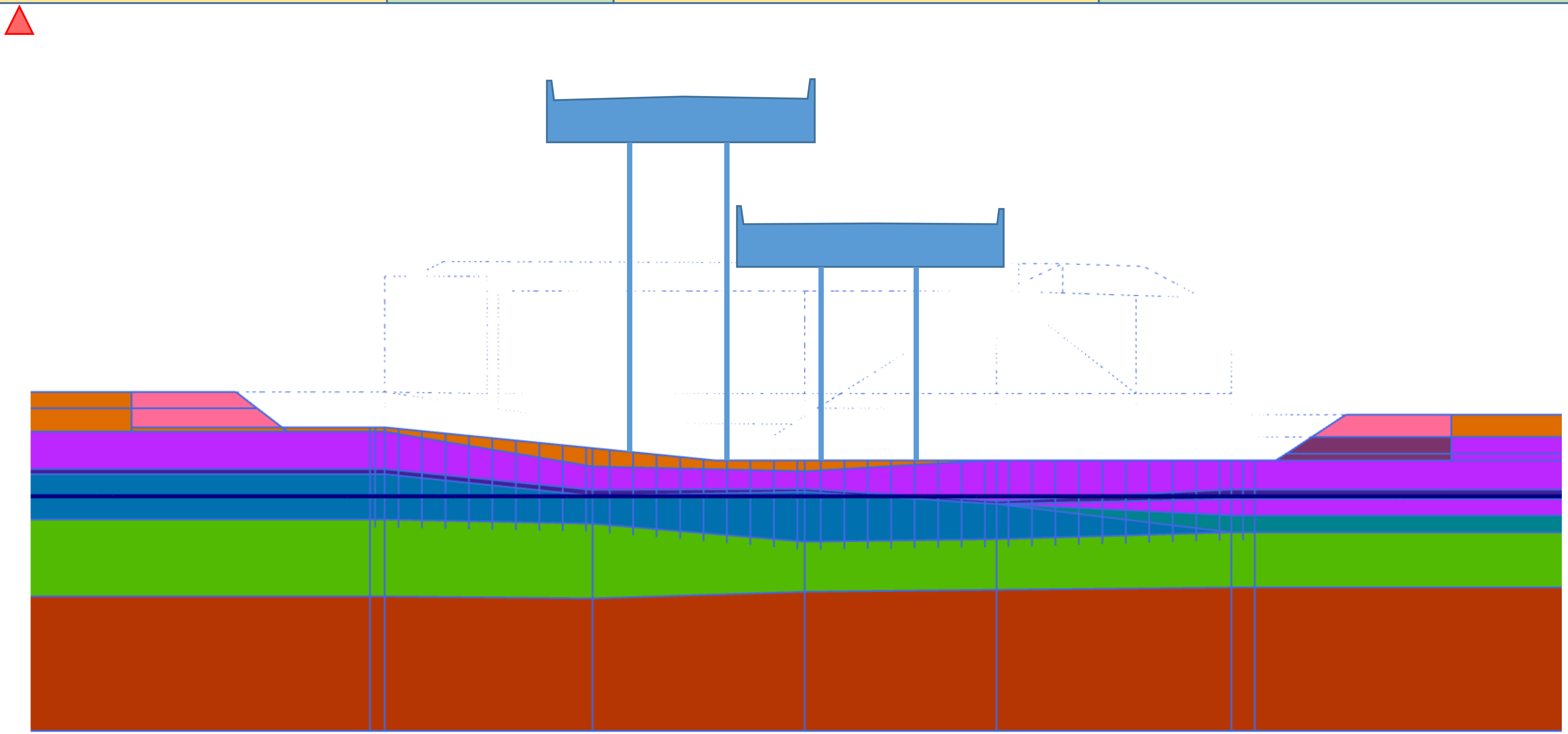

3m deep excavation (to increase headroom for the rig – 12 m instead of 9 m)

Phase 1 - Road N construction	**1 year**	**Phase 2** - Roads A, B, M construction	**35 years**
CMC + Fill + PRELOADING + Pavement	Road N in service	CMC + Fill + PRELOADING + Pavement	All Roads in Service

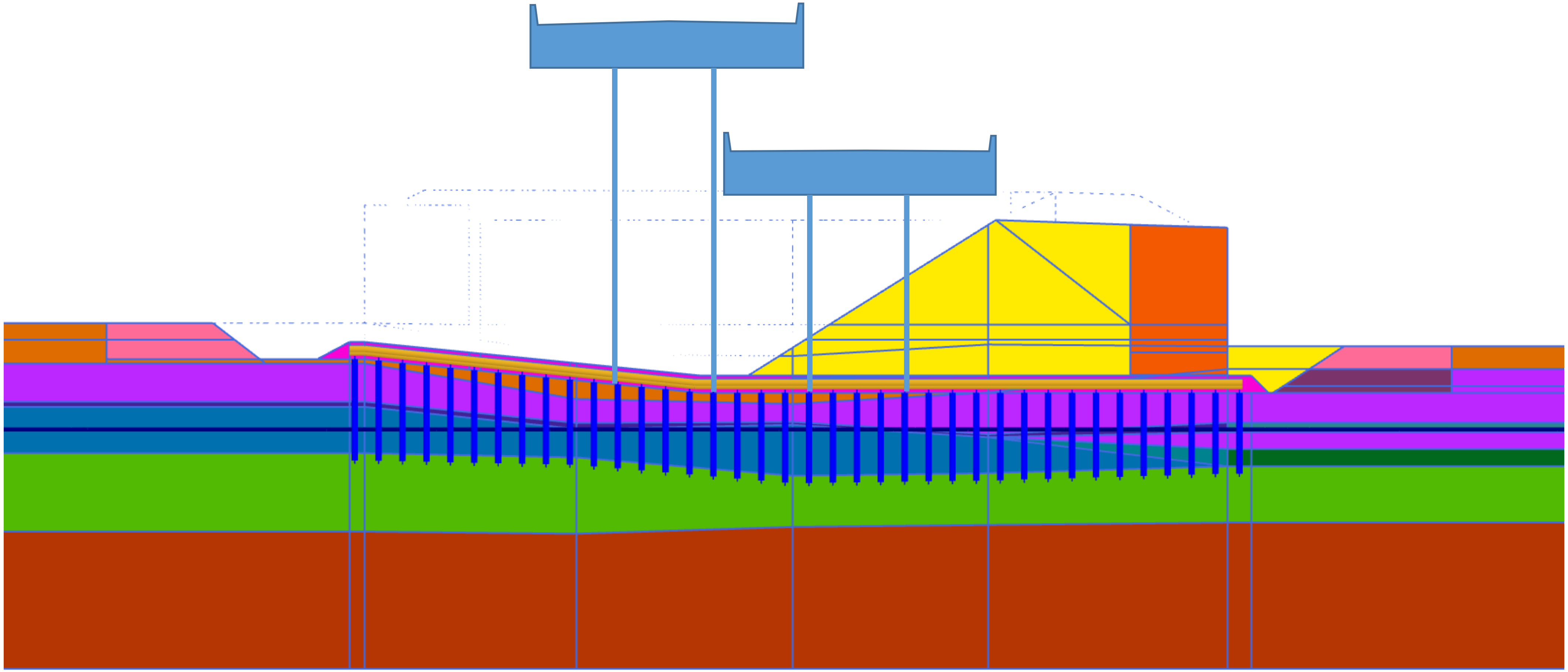

CMC + MSE Wall + Fill installation – Phase 1 (the two bridges are still in operation)

Phase 1 - Road N construction	**1 year**	**Phase 2** - Roads A, B, M construction	**35 years**
CMC + Fill + **PRELOADING** + Pavement	Road N in service	CMC + Fill + **PRELOADING** + Pavement	All Roads in Service

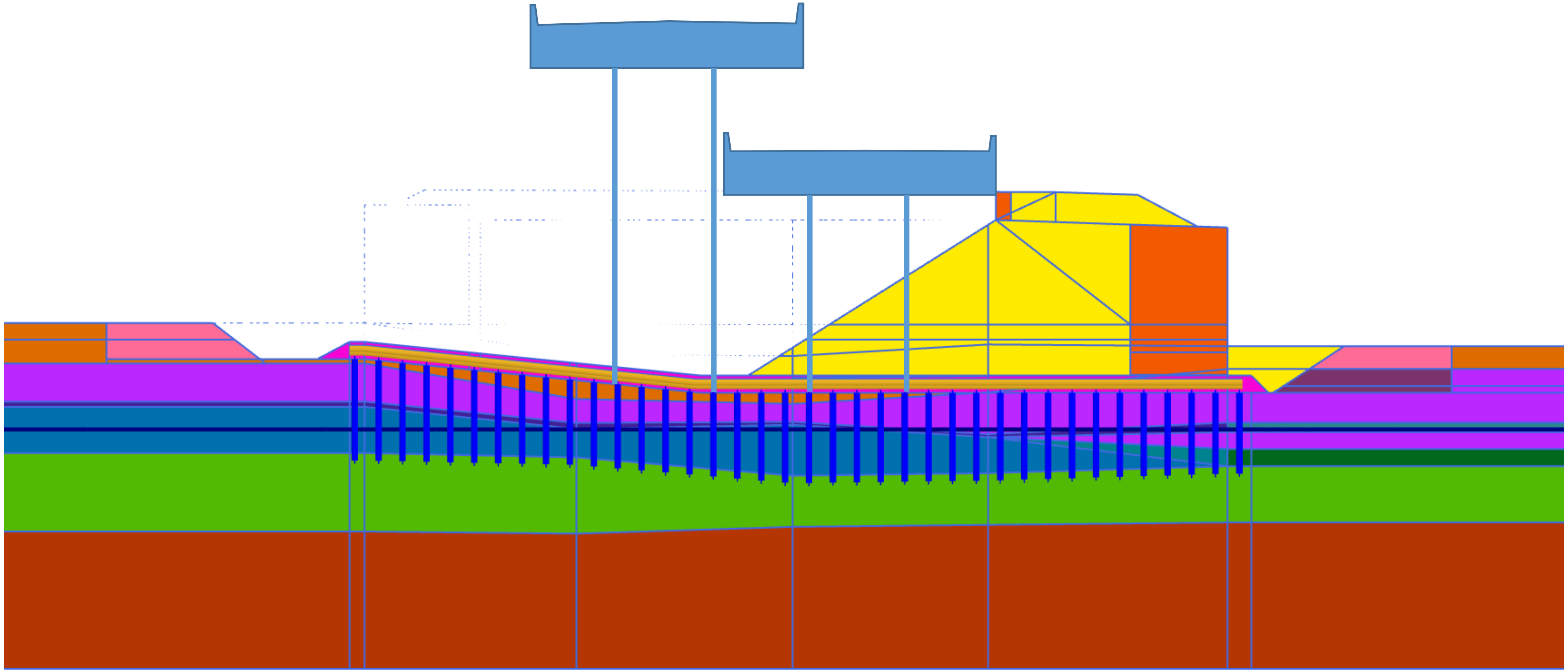

Preloading surcharge (2,0 m during 1 month) to guarantee residual settlement

Phase 1 - Road N construction	**1 year**	**Phase 2** - Roads A, B, M construction	**35 years**
CMC + Fill + **PRELOADING** + Pavement	Road N in service	CMC + Fill + **PRELOADING** + Pavement	All Roads in Service

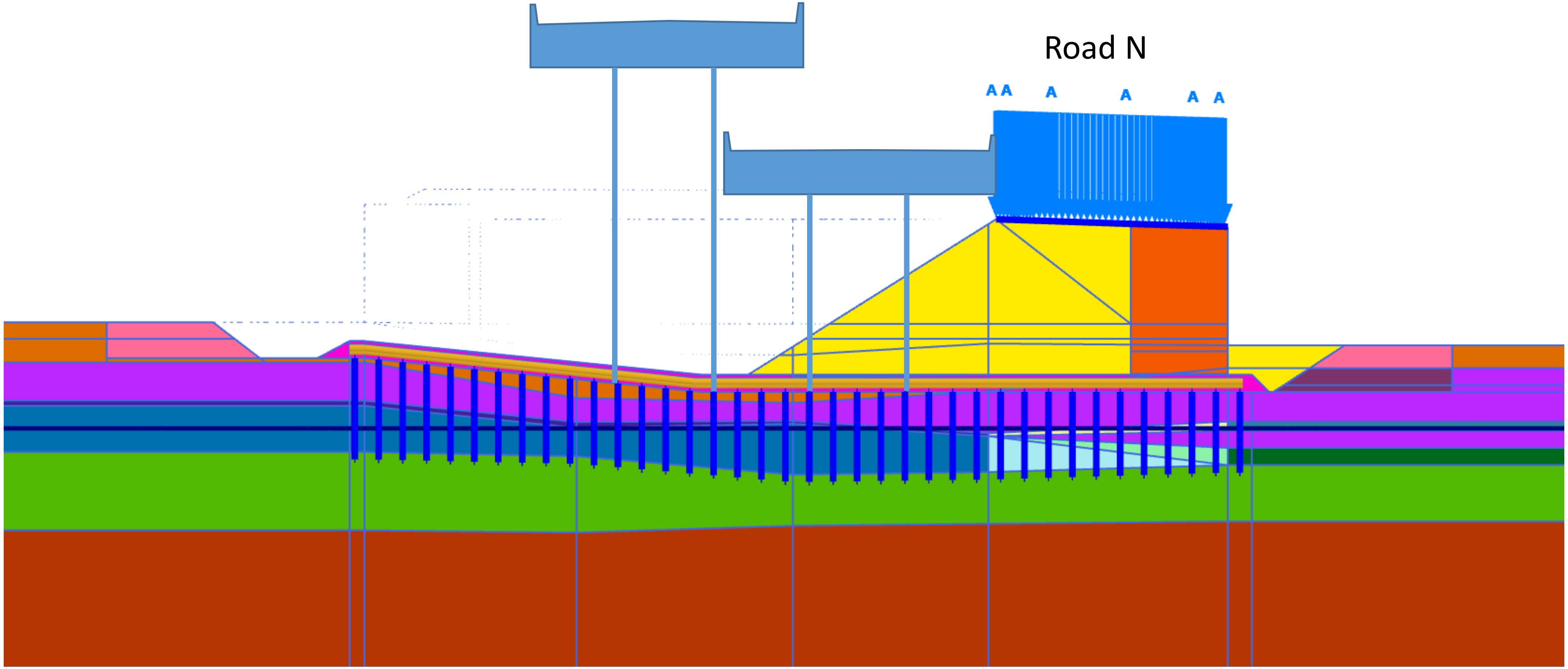

Road N opening

Phase 1 - Road N construction	1 year	Phase 2 - Roads A, B, M construction	35 years
CMC + Fill + PRELOADING + Pavement	Road N in service	CMC + Fill + PRELOADING + Pavement	All Roads in Service

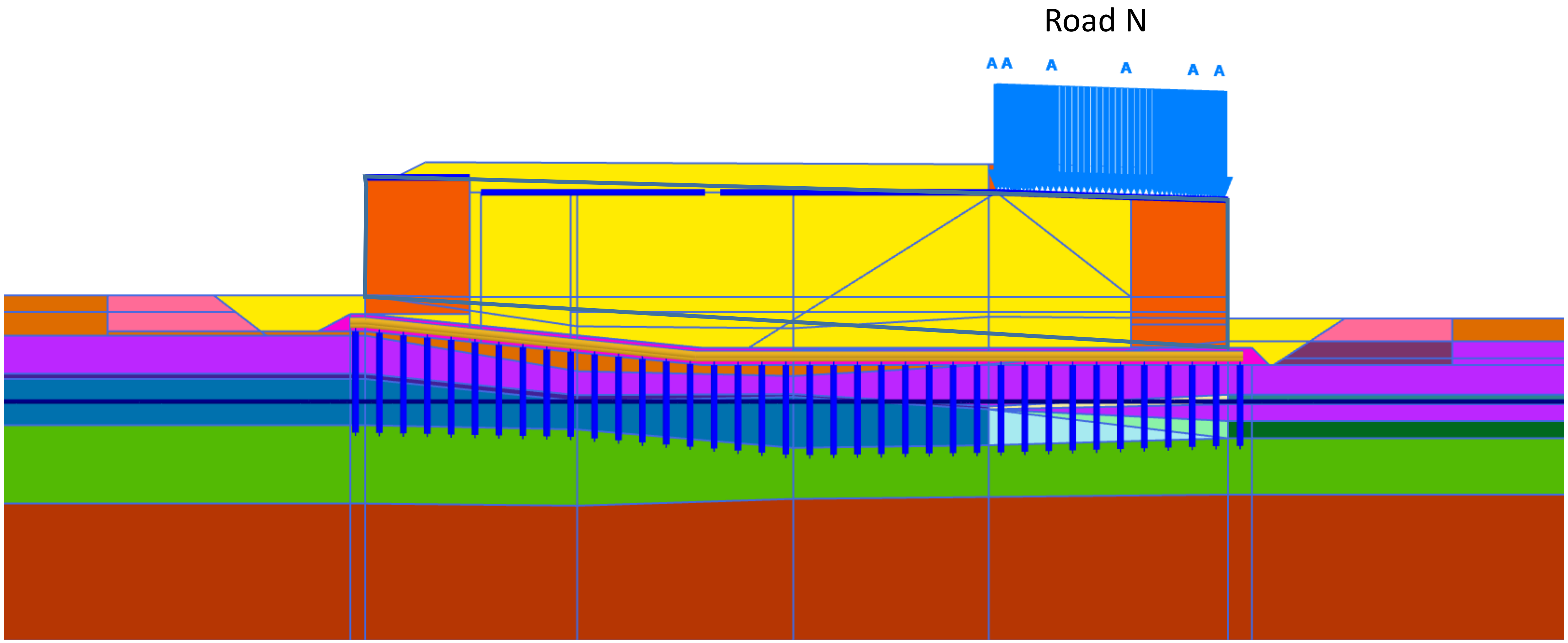

MSE Wall + Fill + Preloading – Phase 2 (one year after road opening)

Phase 1 - Road N construction CMC + Fill + **PRELOADING** + Pavement	**1 year** Road N in service	**Phase 2** - Roads A, B, M construction CMC + Fill + **PRELOADING** + Pavement	**35 years** All Roads in Service

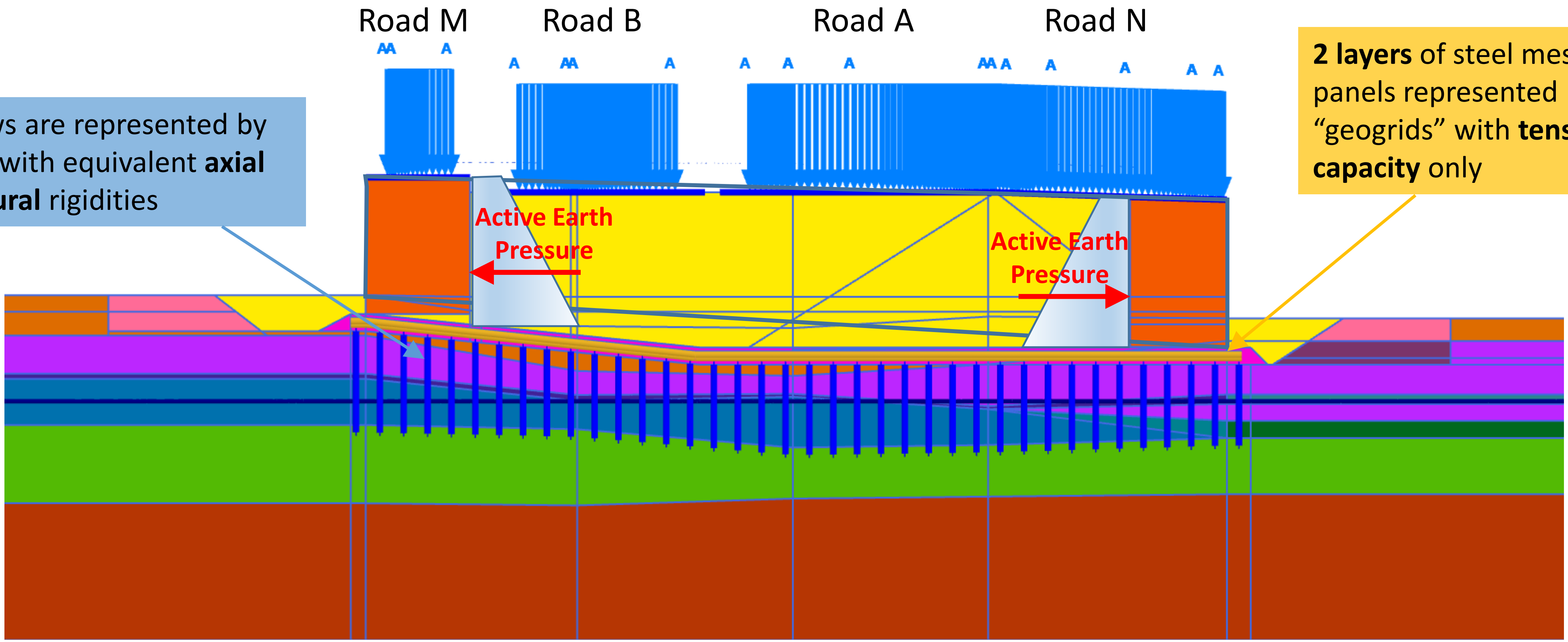

CMC rows are represented by "plates" with equivalent **axial** and **flexural** rigidities

2 layers of steel meshes panels represented by "geogrids" with **tension capacity** only

All roads in operation

Presentation of the project

- Location
- Project description
- Technical specifications

Soil conditions

CMC Ground Reinforcement solution

Design principles

- Analytical approach - Global Bearing Capacity and Settlement
- Finite Element Modelling to fine-tune the design
- Specific verification due to high lateral loads

Execution and controls

Conclusions

Stiffness = 160 000 kN/ml

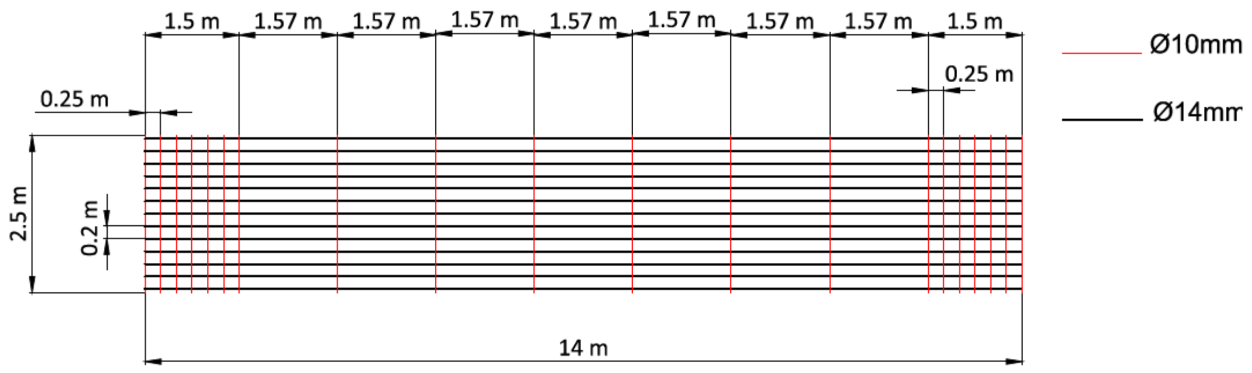

Longitudinal bars (∅ = 14 mm) are designed to withstand tension forces created by active earth pressure.

Transversal bars (∅ = 10 mm) are designed to mobilize tension forces by **friction**. Density is increased at the extremity to reduce overlapping length.

Stiffness = 160 000 kN/ml

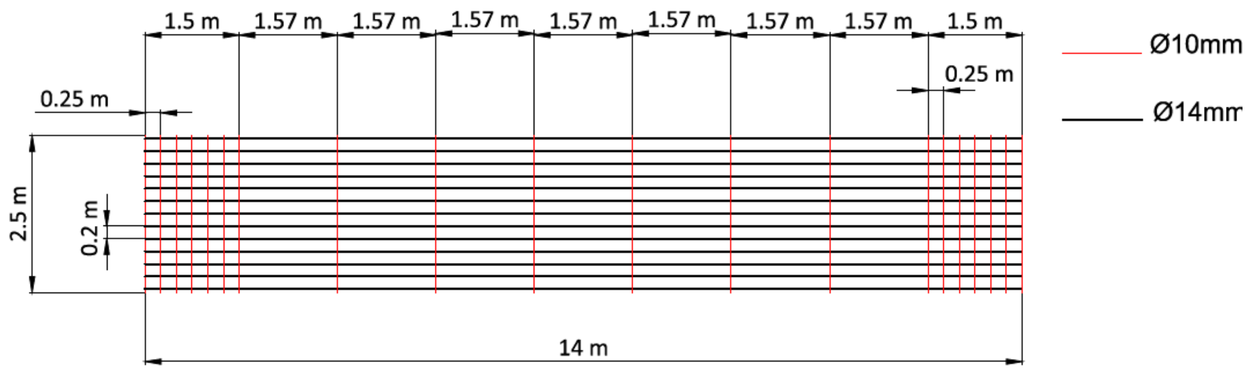

*ULS STR resistance of **one** steel meshes layer*

$$R_{t,d} = \rho_{end}\rho_{deg}\frac{S_0 f_u}{\gamma_{M2}}$$

Reduction factor for damage during fill installation

According to NF P 94-270 Retaining Structures (French National Appendix to EC7)

Stiffness = 160 000 kN/ml

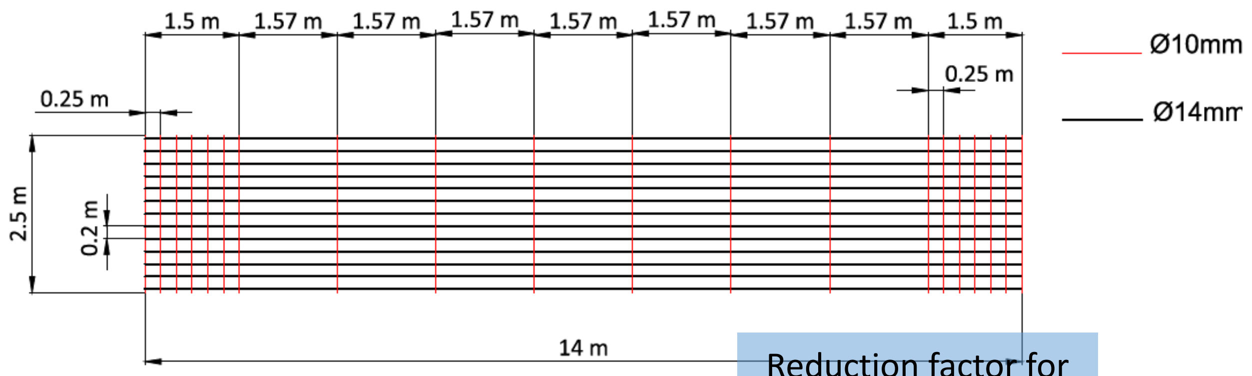

Reduction factor for corrosion

*ULS STR resistance of **one** steel meshes layer*

$$R_{t,d} = \rho_{end}\rho_{deg}\frac{S_0 f_u}{\gamma_{M2}}$$

Stiffness = 160 000 kN/ml

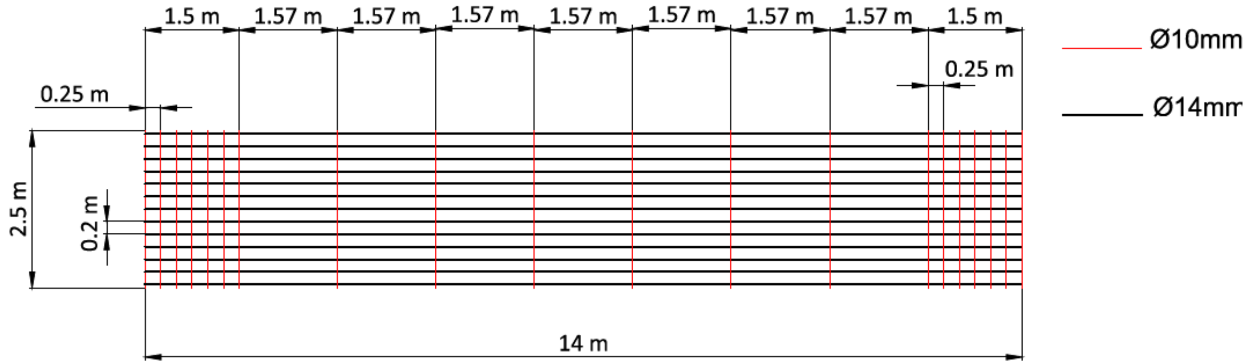

*ULS STR resistance of **one** steel meshes layer*

$$R_{t,d} = \rho_{end}\rho_{deg}\frac{S_0 f_u}{\gamma_{M2}}$$

Partial factor on material

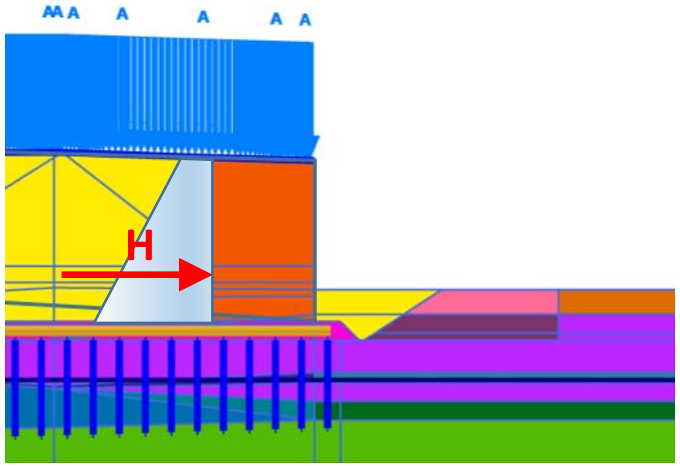

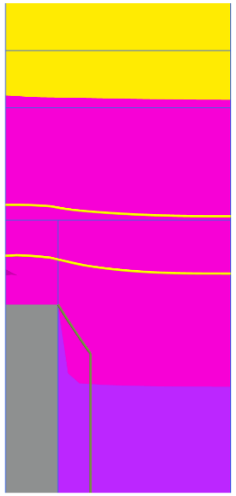

Stiffness = 160 000 kN/ml

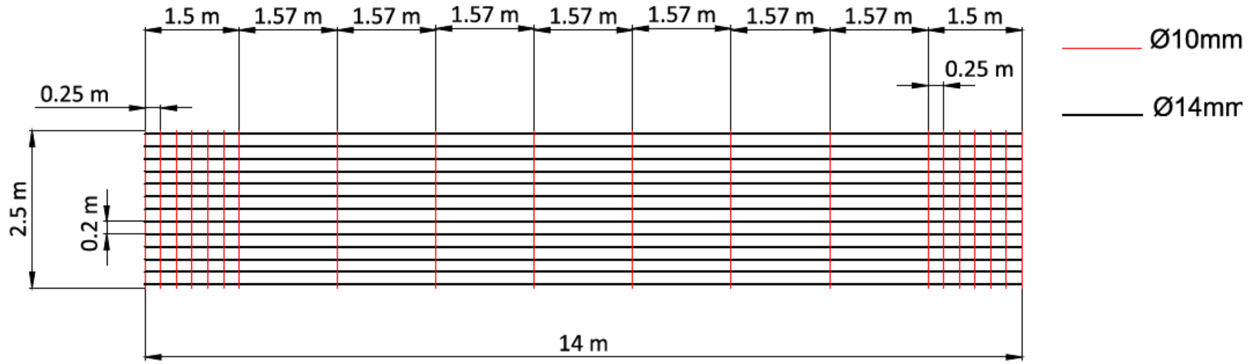

ULS tensile force in the steel meshes layer

a) Active Earth Pressure Effect

$$H = 0{,}5 K_a \gamma_\gamma \gamma_{emb} H_{emb}^2 + K_a \gamma_q q H_{emb}$$

$$\gamma_\gamma = 1{,}35 \qquad \gamma_q = 1{,}5$$

$$K_a = tan^2\left(\frac{\pi}{4} - \frac{\varphi_{emb}}{2}\right) = 0{,}234 \qquad \varphi_{emb} = 38°$$

$$H = 0{,}5 \times 0{,}234 \times 1{,}35 \times 20 \times 11^2 + 0{,}234 \times 1{,}5 \times 17{,}6 \times 11$$

$$H = 450 kN/ml$$

$$T_{active\ force,d} = 225 \text{ kN/ml}$$

*ULS STR resistance of **one** steel meshes layer*

$$R_{t,d} = \rho_{end}\rho_{deg}\frac{S_0 f_u}{\gamma_{M2}}$$

$$S_0 f_u = 5 \times \pi \frac{0{,}014^2}{4} \times 550\ MPa = 423\ kN/ml$$

$$R_{t,d} \approx 0{,}7 S_0 f_u = 300 \text{ kN/ml}$$

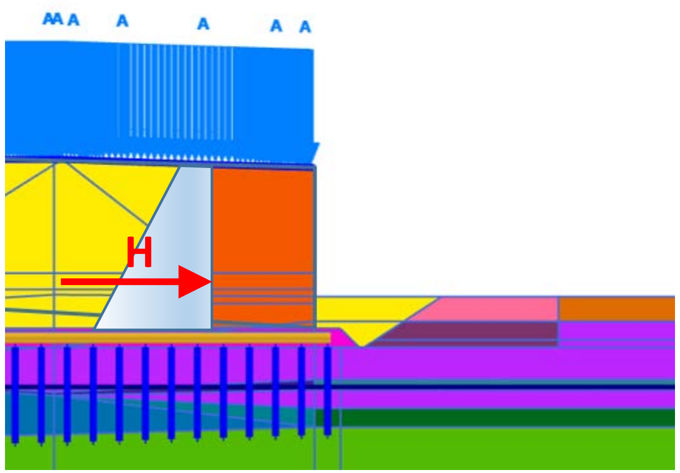

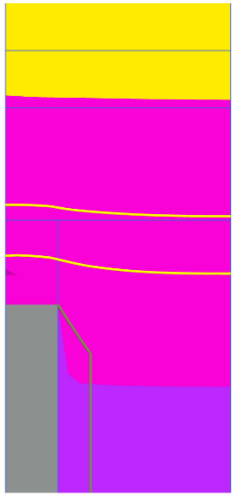

Stiffness = 160 000 kN/ml

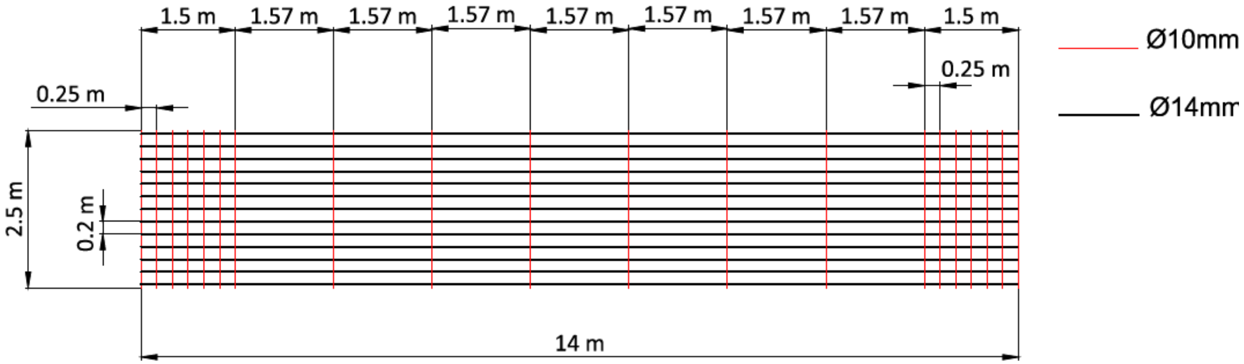

ULS tensile force in the steel meshes layer

a) *Active Earth Pressure Effect*

$$T_{active\ force,d} = 225 \text{ kN/ml}$$

b) *Membrane Effect (from axi-model)*

$$T_{membrane,d} = 50 \text{ kN/ml}$$

$$T_{max,d} = 275 \text{ kN/ml}$$

*ULS STR resistance of **one** steel meshes layer*

$$R_{t,d} = \rho_{end}\rho_{deg}\frac{S_0 f_u}{\gamma_{M2}}$$

$$S_0 f_u = 5 \times \pi\frac{0{,}014^2}{4} \times 550\ MPa = 423\ kN/ml$$

$$R_{t,d} \approx 0{,}7 S_0 f_u = 300 \text{ kN/ml}$$

$$T_{max,d} \leq R_{t,d}$$

Total cumulated deformations

Final results for the proposed solution

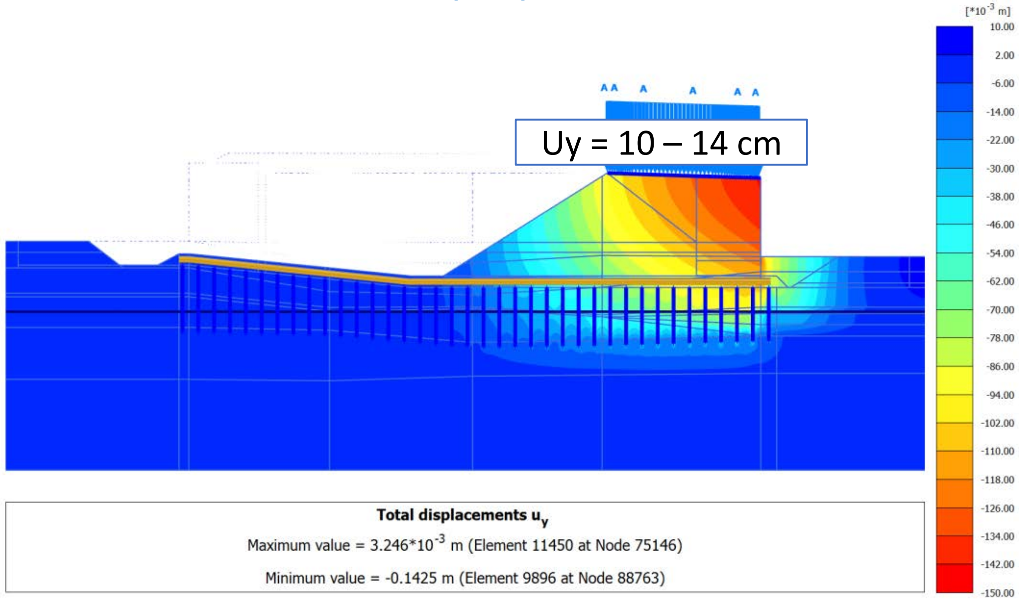

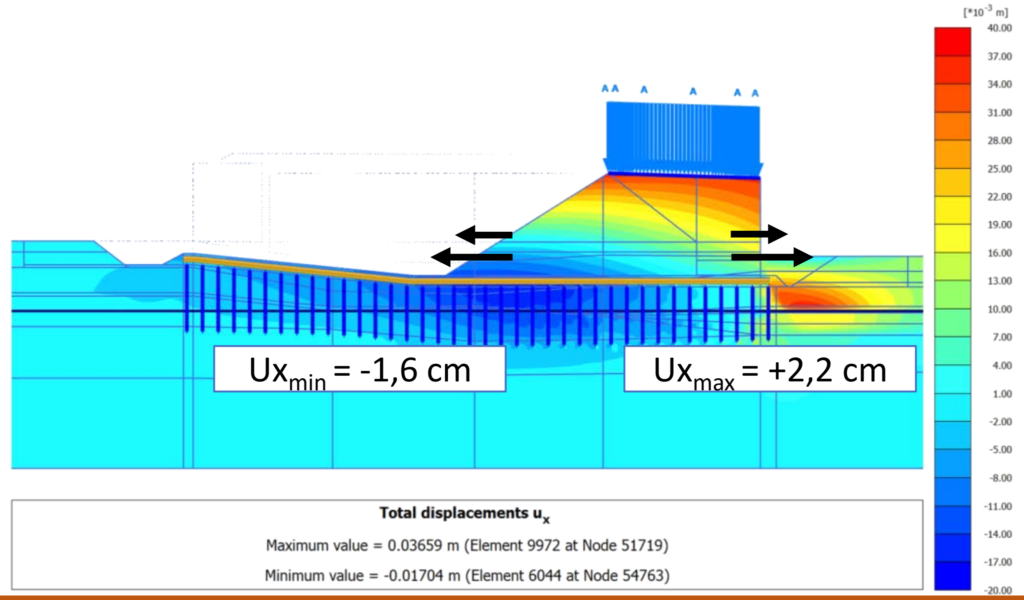

For information – WITHOUT steel meshes

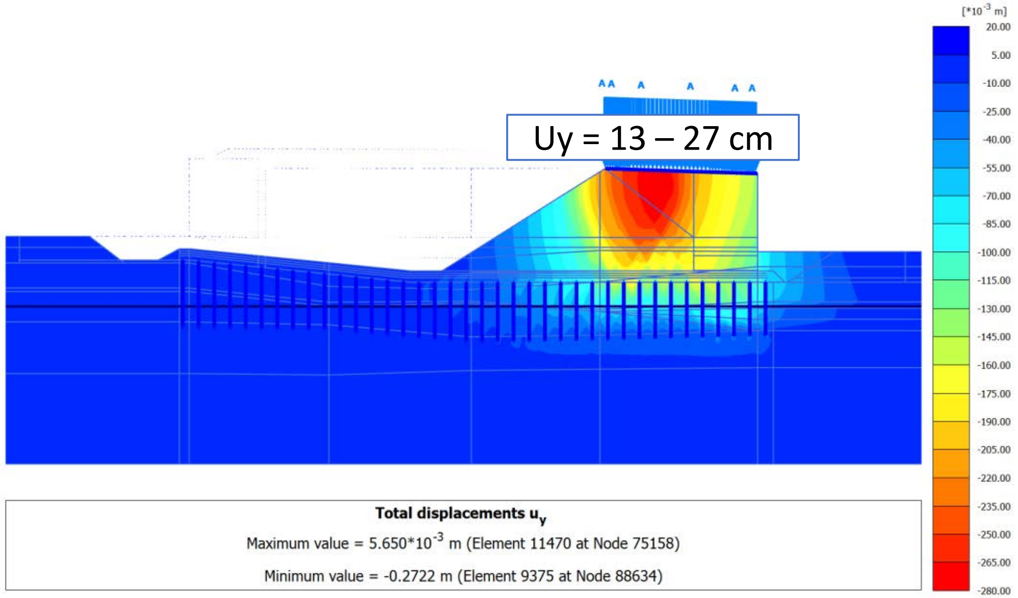

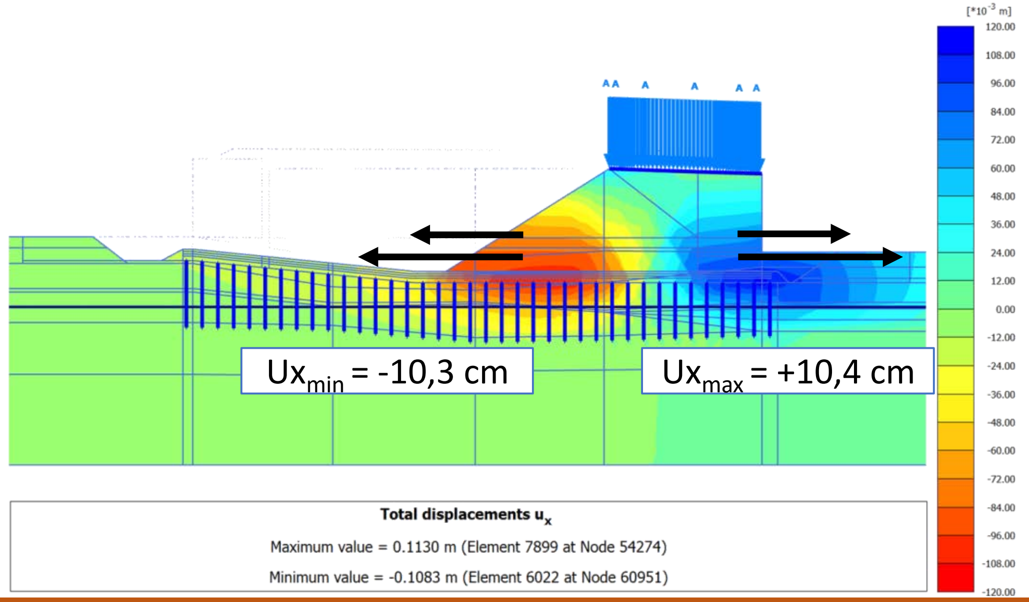

Axial forces and bending moments

Final results for the proposed solution

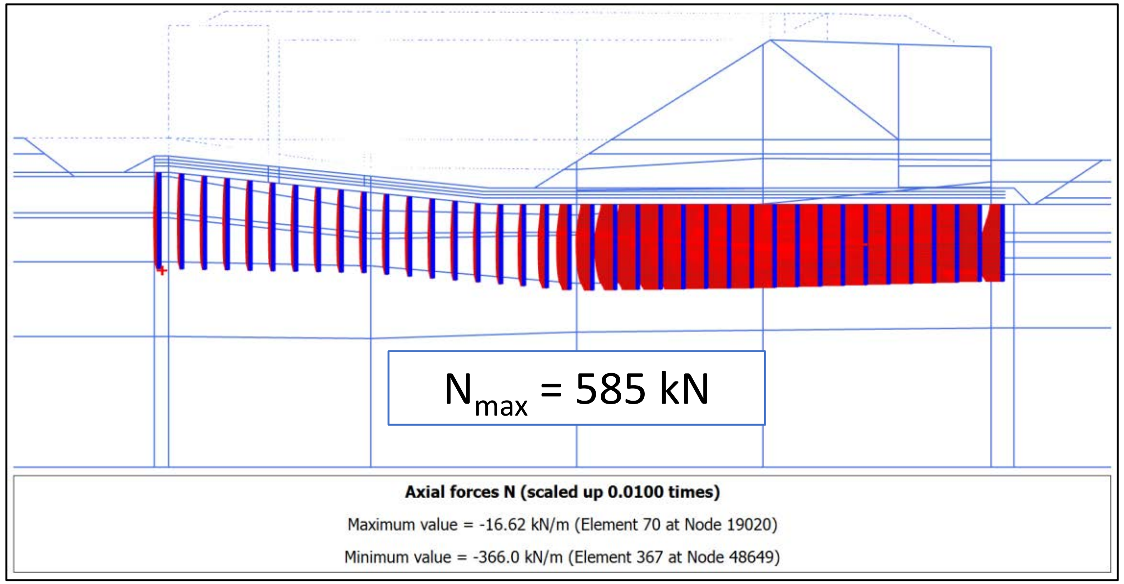

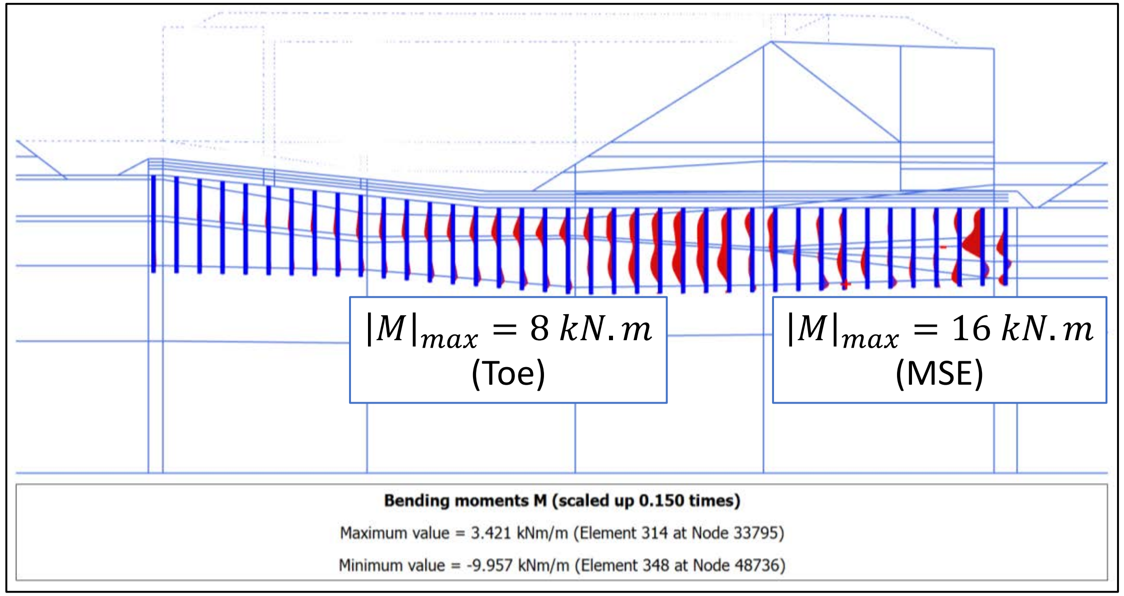

For information – WITHOUT steel meshes

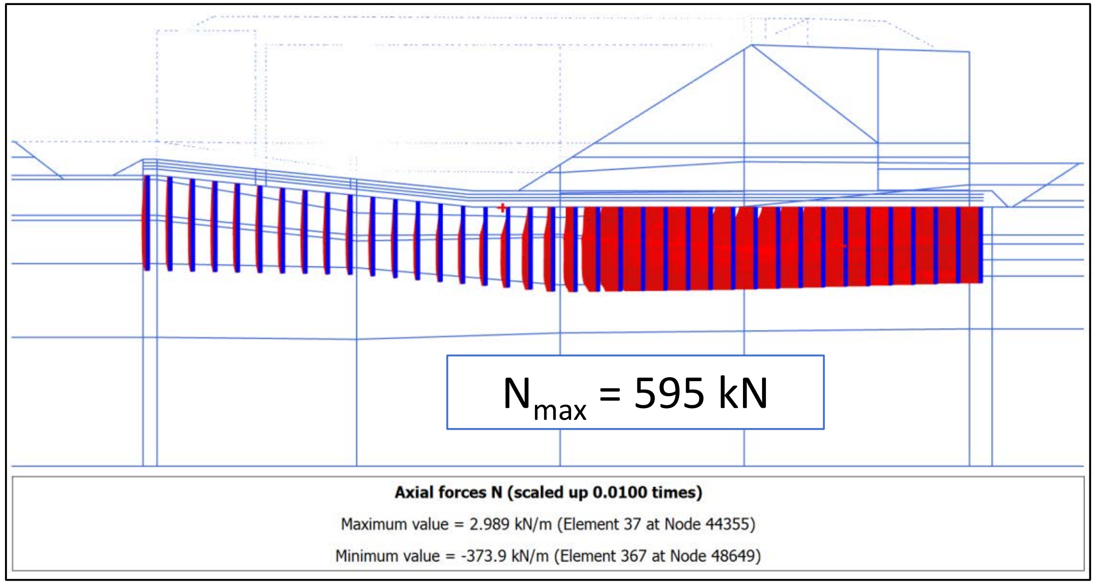

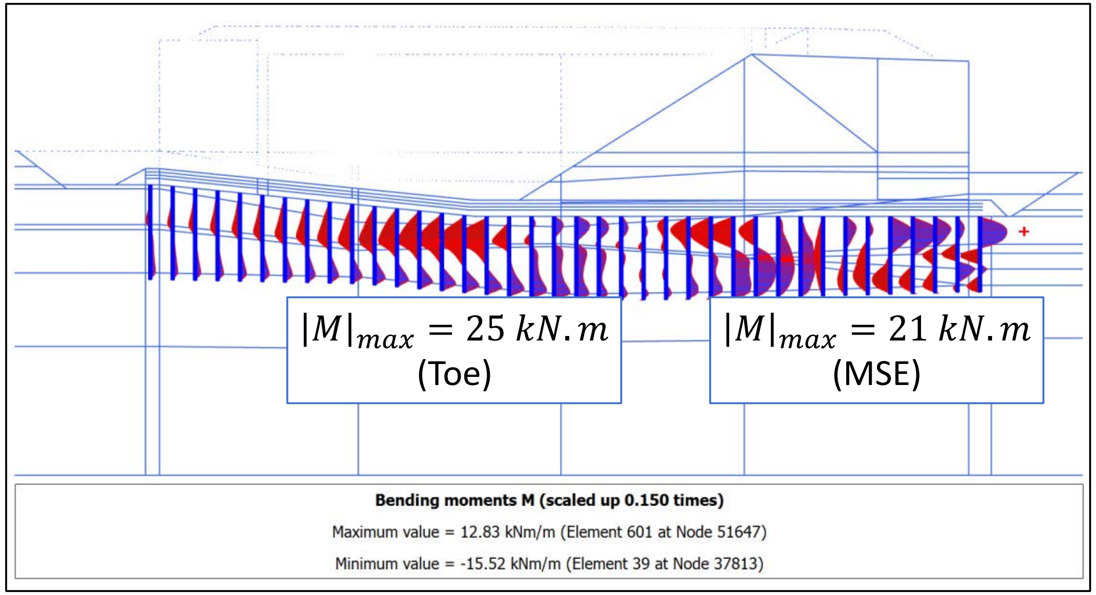

Design resistance to bending and axial force

EC2 - EN 1992-1-1:2004 §12: *Plain and lightly reinforced concrete structures*

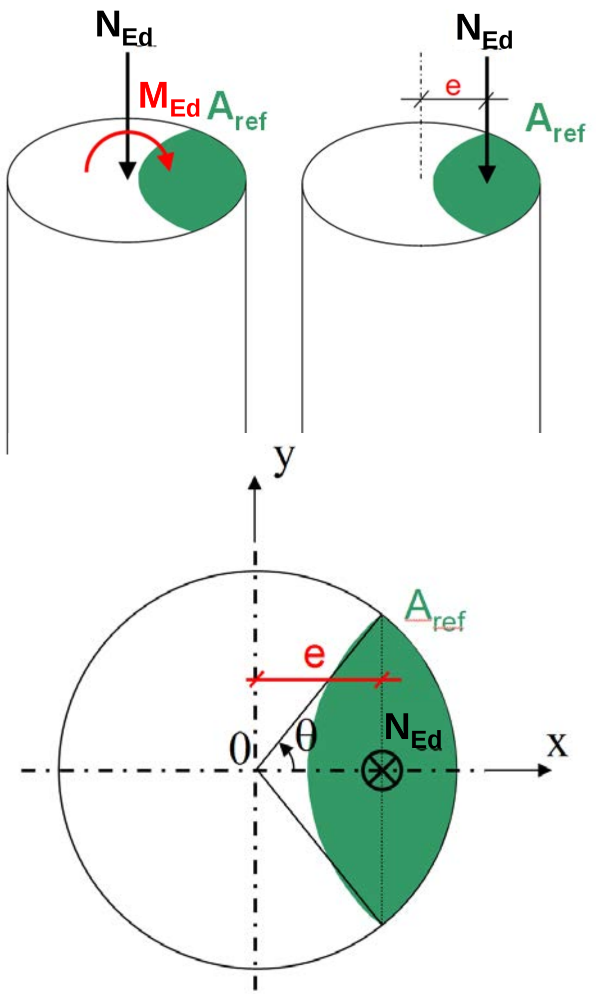

e : eccentricity of loading

$$A_{ref} = R^2.(2\theta - \sin 2\theta)$$

$$\theta = \arccos(e/R)$$

Design resistance to bending and axial force

$$N_{rd} = A_{ref} . f_{cd}$$

f_{cd}: ULS compressive strength

To accept ***unreinforced concrete***, we must check that :

$$N_{Ed} \leq N_{rd}$$

Design resistance to bending and axial force

$$N_{Ed} = \gamma_G N \leq N_{Rd} = f_{cd} A_{ref} = f_{cd}.R^2\left(2\,\mathrm{arccos}\left(\frac{e}{R}\right) - \sin\left(2\,arccos\left(\frac{e}{R}\right)\right)\right)$$

$$ie\ N \leq \frac{f_{cd}}{\gamma_G}.R^2\left(2\,\mathrm{arccos}\left(\frac{M/N}{R}\right) - \sin\left(2\,arccos\left(\frac{M/N}{R}\right)\right)\right)$$

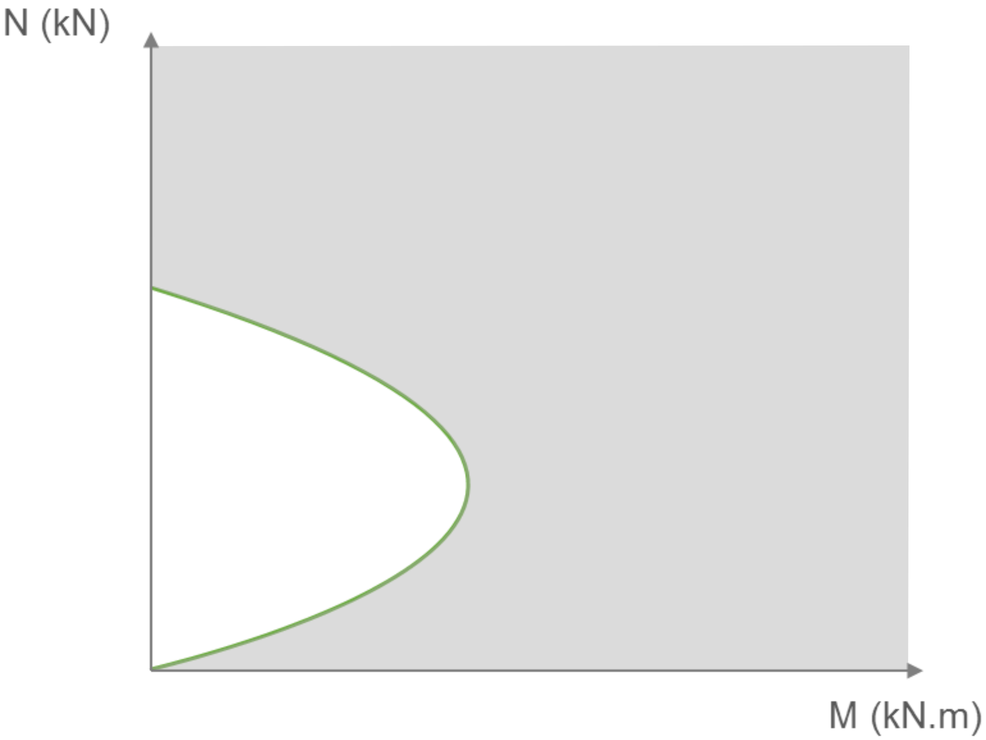

Note: f_{cd} = 10 MPa for UCS (28 days) = 20 MPa

Design resistance to bending and axial force

Final results for the proposed solution

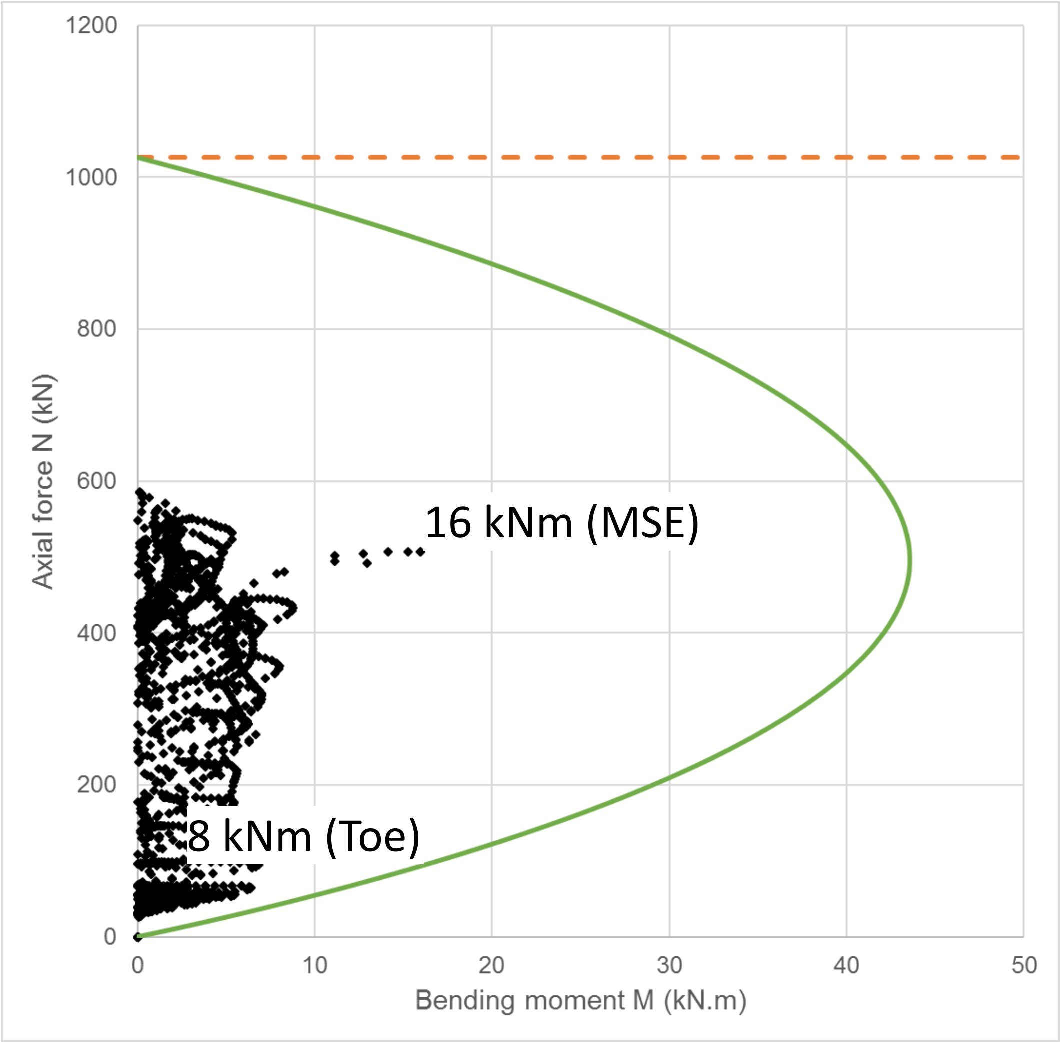

For information – WITHOUT steel meshes

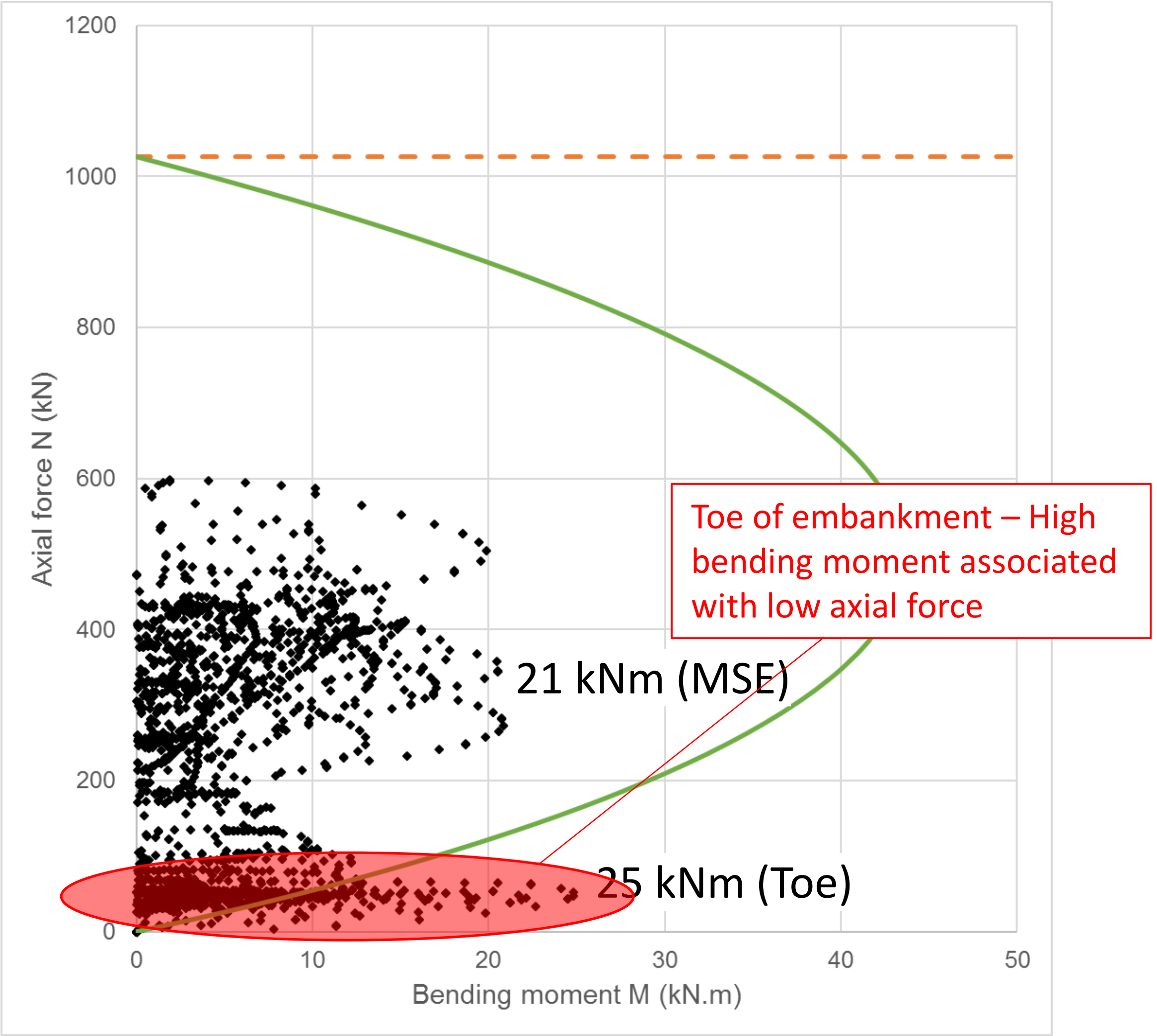

Presentation of the project

- Location
- Project description
- Technical specifications

Soil conditions

CMC Ground Reinforcement solution

Design principles

- Analytical approach - Global Bearing Capacity and Settlement
- Finite Element Modelling to fine-tune the design
- Specific verification due to high lateral loads

Execution and controls

Conclusions


GEOPAC
MSE Walls
Photographer position


750-18X
P403
GEOPAC


MSE Walls
Photographer position


MSE Walls
Photographer position

Static Isolated Load Tests

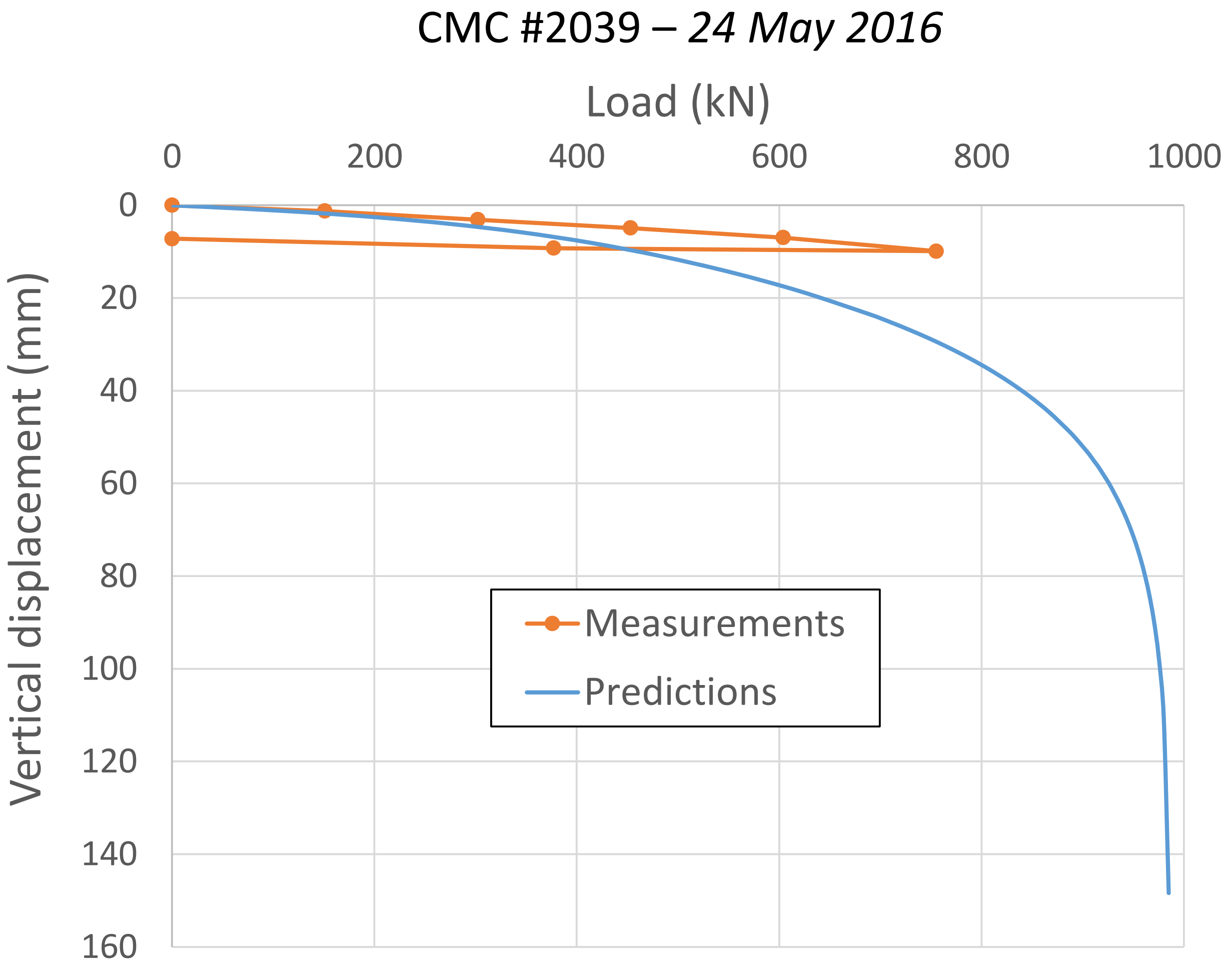

Dynamic Isolated Load Tests

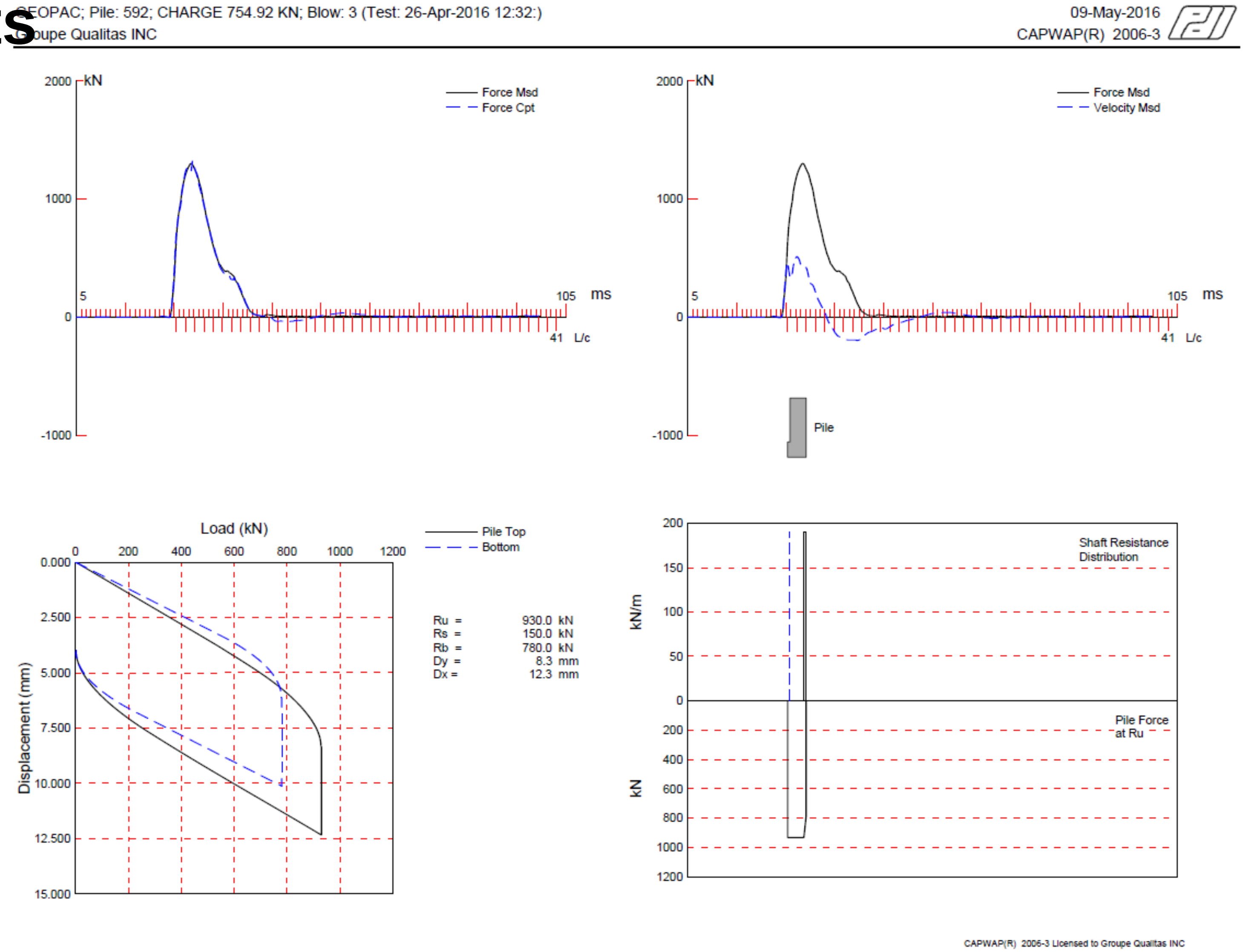

By way of anecdote

Archeological remains of several old tanneries found during Working Platform preparation !

Conclusions

- CMC Rigid inclusions was proved to be a **competitive alternative to the "dig-out and replace" base solution** on the Turcot project for this section.

- Generally speaking, CMC rigid inclusions solutions are based on an **advanced design** that takes into account the **soil capacity**. The **ASIRI** guideline (edited in 2012 & 2013) gives an excellent overview of the design philosophy. Local standards may be used in addition to set the required level of partial safety factors on actions, materials and resistance.

- CMC may be subjected in some situations to **high lateral loads** (toe of embankment, seismic conditions, wind areas). CMC integrity must be then checked carefully. **Steel reinforcement (cages, rebars) is sometimes required**.

- **Several tests are necessary to control the construction of CMC rigid inclusions**: UCS tests on concrete, reflection or impedance tests, static and dynamic isolated tests.

Before (Aerial structure)

After (MSE Wall + bridge)

Thank you for your attention

Basal Reinforced Piled Embankments: how to decide, how to design?

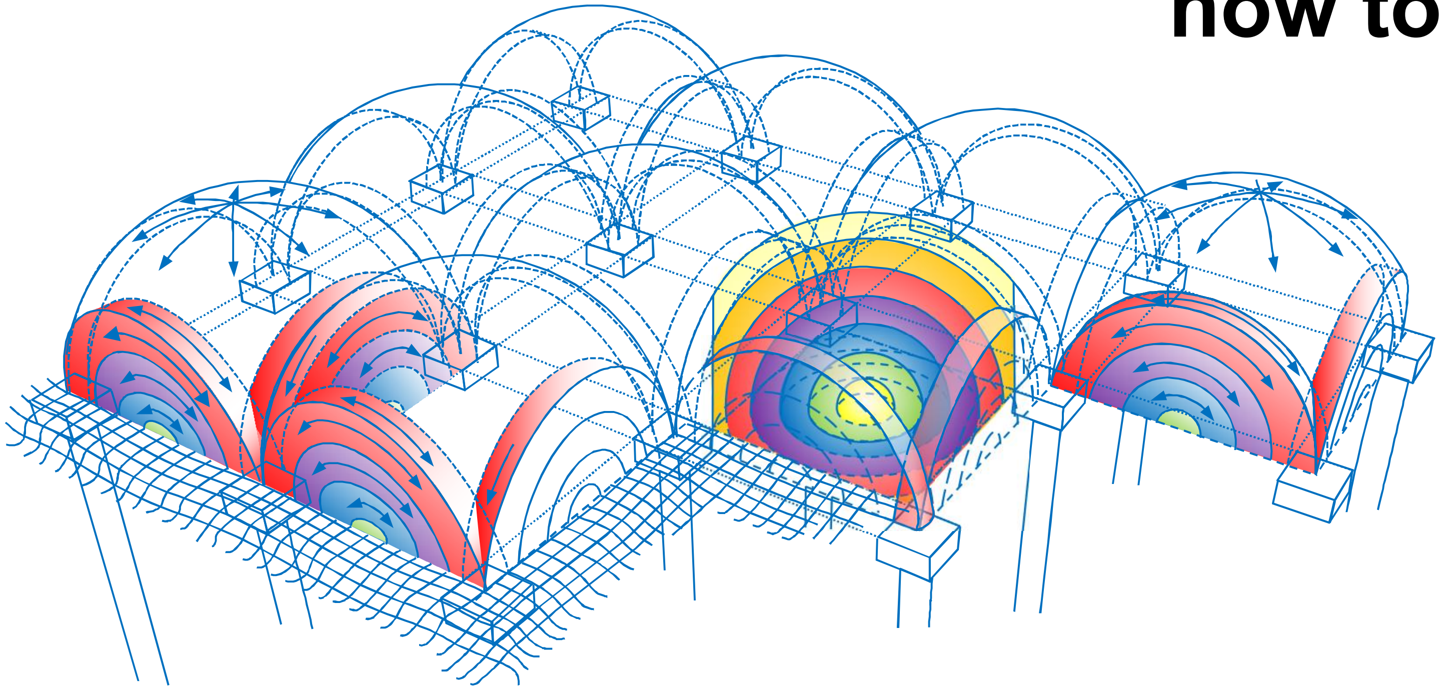

Arjan A.M. Venmans

Suzanne J.M. van Eekelen

Deltares, The Netherlands
arjan.venmans@deltares.nl
suzanne.vaneekelen@deltares.nl

Basal Reinforced Piled Embankments

- How to decide?
- How to design?

Arjan Venmans

Suzanne van Eekelen

What is a (Basal Reinforced) Piled Embankment?

GR = geosynthetic reinforcement

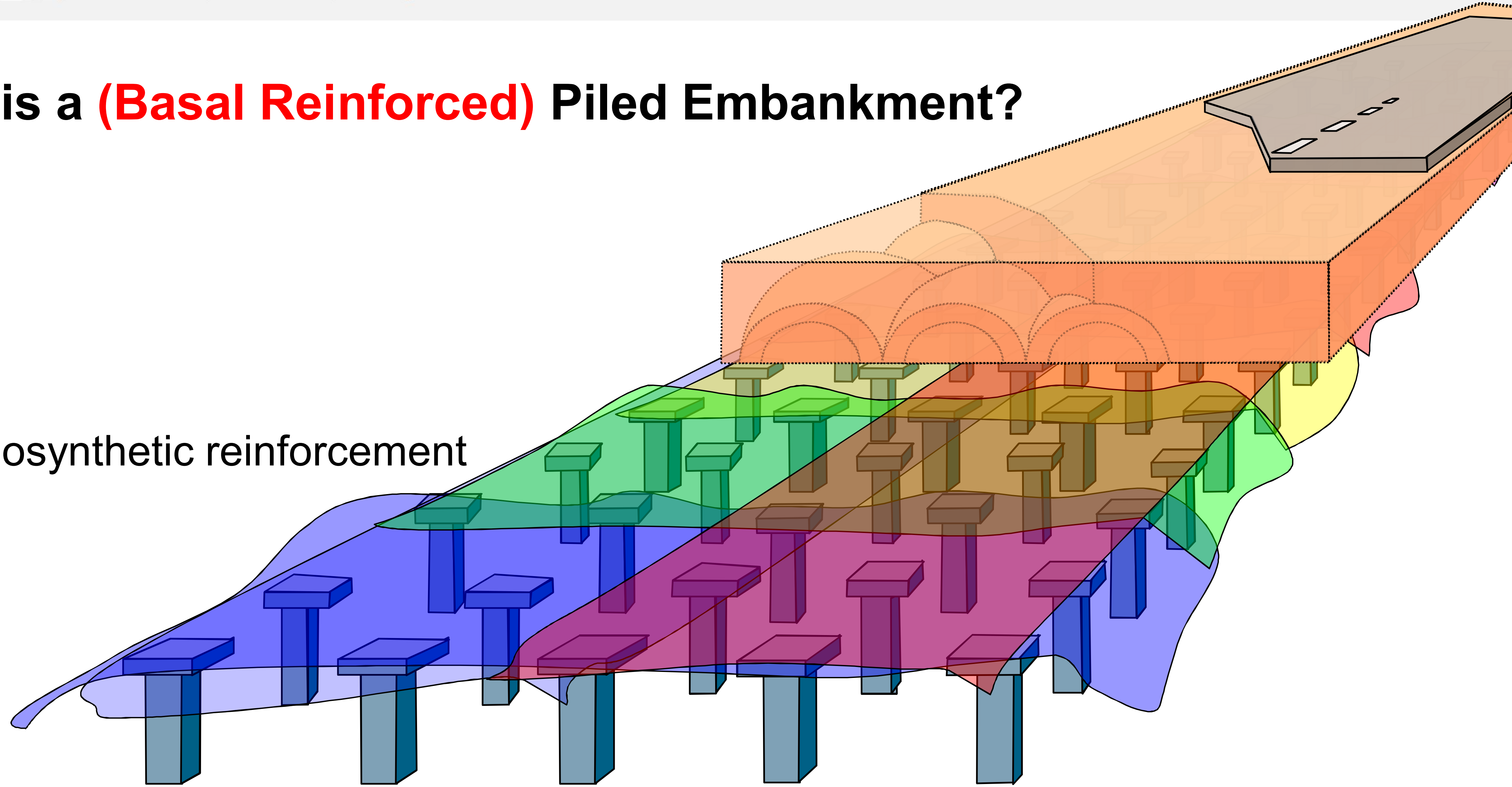

How to decide?

Piled embankment or not?

Often based on assumptions

Two cases, two rational criteria:

Case 1 + 2: Whole life costs

Case 2: Life cycle analysis

Case 1 Bridge approach zones (a) Whole life costs

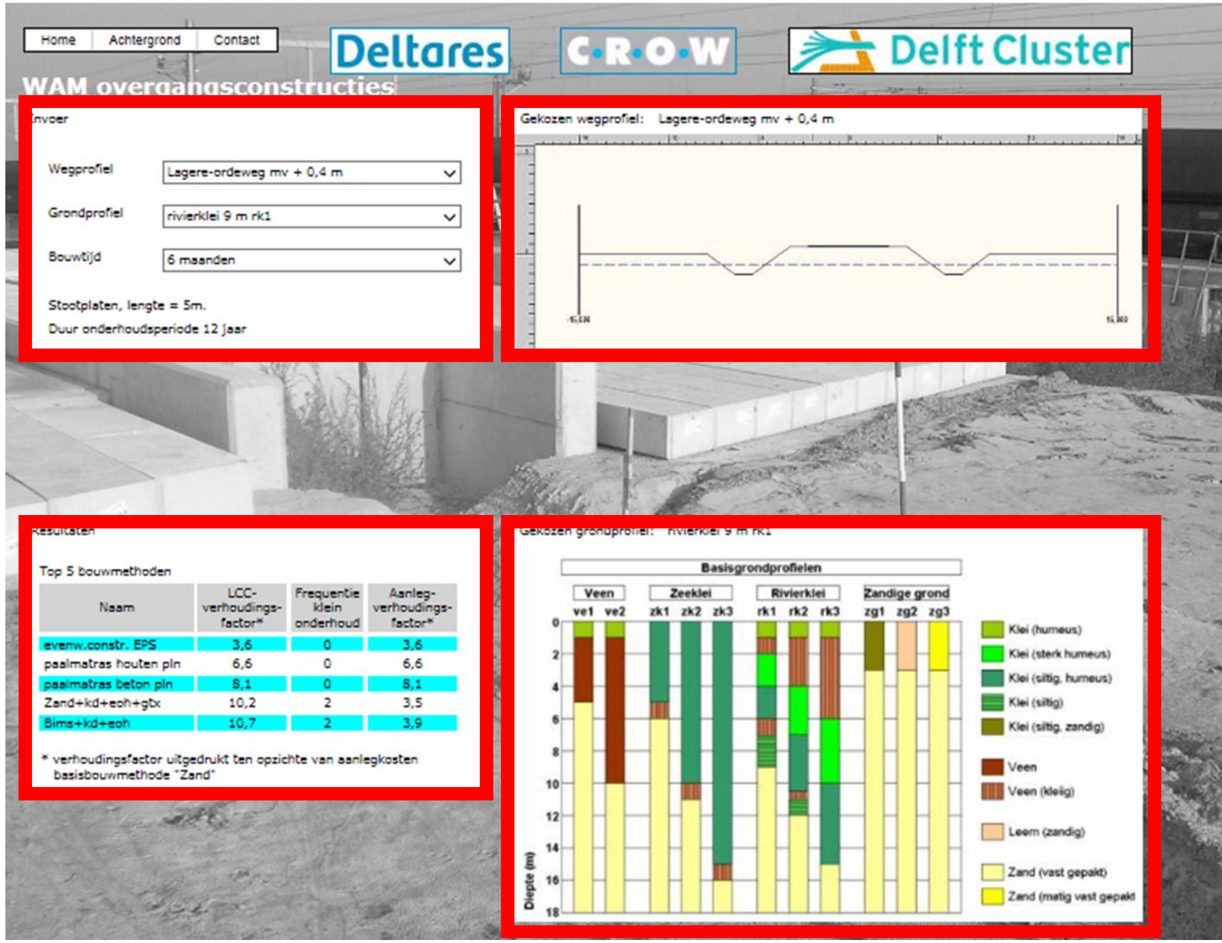

http://dtvirt57.deltares.nl/applications/intraweb/dminiroad/dminiroad.dll

Case 1 Bridge approach zones (a) Whole life costs

slope ≥ 1:100 → maintenance

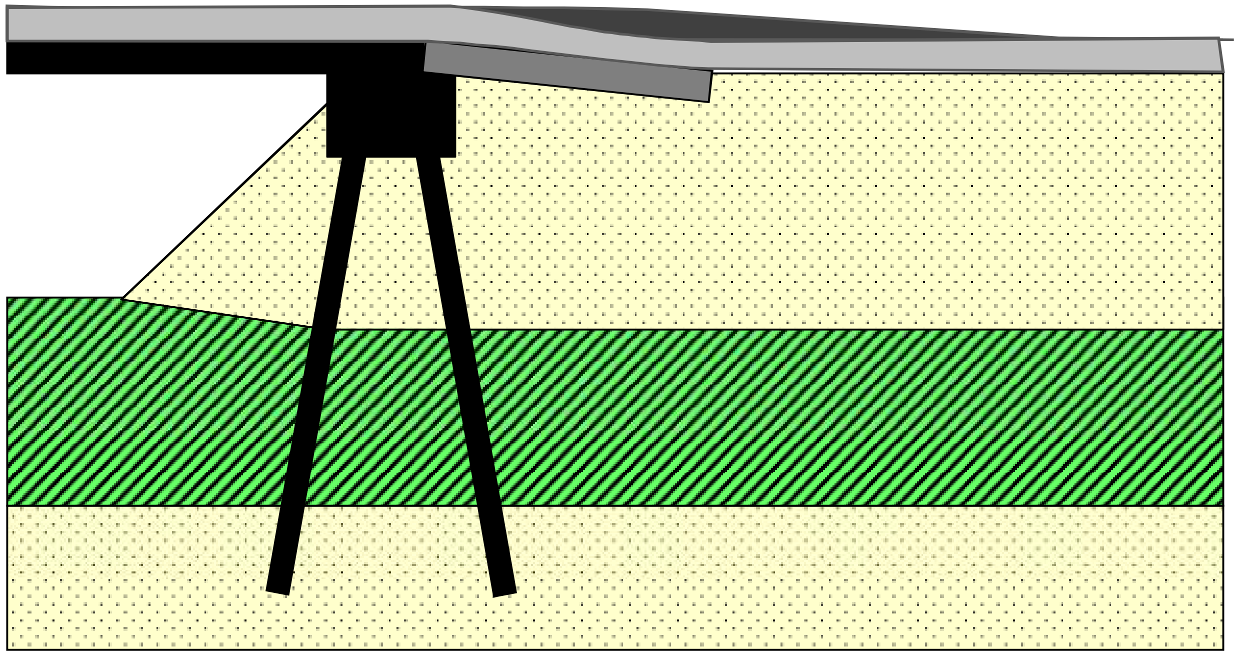

Dense sand

Silty clay

Organic silty clay

Very organic clay

Clayey peat

Peat

Organic clay

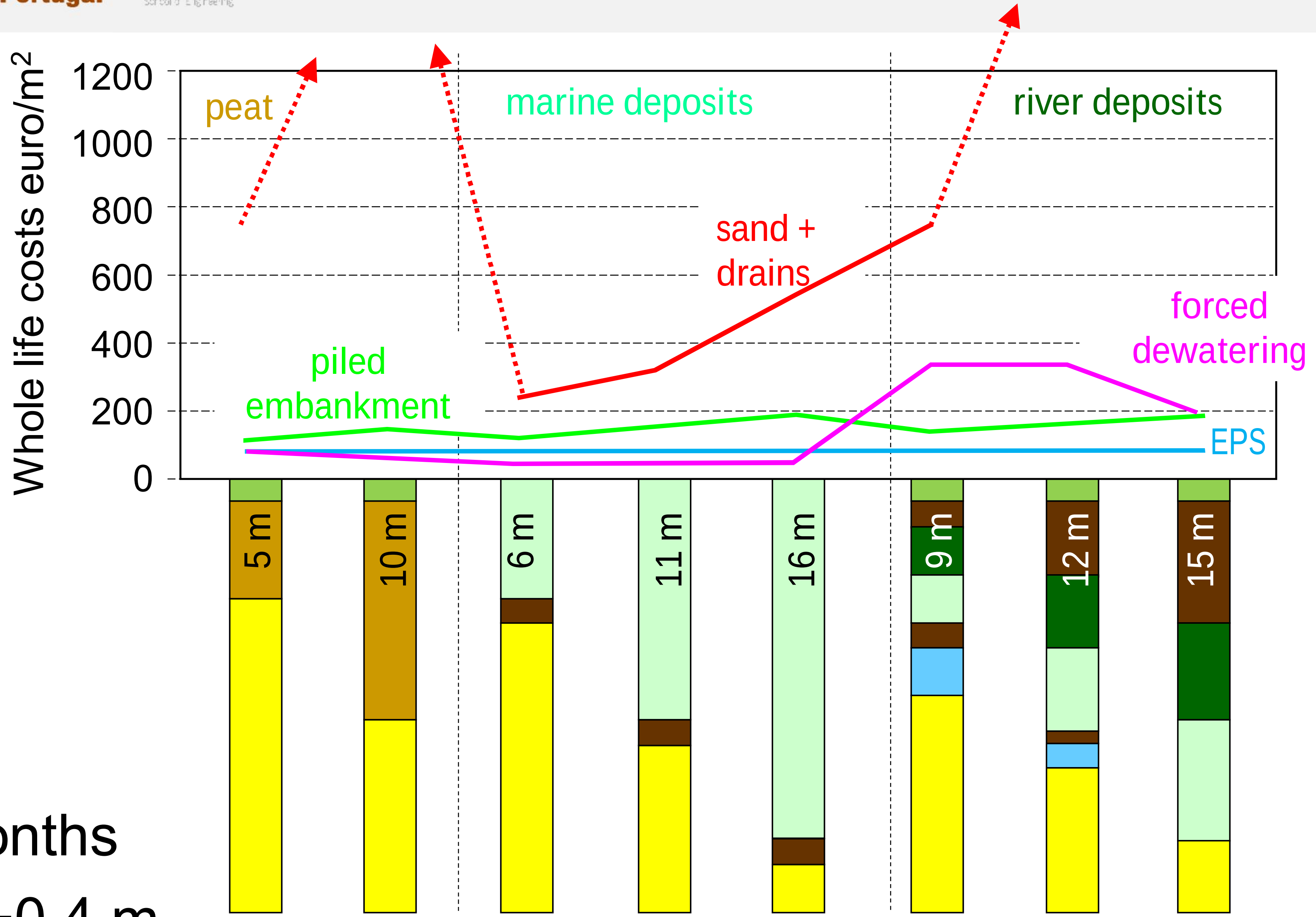

Construction time 6 months

Low volume road, GL +0.4 m

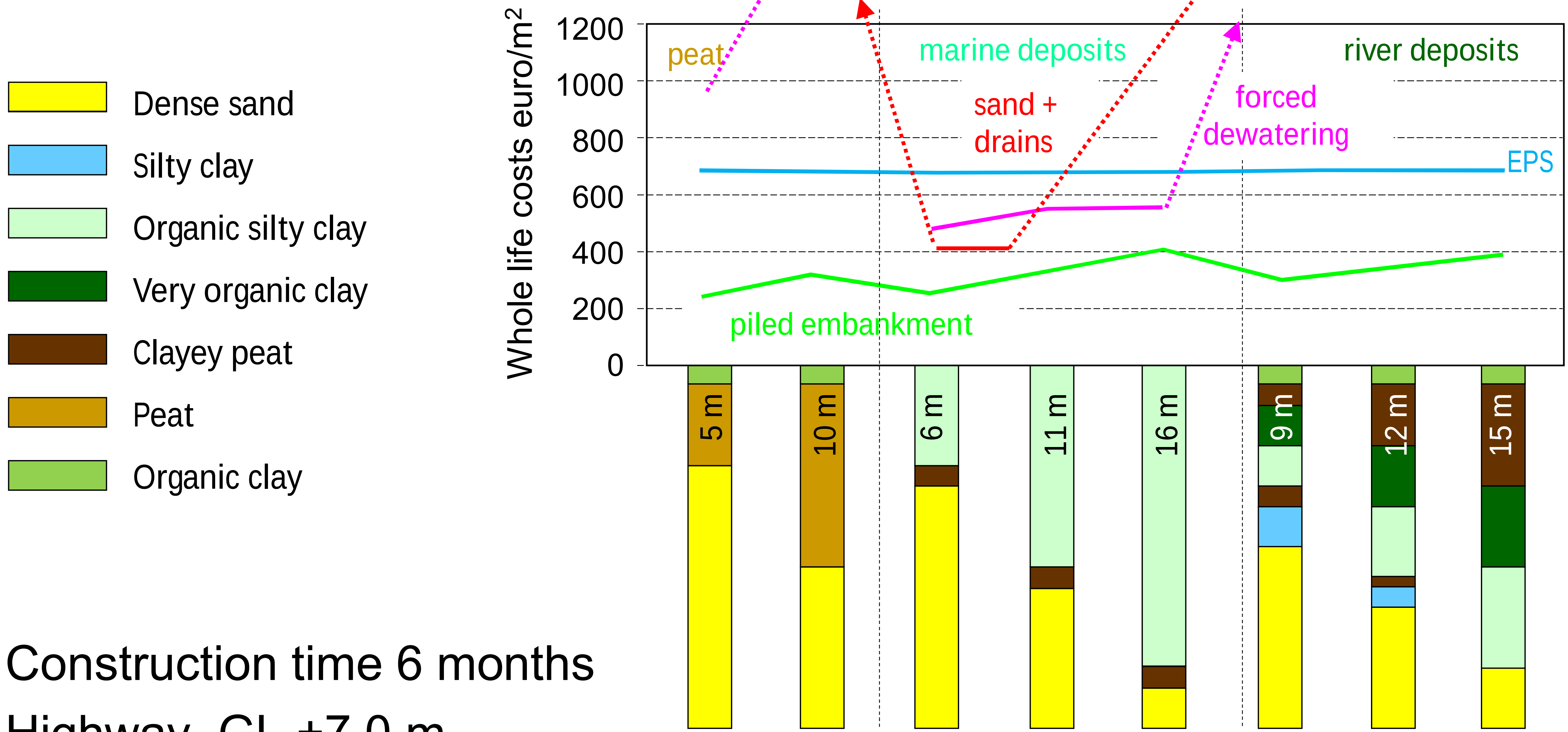

Construction time 6 months

Highway, GL +7.0 m

Case 2 Kamerik local road (a) Whole life costs + (b) Life cycle analysis

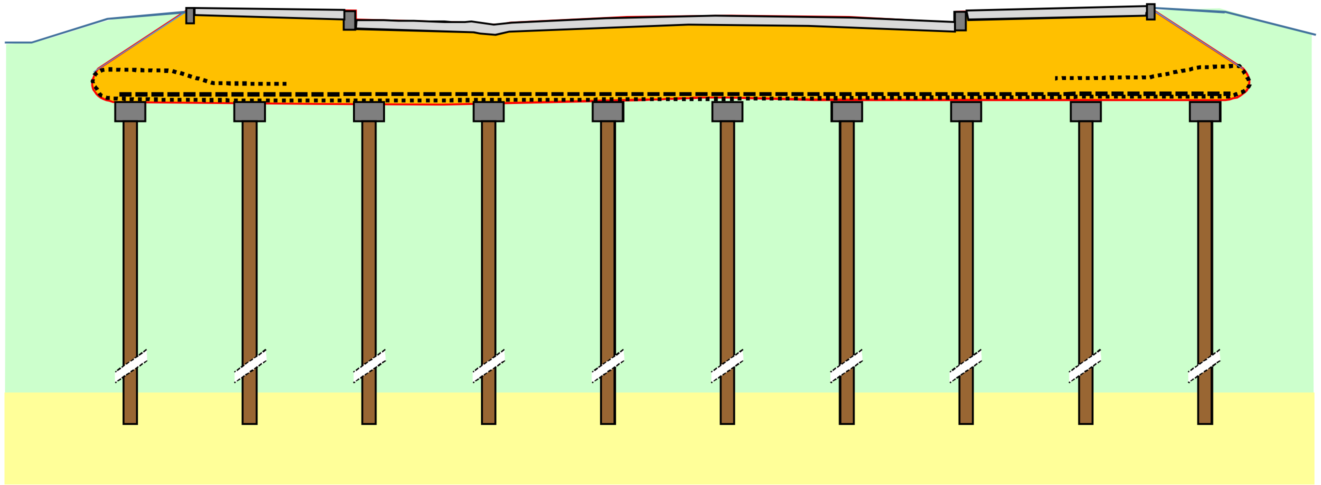

Case 2 Kamerik local road (a) Whole life costs + (b) Life cycle analysis

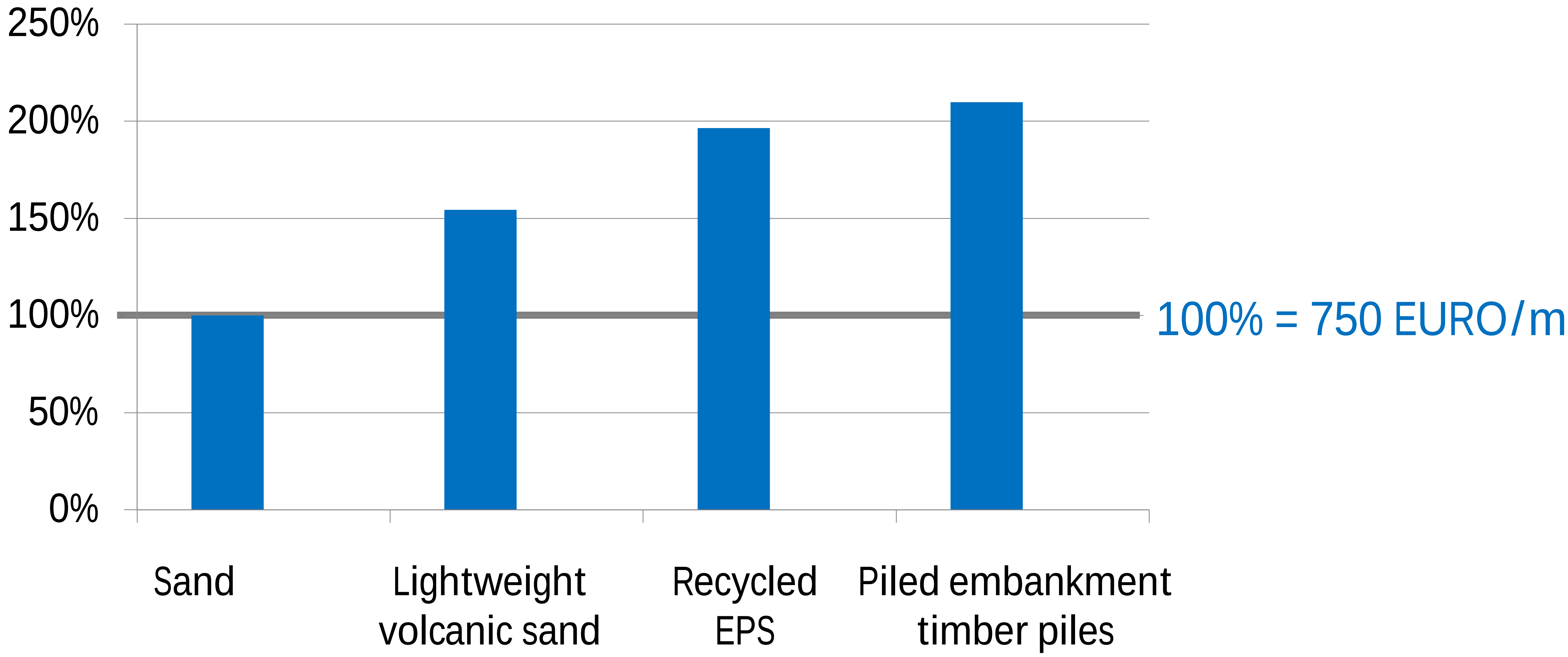

Case 2 Kamerik local road (a) Whole life costs + (b) Life cycle analysis

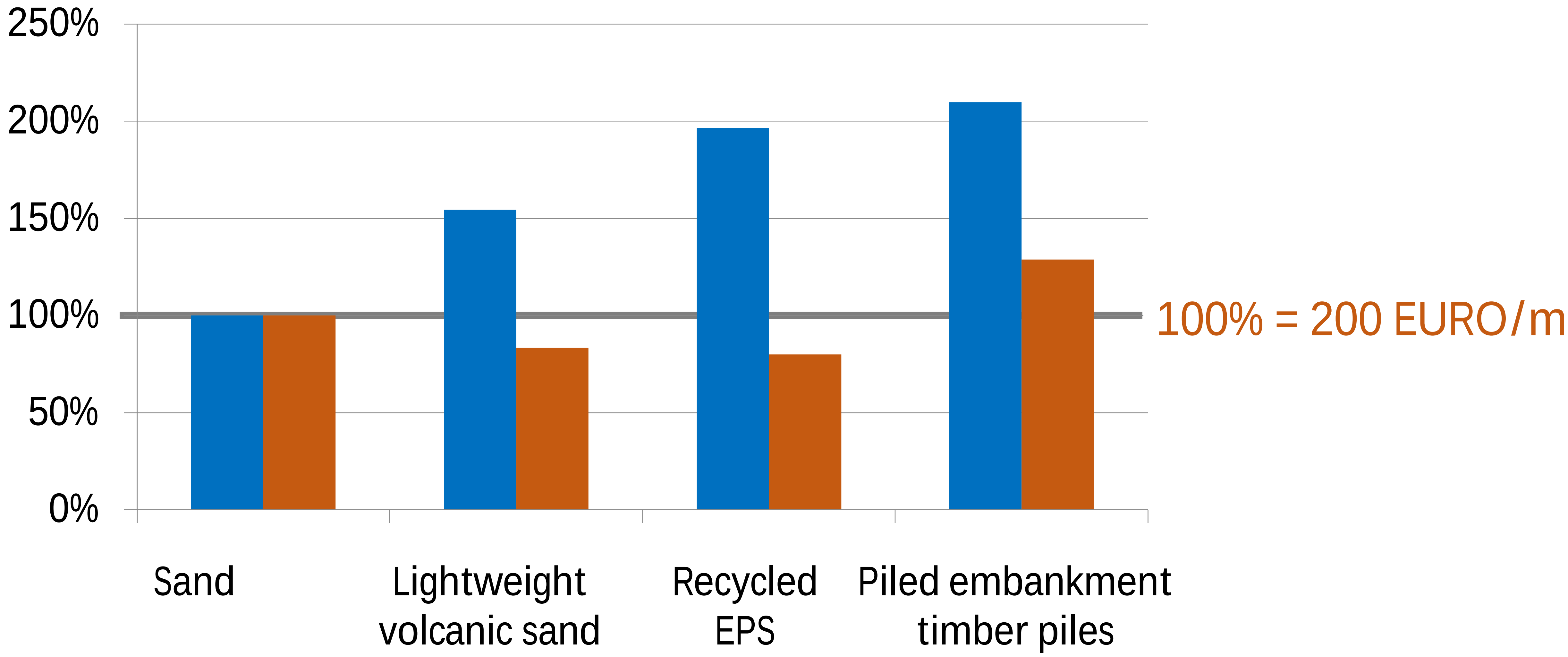

Lessons learned

(a) whole life costs of piled embankments

Case 1: interesting for:

- Short construction time
- High embankment
- High soil compressibility

Case 2: not interesting for:

- Reconstruction of existing embankment

Lessons learned

(b) Case 2: Life cycle analysis

- Timber piles **>>** concrete piles
- Sand fill **>>** crushed concrete fill

Suzanne van Eekelen

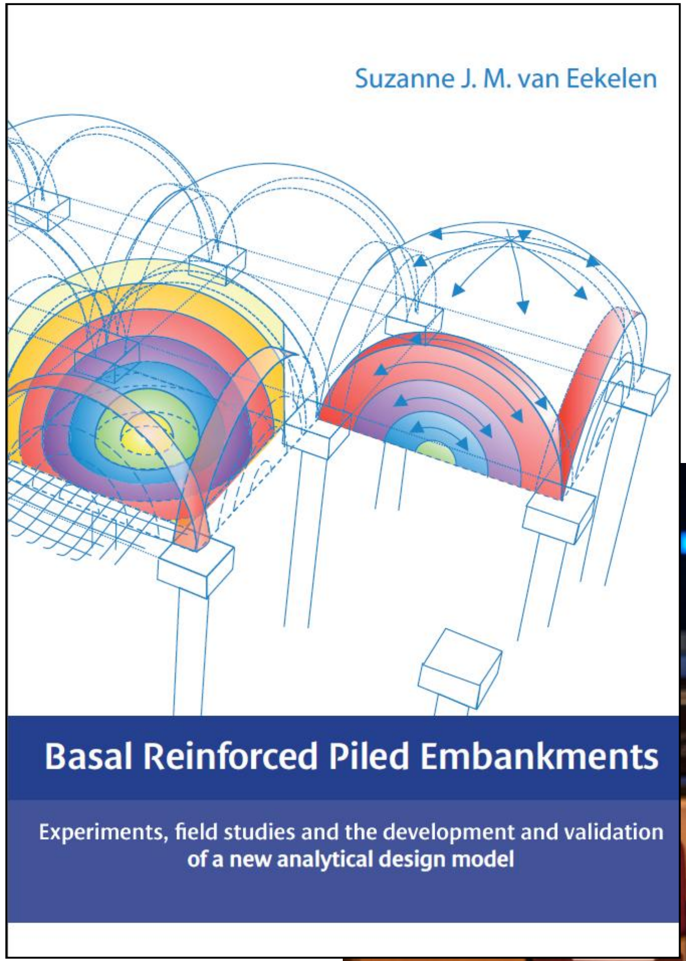

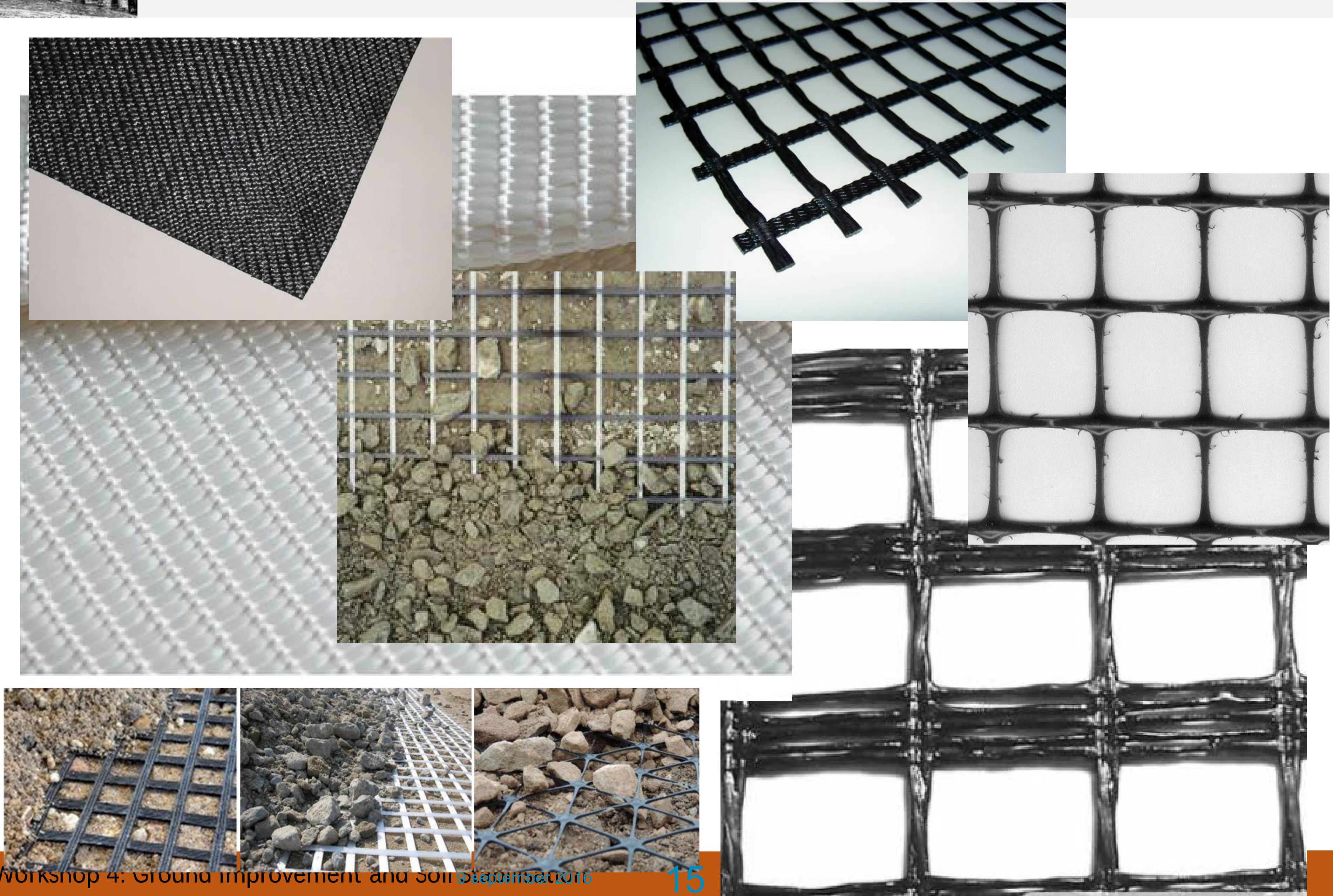

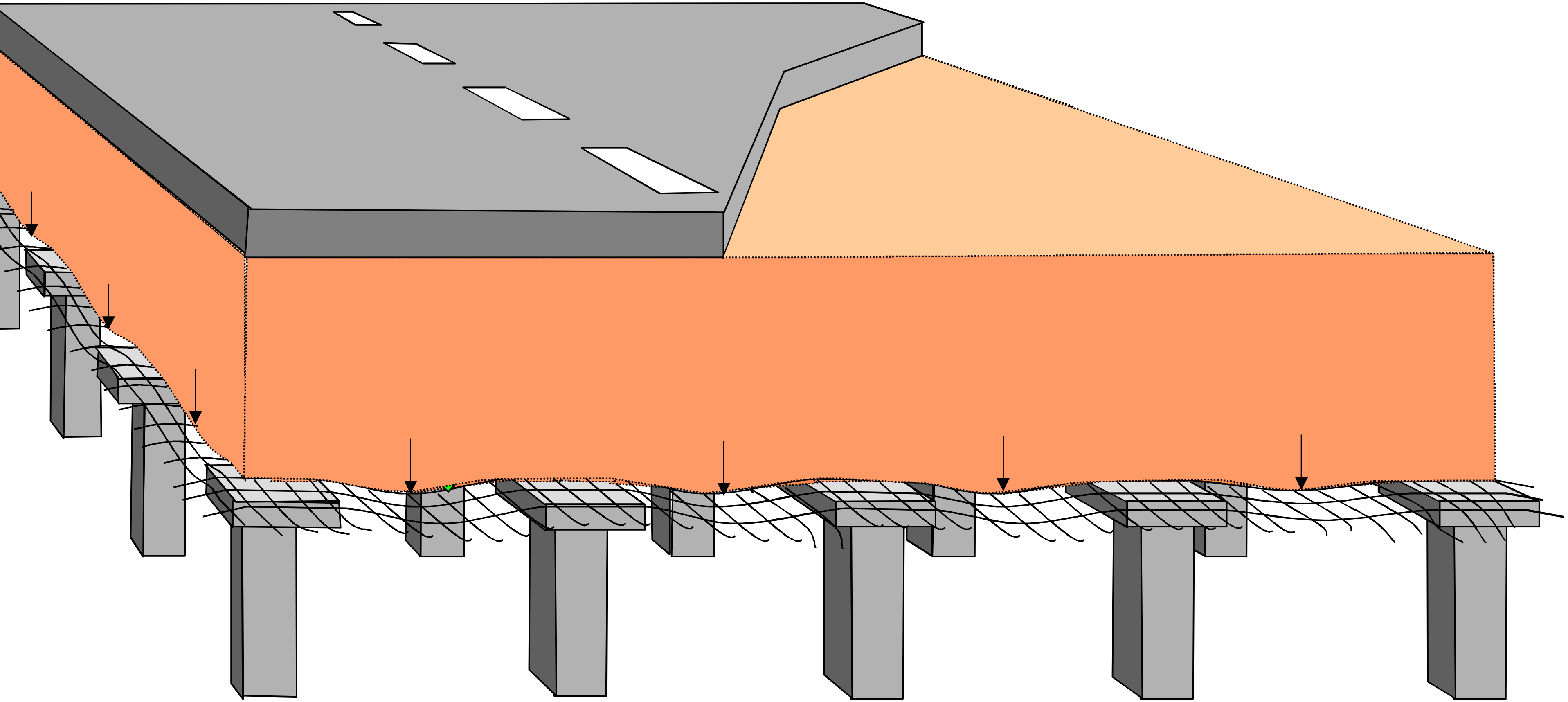

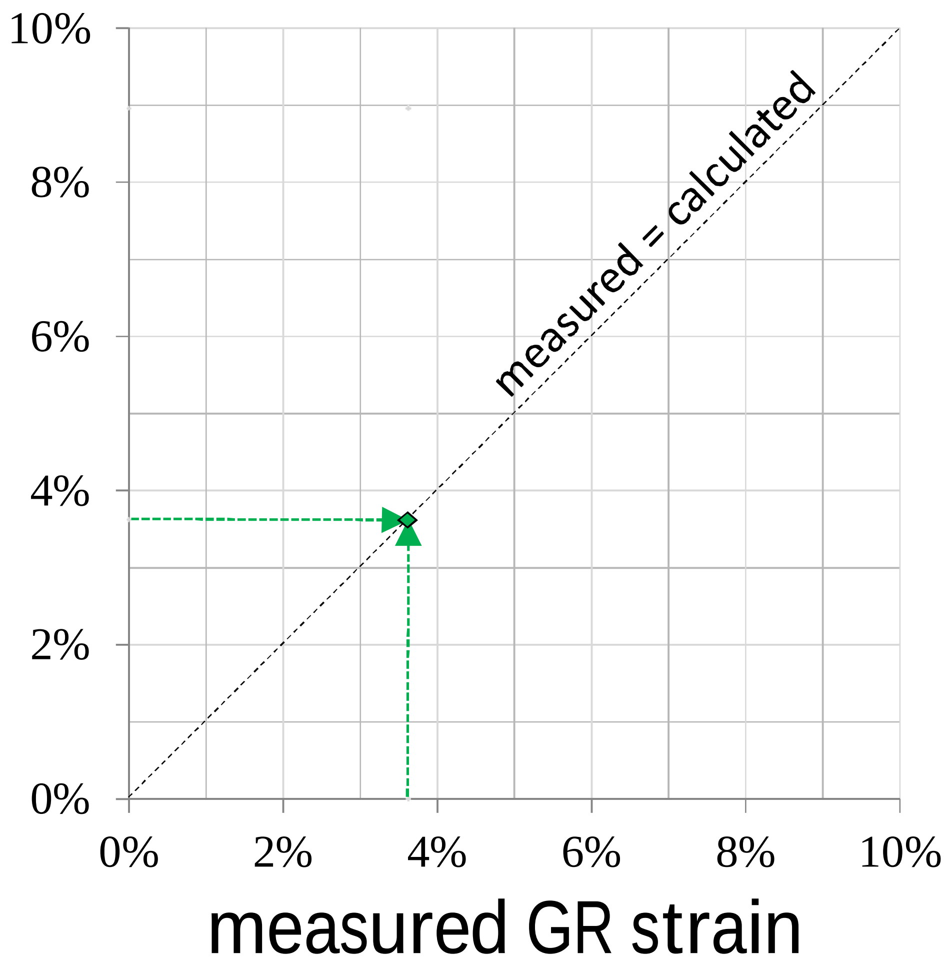
10%
8%
6%
4%
2%
0%
0%
2%
4%
6%
8%
10%
measured = calculated
measured GR strain

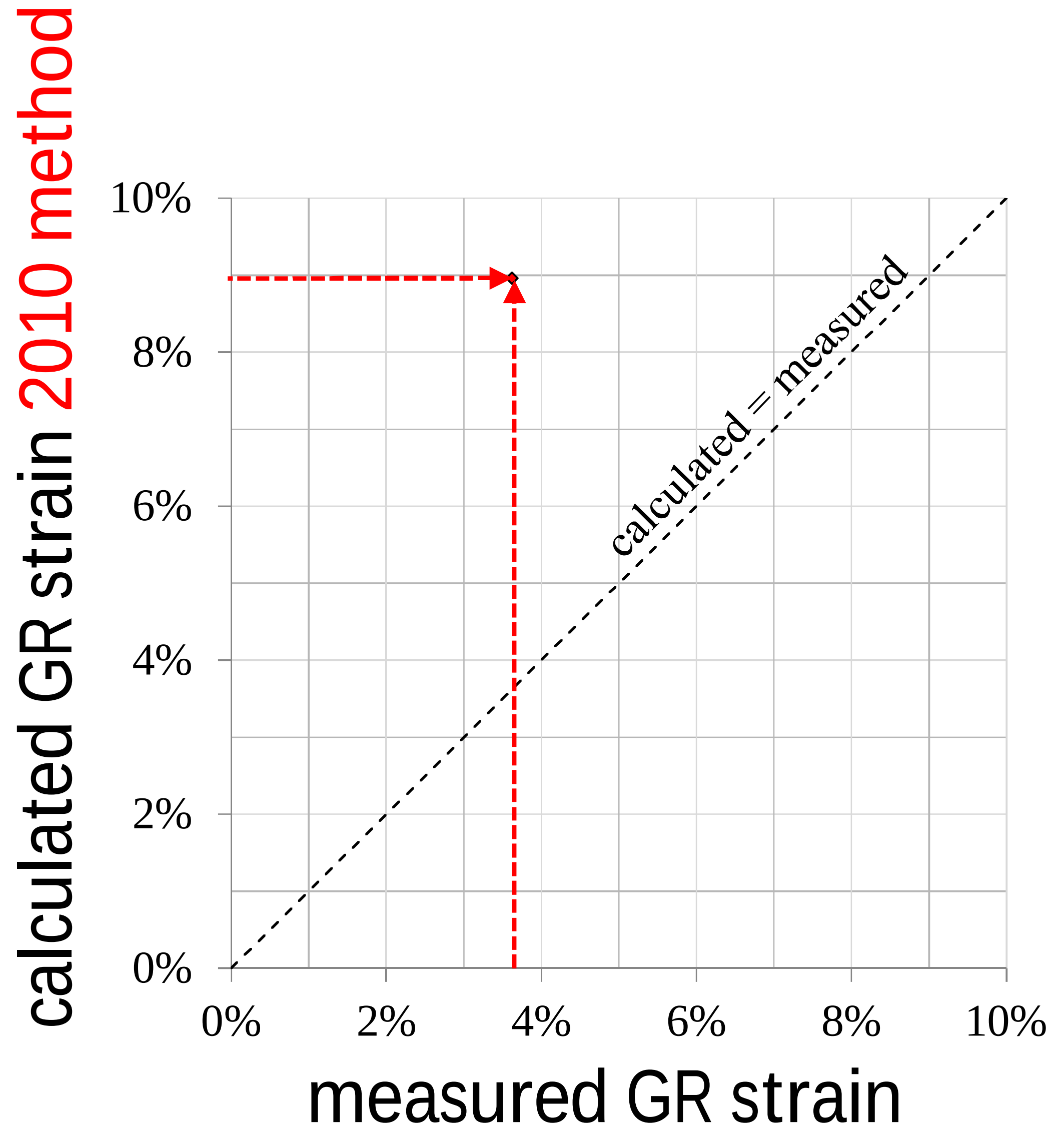

2010 method **(Zaeske 2001, adopted in the German EBGEO and the Dutch CUR226 (2010)**

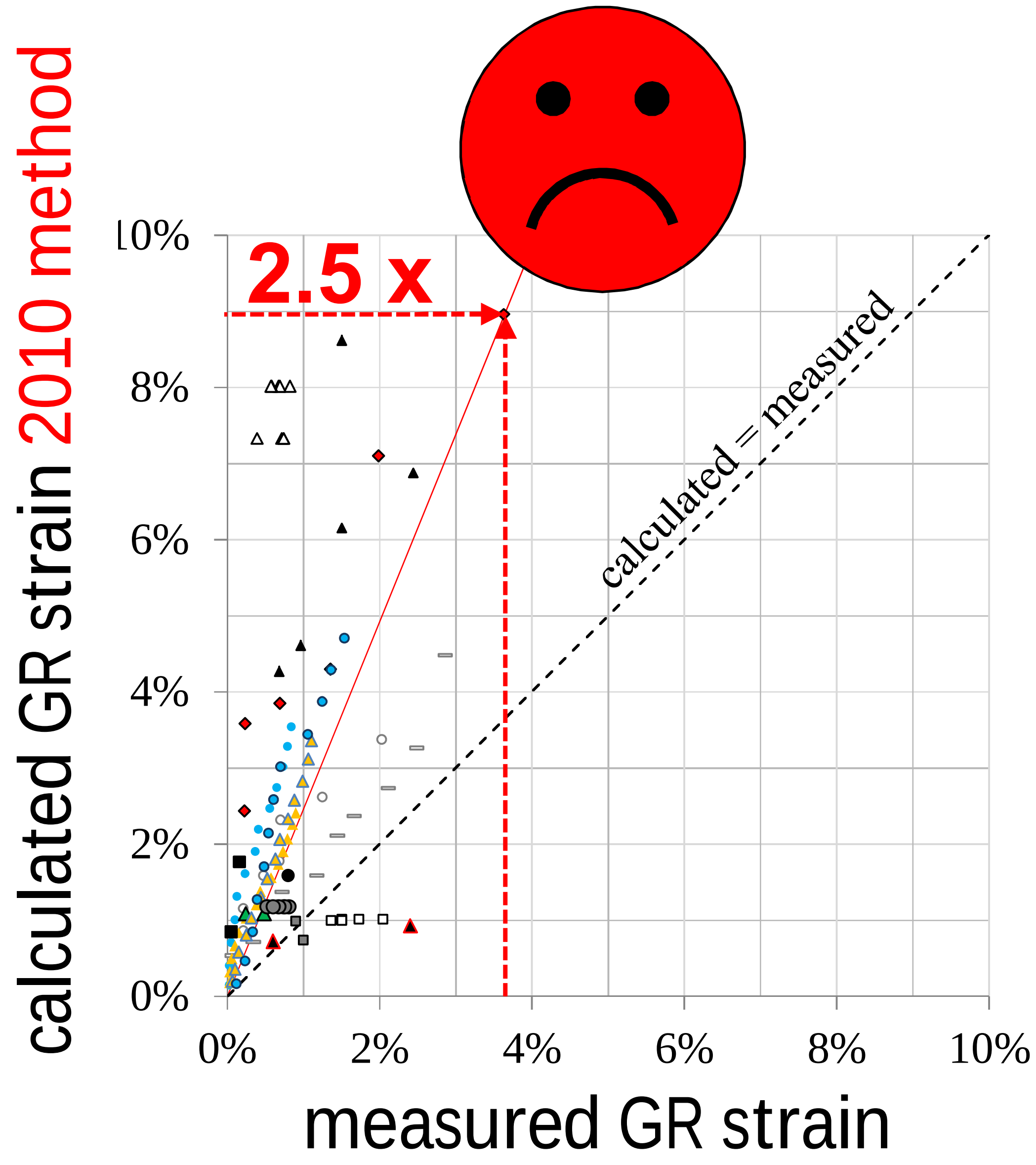

Measurements in field tests and series of experiments taken from:

Zaeske 2001, Germany
Van Duijnen et al 2010, Netherlands
Huang et al 2009, Finland
Oh and Shin 2007, Korea
Haring et al, 2008, N210, Netherlands
Weihrauch 2013, Hamburg, Germany
Vollmert et al 2007, Bremerhafen, Germany.
Almeida et al 2007, Rio de Janeiro, Brazil
Briancon and Simon 2012, France
Van Eekelen et al 2012a, Netherlands
Van Eekelen et al 2012b, Woerden, Netherlands

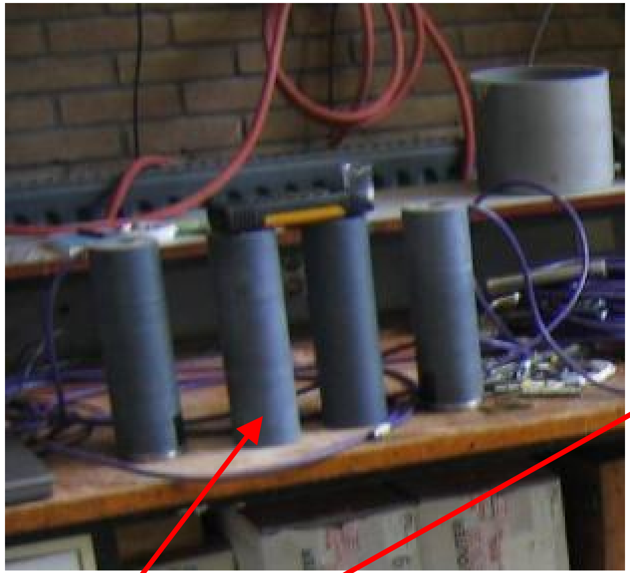

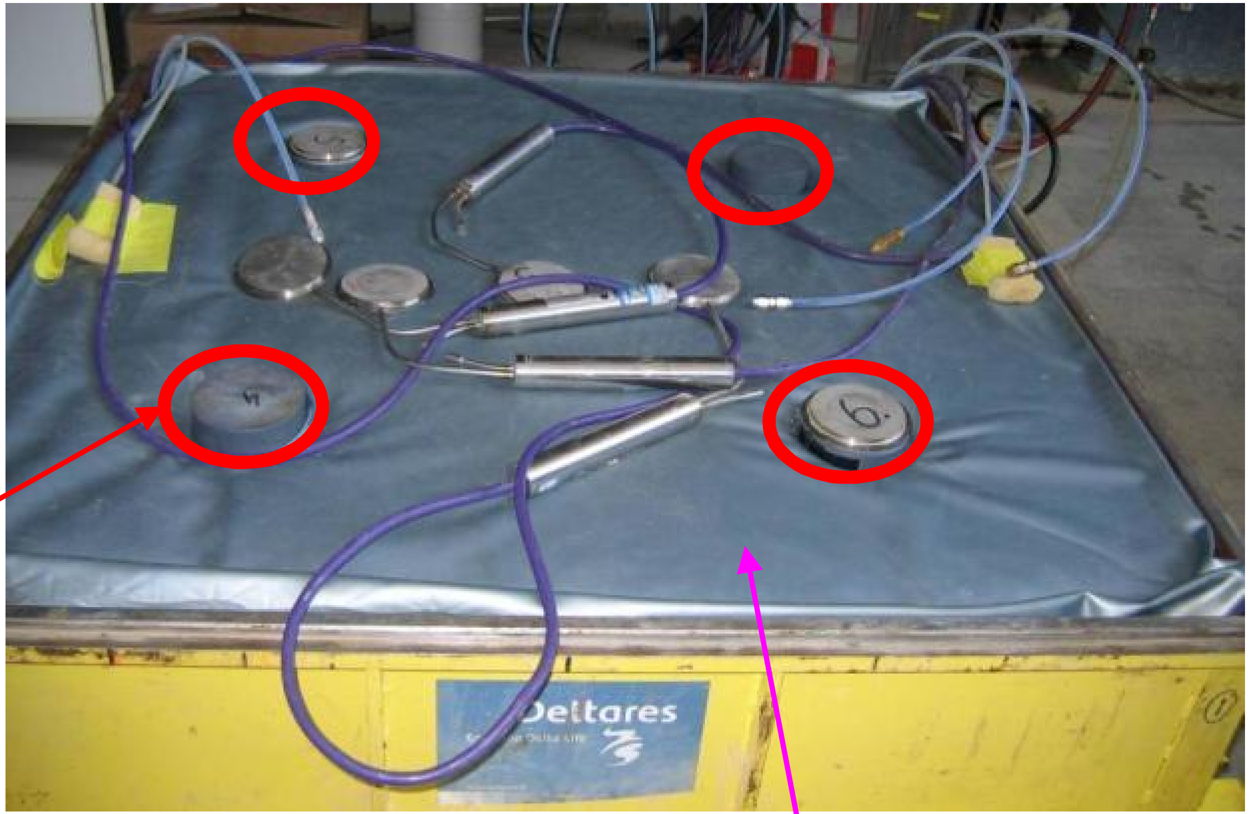

piles

"soft soil"

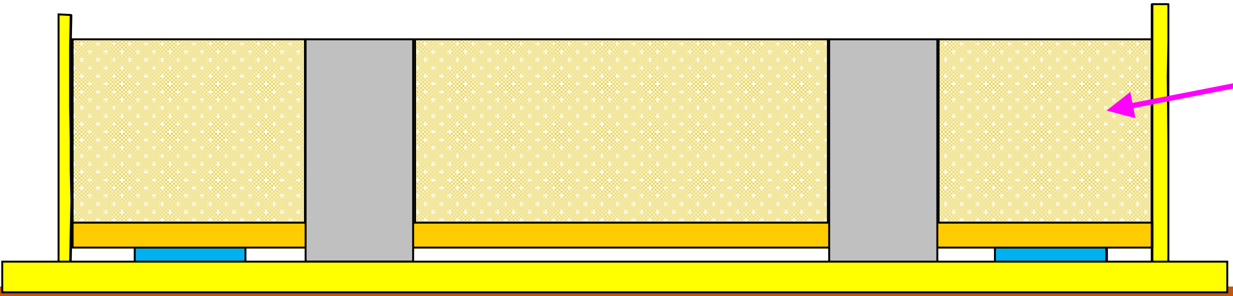

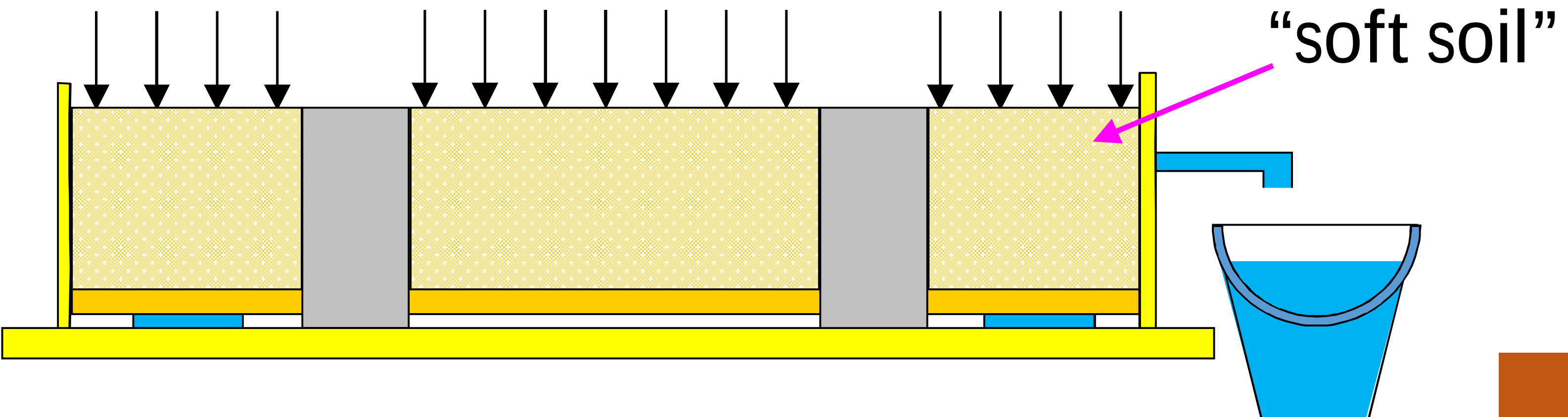
“soft soil”

Geosynthetic reinforcement

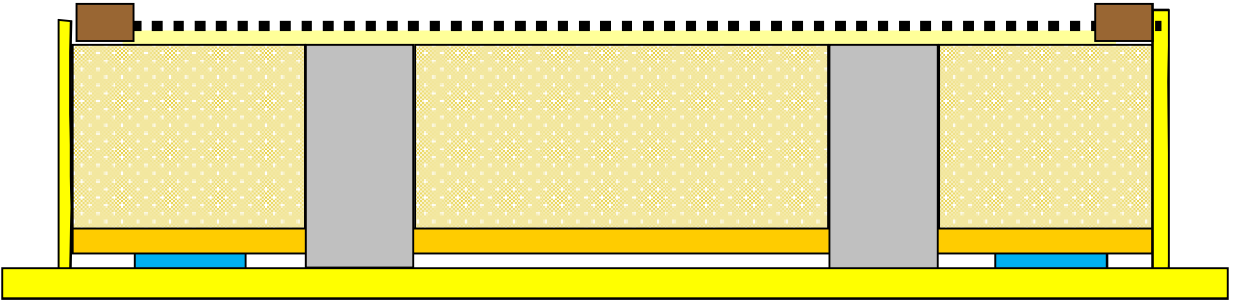

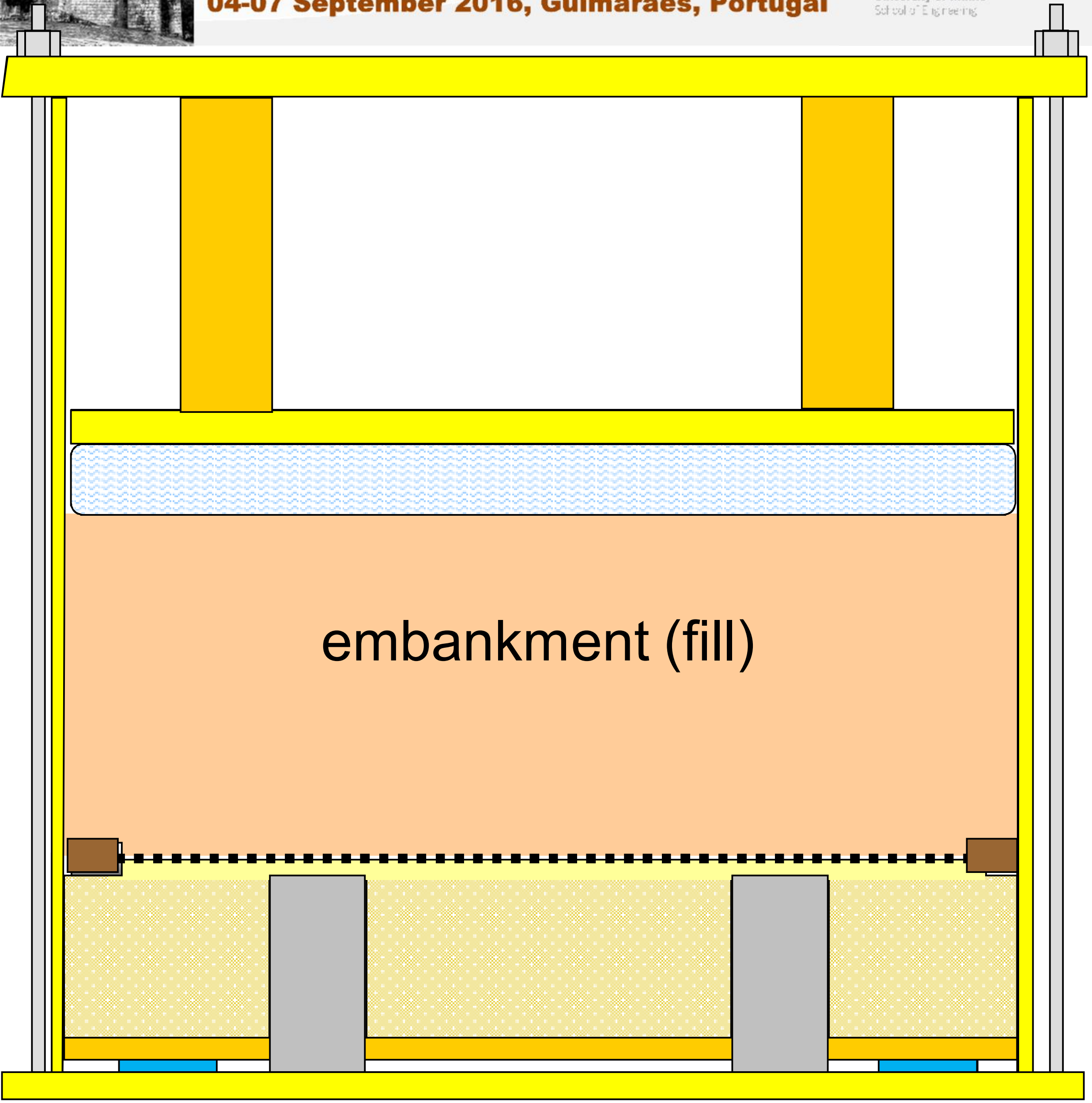
embankment (fill)

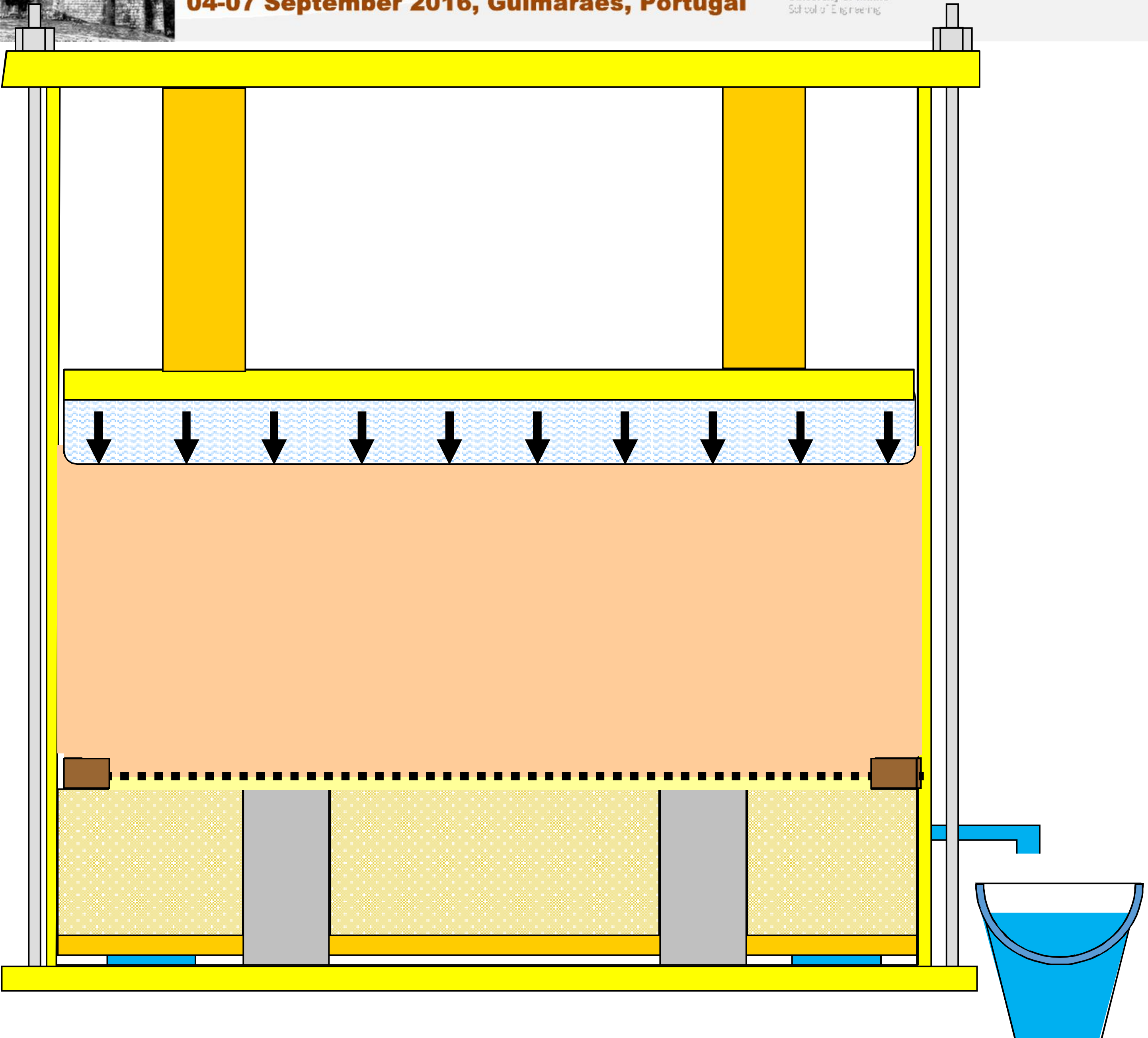

Load → step 1 arching → load part A

step 1 arching → "residual" → step 2 → strain

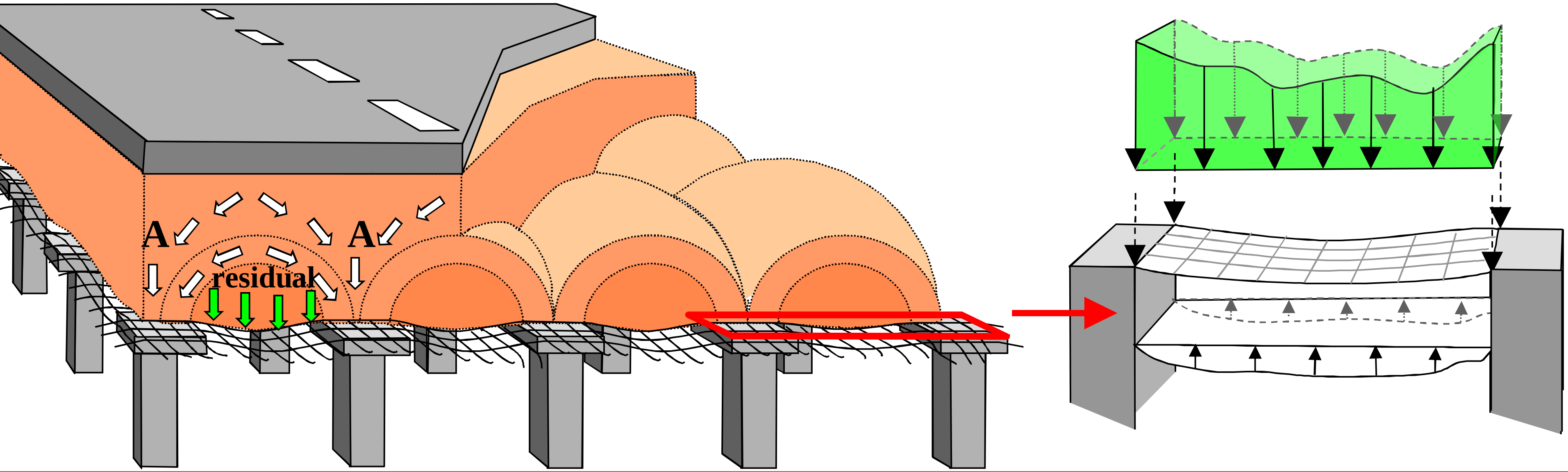

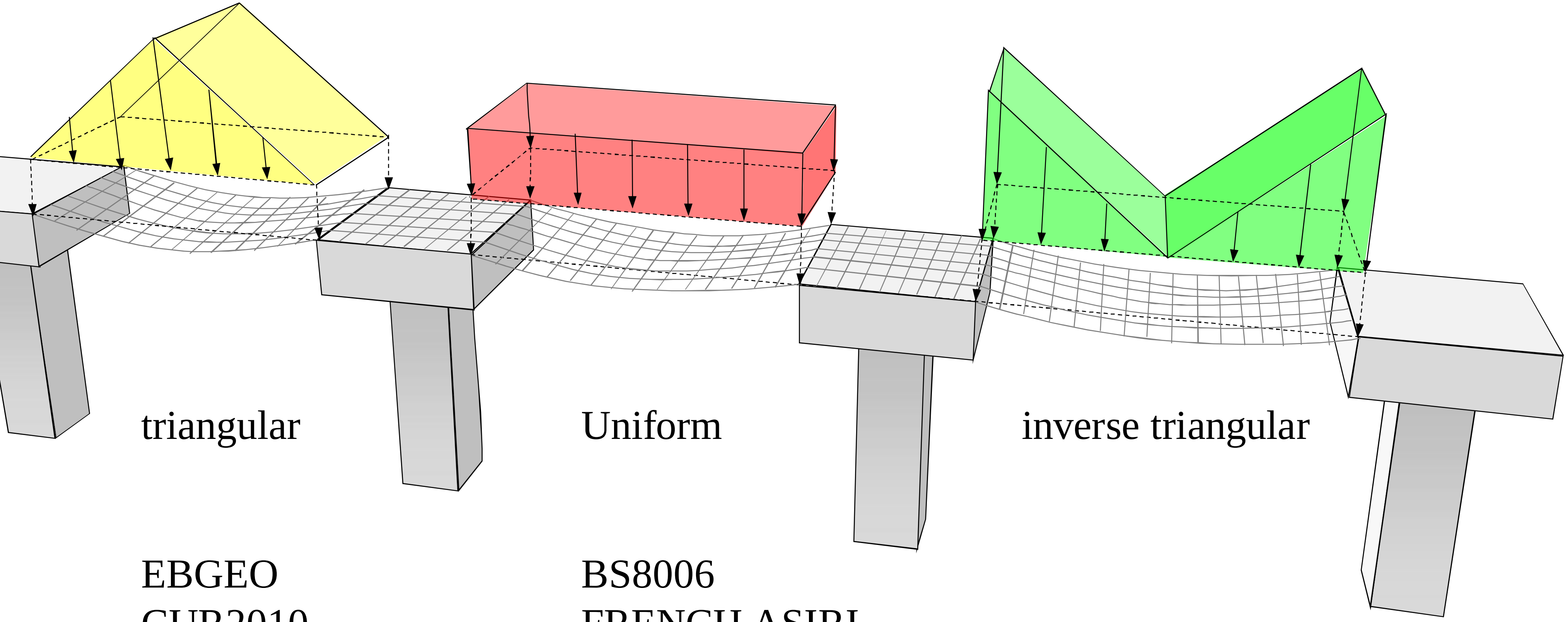

EBGEO
CUR2010

BS8006
FRENCH ASIRI

Observed load distribution (simplified for this presentation):

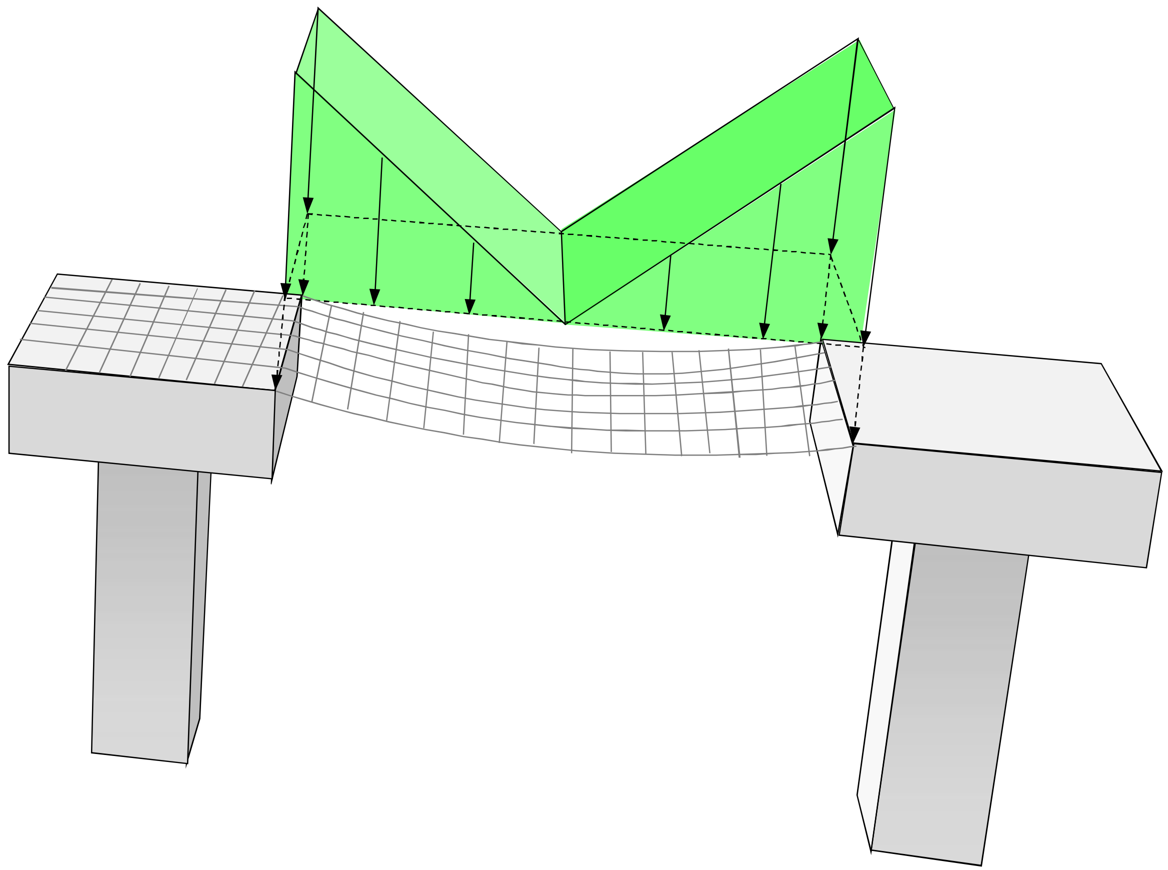

More precise (van Eekelen et al., 2015):

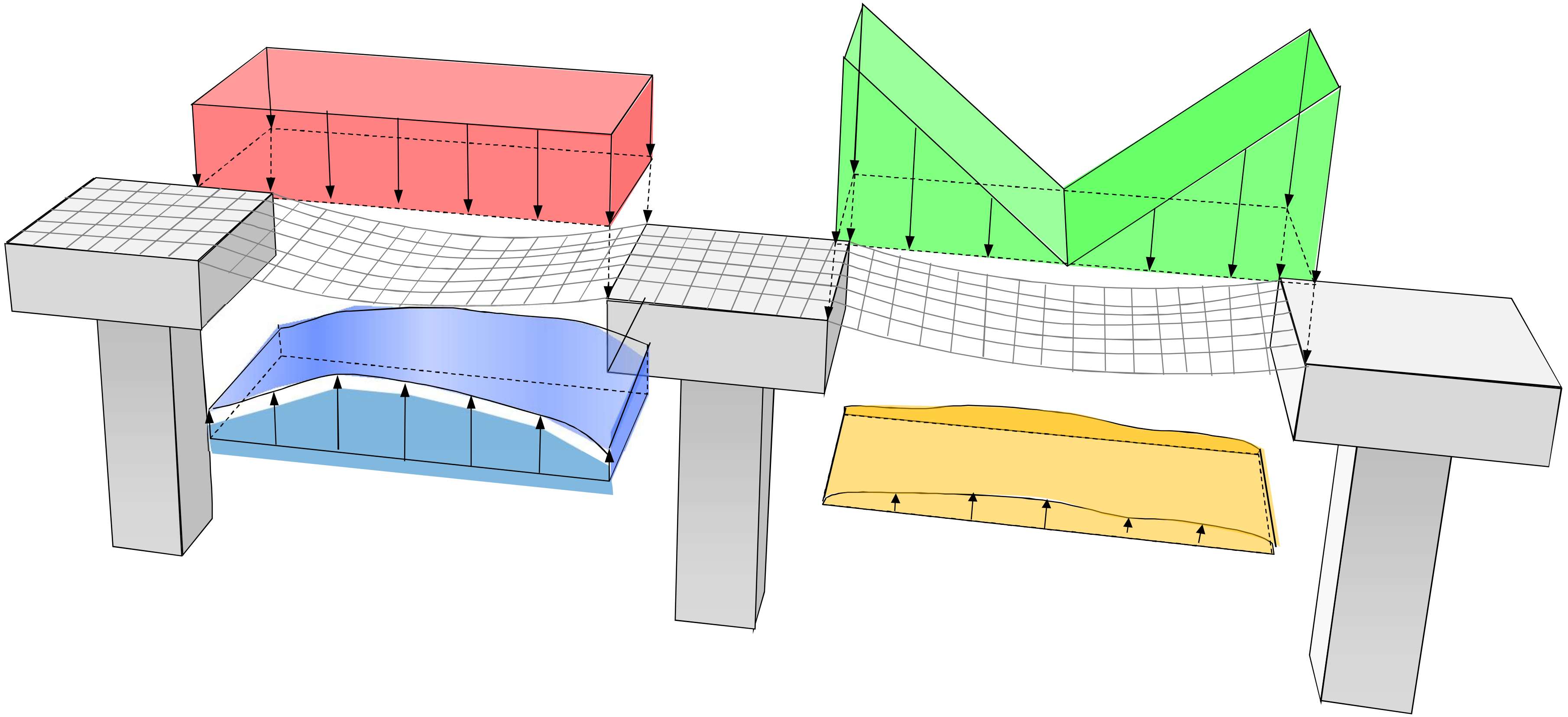

Load → step 1 arching → load part A / "residual" → step 2 → strain

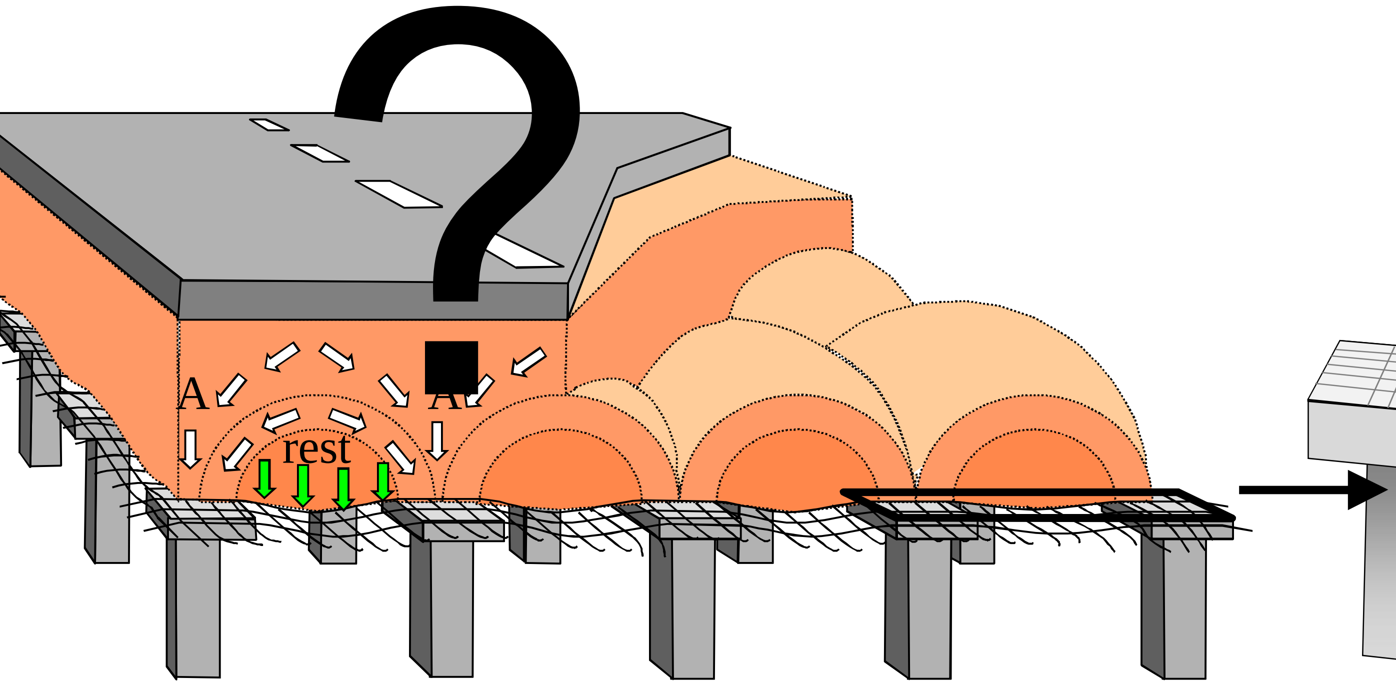

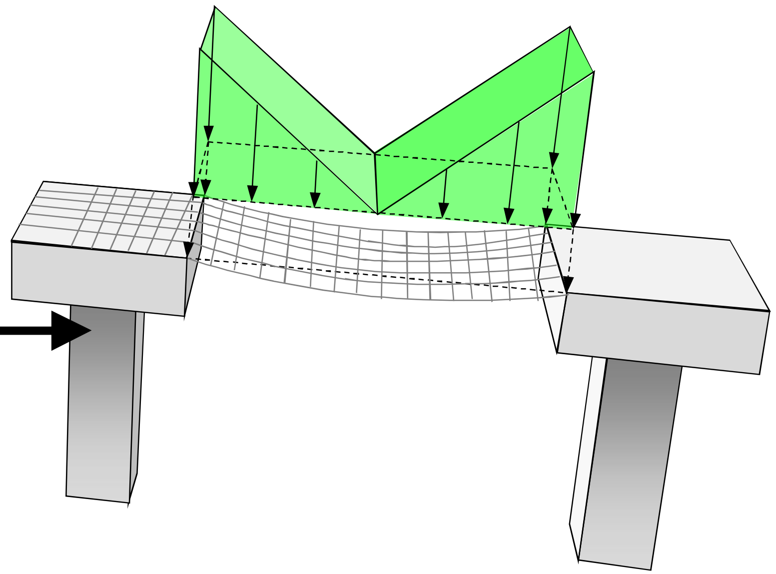

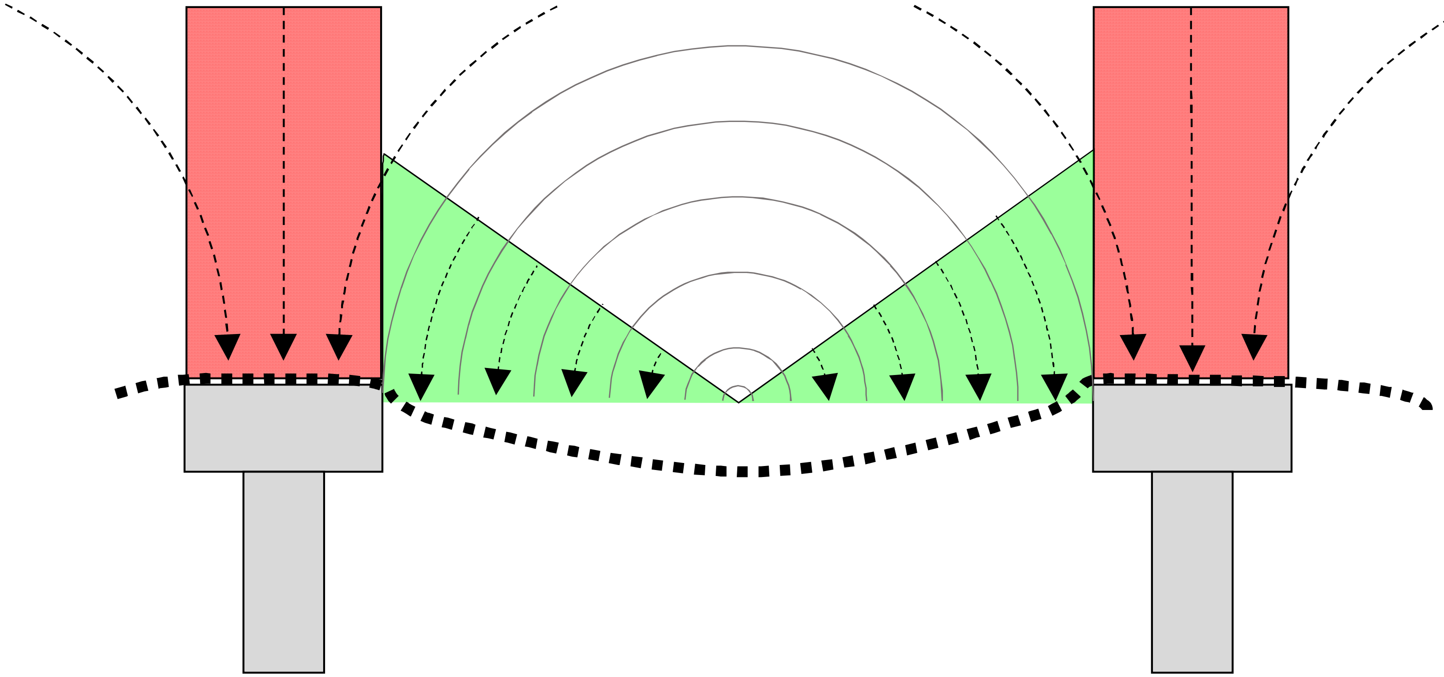

Concentric Arches Model
[van Eekelen 2015]

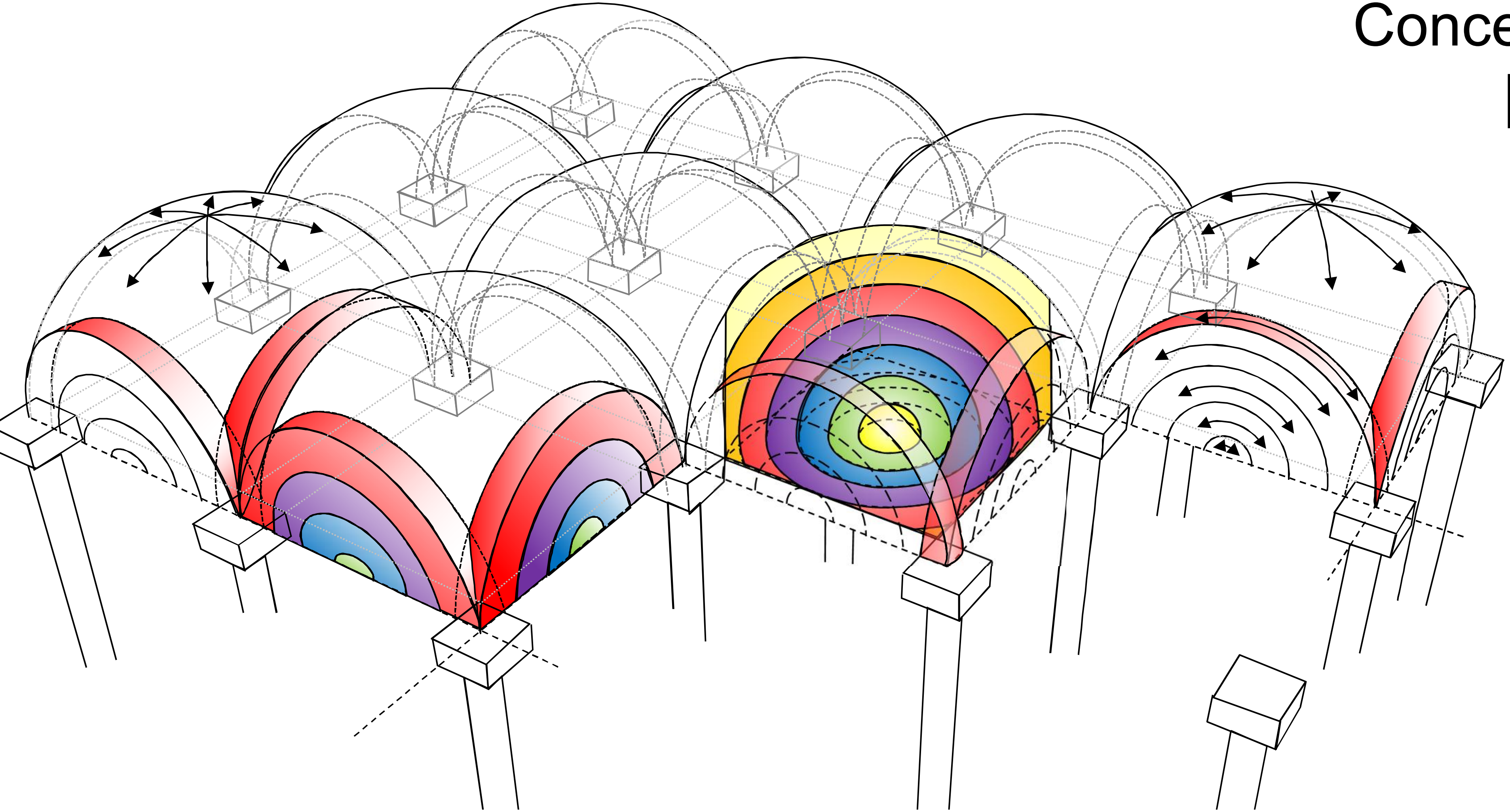

Excel sheet with equations: www.piledembankments.com

2010 Method

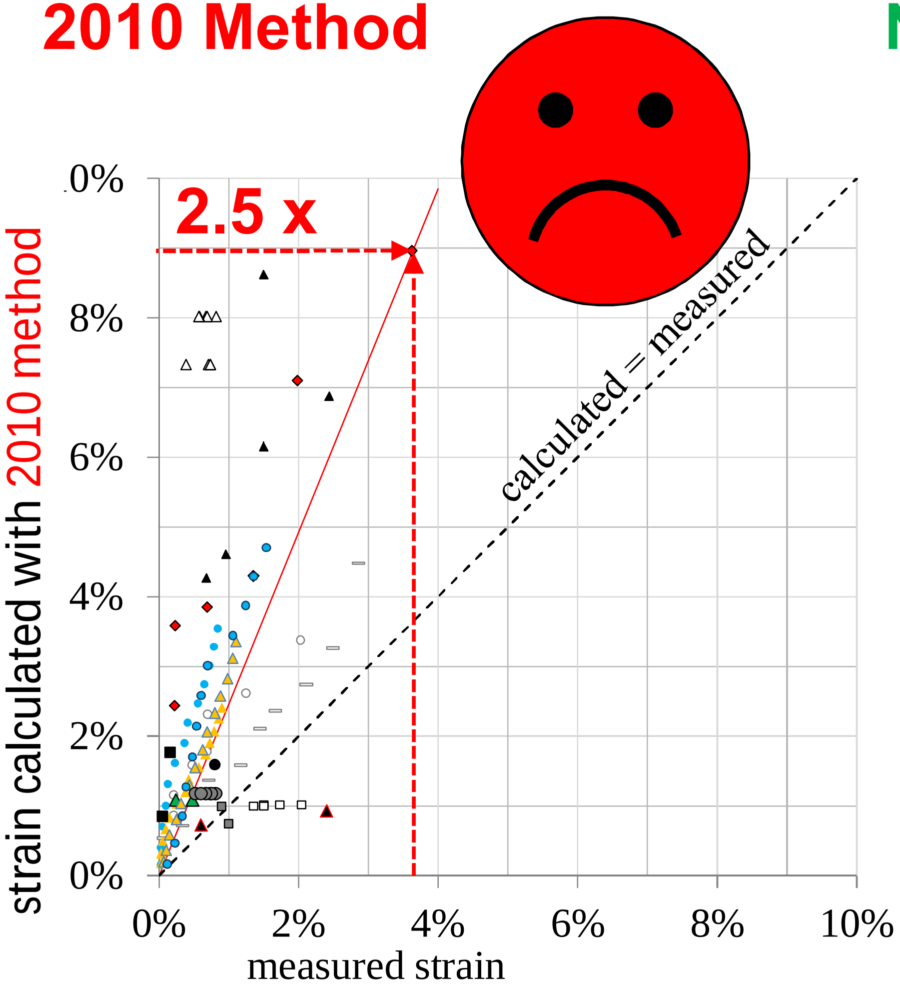

New Concentric Arches model

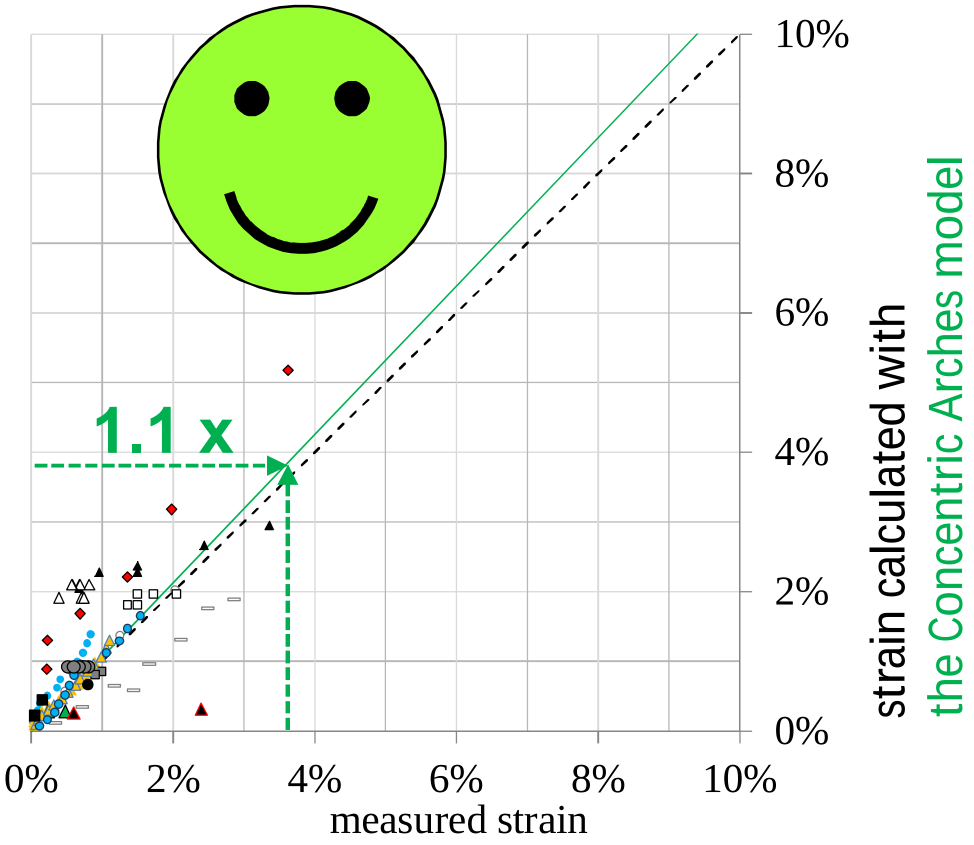

Conclusions

2010 method (EBGEO/CUR 226): calculates 2.5 times the measured strain

Experiments: load distribution inversed triangular

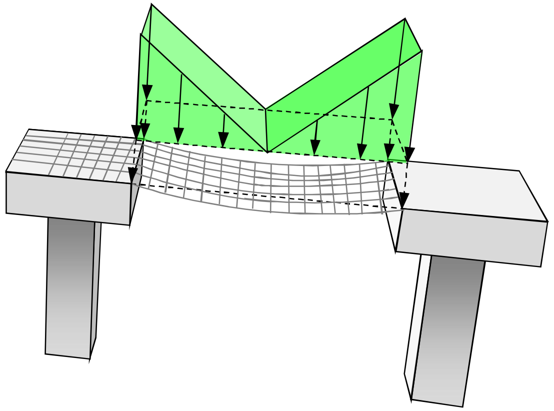

Explanation: new Concentric Arches model

Result: 1.1 times the measured strain

"perfect" match

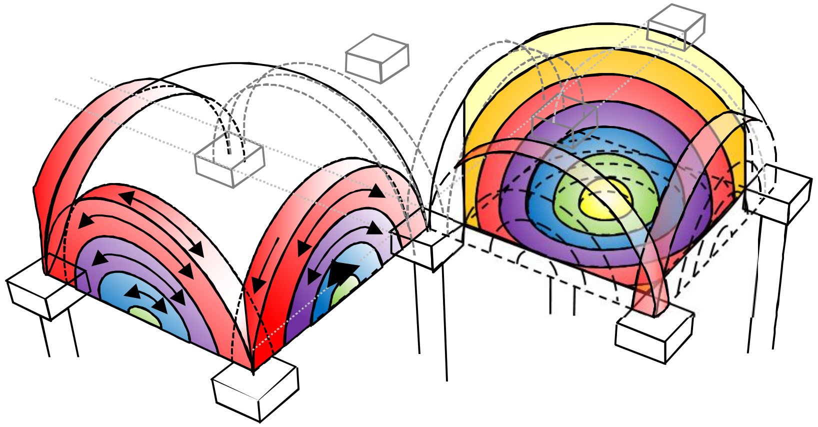

Therefore: adopted in the new Dutch design guideline

OBRIGADO!

Design Guideline
CRCpress.com or amazon.com
Search for “eekelen”

Free excel with the equations:
www.piledembankments.com

International course:
15/16 November in Delft, Netherlands
https://paotm.nl search for “basal”

Most important publications about this research:

CUR 226 (2016). S.J.M van Eekelen and M.H.A. Brugman, Eds. Design Guideline Basal Reinforced Piled Embankments. SBRCURnet & CRC Press, ISBN 9789053676240, https://www.crcpress.com/Design-Guideline-Basal-Reinforced-Piled-Embankments/Eekelen-Brugman/9789053676240

Van Eekelen, S.J.M. (2015). Basal Reinforced Piled Embankments. *PhD thesis Technical University of Delft, Netherlands. ISBN 978-94-6203-825-7 (print), ISBN 978-94-6203-826-4 (electronic version). Downloadable at: www.piledembankments.com, incl. an excel calculation file.*
This PhD thesis include:

- Van Eekelen, S.J.M., Bezuijen, A., Lodder, H.J., van Tol, A.F. (2012a). Model experiments on piled embankments Part I. *Geotextiles and Geomembranes 32: 69 - 81.*
- Van Eekelen, S.J.M., Bezuijen, A., Lodder, H.J., van Tol, A.F. (2012b). Model experiments on piled embankments. Part II. *Geotextiles and Geomembranes 32: 82 – 94.*
- Van Eekelen, S.J.M., Bezuijen, A., Van Tol, A.F. (2013). An analytical model for arching in piled embankments. *Geotextiles and Geomembranes 39: 78 – 102.*
- Van Eekelen, S.J.M., Bezuijen, A. van Tol, A.F. (2015). Validation of analytical models for the design of basal reinforced piled embankments. *Geotextiles and Geomembranes. 43:1, 56 - 81.*

Van Eekelen, S.J.M. (2016). The 2016-update of the Dutch Design Guideline for Basal Reinforced Piled Embankments. *In: Proc. of ICTG3, Portugal.*

Van Eekelen, S.J.M. and Venmans, A.A.M. (2016). Piled embankment or a traditional sand construction: how to decide? A case study. *In: Proc. of ICTG3, Portugal.*

Most important publications about this research:

DuboCalc (2015). https://www.rijkswaterstaat.nl/zakelijk/zakendoen-met-rijkswaterstaat/inkoopbeleid/duurzaam-inkopen/duurzaamheid-bij-contracten-en-aanbestedingen/dubocalc/index.aspx

Venmans, A.A.M (2013). Building with the subsurface for realizing cost-efficient infrastructure. Proceedings of 18th International Conference on Soil Mechanics and Geotechnical Engineering, Paris. Vol. 2, pp. 1781-1784.

Venmans, A.A.M., Förster, U., Hooimeijer, R.H. (2005). Integral design of motorways on soft soil on the basis of whole life costs. Proceedings 16th International Conference on Soil Mechanics and Geotechnical Engineering, Osaka. Millpress Science Publishers Rotterdam, vol. 4, pp 2867-2870.

Venmans, A.A.M., Kwast, E., (2011). Life cycle cost optimization of bridge approach constructions in local and national roads in the Netherlands. In: Proceedings EPS 2011, Oslo.

WAM-software decision support tool for ground improvement for bridge approach constructions http://dtvirt57.deltares.nl/applications/intraweb/dminiroad/dminiroad.dll

Behaviour of a compacted subgrade soil and the influence of planar reinforcement in track substructure

Ana Heitor, Buddhima Indraratna and Cholachat Rujikiatkamjorn[1]

1. University Of Wollongong, Australia

Part A – Small strain behaviour of compacted subgrade soil

- Track substructure:
- Ballast
- Subballast
- **Subgrade**

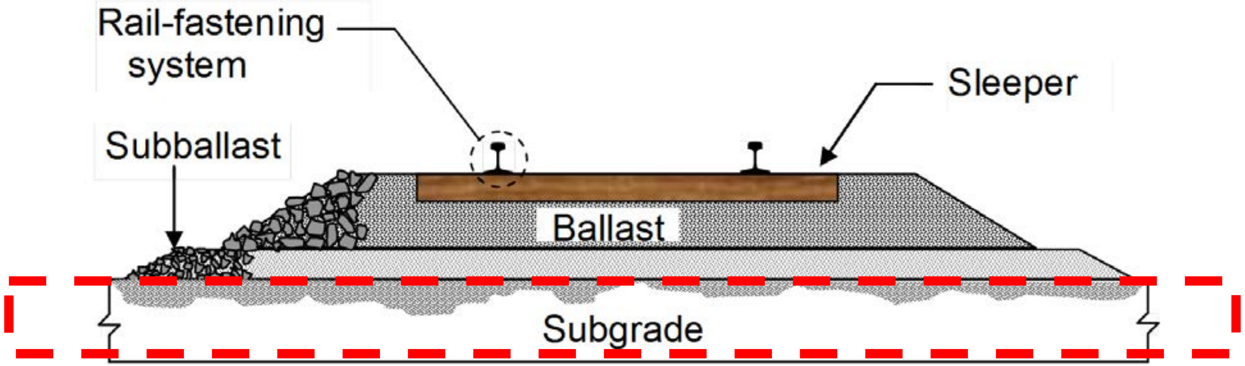

Strain limits

- Small strain shear modulus

$$G_0 = \frac{\gamma}{g} V_s^2$$

  - Higher loads during compaction cause non-linear stress-strain behavior

  - The stiffness values measured during compaction will therefore be lower than those obtained by non-destructive testing (i.e. MASW or BE)

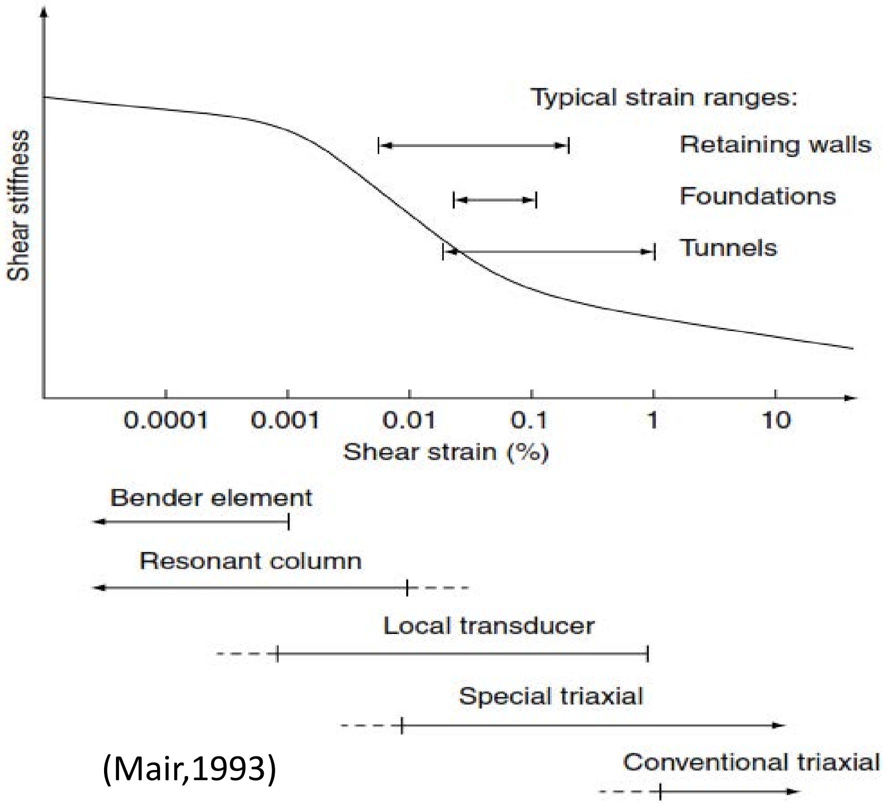

(Mair,1993)

• Compaction characteristics

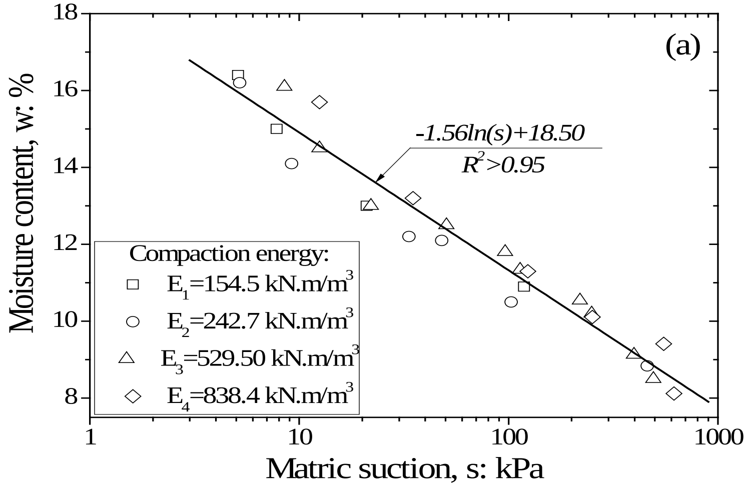

- Silty sand (Penrith, NSW) : SP-SC 89% sand and 11% fines
- LL = 25.5%, PI = 10 and Gs = 2.7

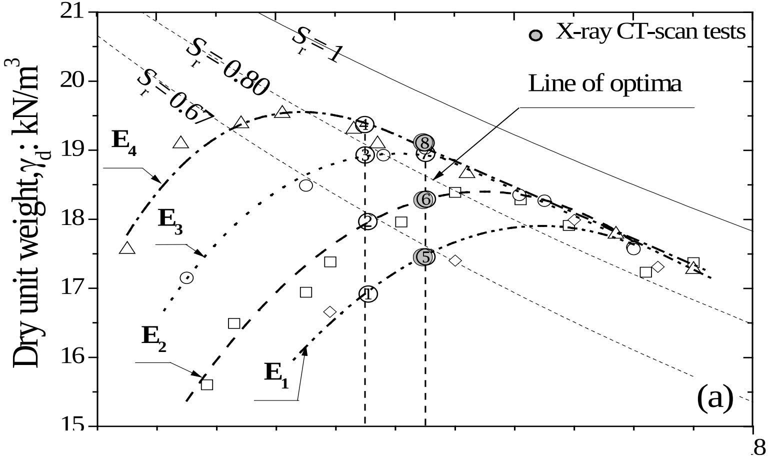

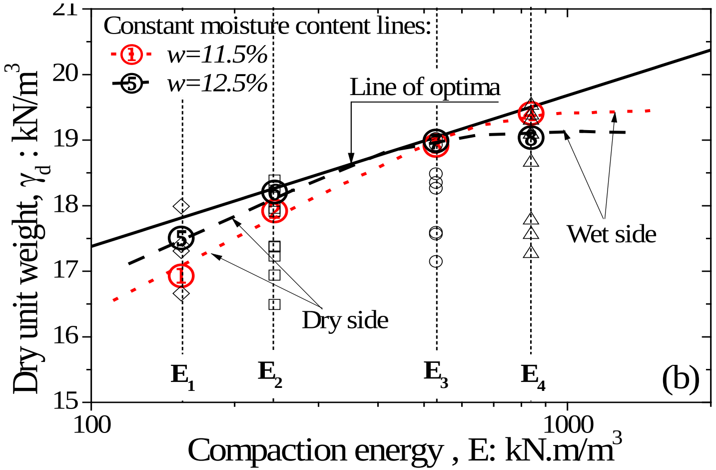

Heitor et al. (2013) *CGJ* 50 (2): 179-188

Modulus across the compaction plane

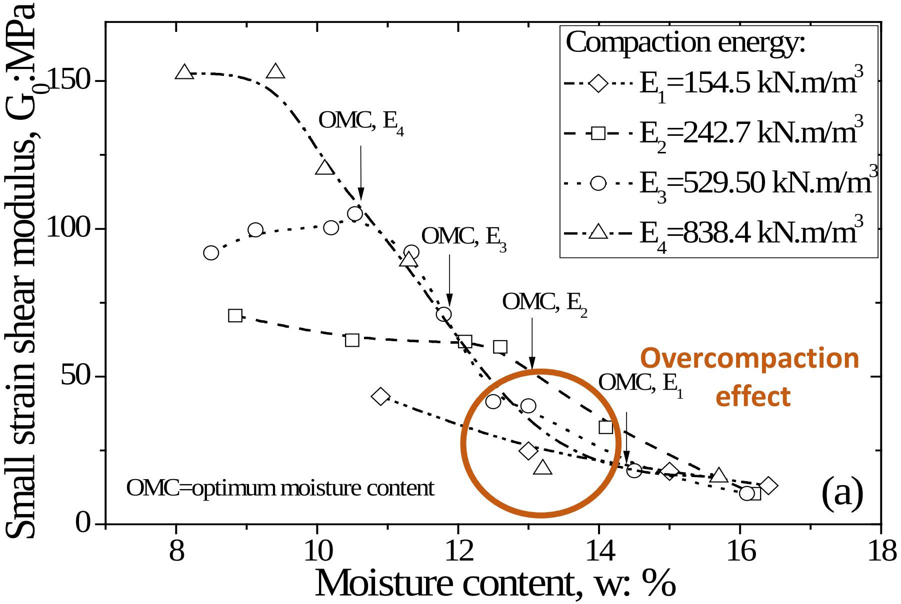

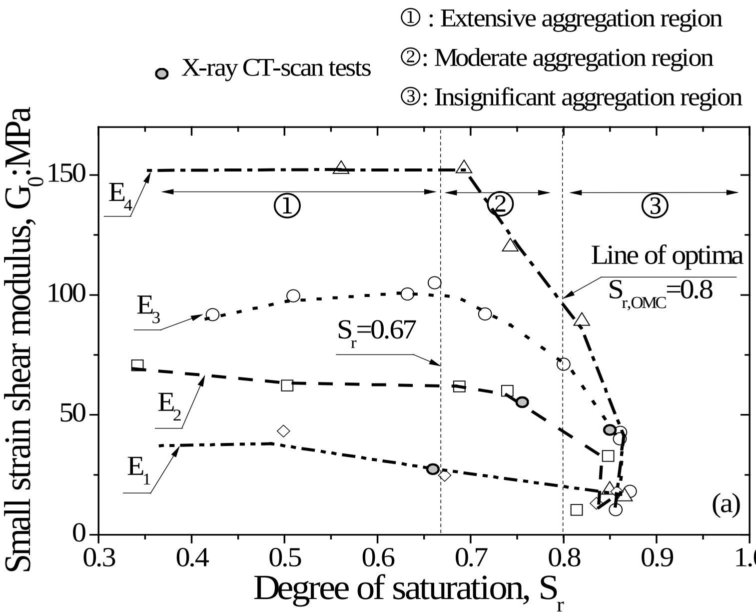

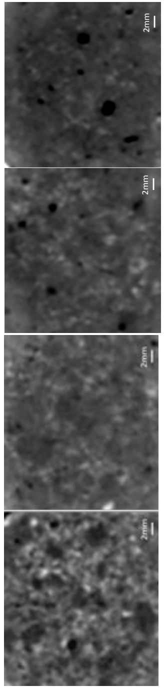

Heitor et al. (2013) *CGJ* 50 (2): 179-188

G_0 and End-Product Specifications

$$\frac{G_0}{G_{ref}} = Af(e)\left[\frac{(p-u_a)+(u_a-u_w)S_r}{p_r}\right]$$

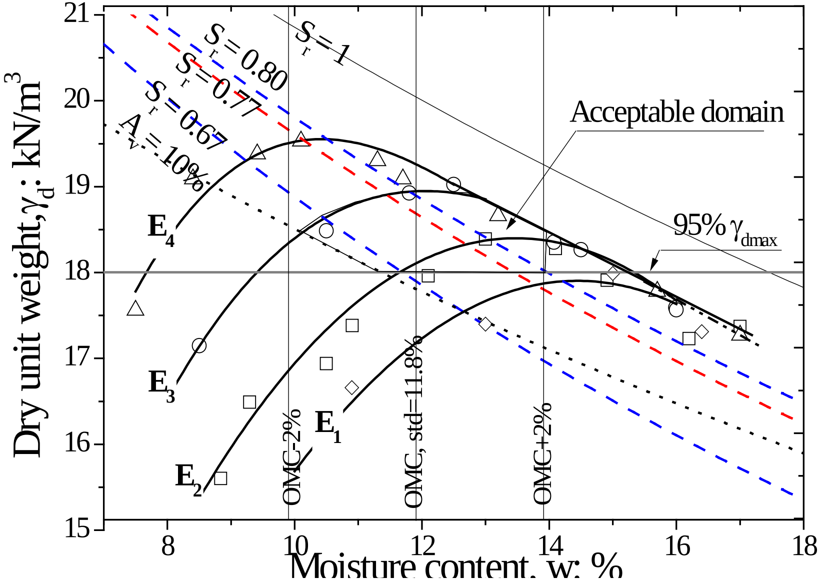

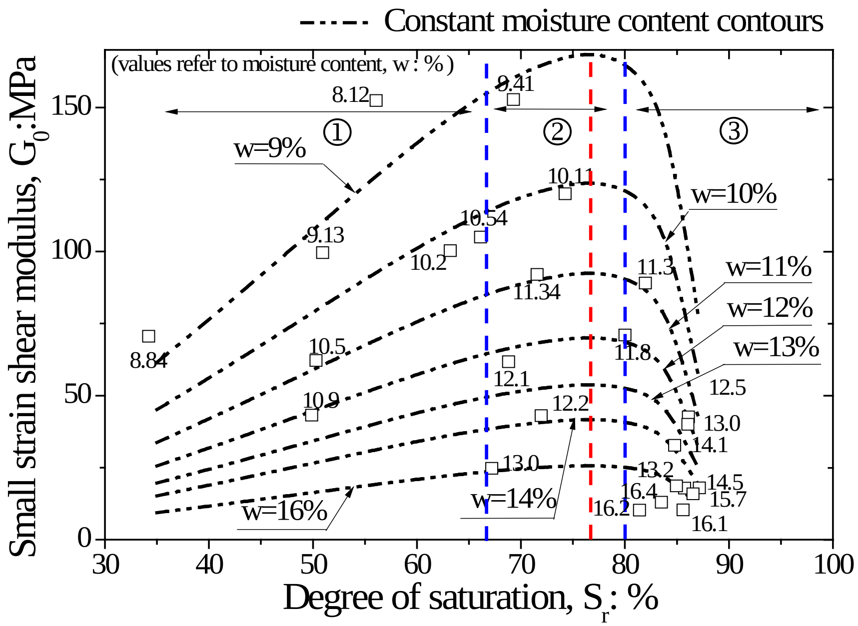

Heitor et al. (2013) *CGJ* 50 (2): 179-188

Suction history: wetting/drying cycles

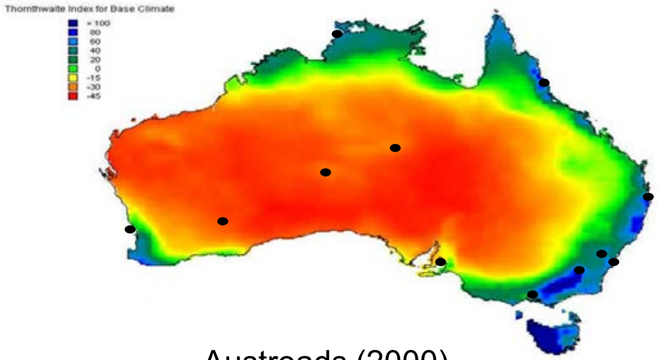

Austroads (2000)

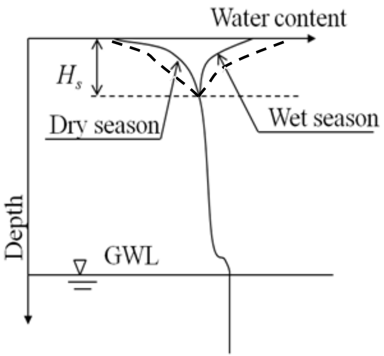

The effect of suction history on G0 (Ng et al., 2012 and Heitor et al., 2014) :

- hydraulic cycles,
- recent suction history
- the current suction ratio (CSR) with $CSR = \frac{s_{max}}{s_{current}}$

G0 during a drying-wetting cycle

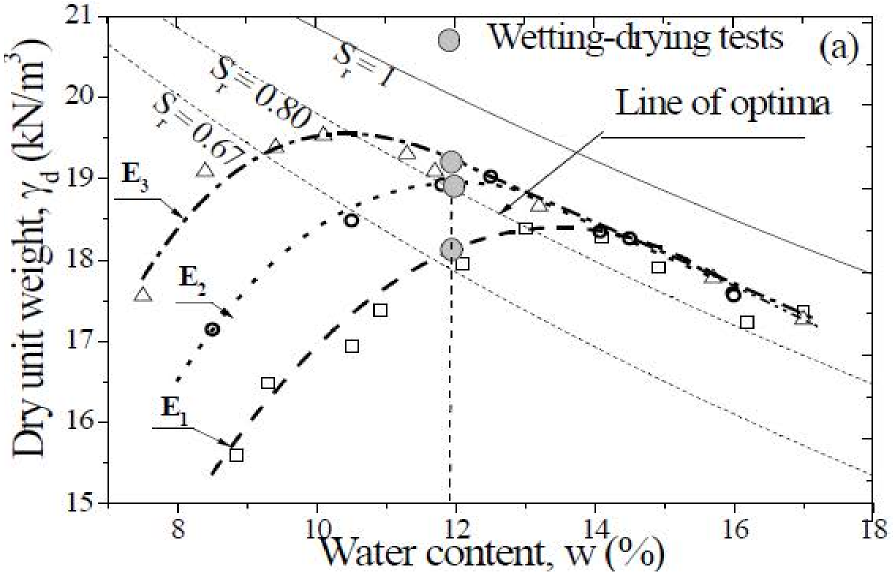

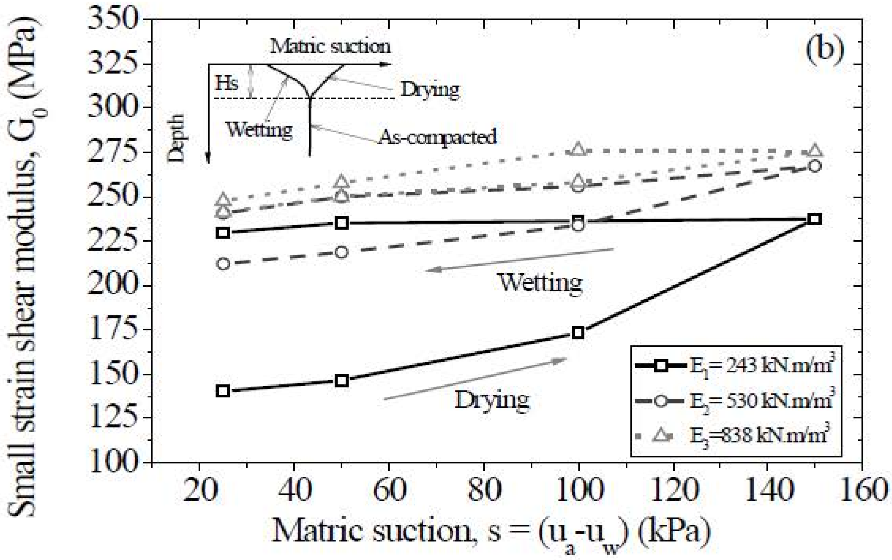

modified after Heitor et al.(2015) *Géotechnique.* Vol. 65 (9), pp. 717-727

Part B: Influence of planar reinforcement in the track substructure

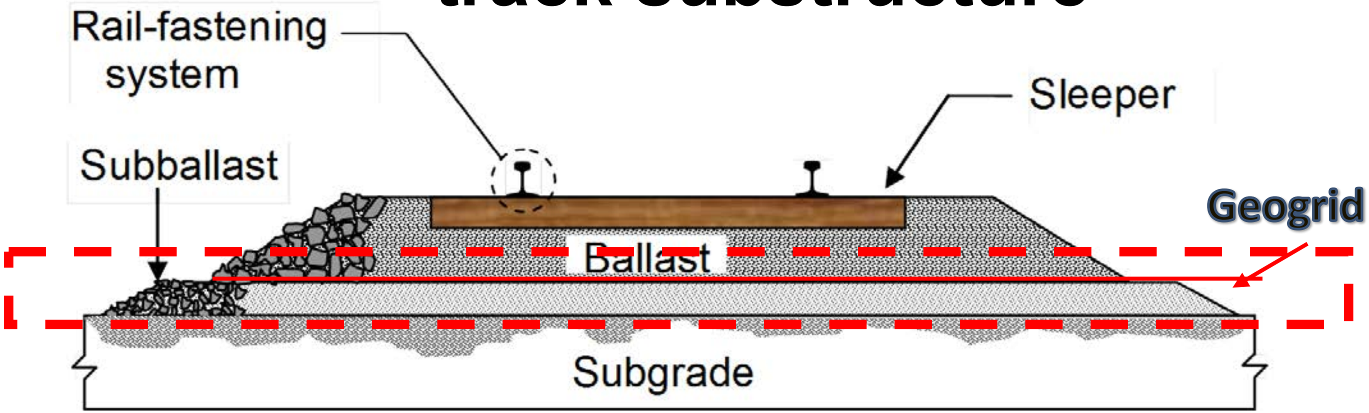

Track substructure:

- Ballast
- Subballast
- Subgrade
- **Geogrid at interface ballast/ subballast**

The use of geosynthetics in rail tracks

- Geogrids / geocells reinforce and confine ballast, resulting in a reduced settlement and decreased lateral movement of ballast

- Lack of availability of a comprehensive computational model to study the interaction of ballast aggregates with geogrids (i.e. interlocking /confinement effects)

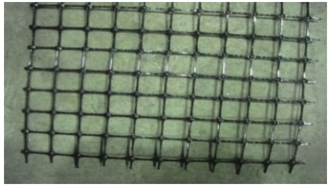

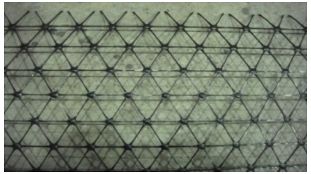

Tensar, 2012

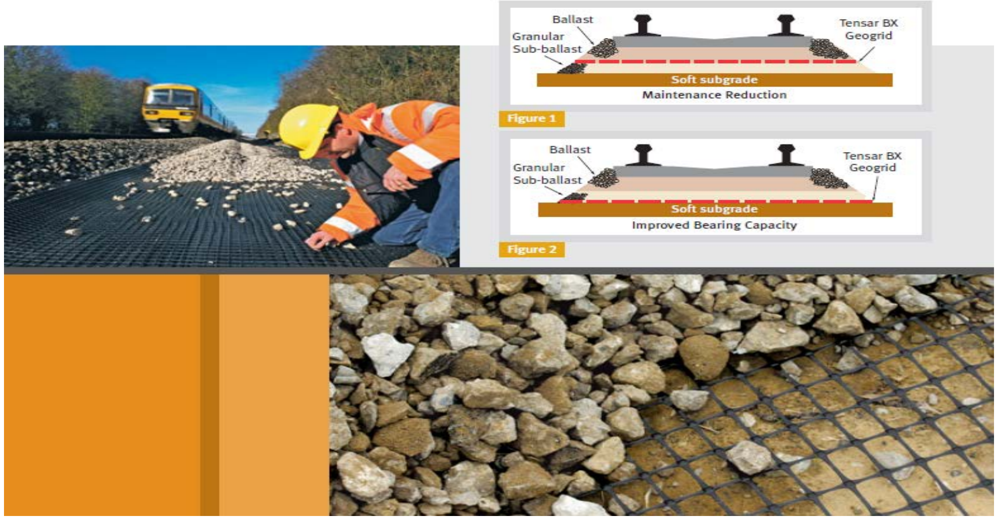

Cyclic loading tests for geogrid-reinforced ballast

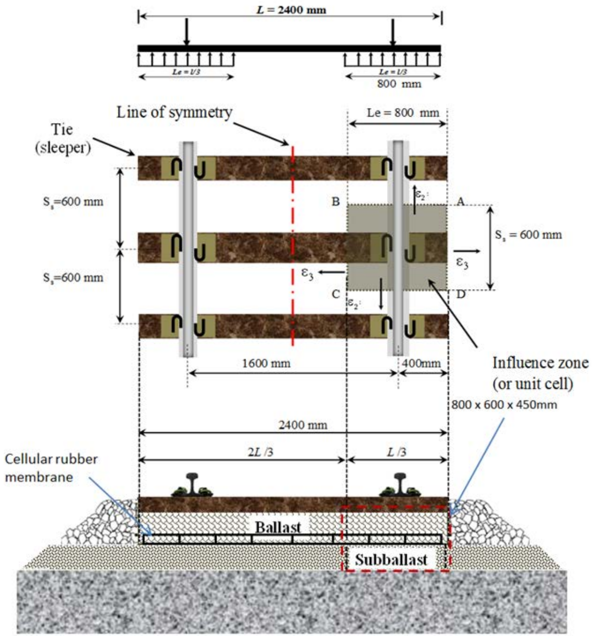

Cubical Triaxial Apparatus to Simulate a Track Section (Specimen: 800x600x600 mm)

Indraratna, B., Ngo, N. T. , and Rujikiatkamjorn, C. (2013). Journal of Geotechnical and Geoenvironmental Engineering-ASCE. 139(8): 1275–1289.

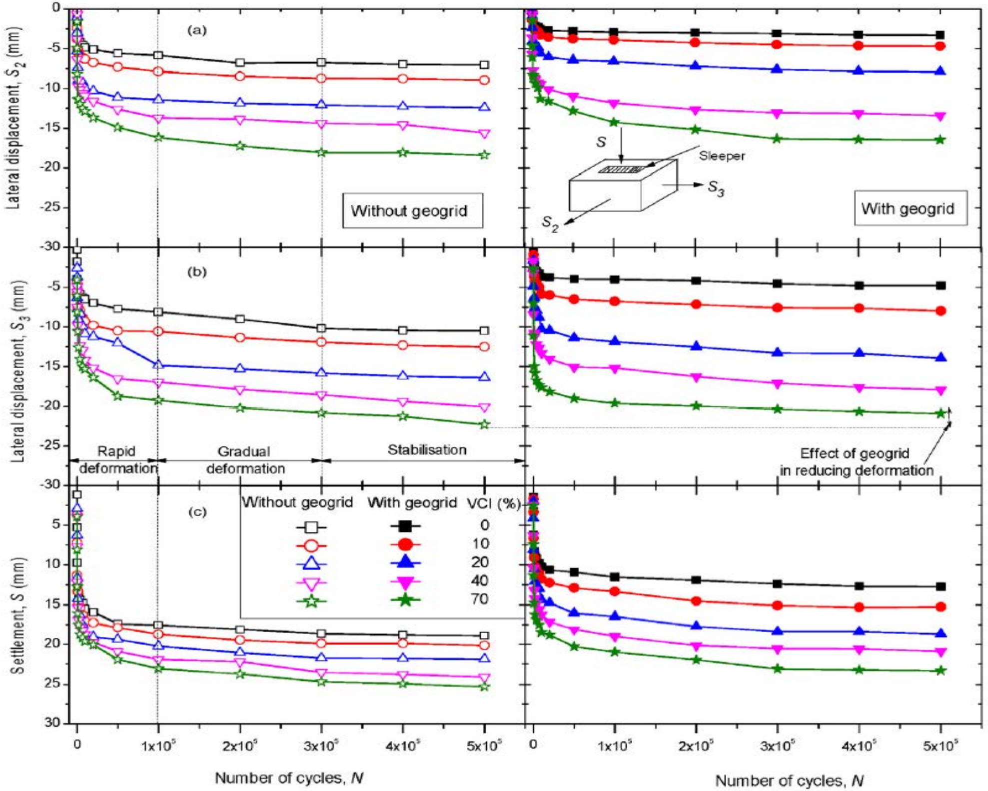

$$VCI = \frac{(1+e_f)}{e_b} \times \frac{G_{s.b}}{G_{s.f}} \times \frac{M_f}{M_b} \times 100$$

e_b = Void ratio of clean ballast

e_f =Void ratio of fouling material

$G_{s\text{-}b}$ = Specific gravity of ballast material

$G_{s\text{-}f}$ = Specific gravity of fouling material

M_b = Dry mass of clean ballast

M_f = Dry mass of fouling material

Variations in the deformation of fresh and fouled ballast with and without geogrid with varying VCIs (Indraratna et al. 2013)

Optimum aperture size of geogrids

Geogrids Used for Testing

Geogrid type	*Aperture shape*	*Aperture size (mm)*	T_{ult} (kN/m)
G1	Square	38 × 38	30
G2	Triangle	36	19
G3	Square	65 × 65	30
G4	Rectangle	44 × 42	30
G5	Rectangle	36 × 24	30
G6	Square	33 × 33	40
G7	Rectangle	70 × 110	20

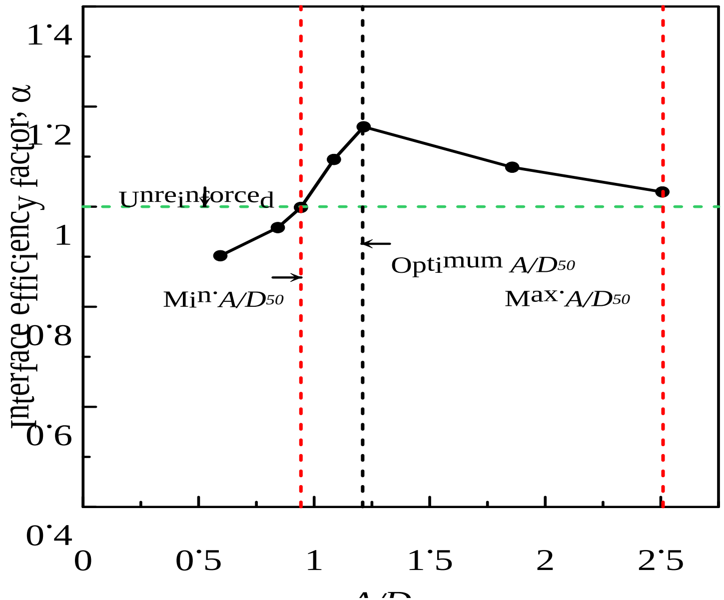

Optimum Aperture Size of Geogrids

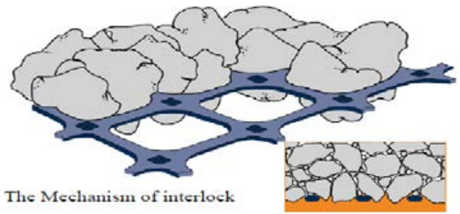

The mechanism of particle interlock within the geogrid aperture (Wrigley 1989)

Indraratna, Hussaini and Vinod (2011)

Field Trial on Instrumented Tracks

Locations of instrumented track sections at Singleton (data sourced from RCA, 2008)

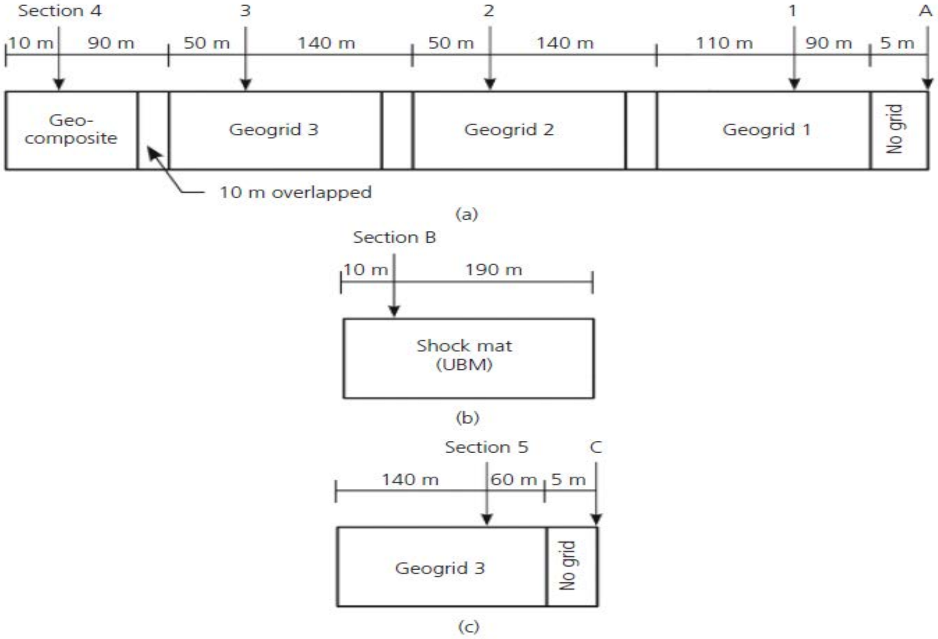

Figure 2. Reinforcement of track substructure with different geosynthetics at (a) sections A to 4, (b) section B, and (c) sections 5 and C

Indraratna & Nimbalkar 2014

Magnitude of strains

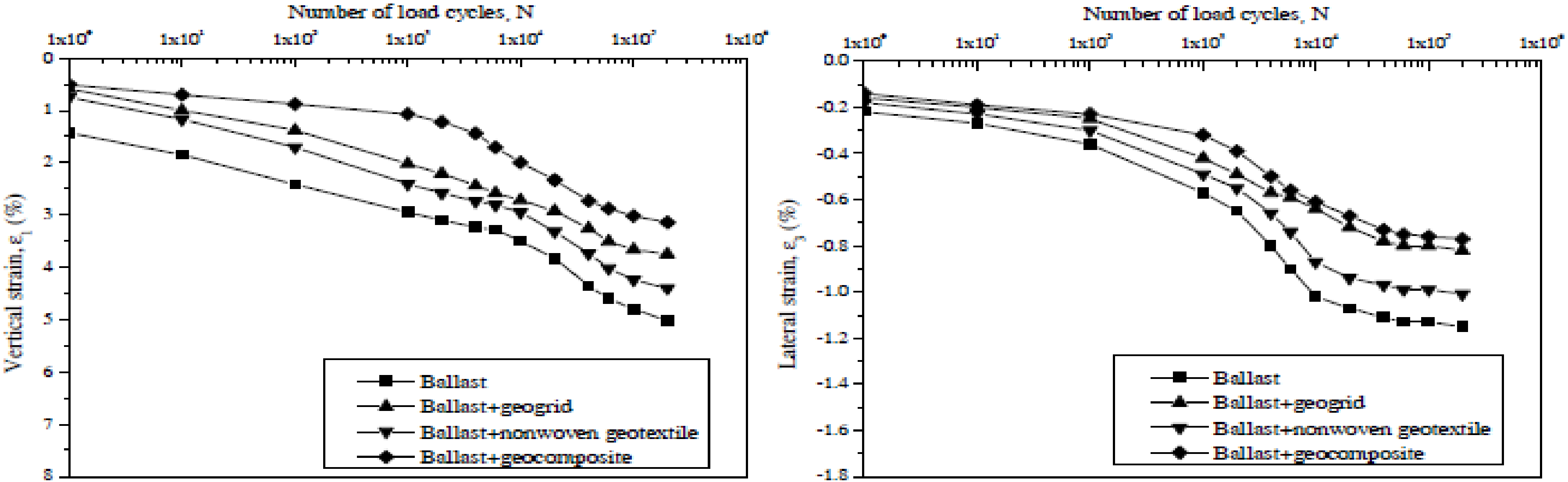

Variation of (a) vertical strain (ε_1) and (b) lateral strain (ε_3) with number of load cycles (N) (data sourced from Indraratna & Nimbalkar 2013).

Ballast breakage with and without inclusion of geosynthetics

Test No.	Material type	Ballast breakage index (*BBI*)		
		Top zone	Central zone	Bottom zone
1	Fresh ballast	0.140	0.059	0.046
2	Ballast + geogrid	0.119	0.030	0.015
3	Ballast + geotextile	0.093	0.066	0.031
4	Ballast + geocomposite	0.086	0.034	0.005

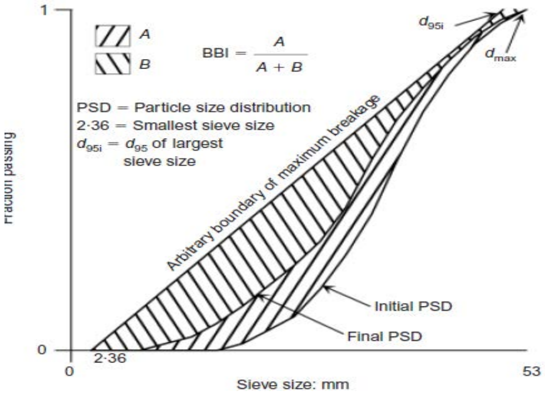

Lackenby et al. 2007

Final Remarks

- Compacted Subgrade performance is strongly dependent of the compaction state
- There is a intimate relationship between G_0, degree of saturation and soil macrostructure that governs the performance of compacted materials
- A series of filed trials and large-scale Track Process Simulation Apparatus (TPSA) were conducted with and without geogrid inclusion show the behaviour of the track substructure is enhanced with geogrids and its inclusion also controls the incidence of ballast breakage.
- Geogrid decreases deformation and breakage of ballast specimens associated with interlocking effects.

REFERENCES

Heitor, A., Indraratna, B. and Rujikiatkamjorn, C. (2013). Laboratory study of small strain behavior of a compacted silty sand. *Canadian Geotechnical Journal*, 50(2), 179-188.

Heitor, A., Indraratna, B. and Rujikiatkamjorn, C. (2015) The role of compaction energy on the small strain properties of a compacted silty sand subjected to drying-wetting cycles *Géotechnique.* Vol. 65 (9), pp. 717-727 (DOI: http://dx.doi.org/10.1680/geot.14.P.053)

Indraratna, B., Ngo, N. T. , and Rujikiatkamjorn, C. (2013). "Studying the deformation of coal fouled ballast stabilised with geogrid under cyclic load". *Journal of Geotechnical and Geoenvironmental Engineering-ASCE*. 139(8): 1275–1289.

Indraratna, B., Karimullah Hussaini, S. K., and Vinod, J. S., "On The Shear Behavior of BallastGeosynthetic Interfaces," Geotechnical Testing Journal, Vol. 35, No. 2, 2012, pp. 18, http://dx.doi.org/10.1520/GTJ103317. ISSN 01496115

Indraratna, B., Nimbalkar, S. & Neville, T. (2014). Performance assessment of reinforced ballasted rail track. Proceedings of the ICE: Ground Improvement, 167 (1), 24-34.

Selig, E.T. and Waters, J.M. (1994). Track geotechnology and substructure management, Thomas Telford, London.

Thank You!

Dynamic Rollers in Earthworks: Compaction and Continuous Compaction Control

Johannes Pistrol[1], Dietmar Adam[1]

1. *Vienna University of Technology, Austria*

Roller Compaction

1. **Static** rollers
2. **Dynamic** rollers

    2.1 **Vibratory** rollers

    2.2 **Oscillatory** rollers

    2.3 Rollers with **control of vertical centrifugal force**

    2.4 **Feedback controlled** rollers (VARIOCONTROL, VARIOMATIC, ACE)

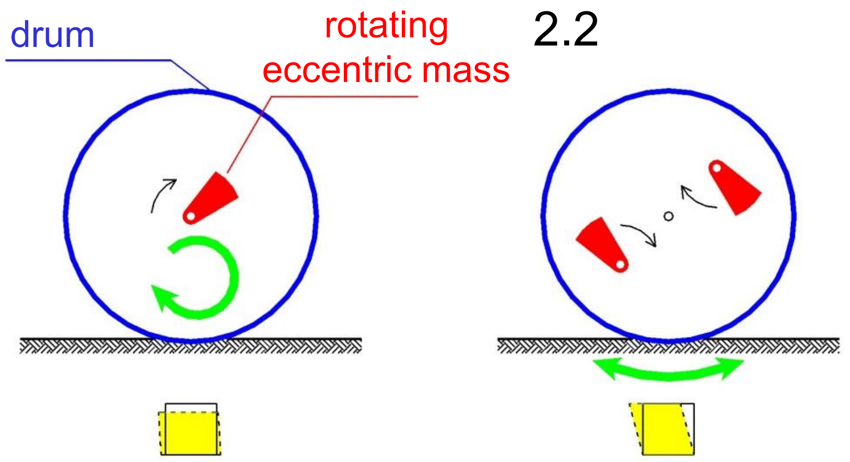

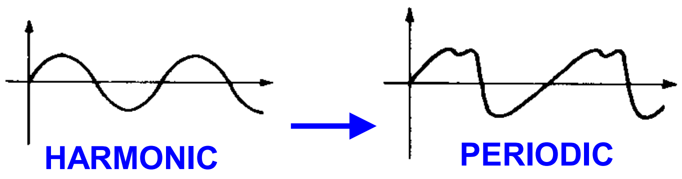

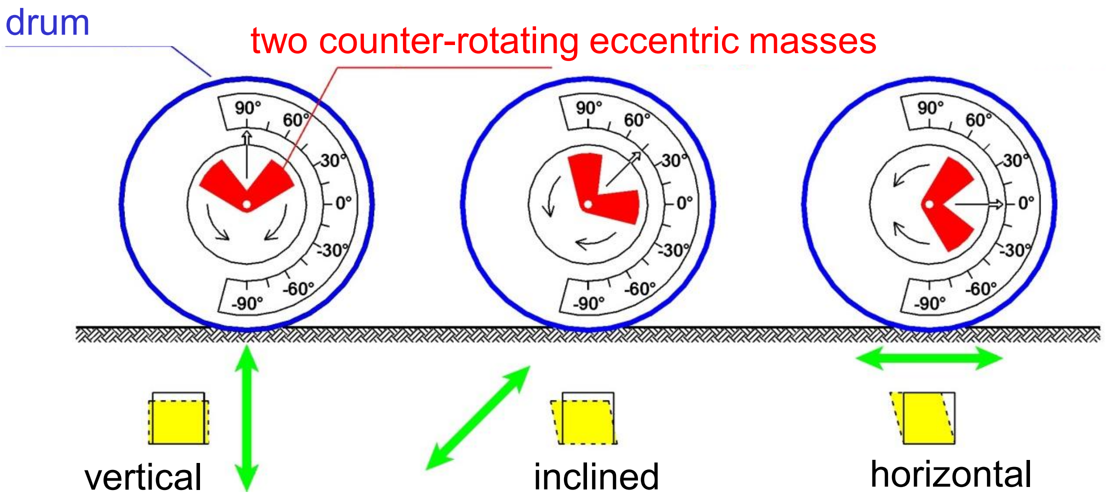

2.3 & 2.4

Oscillating rollers:

- two eccentric masses – eccentric but point symmetric to the drum axis
- same sense of rotation
  ⇒ sinusoidal torque around drum axis
- mainly dynamic shear forces
- low ambient vibrations

Vibrating rollers:

- eccentric mass in the drum axis
- circular translational vibration of the drum
- mainly vertical loading
- better compaction depth

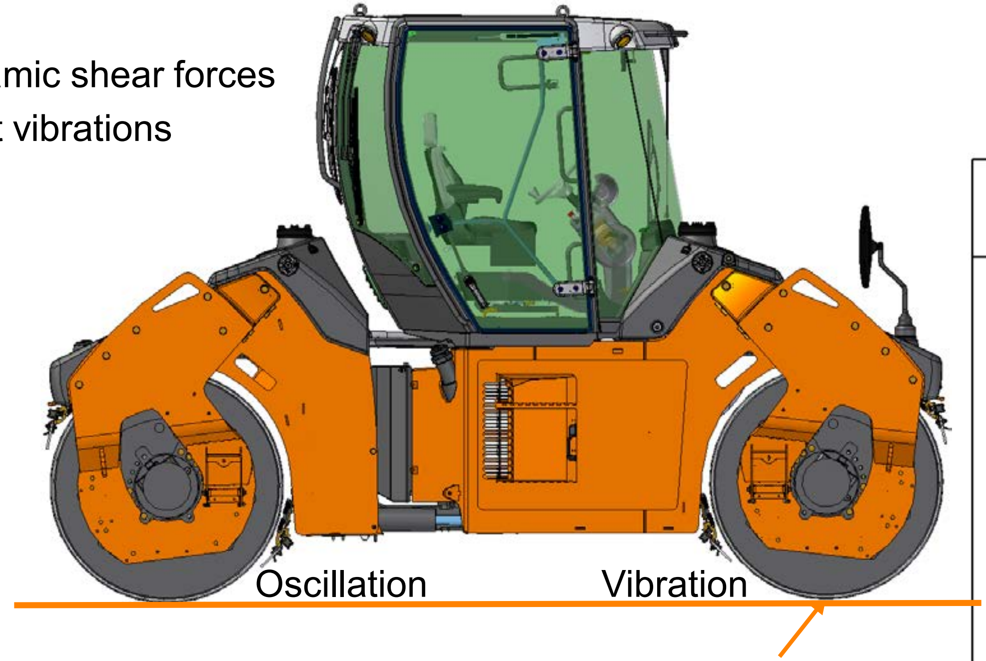

Modes of operation:

Continuous Contact, Partial Uplift, Double Jump, Rocking Motion, Chaotic Motion

drum motion	interaction drum-soil	mode of operation	soil contact force	application of CCC	soil stiffness	roller speed	drum amplitude
periodic	cont. contact	Continuous Contact		yes	low	fast	small
periodic	periodic loss of contact	Partial Uplift		yes			
periodic	periodic loss of contact	Double Jump		yes			
periodic	periodic loss of contact	Rocking Motion	left right	no			
chaotic	non-periodic loss of contact	Chaotic Motion		no	high	slow	large

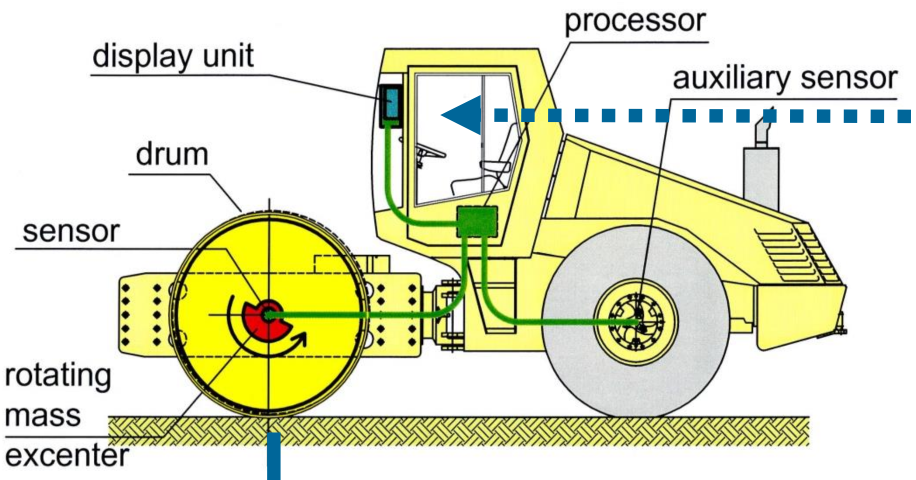

drum acceleration

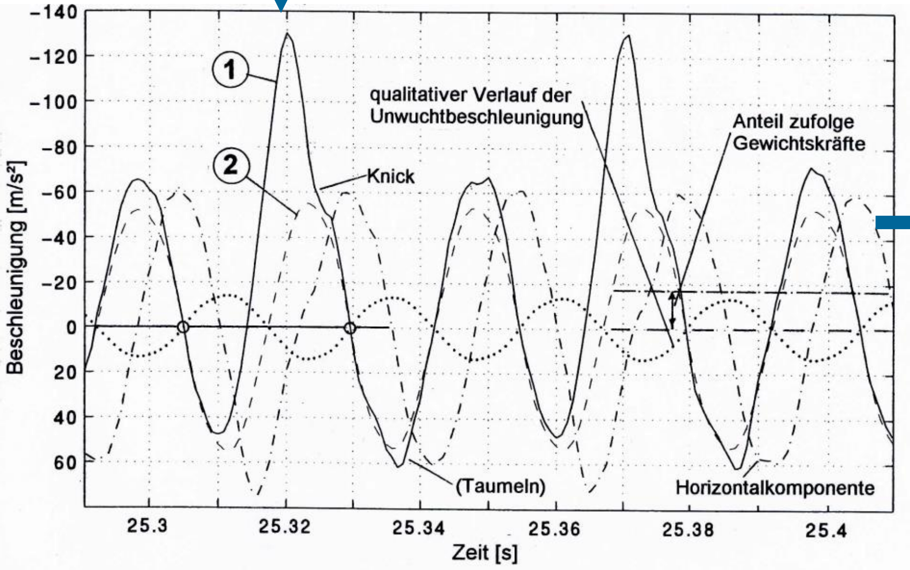

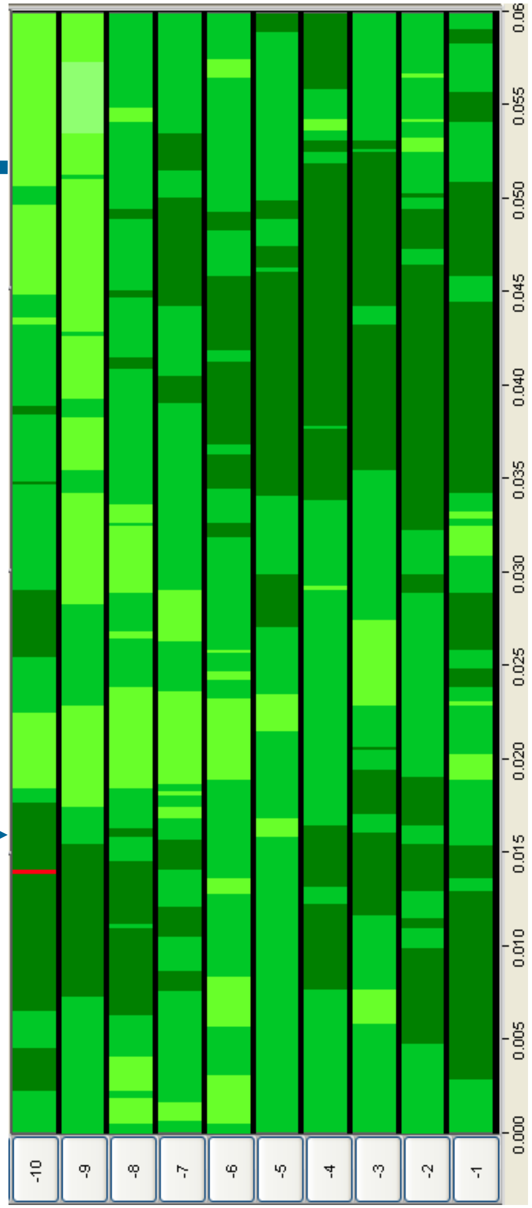

Compactometer

CMV

$$CMV = Faktor_1 \frac{a(2\omega_0)}{a(\omega_0)}$$

$$RMV = Faktor_2 \frac{a(0.5\omega_0)}{a(\omega_0)}$$

is based on the evaluation of the acceleration in the *frequency domain*

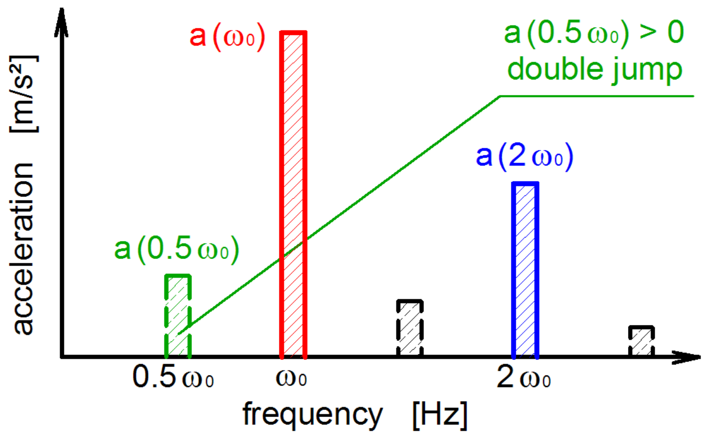

Terrameter

OMEGA

is based on the evaluation of the energy transmitted to the soil in the *time domain*

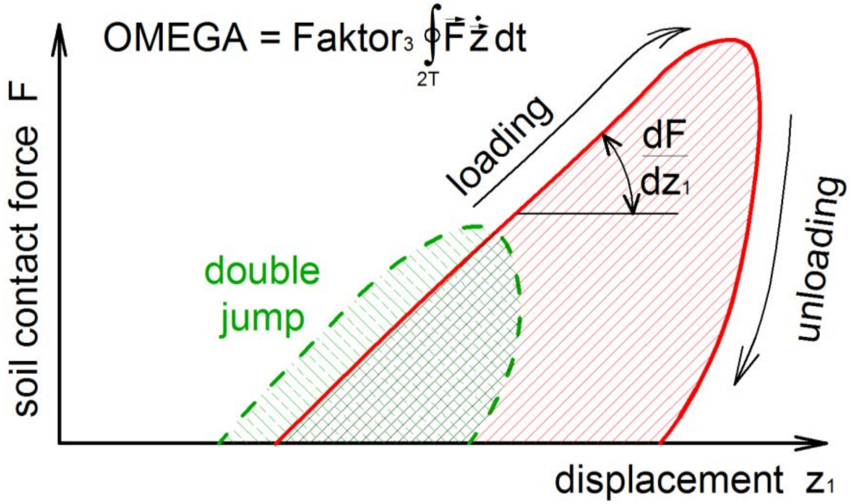

CCC Values

Terrameter

E_{VIB}

⇨ inclination of the soil contact force displacement relationship during loading; *time domain*

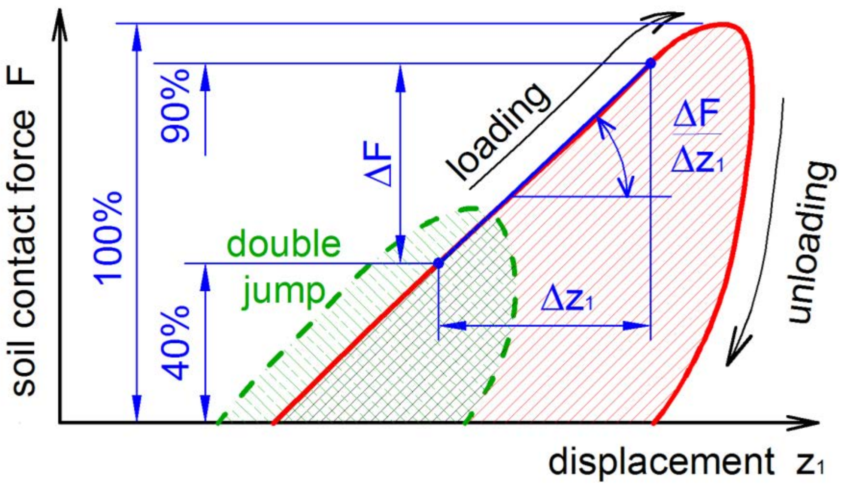

ACE

k_B

⇨ derived from the soil contact force displacement relationship at maximum drum deflection; *time domain*

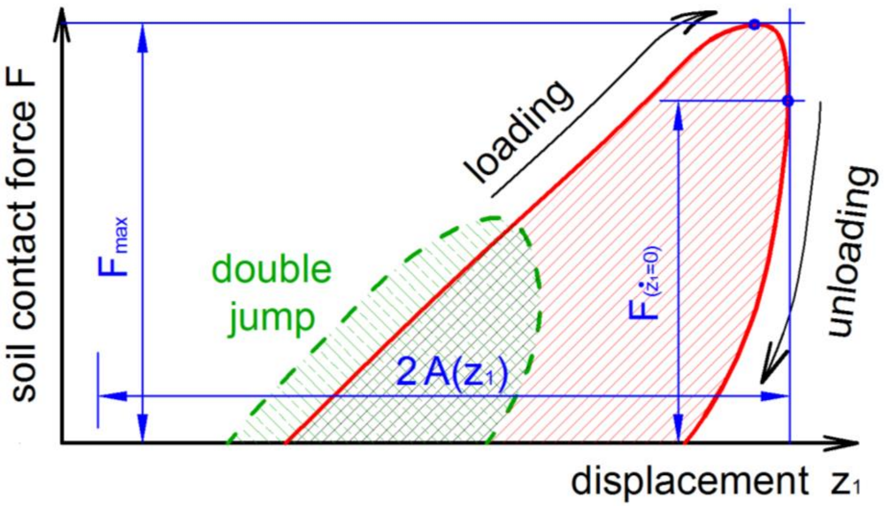

Modelling of the dynamic soil roller interaction system

Semi-analytical modelling

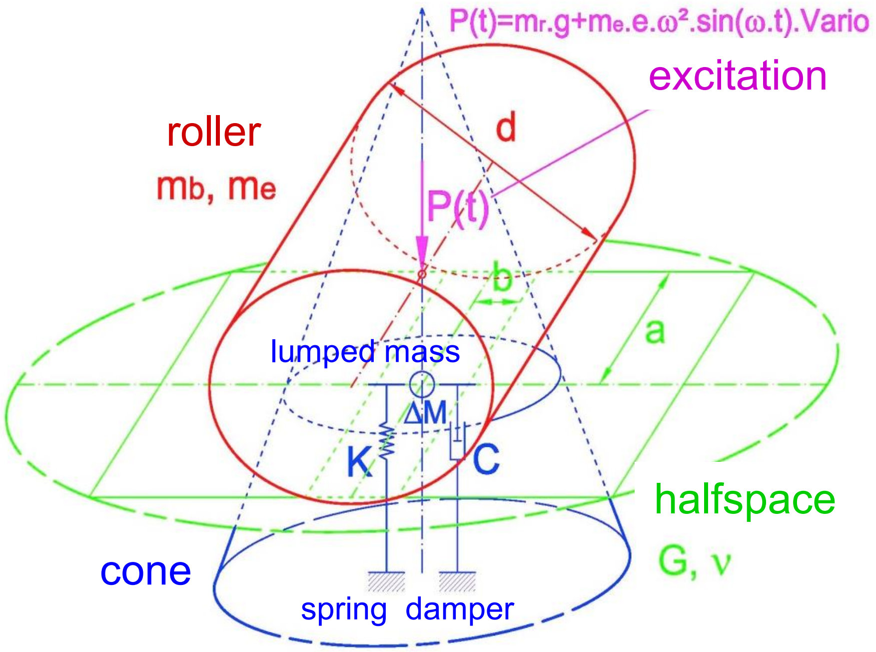

Finite element modelling

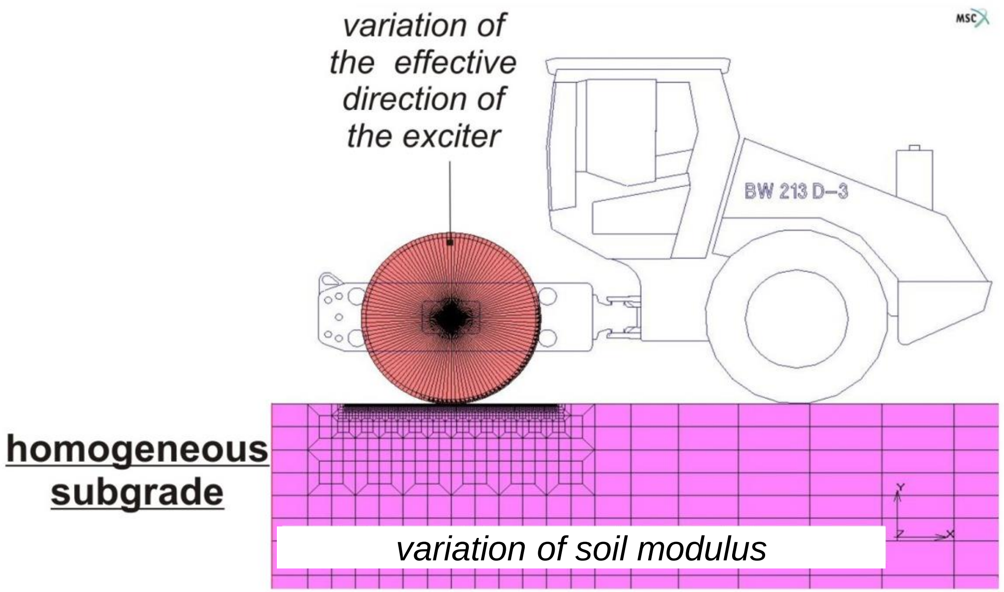

Roller drum: rigid body with directed excitation unit
Ground: approximation of linear elastic halfspace
→ cone model (SDOF) (*Wolf*, 1994)

→ linear elastic elements

Contact problem: relevant non-linearity in the interaction system

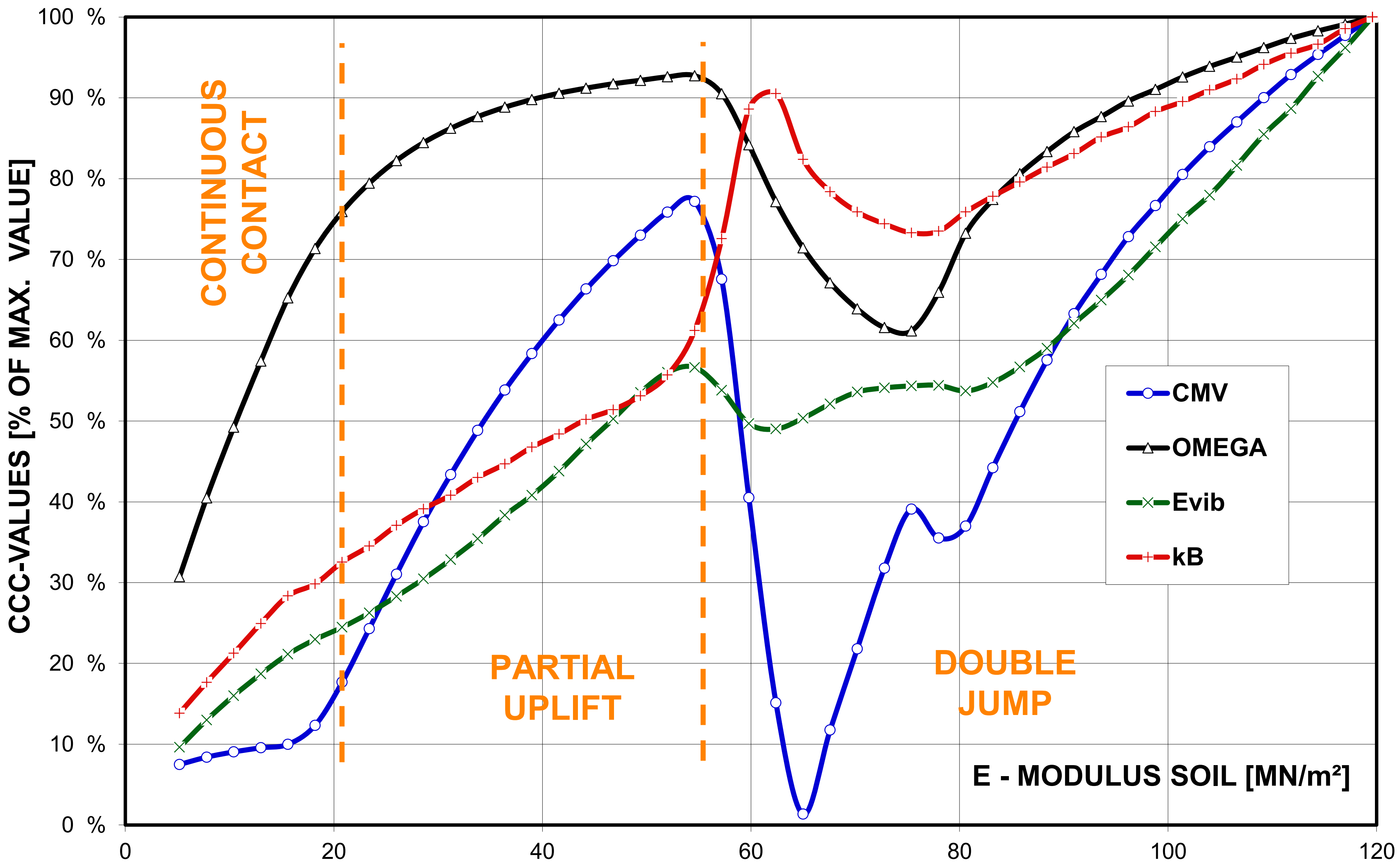
100 %
90 %
80 %
70 %
60 %
50 %
40 %
30 %
20 %
10 %
0 %
CCC-VALUES [% OF MAX. VALUE]
CONTINUOUS CONTACT
PARTIAL UPLIFT
DOUBLE JUMP
CMV
OMEGA
Evib
kB
E - MODULUS SOIL [MN/m²]
0
20
40
60
80
100
120

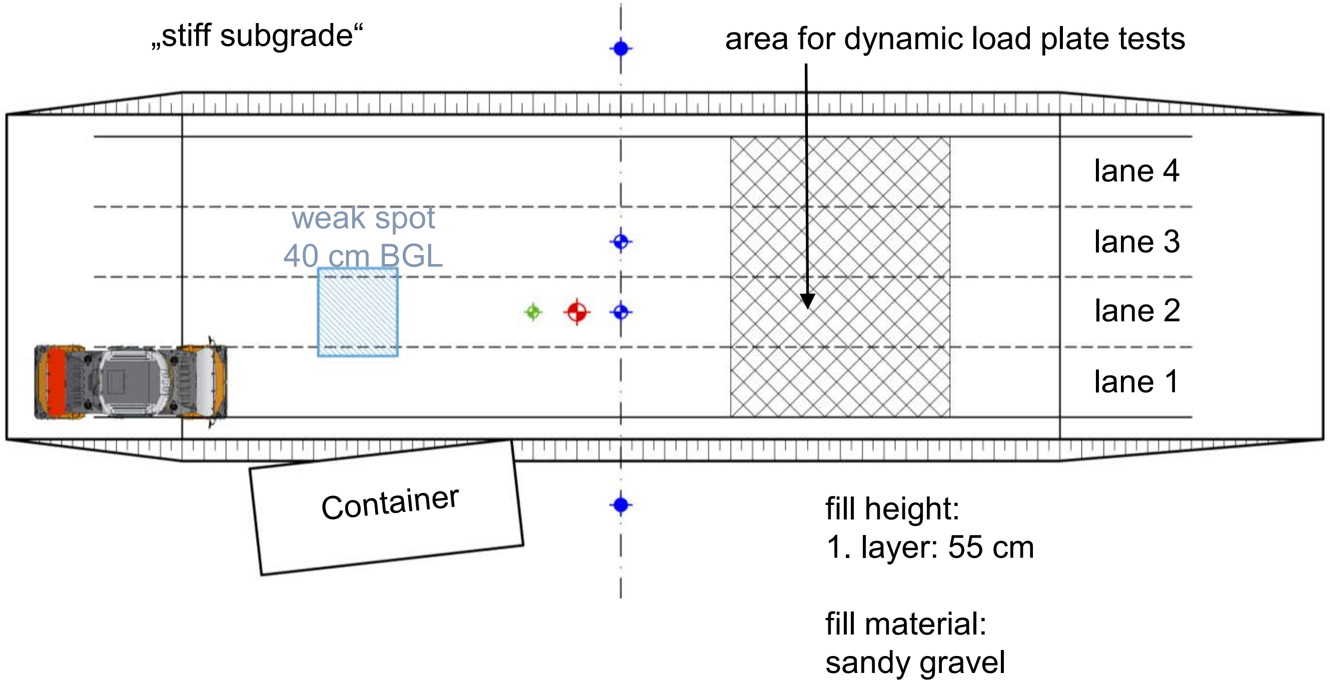

- Tri-axial accelerometer 55 cm BGL
- Tri-axial accelerometer on the surface
- Deformation measurement device
- Dynamic soil pressure 55 cm BGL
- Reference point of geodetic levelling

Compaction device:
HAMM HD^{+} 90 VO tandem roller (ca. 9.8 t)

Vibration (ca. 1.9 t drum mass):
Small amplitude: 0.34 mm at 50 Hz
Large amplitude: 0.62 mm at 40 Hz

Oscillation (ca. 1.9 t drum mass):
Tangential amplitude: 1.44 mm at 39 Hz

Calculation of the CCC values based on acceleration measurements:

Lane 2, Vibration, f = 50 Hz, v = 2-6 km/h

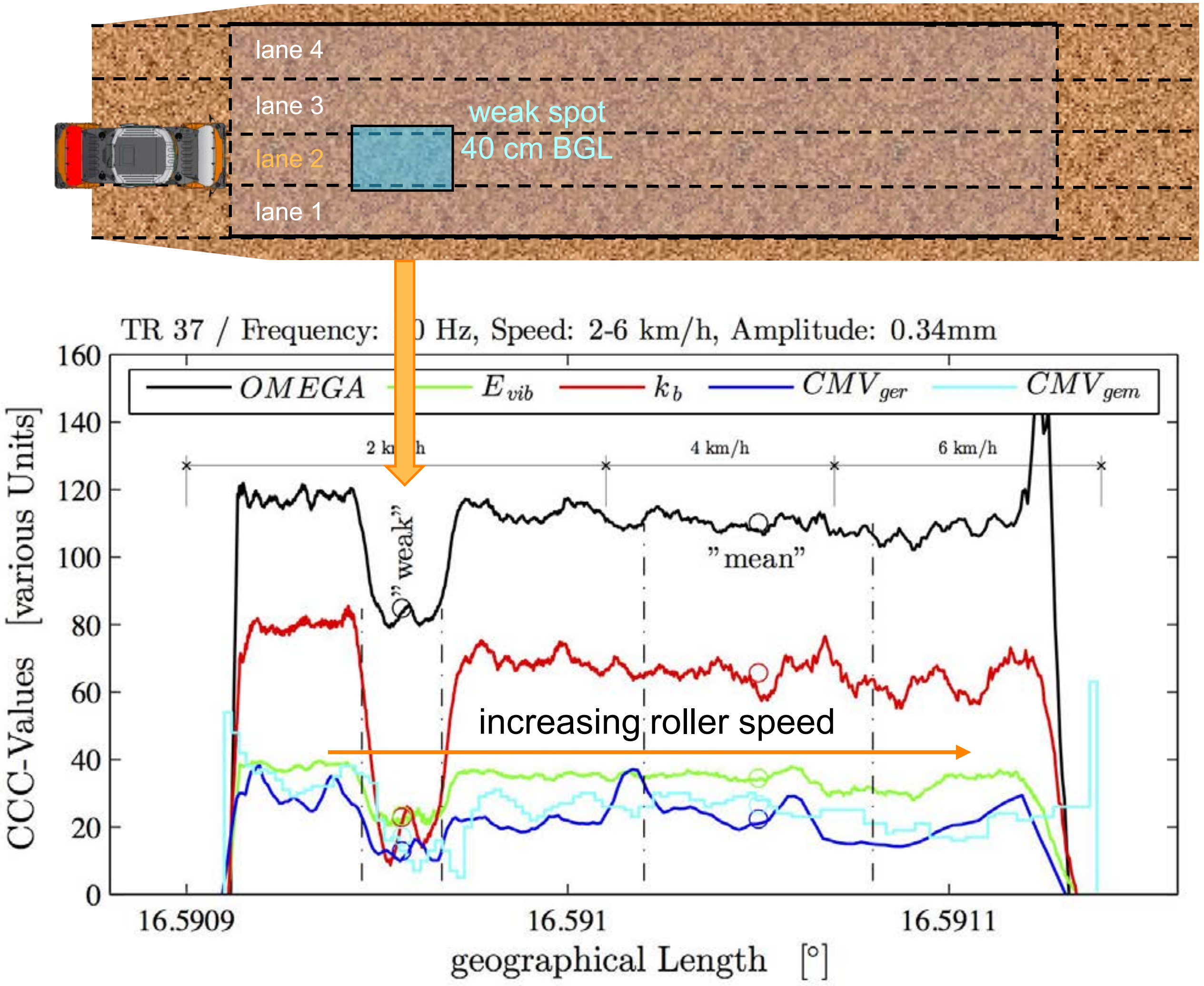

Installation of the artificial weak spot

Dynamic load plate tests after each roller pass

Comparison of two test runs:

f = 40 Hz (thin line) and f = 30 Hz (bold line)

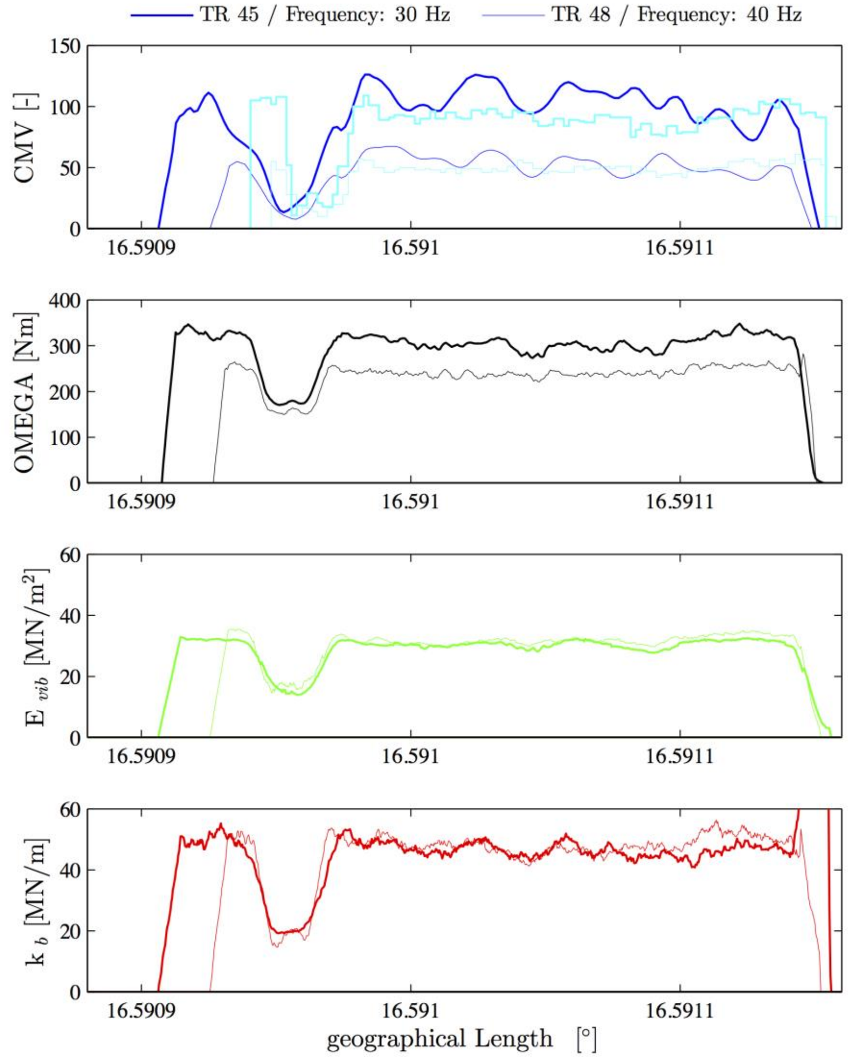

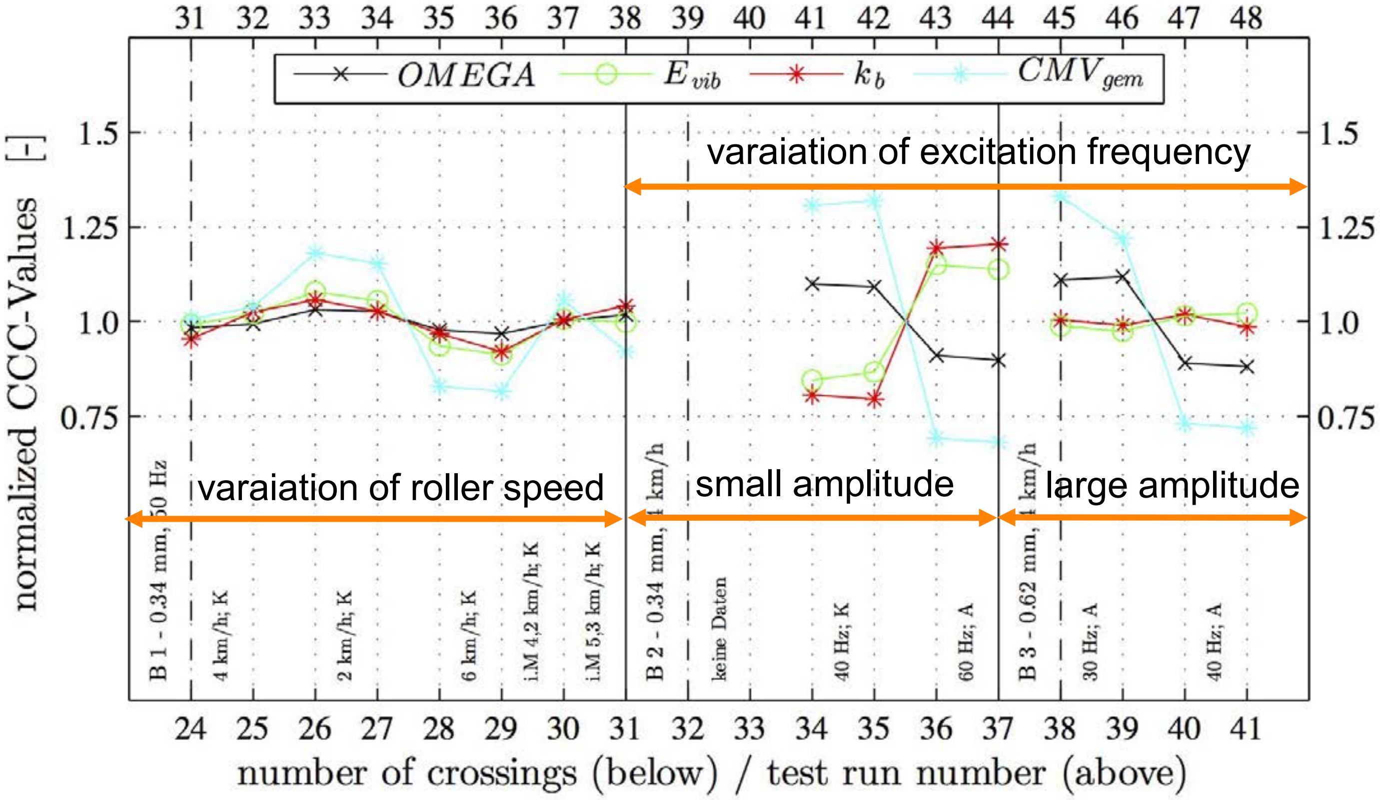

Main influence on CCC values:

- Modes of operation
- Roller speed
- Excitation frequency
- Excitation amplitude

Oscillating rollers:

- Two eccentric masses – eccentric, but point symmetric to the drum axis
- Same sence of rotation
  ⇒ sinusoidal torque around drum axis
- Mainly dynamic shear forces
- Low ambient vibrations
- Until recently:
  no CCC system!

Vibrating rollers:

- Eccentric mass in the drum axis
- Circular translational vibration of the drum
- Mainly vertical loading
- Better compaction depth

interaction drum-soil	mode of operation	horizontal acceleration in the bearing	app. of CCC	roller speed	soil stiffness	excitation amplitude	excitation frequency
continuous contact	Stick	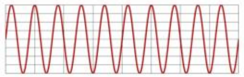	yes	slow	low (Stick)	small (Stick)	low (Stick)
periodic loss of contact	One-sided Slip	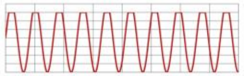	yes	↓	↓	↓	↓
	Asymmetric Slip	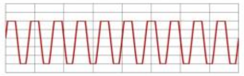	yes	↓	high (Slip)	large (Slip)	high (Slip)
	Symmetric Slip	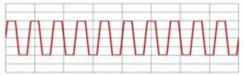	yes	fast			

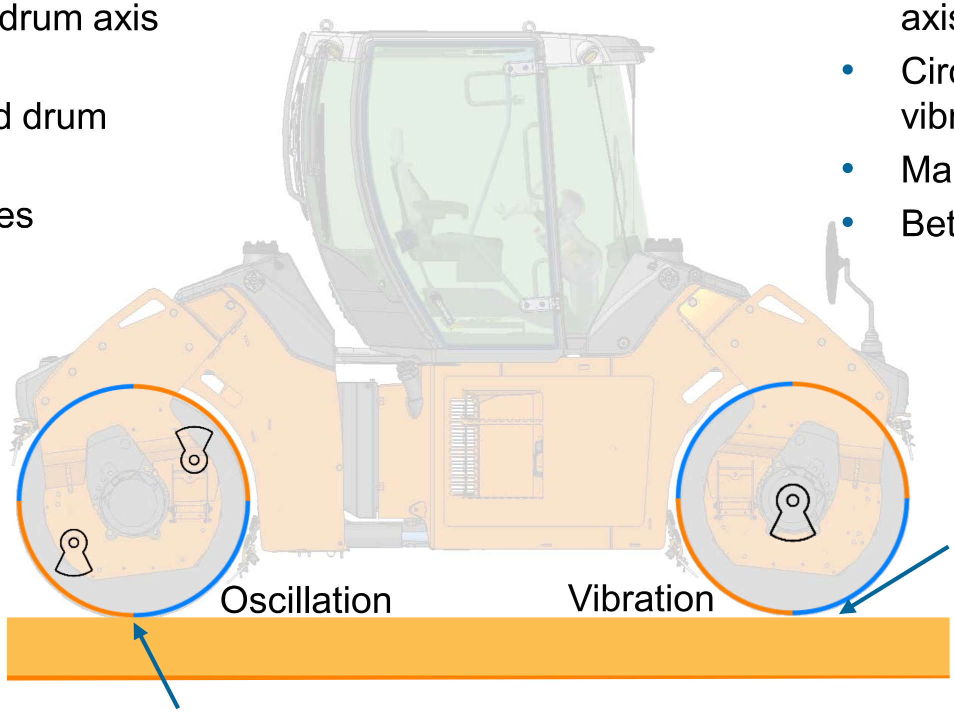

Modes of operation:
Stick, One-sided Slip, Asymmetric Slip, Symmetric Slip

Modes of operation:
Continuous Contact, Partial Uplift, Double Jump, Rocking Motion, Chaos

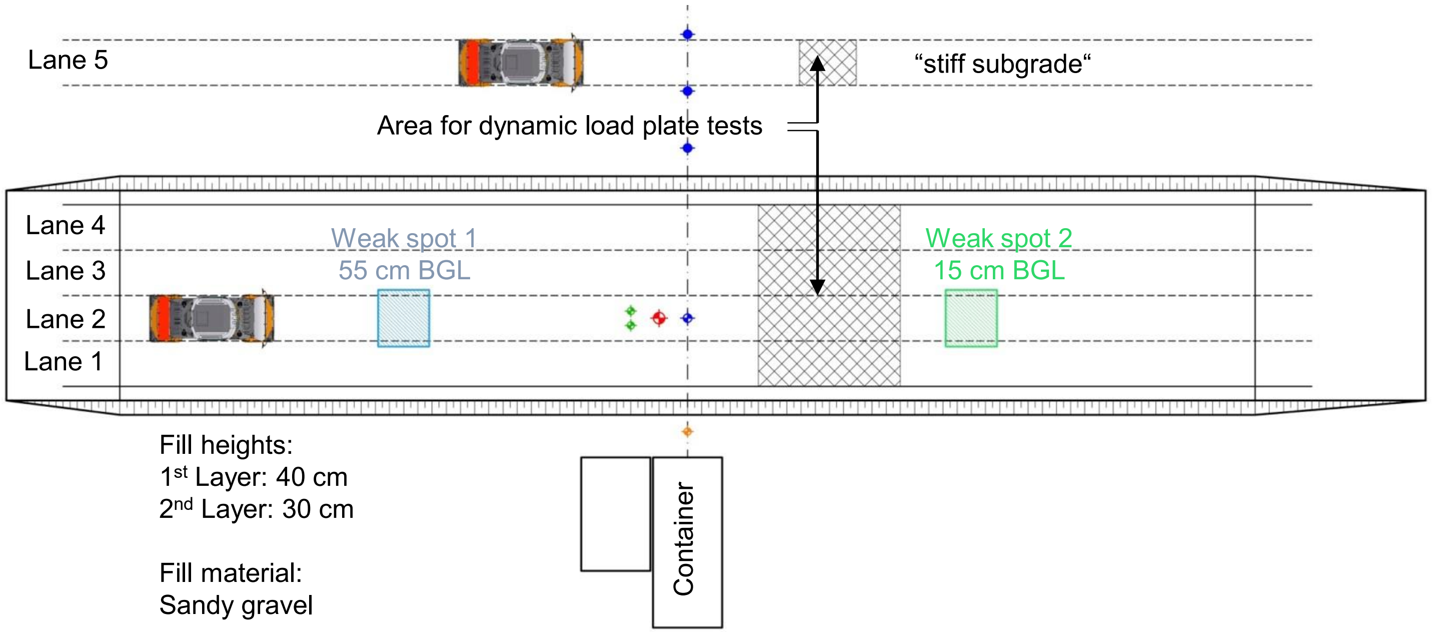

- Tri-axial accelerometer 70 cm BGL
- Tri-axial accelerometer on the surface
- Deformation measurement device
- Dynamic earth pressure cell 70 cm BGL
- Reference point of geodetic levelling

Compaction device:
HAMM HD$^+$ 90 VO tandem roller (ca. 9.8 t)

Vibration (ca. 1.9 t drum mass):
Small amplitude: 0.34 mm at 50 Hz
Large amplitude: 0.62 mm at 40 Hz

Oscillation (ca. 1.9 t drum mass):
Tangential amplitude: 1.44 mm at 39 Hz

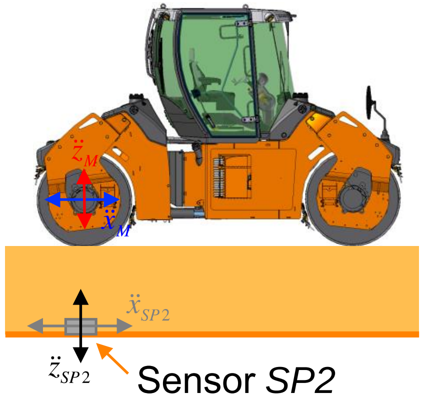

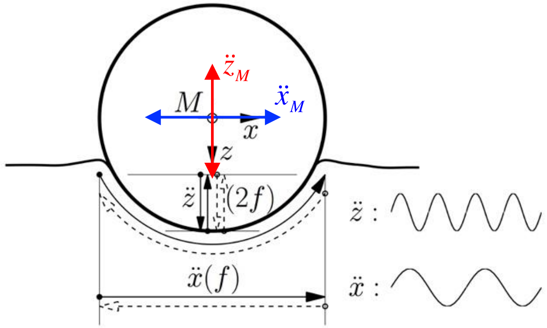

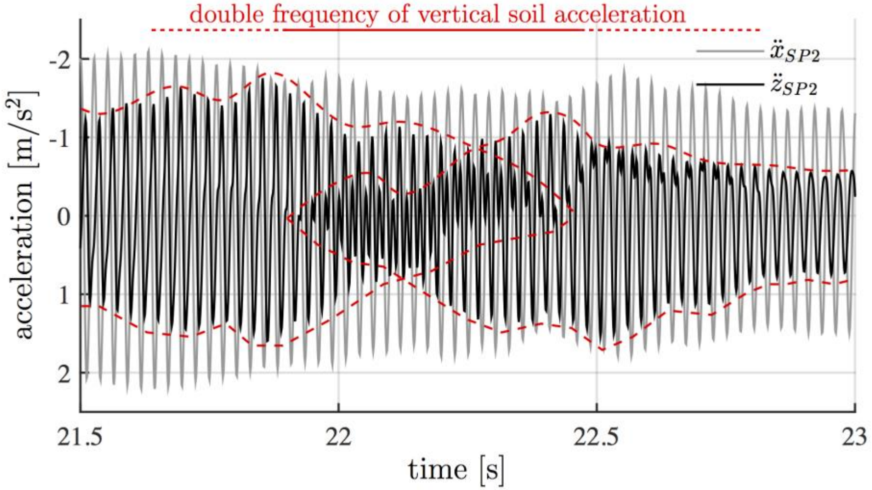

Accelerations in the bearing of the drum (point *M*):

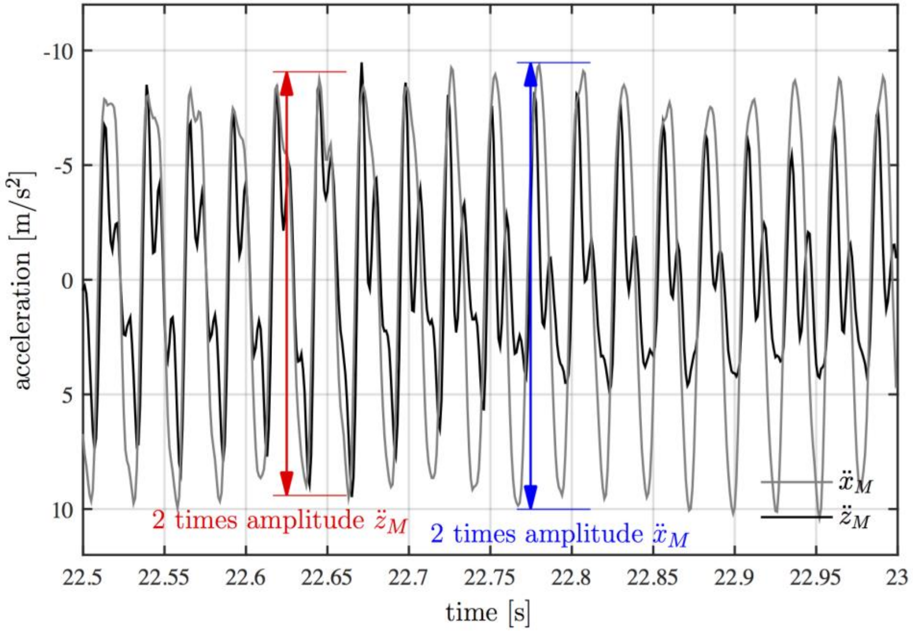

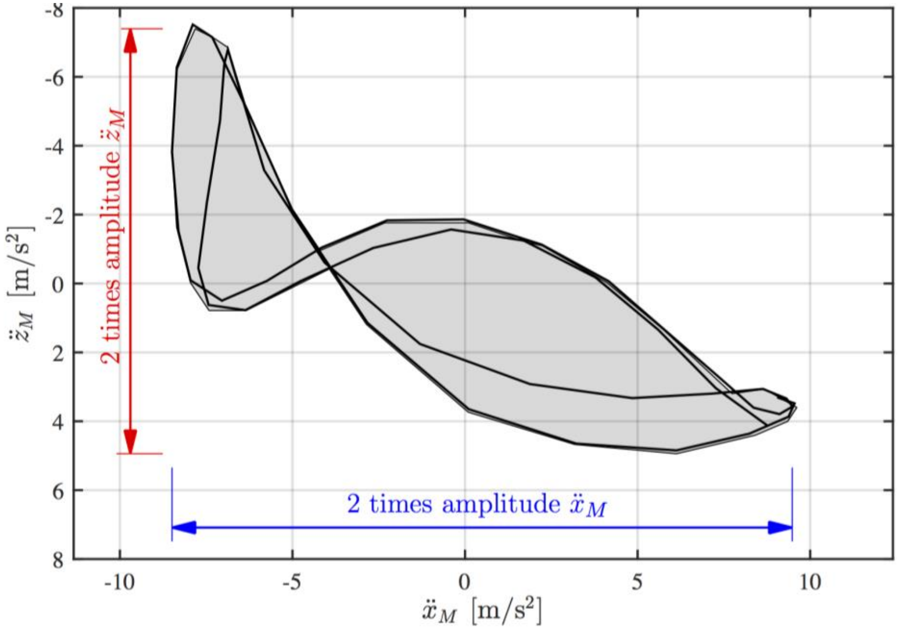

Motion behaviour of point *M*:

Rotary motion:

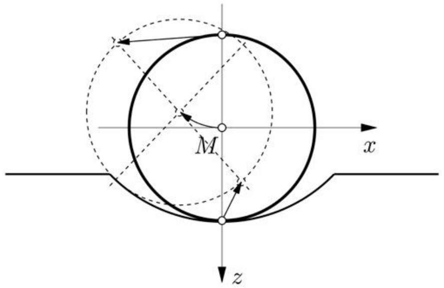

Mode of operation **Stick**

Translatory motion:

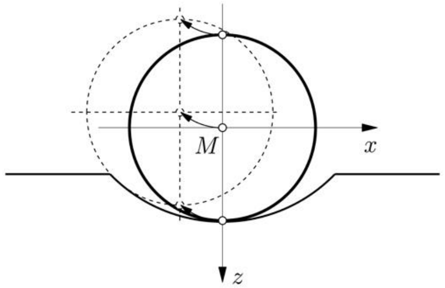

Mode of operation **Slip**

Mode independence!

Formulation of the equations of motion:

$$m\ddot{x}_A + \frac{mr(R-r)}{R}\ddot{\theta} - \frac{mr^2(R-r)}{R^2}\dot{\theta}^2\theta + k_H x_A + c_H \dot{x}_A = 0$$

$$(m+\Delta m)\ddot{z}_A - \frac{mr(R-r)}{R}\frac{r}{R}\ddot{\theta}\theta - \frac{mr^2(R-r)}{R^2}\dot{\theta}^2 + k_V z_A - mg + c_V \dot{z}_A = F_z$$

$$\left[I + \frac{mr^2(R-r)^2}{R^2}\right]\ddot{\theta} + \frac{mr(R-r)}{R}\ddot{x}_A - \frac{mr^2(R-r)}{R^2}\ddot{z}_A\theta + mg(R-r)\frac{r^2}{R^2}\theta = M_0 \sin(\xi t)$$

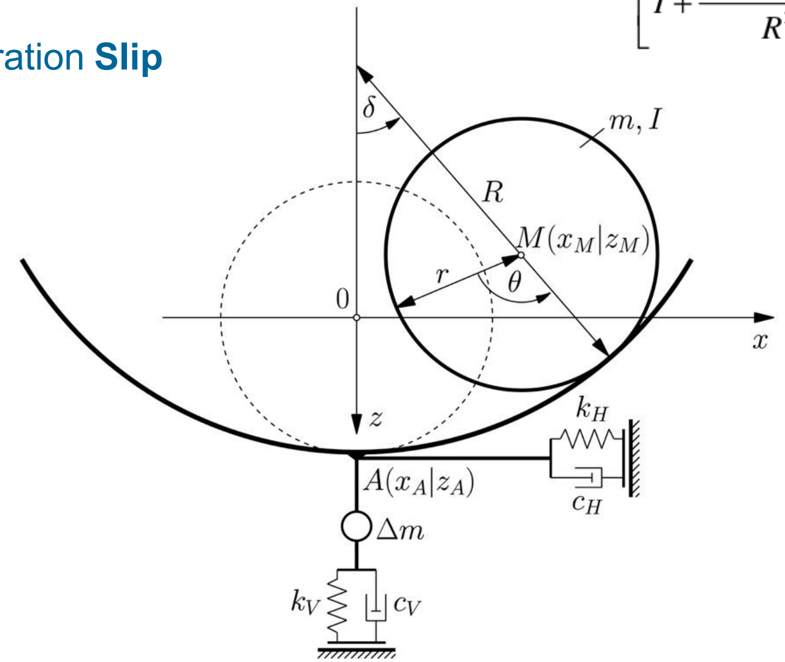

Mechanical model

- Results of the experimental measurements:

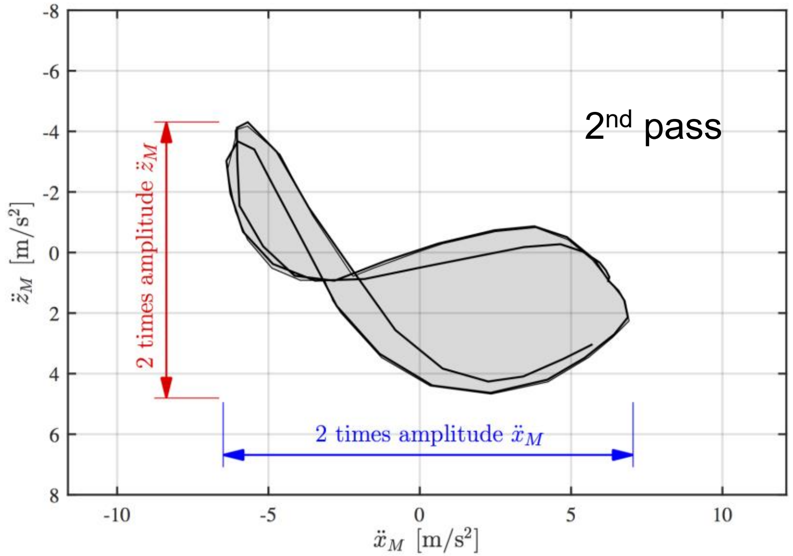

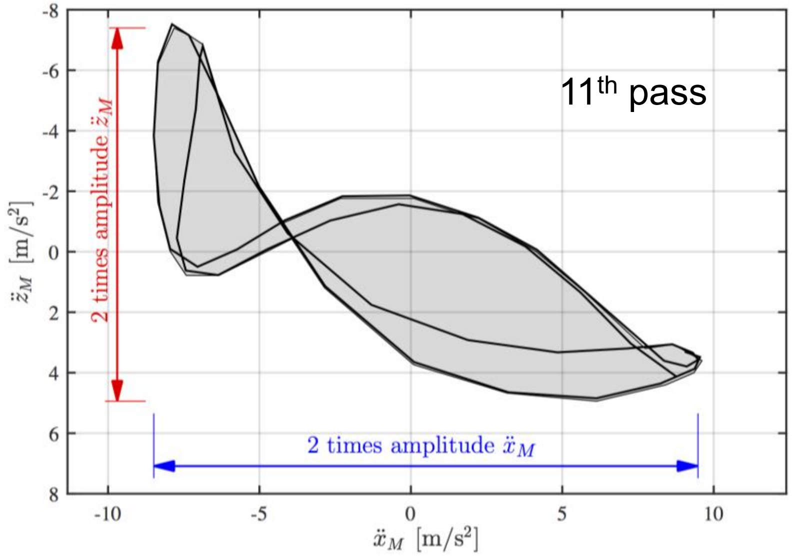

- Results of the model analysis:

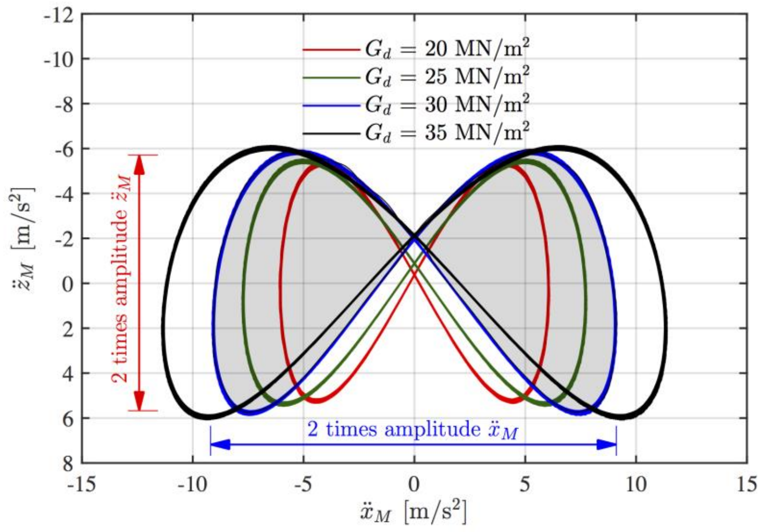

- Expansion of the eight shape
  - with increasing number of passes
  - with increasing soil stiffness
- Distortion of the shape caused by travelling motion
- Characterisation of the shape = possible CCC
- Definition: area of the shape = CCC value for oscillating rollers

Application of the CCC algorithm on acceleration measurements:

2nd layer, lane 2, Oscillation, f = 39 Hz, v = 4 km/h

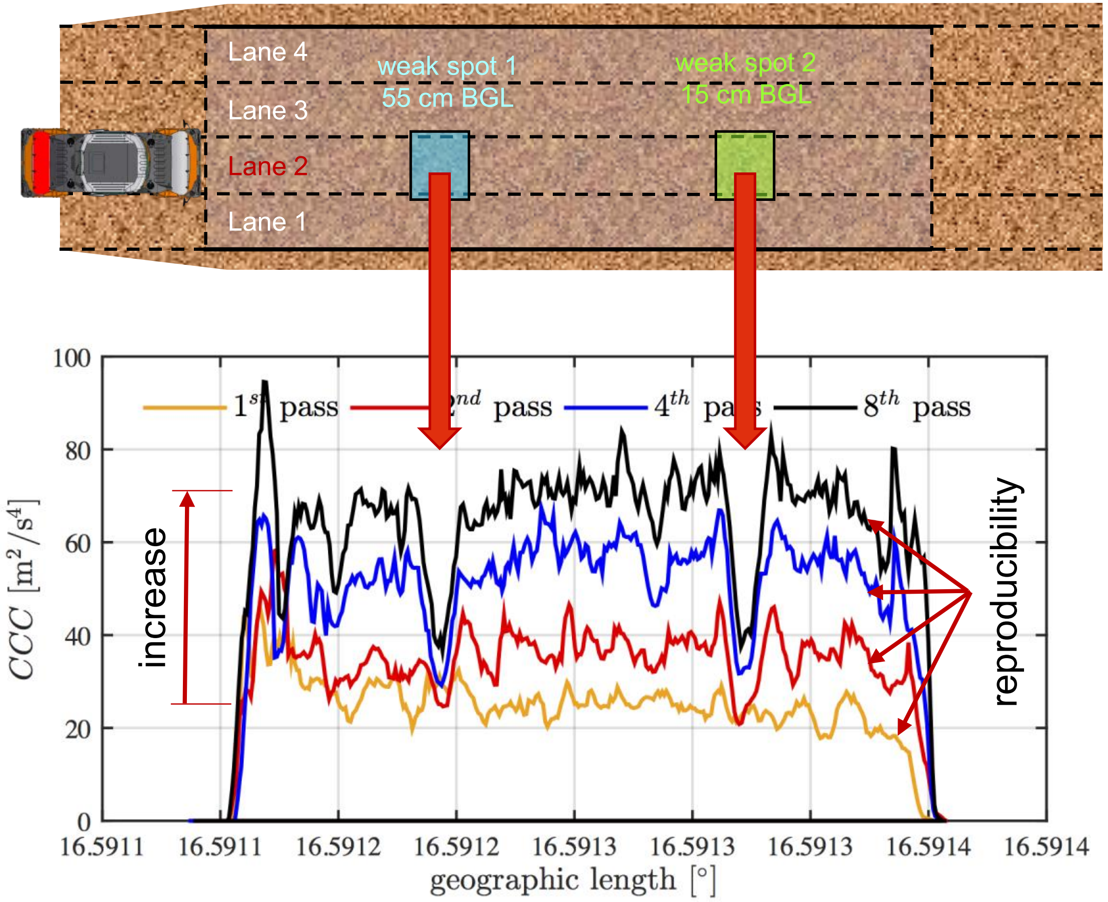

Comparison to dynamic load plate tests:

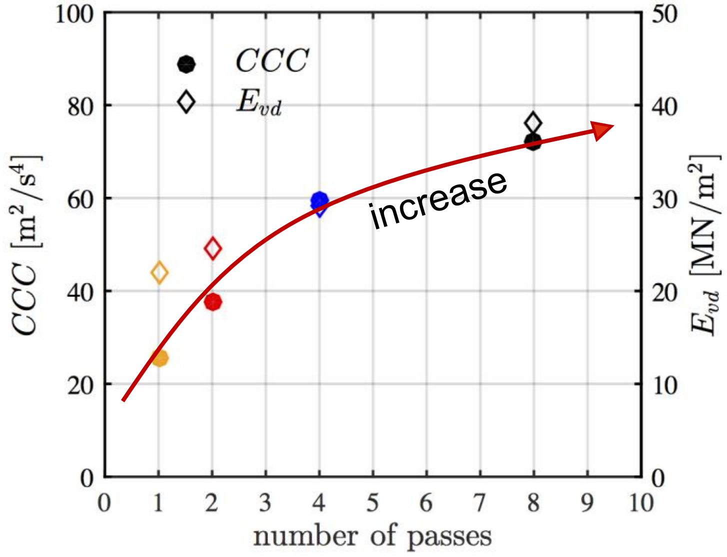

Dynamic Rollers in Earthworks: Compaction and Continuous Compaction Control

Johannes Pistrol[1], Dietmar Adam[1]

1. *Vienna University of Technology, Austria*

University of Minho
School of Engineering

SIMSG ISSMGE

GEO-INSTITUTE TRB

Workshop 4
Ground Improvement and Soil Stabilization
Keynote Lecture

Performance of test embankment under vacuum consolidation: numerical analysis

Marcio Almeida[1], Esther Marques[2],

Leonardo Deotti[1], Maria Cascão[1]

Instituto Alberto Luiz Coimbra de Pós-Graduação e Pesquisa de Engenharia
COPPE UFRJ

1. *Federal University of Rio de Janeiro*
2. *Military Institute of Engineering*

EXÉRCITO BRASILEIRO
IME
INSTITUTO MILITAR DE ENGENHARIA

Objectives:

- To present the numerical prediction of the behaviour of a test embankment on structured clay subjected to vacuum and embankment loading.
- To show some recent case studies performed in Norh and South America

Marques (2001), D.Sc. COPPE – Test embankment: site investigation, soil parameters, field monitoring

Deotti (2015), D.Sc. COPPE – Numerical modelling of test embankment under vacuum loading

Contents:

Vacuum consolidation on soft soils

- Originally proposed by Kjellman (1952);
- Successfully used in different parts of the world: Cognon, 1991; Cognon et al., 1994; Jacob et al., 1994; Chu et al., 2000; Marques, 2001; Indraratna et al 2005; Chai and Carter, 2011;
- Two vacuum application methods used in Geotechnics:

a) Air-tight Sheet Method

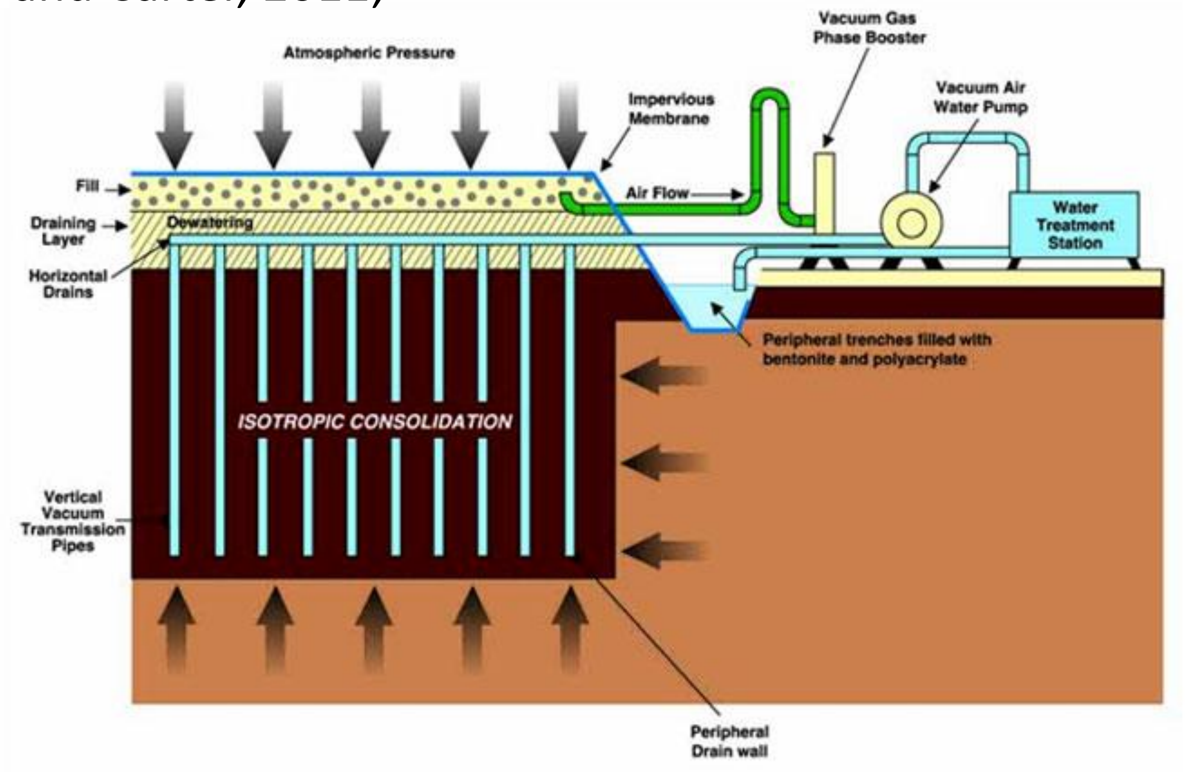

Vacuum consolidation on soft soils

b) Vacuum-Drain Method

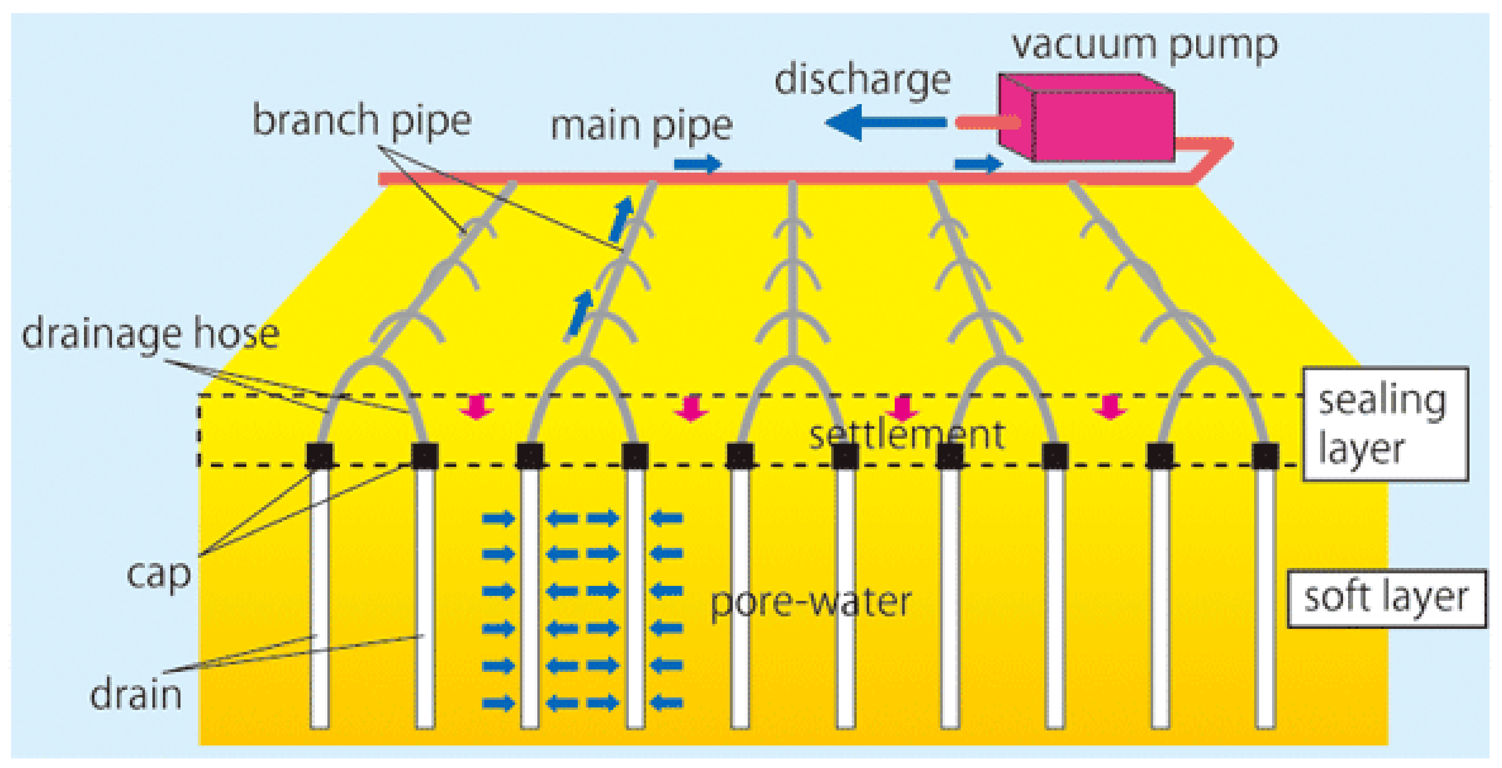

Conventional pre-loading fill vs. Vacuum consolidation method

$\sigma' = \sigma - u$

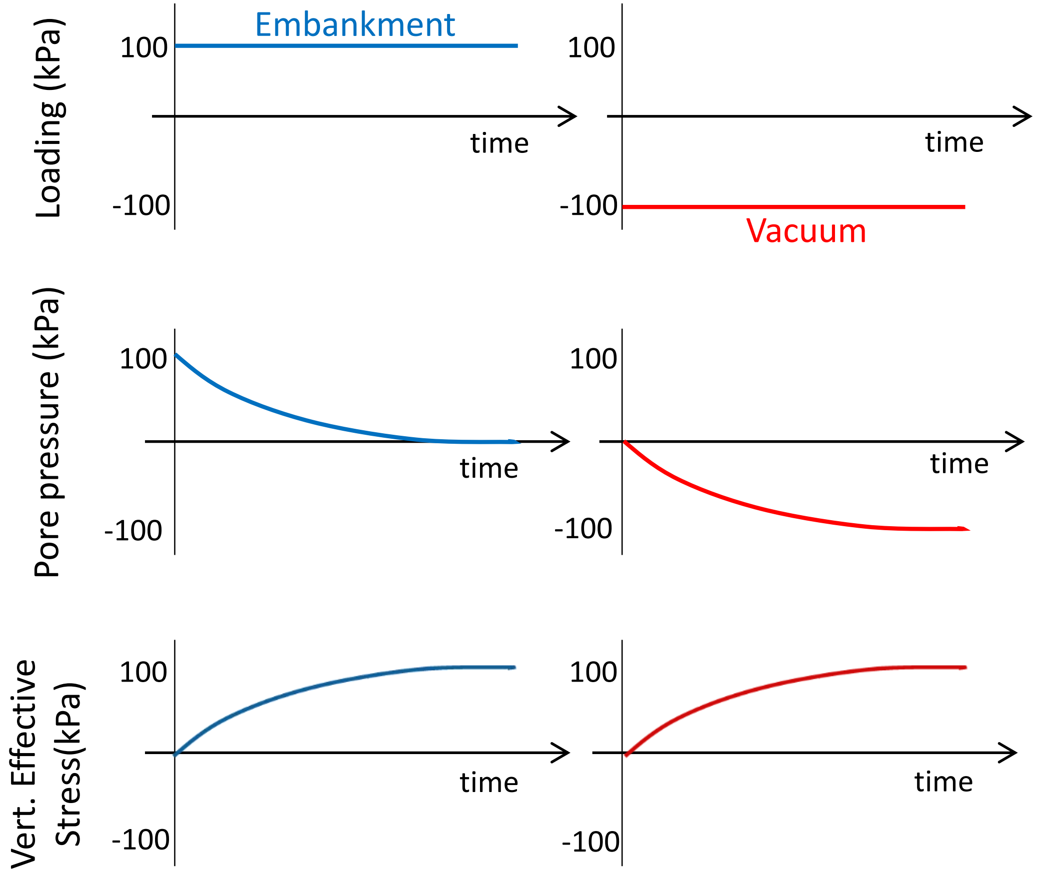

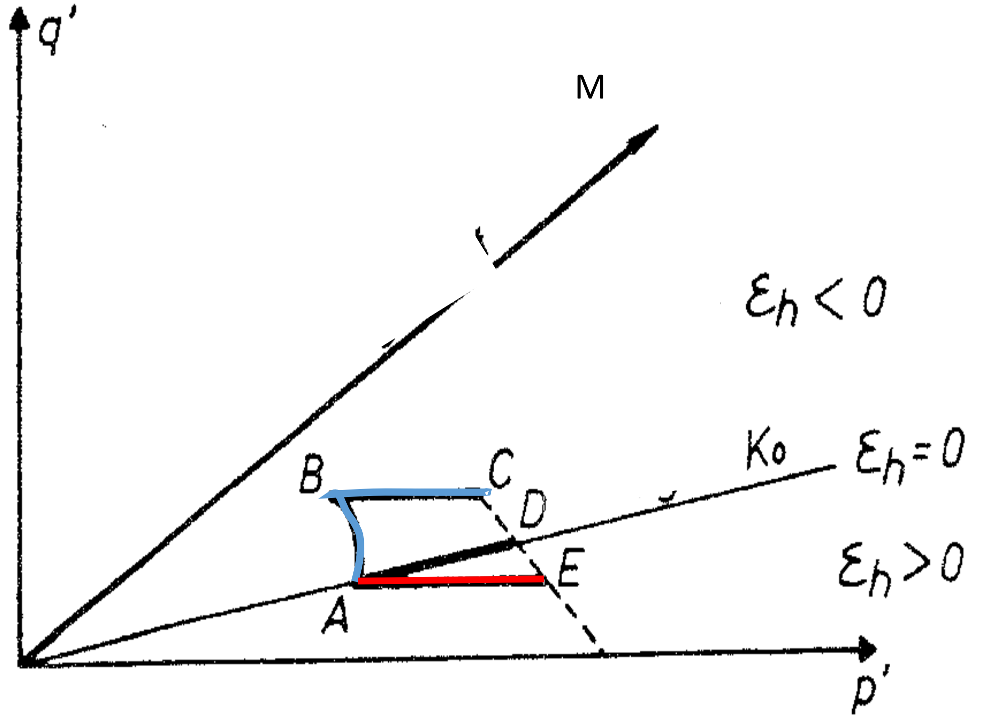

Advantages

- It is the most suitable solution at sites where stability is a concern (failure does not occur under pure vacuum consolidation);
- Hydrostatic suction results in "negative" horizontal displacements in theory;
- Vacuum consolidation requires less volumes of fill material;

Disadvantages

- Special electrical system and periodic maintenance are required;
- It is not an economic technique in cases of small embankments.

Saint-Roch-de-l'Achigan trial embankment

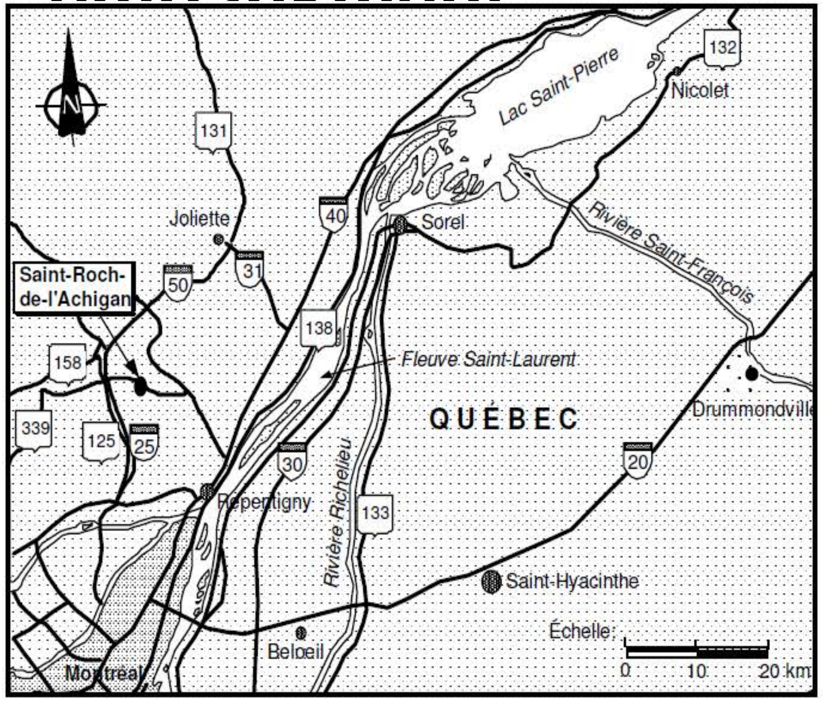

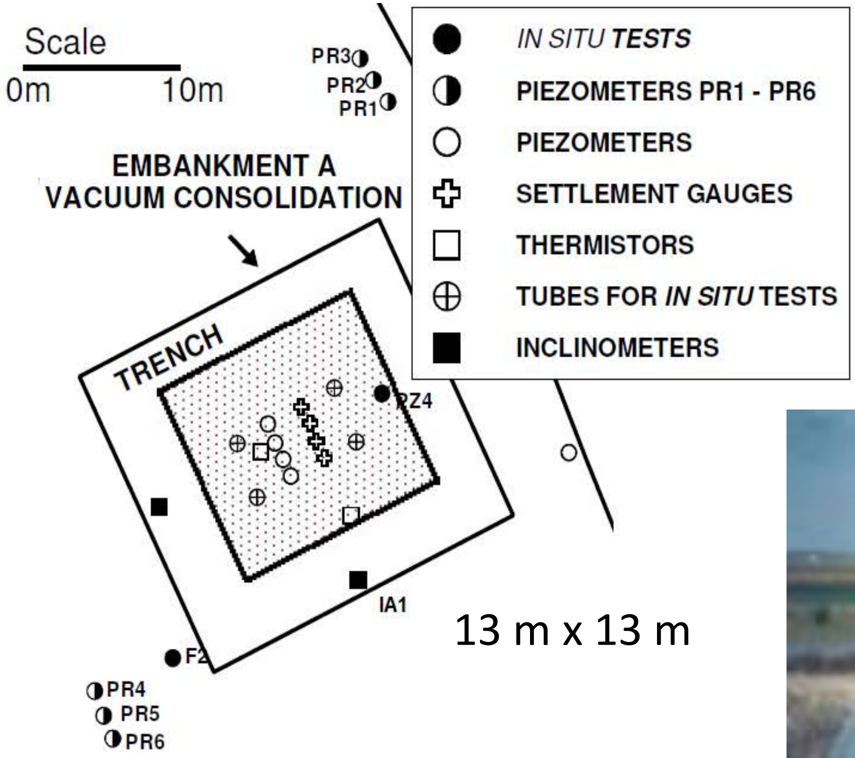

13 m x 13 m

Embankment A - vacuum

Embankment B - vacuum + heating

Cooperation Laval Univ. – Federal Univ. of Rio de Janeiro
Marques (2001) DSc

Saint-Roch-de-l'Achigan trial embankment

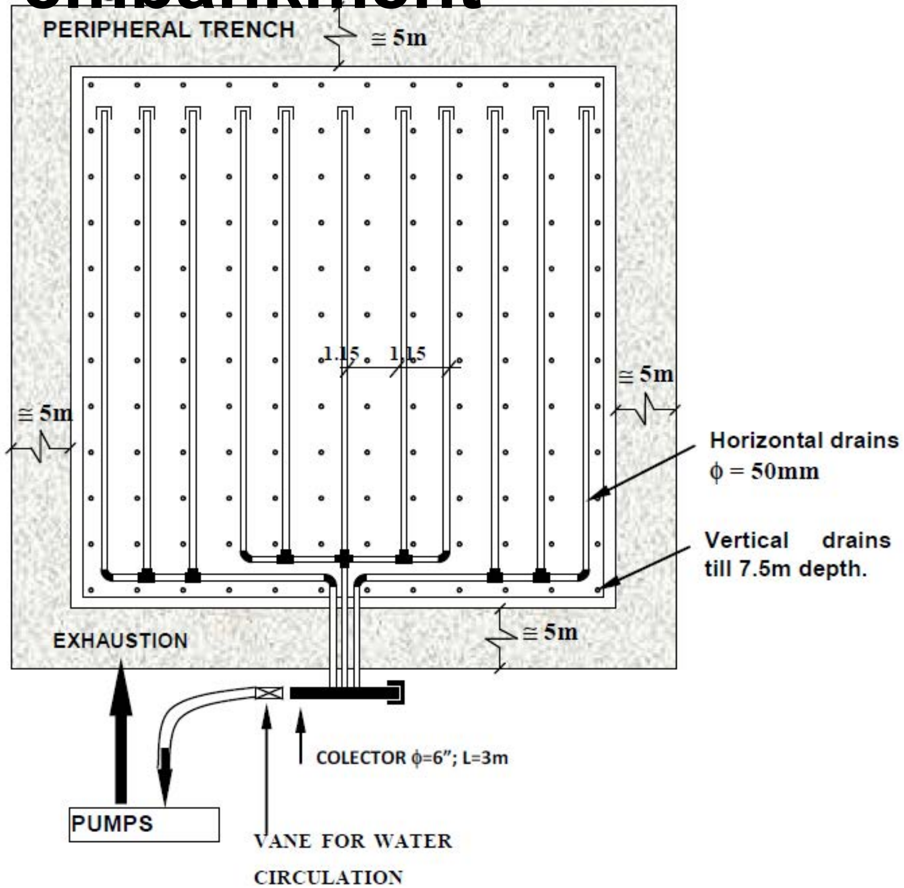

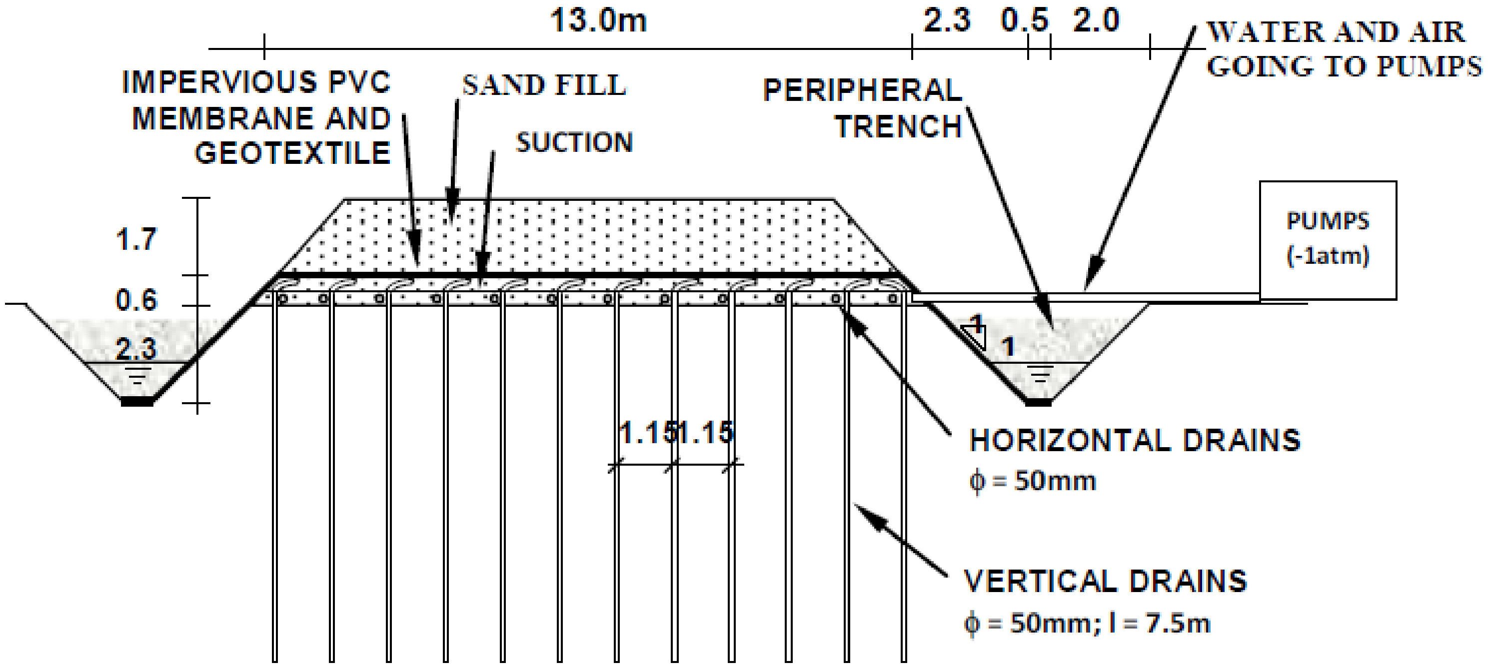

Saint-Roch-de-l'Achigan trial embankment

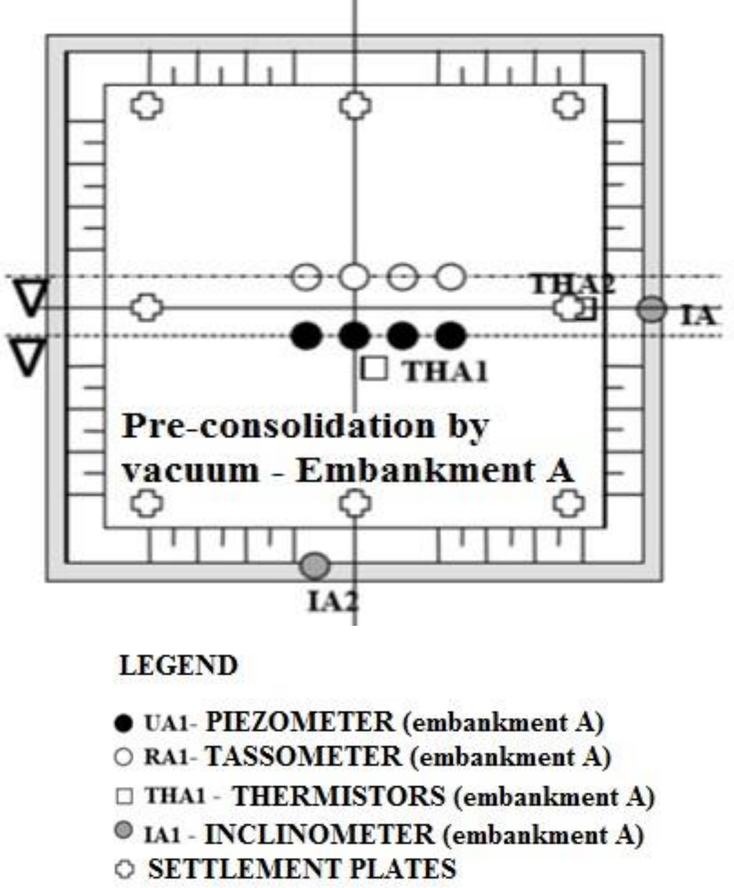

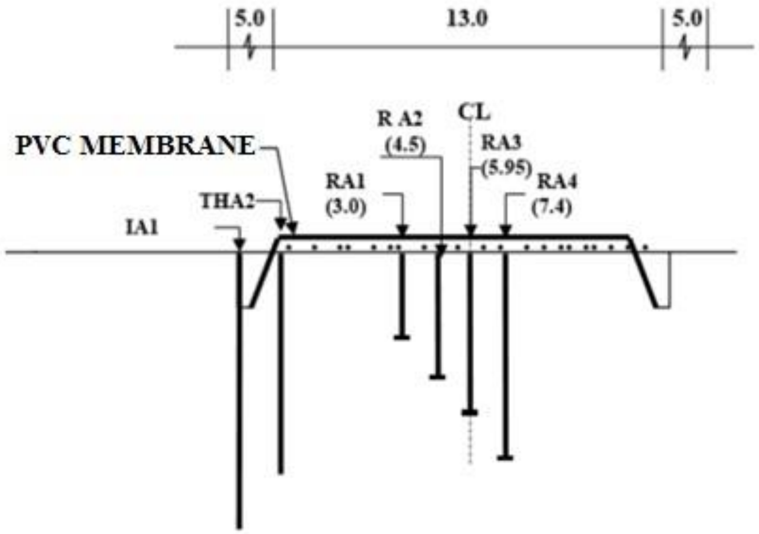

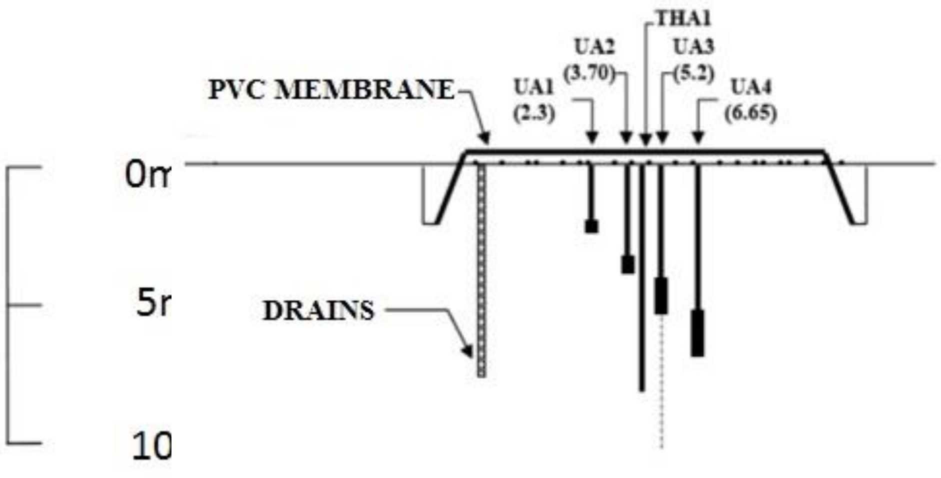

Geotechnical Characteristics

CPTu
Vane tests
Index tests
Oedometer tests
Triaxial tests

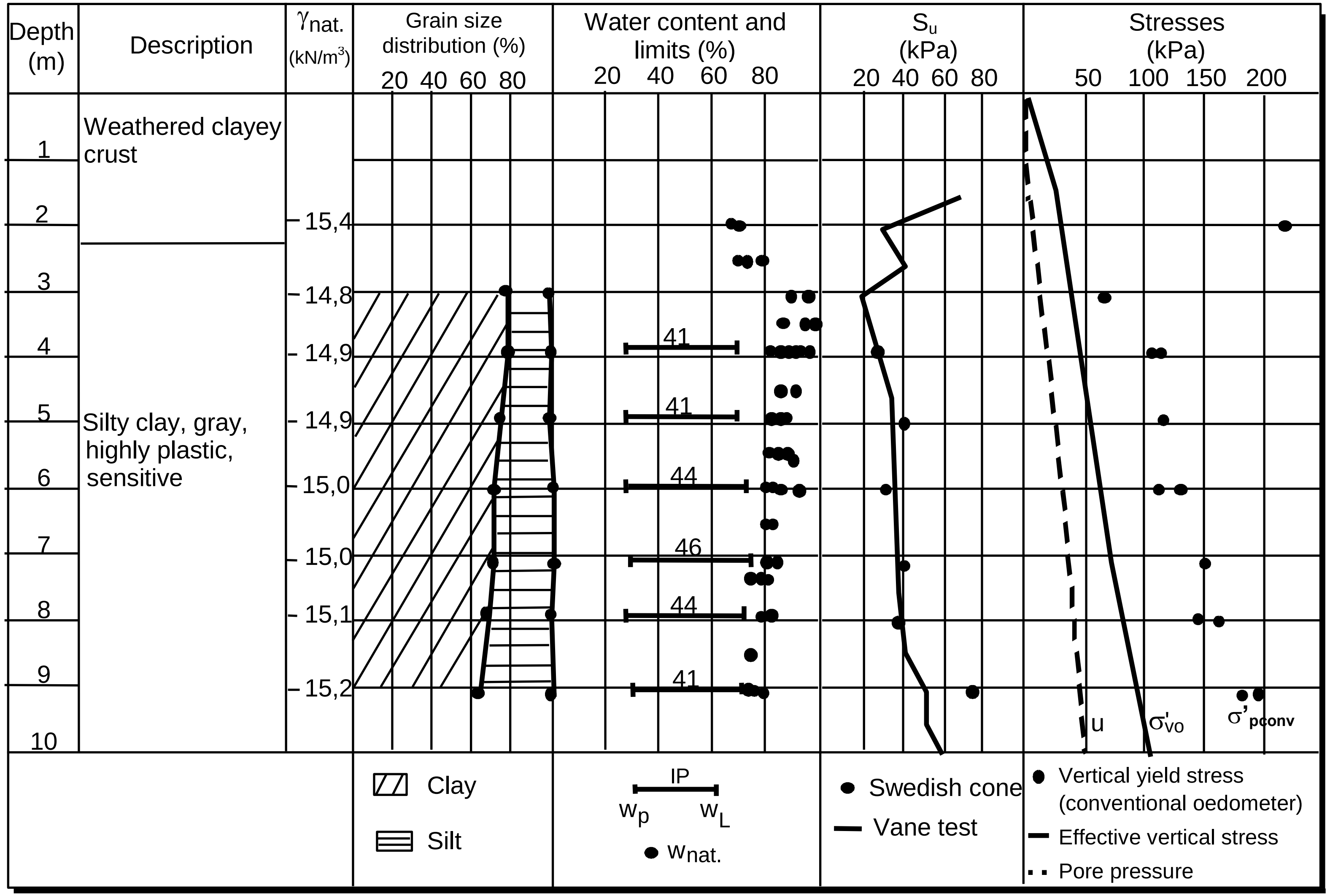

Non hydrostatic water level (piezometer data)

+

Low water table

≅ 1.5 m bellow GL

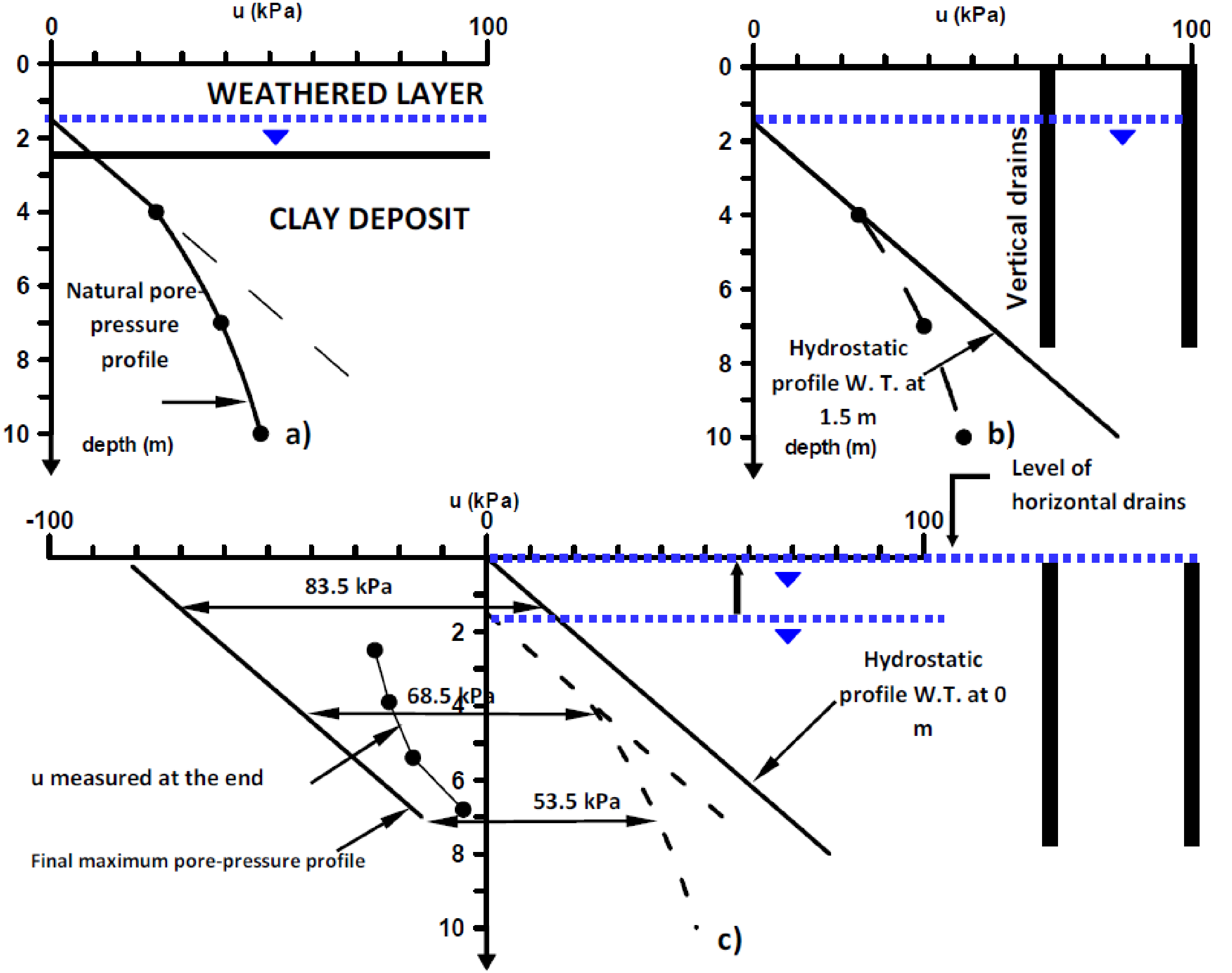

Construction stages

Stages	H embank. (m)	T days after vacuum	Comments
A1	0.0	-	Before drains installation. Non-hydrostatic profile WL= -1.5 m
A2	0.3	-	20 cm excavation, 30cm embankment and drains installation
A3	0.6	-	30 cm embankment and placement of PVC membrane
A4	0.6	-	Excavation of trenches
A5	0.6	0	Vacuum application
A6	0.6	11	Problems on vacuum application system
A7	1.37	22	70 cm sand fill and 7cm gravel
A8	2.37	62	1m sand fill
A9	2.37	144	Problems on vacuum application system
A10	2.37	159	End of vacuum application.

Construction stages

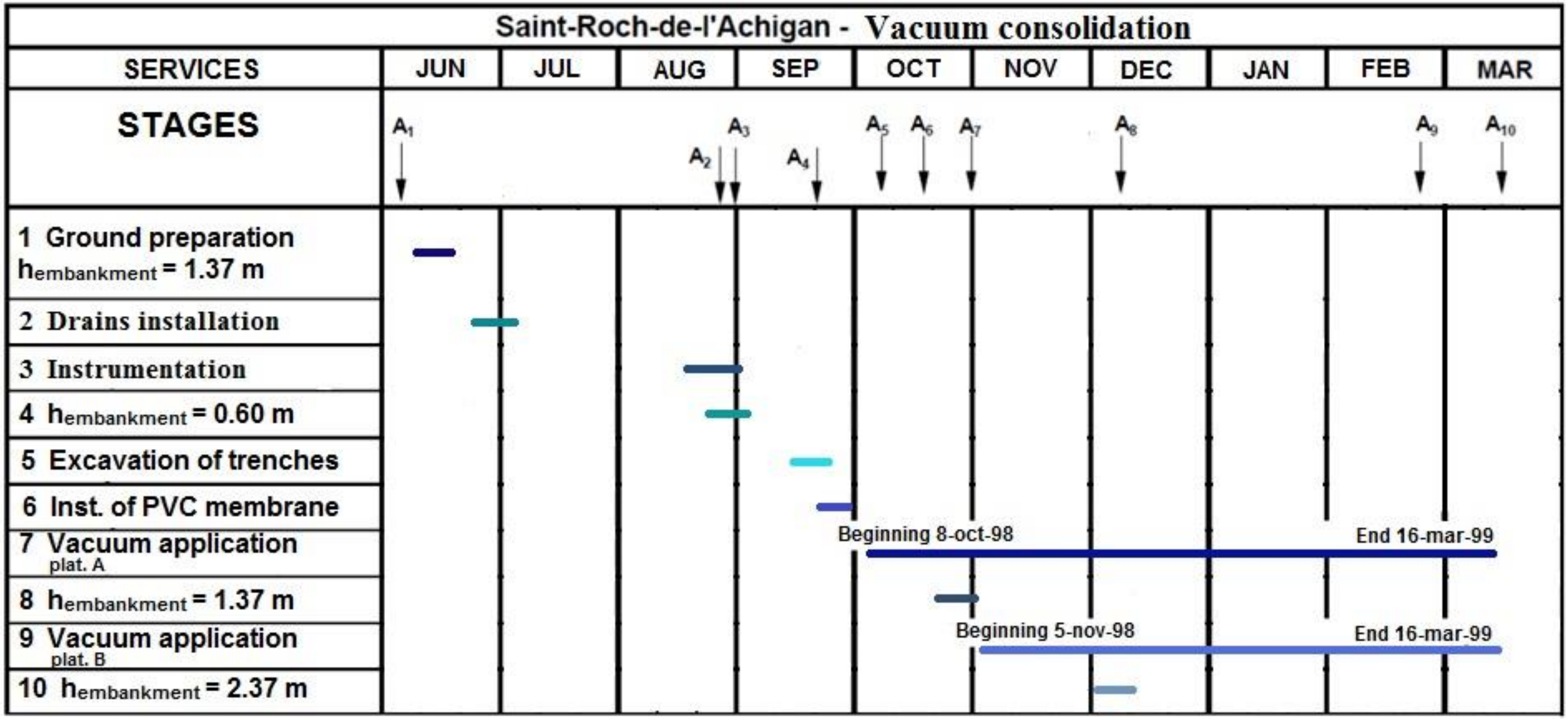

Elastoplastic model (S-CLAY 1S)

Saint-Roch-de-l'Achigan Clay: structured behaviour

S-CLAY 1S model (Koskinen et al., 2002):

- Based on the Modified Cam Clay model
- Able to represent the anisotropy and structure in normally and slightly overconsolidated clays

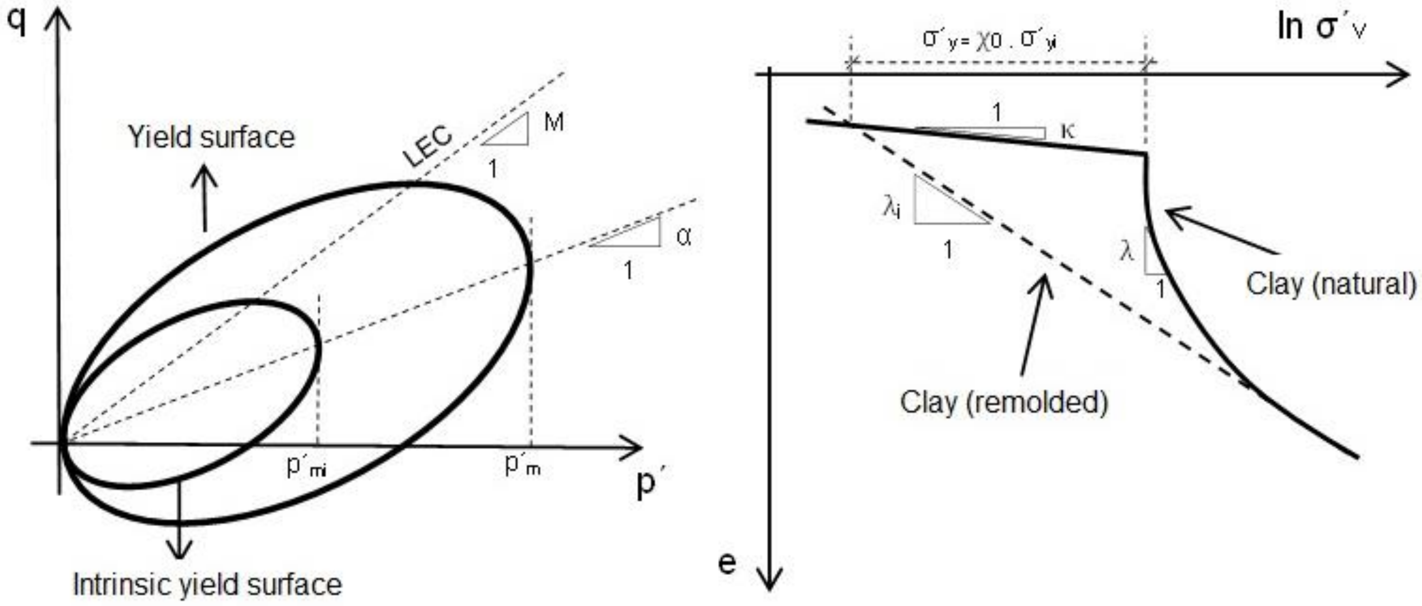

Determination of the soil profile and geotechnical parameters

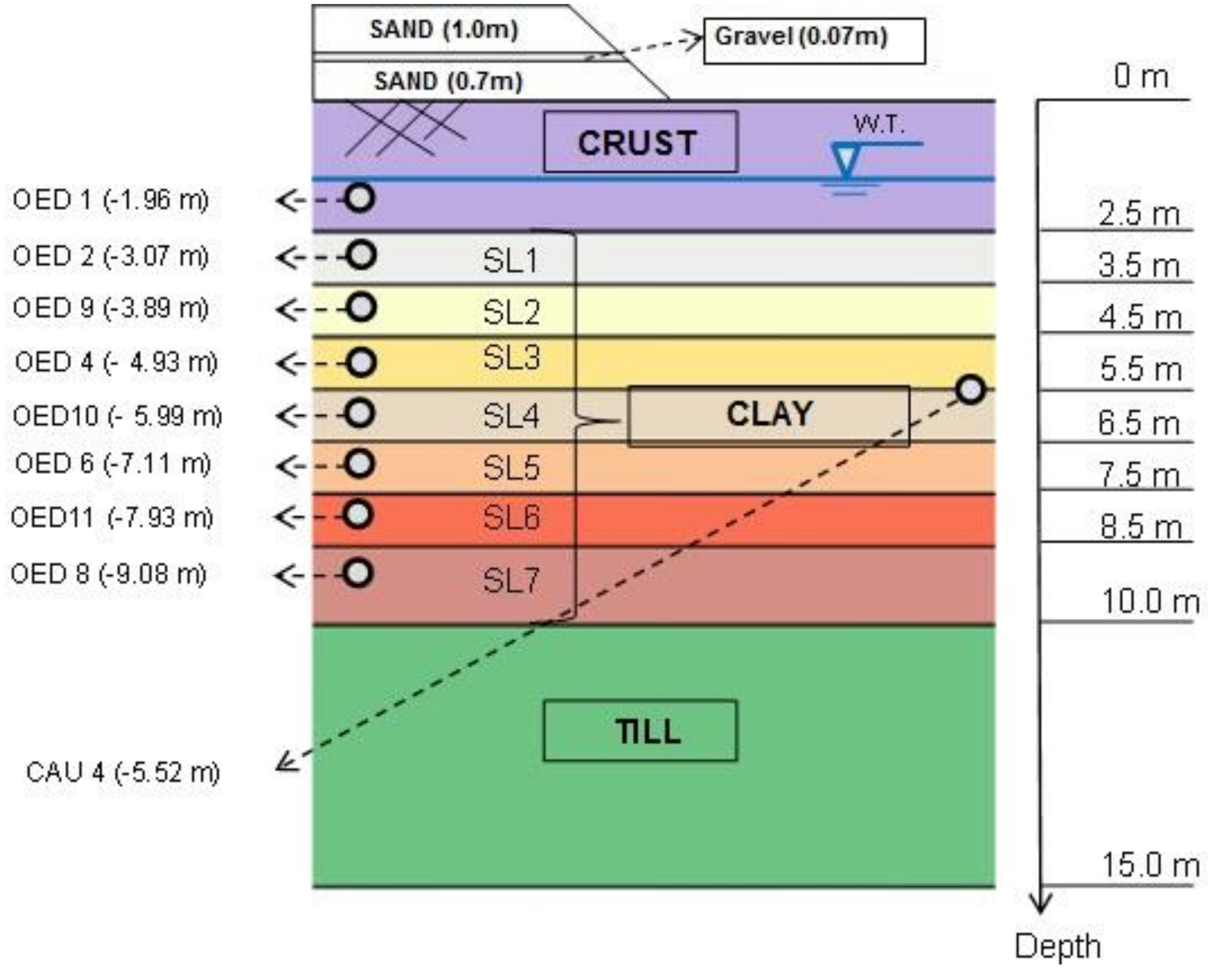

Sand, Gravel & “Till”:
MC model

Crust:
MCC Model

Clay:
S-CLAY 1S model

Material parameters

Mod. Cam-Clay Model

	Crust
Depth (m)	0.0 - 2.5
σ´$_p$ (kPa)	240.00
e_0	2.00
e_{v0}	1.95
k_{vo} (m/s)	2.00E-09
C_k	1.14
κ	0.02
λ	0.6
M	1.545
$\nu´$	0.2

Mohr Coulomb Model

	Till	Sand	Gravel
Depth (m)	10.0 – 15.0	-	-
γ_n(kN/m3)	15.0	19	19
e_0	0.50	0.50	0.5
k_{vo} (m/s)	5.00E-06	1.00E-03	1.00E-03
$\varphi´_{cv}(^\circ)$	40	30	35
$\nu´$	0.30	0.30	0.30
E (kPa)	1.00E-07	1.00E-05	1.00E-06
c´ (kPa)	1	5	5

SCLAY1-S Model

	SL1	SL2	SL3	SL4	SL5	SL6	SL7
Depth (m)	2.5 - 3.5	3.5 - 4.5	4.5 - 5.5	5.5 - 6.5	6.5 - 7.5	7.5 - 8.5	8.5 - 10.0
σ´$_p$ (kPa)	66.50	102.6	108.3	106.4	141.5	150.1	180.5
e_0	2.54	2.47	2.46	2.40	2.40	2.34	2.19
e_{v0}	2.47	2.37	2.36	2.30	2.32	2.16	2.08
k_{vo} (m/s)	2.0E-09	3.3E-09	3.2E-09	2.2E-09	1.6E-09	1.8E-09	2.3E-09
C_k	1.04	1.03	1.04	1.11	1.22	1.02	0.97
κ	0.02	0.04	0.04	0.04	0.02	0.04	0.04
λ	0.90	1.34	1.20	1.06	1.13	1.13	1.21
χo	25.71	9.66	9.66	9.66	9.66	9.66	9.66
λ_i	0.22	0.28	0.22	0.28	0.27	0.27	0.23
μ	6.67	11.20	12.55	14.20	13.27	13.27	12.7
a	12.00	12.00	12.00	12.00	12.00	12.00	12.00
b	0.25	0.25	0.25	0.25	0.25	0.25	0.25
η_{K_o}	1.040	1.040	1.040	1.040	1.040	1.040	1.040
M	1.545	1.545	1.54	1.545	1.545	1.545	1.545
α_{K_o}	0.605	0.605	0.605	0.605	0 605	0.605	0.605
β	1.013	1.013	1.013	1.013	1.013	1.013	1.013
$\nu´$	0.2	0.2	0.2	0.2	0.2	0.2	0.2

Parameter Validation - Oedometer tests – (12)

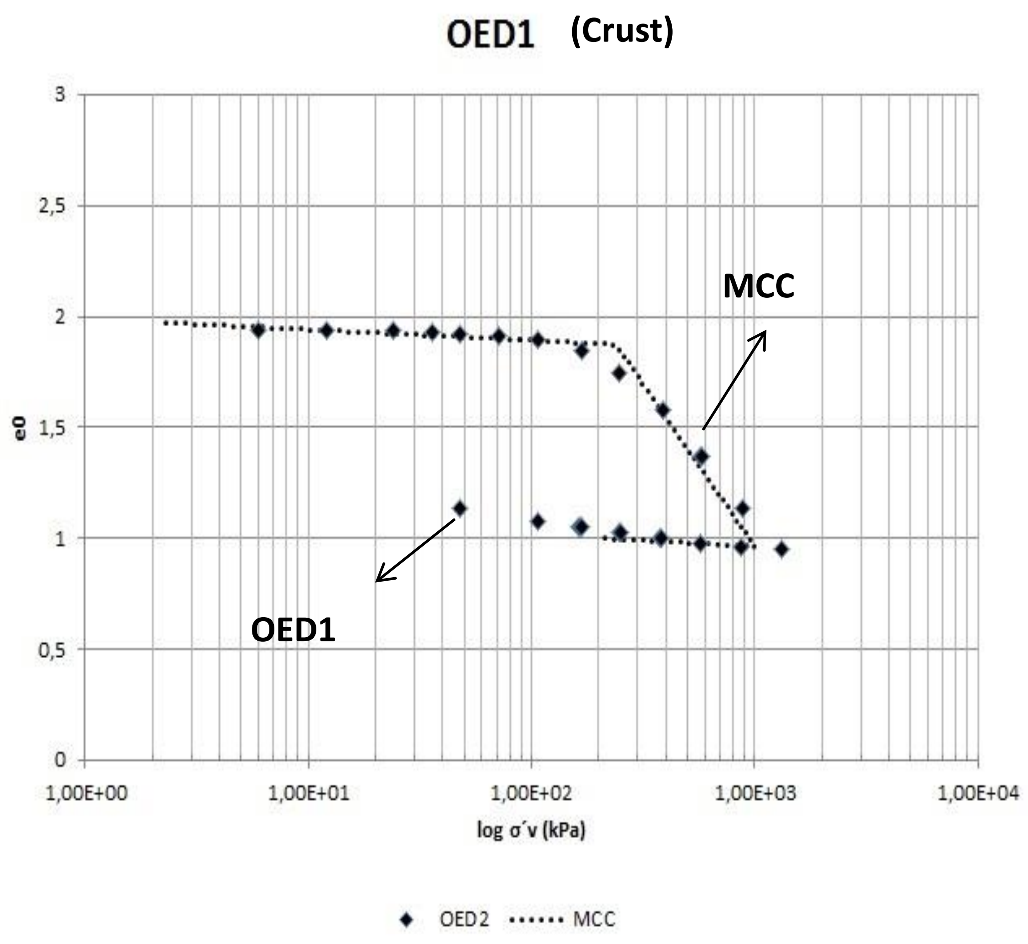

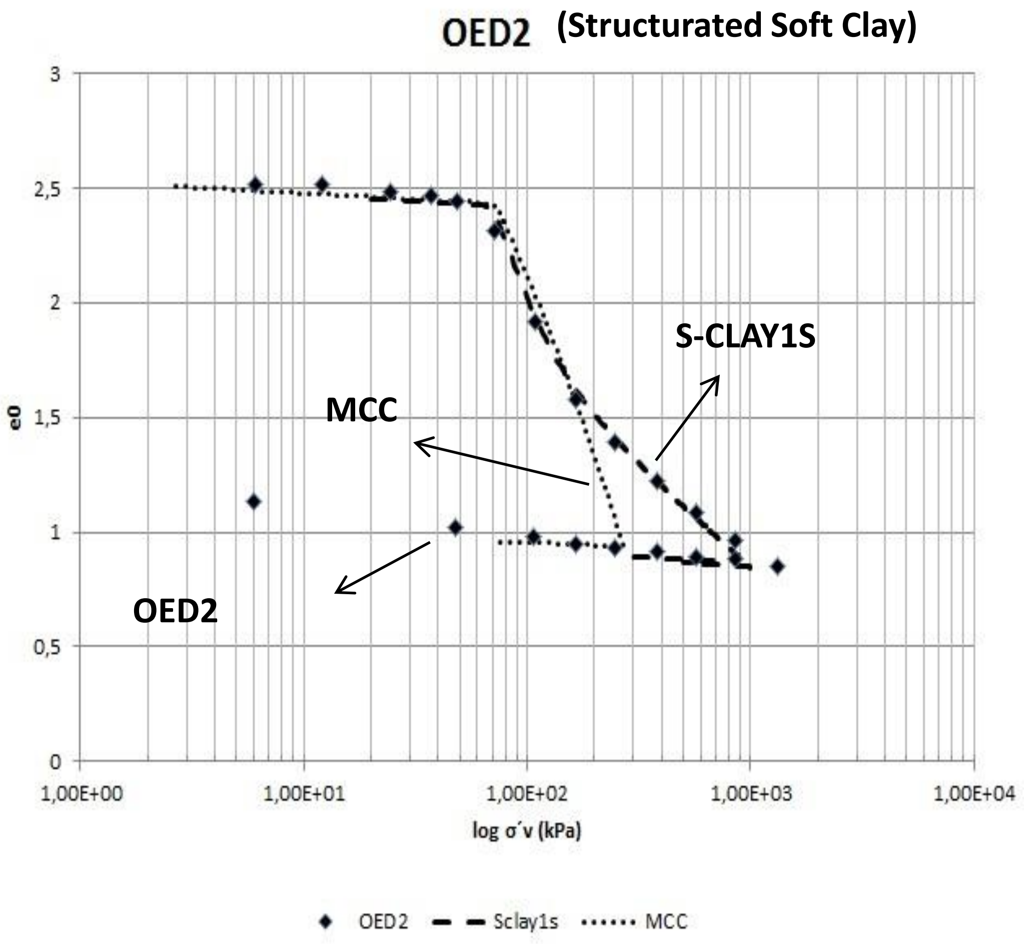

Parameter Validation - Triaxial tests (7)

CAU4

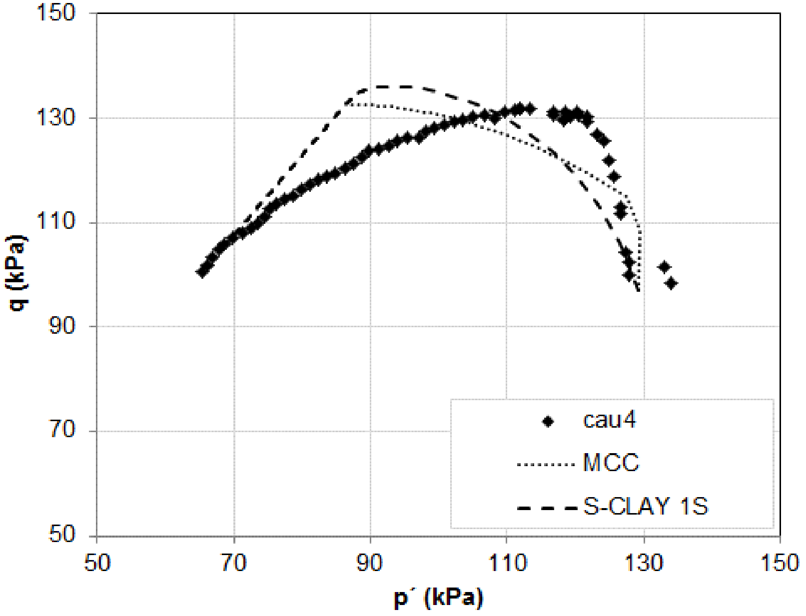

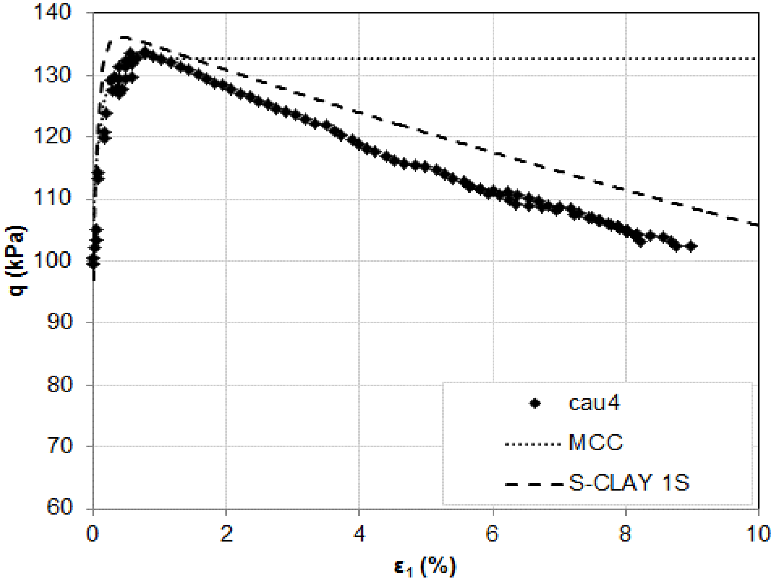

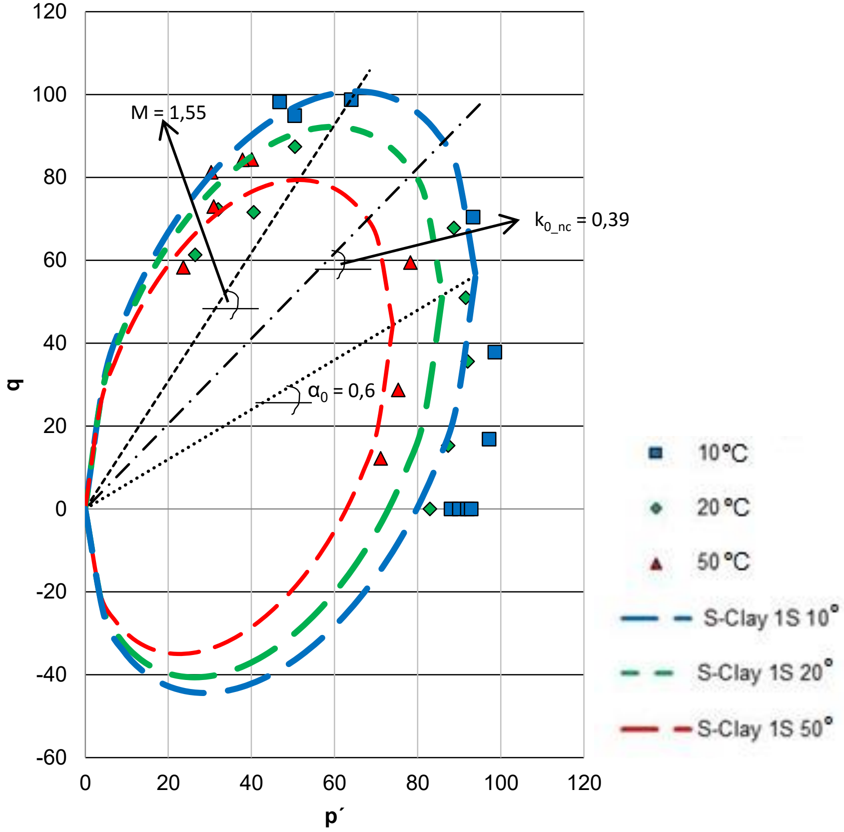

Conversion of the unit cell to the plane strain state

Hird el al. (1992)

$$\frac{k_{hp}}{k_h} = \frac{2B^2}{3R^2[ln\left(\frac{R}{r_s}\right) + \left(\frac{k_h}{ks}\right) ln\left(\frac{r_s}{r_w}\right) - \left(\frac{3}{4}\right)]}$$

	Coefficient of permeability (m/s)					
	Crust	SC 1	SC 2	SC 3	SC 4	SC 5
k_{h0}	2,00E-09	2,00E-09	3,30E-09	3,20E-09	2,20E-09	1,60E-09
$k_{h\,ps}$ (Hird)	3,37E-10	3,37E-10	5,56E-10	3,38E-10	3,7E-10	2,7E-10

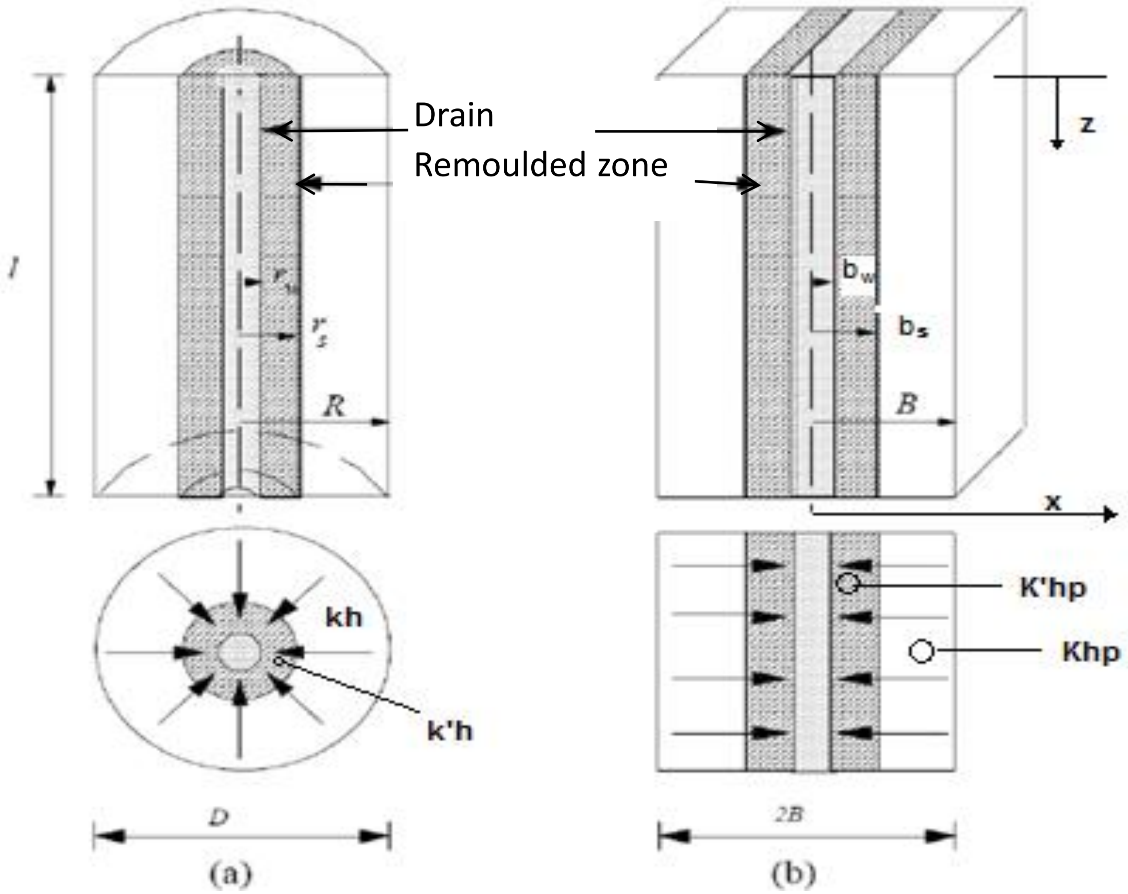

Finite element analysis

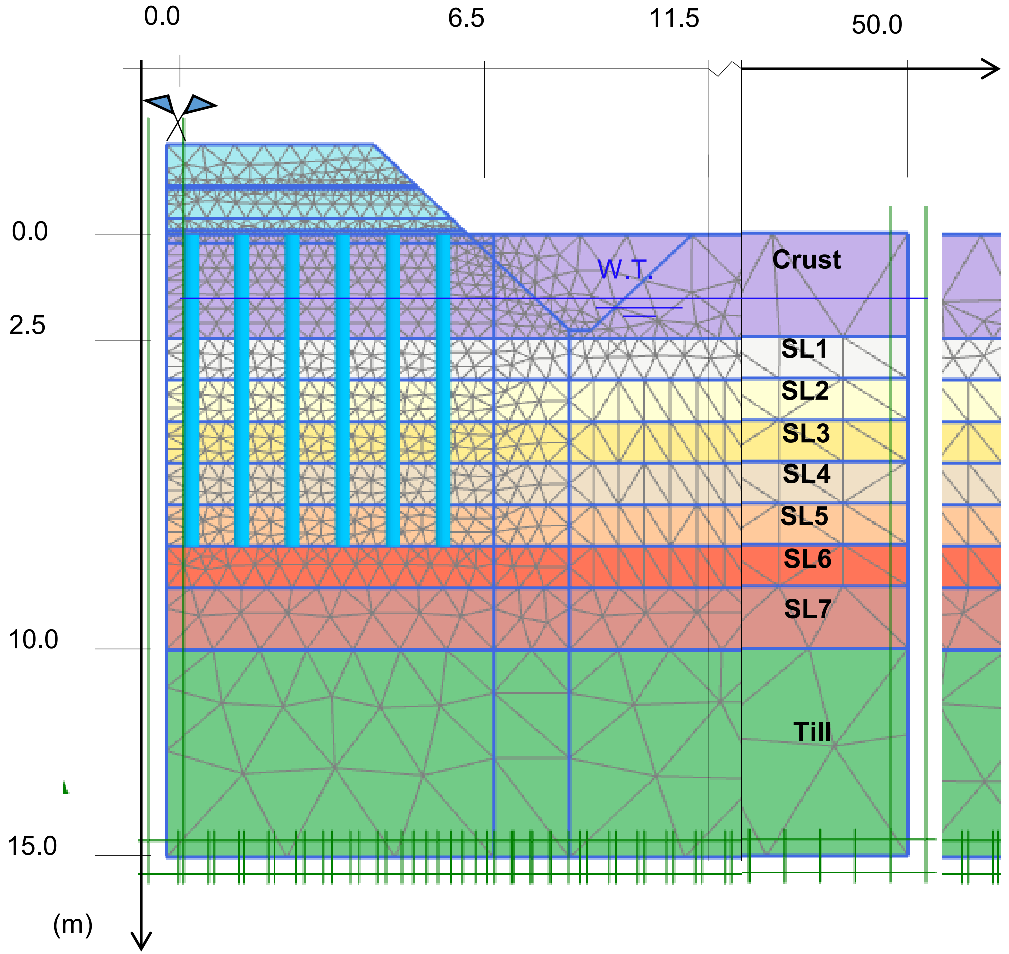

23 calculation steps were adopted to represent all (10) events involved

Original Plaxis is not able to perform Vacuum loading analysis => Plaxis-UFRJ collaboration set up for Plaxis alterations

In situ stress conditions

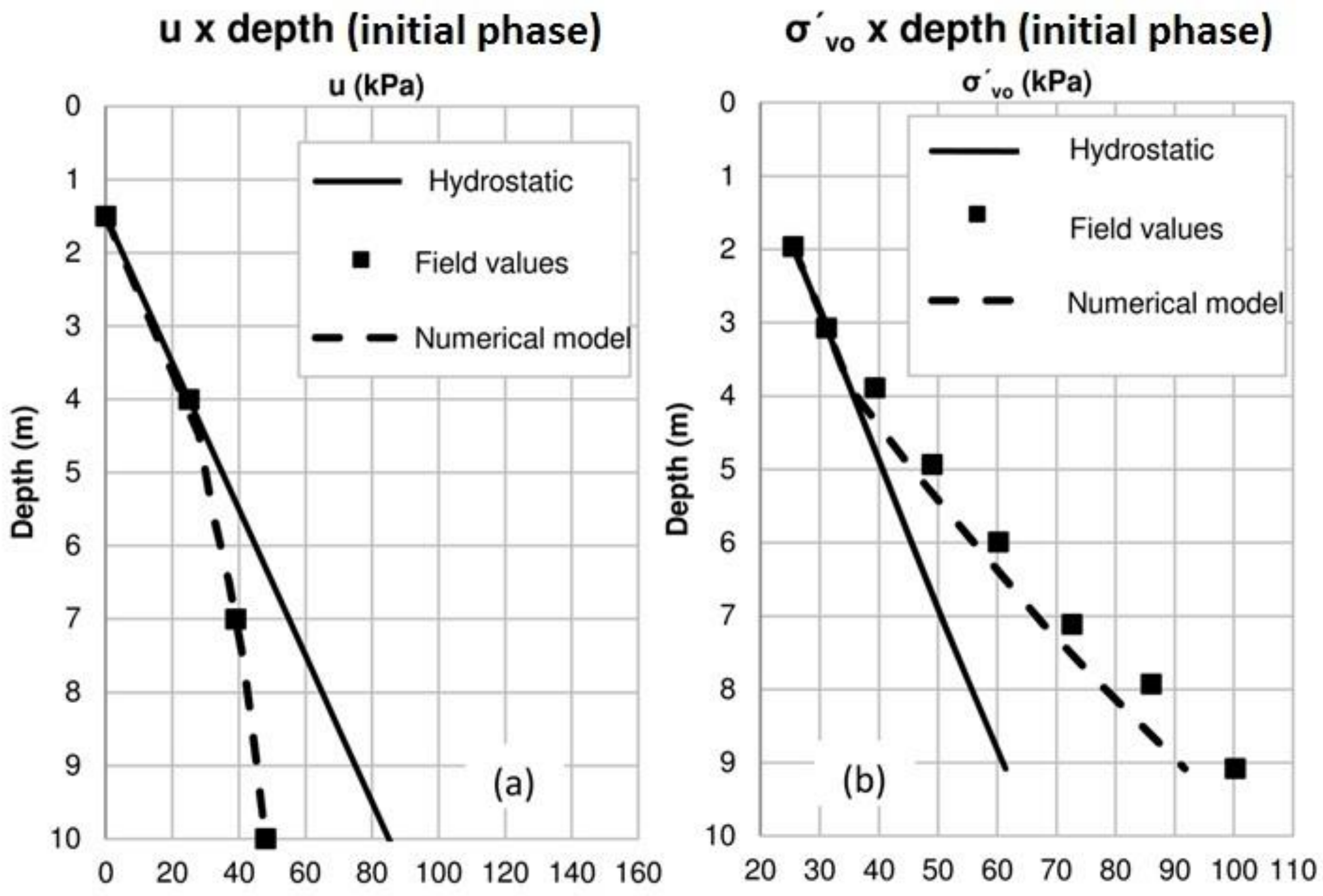

Stress Paths

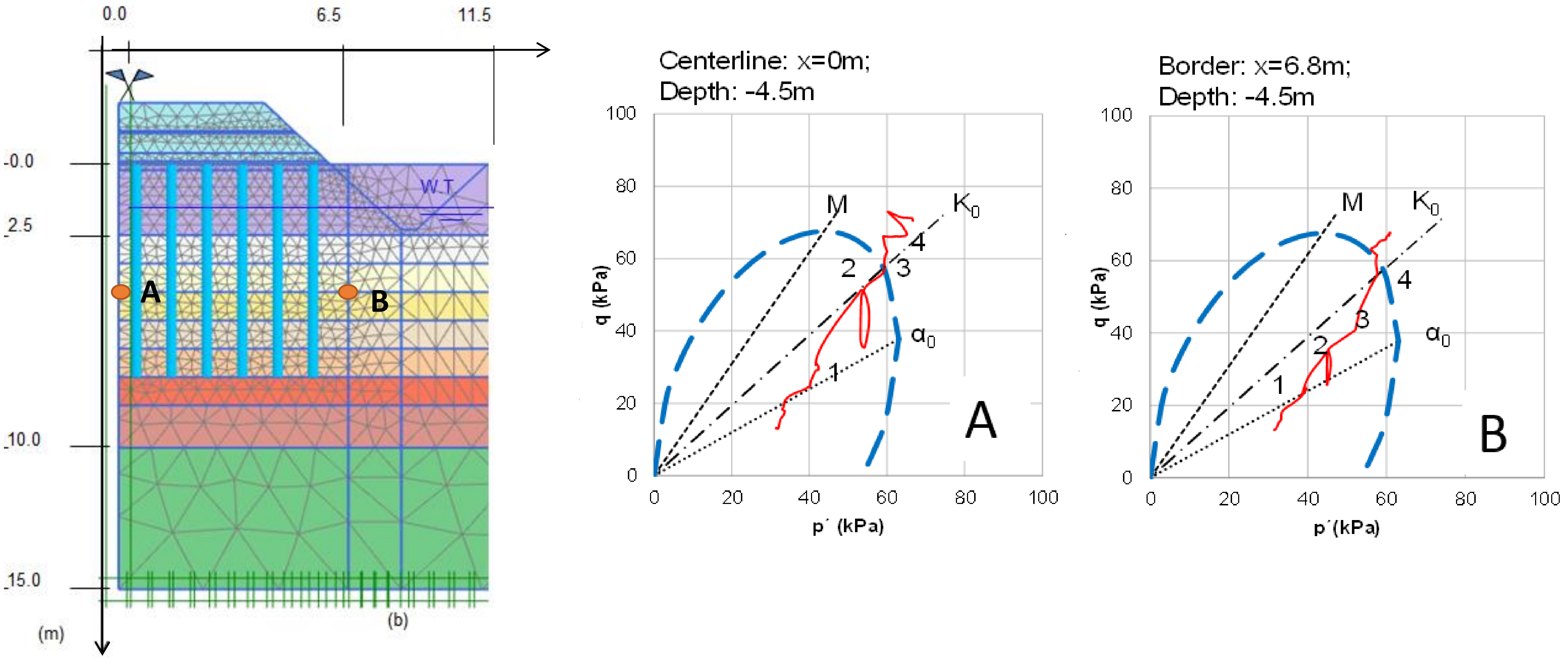

Laboratory Tests in Brazil (Oedometer and Triaxial Tests)

- **Oedometer Tests**

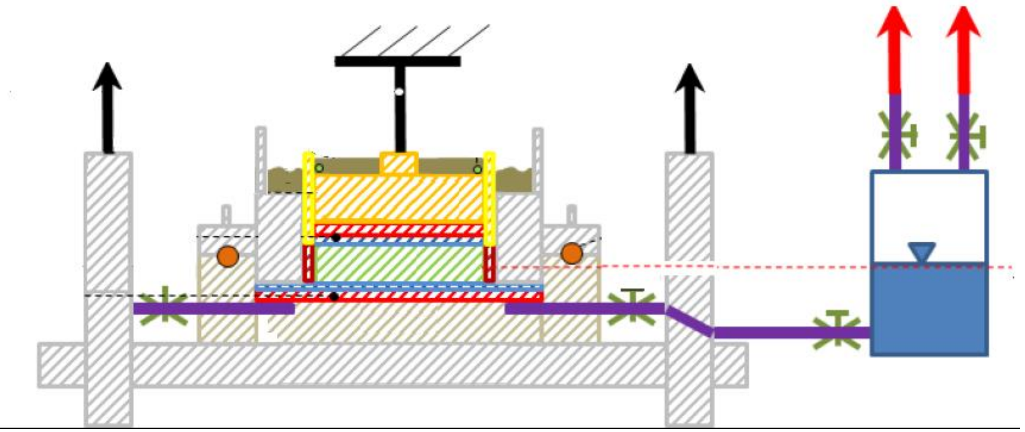

Correa, M.R.B.C., Sandroni, S.S. 2014. Vacuum application in 1D and isotropic Trials (in Portuguese). In: *XVI Brazilian Conference on Soil Mechanics and Geotechnical Engineering, 9-13 September 2014, Goiania.*

- **Isotropic Triaxial Tests**

Vacuum load test in Brazil: test embankments

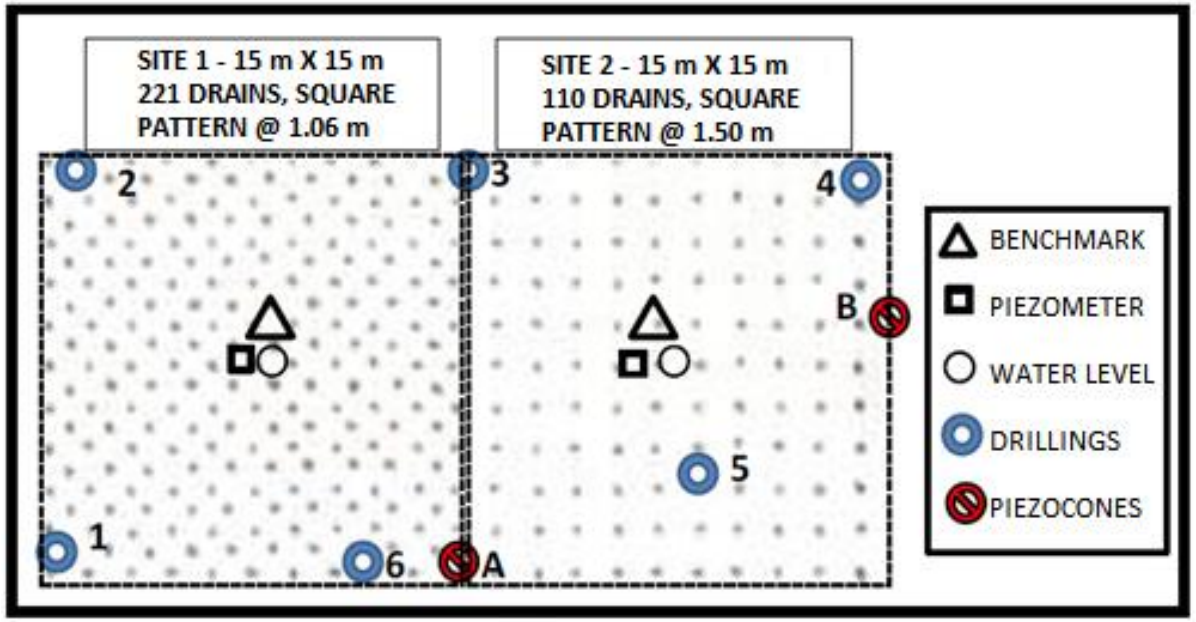

Sandroni, S.S., Andrade, G.G., Odebrecht, E. Vacuum consolidation pre-loading on soft soils: a first field experience (in Portuguese). In: *XVI Brazilian Conference on Soil Mechanics and Geotechnical Engineering, 15-18 September 2012, Pernambuco.*

Road Infrastructure – A Case Study in South America (Colombia)

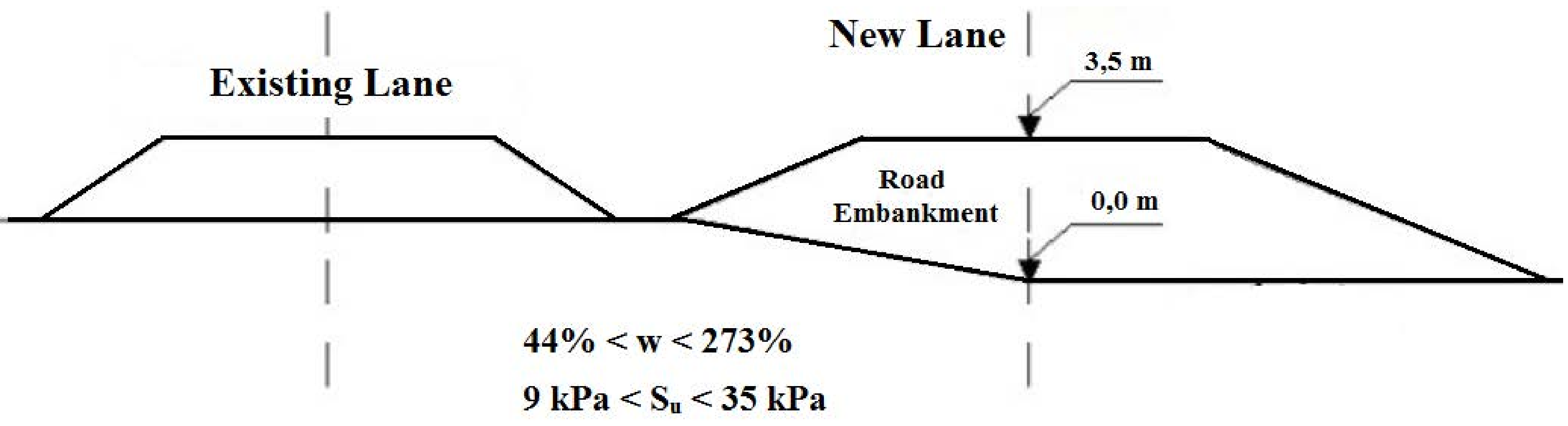

Correa, M.R.B., Brandt, J.R., Andrade, G.G., Yanez, D.G. 2016. Soft soil improvement through use of vacuum consolidation method in a road infrastructure construction site in South America (in Portuguese). In: *XVIII Brazilian Conference on Soil Mechanics and Geotechnical Engineering, 19-22 October 2016, Belo Horizonte, Minas Gerais.*

Petrochemical Plant, México

Petrochemical Plant, México

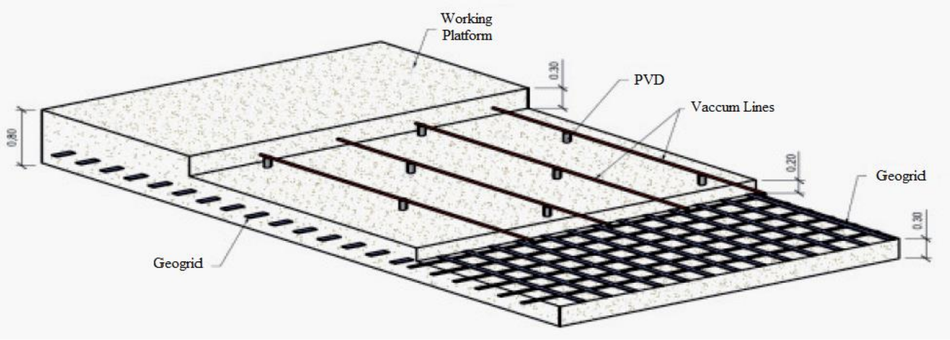

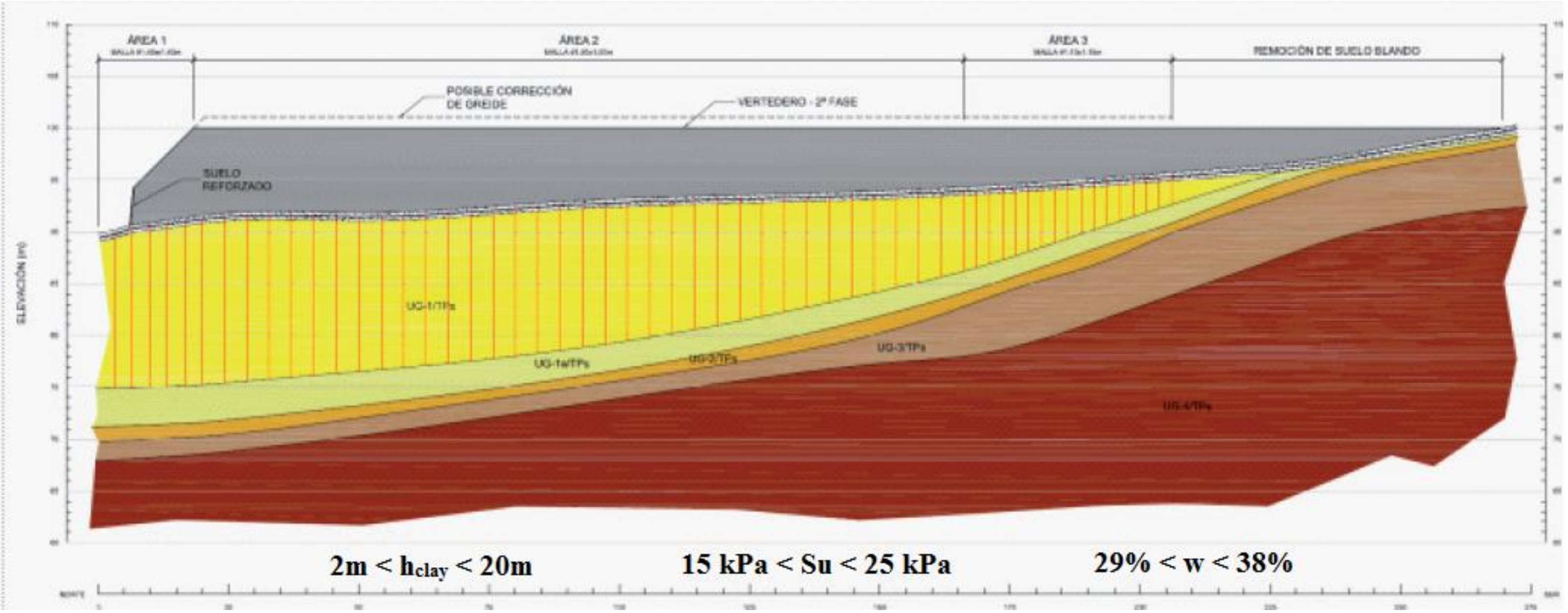

Kochen, R., Neto, H.G.B., Bastos, I.G., Araujo, R. 2015. Soft soil improvement through use of vacuum consolidation method (in Portuguese). *Revista Engenharia.* 624/2015, pp.54-59.

Petrochemical Plant, México – Settlements data

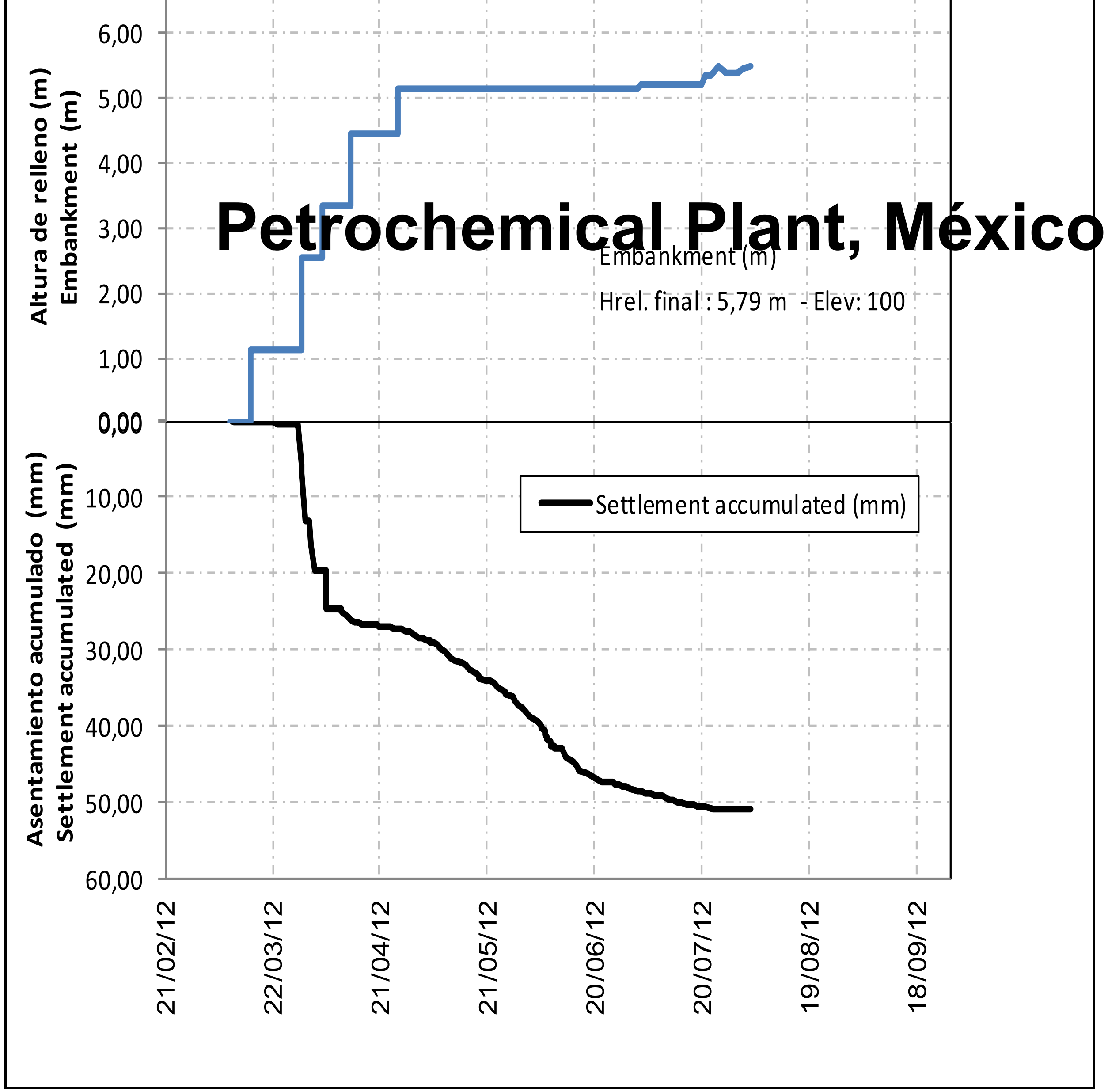

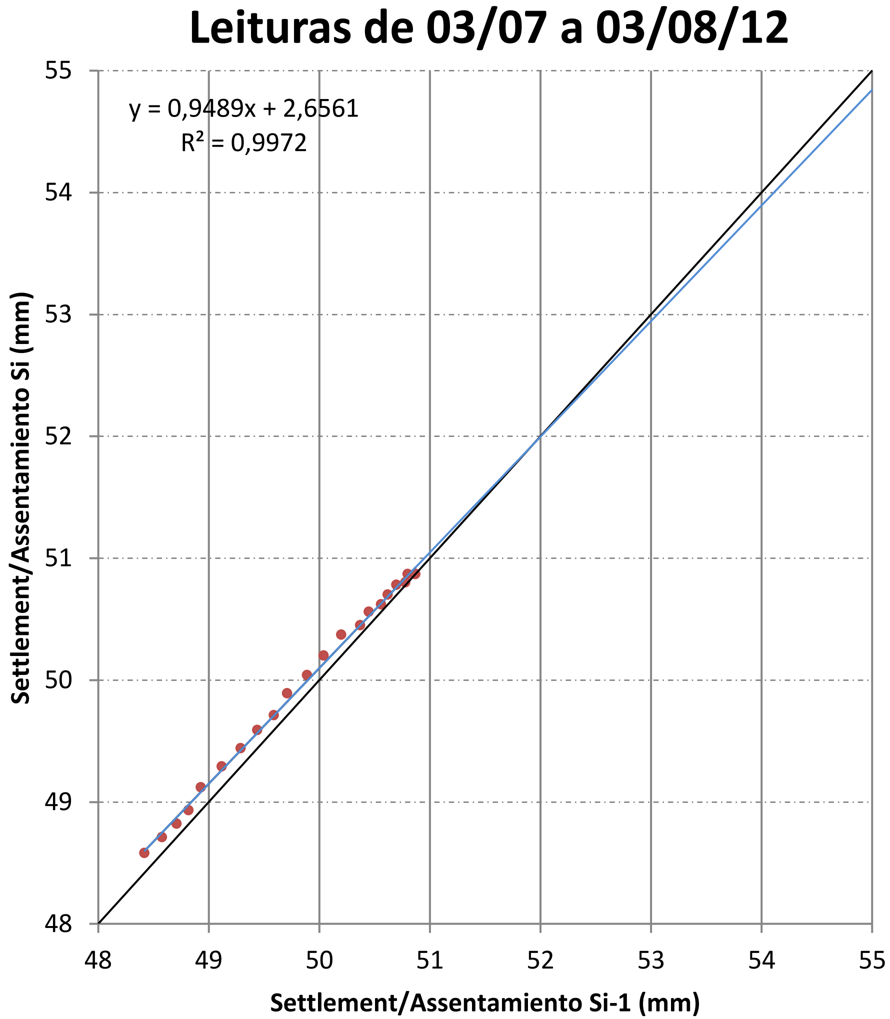

Conclusions

- Good agreement between measured and predicted settlements, pore pressures and horizontal displacements, these being almost negligible.
- Compression curves: overall agreement between laboratory data, field data and numerical calculations.
- Vacuum loading results results in stress paths away from failure, therefore more suitable in cases stability is a major concern.
- Consistent overall numerical modelling of the structured clay subjected to vacuum loading.
- Increasing use of vacuum loading in South America

Acknowledgements

- Field studies in Canada: U. Laval, S. Leroueil; Menard, S. Varaksin
- Numerical studies: Plaxis, R. Brinkgreve; Chalmers Univ., M. Karstunen
- Brazilian studies: Tecnogeo, G. Andrade; Geocompany, R. Kochen; PUC-Rio, S. Sandroni.

Activated Binders in Soil Stabilisation Applications

Tiago Miranda[1], Nuno Cristelo[2] and Sara Rios[3]

1. University of Minho, Guimarães, Portugal
2. University of Trás-os-Montes e Alto Douro, Vila Real, Portugal
3. CONSTRUCT-GEO, University of Porto, Portugal

Contents

Introduction

➢ *Why alkaline activation?*

Ground improvement methods

Chemical stabilisation

Traditional binders: **Ordinary Portland Cement and Lime**

Development of more sustainable binders: - reduce the CO_2 production
- use of waste materials

Introduction

➢ *What is alkaline activation (AA)?*

AA is the polimerization of aluminium and silicon ions, when aluminosilicate sources are dissolved in high pH solutions.

The final material is a 3D aluminosilicated polymer formed by several amorphous to semi-crystaline phases (SiO_4 and AlO_4 tetrahedrons sharing O)

PERCURSOR

Solid aluminosilicate source

+

ACTIVATOR

Activating **solution**

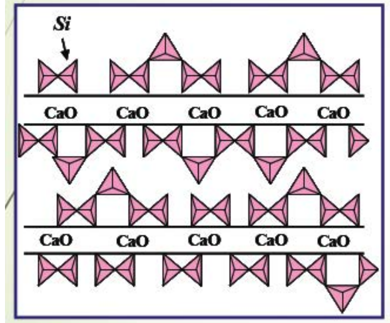

2D C-S-H Gel existing in high calcium binders

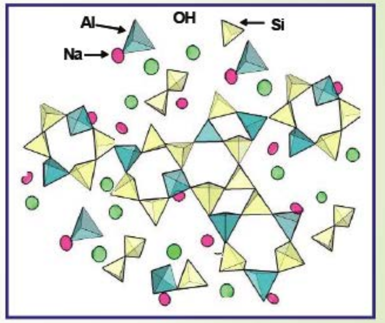

3D N-A-S-H Gel formed by the AA of silicon and aluminium

Introduction

➢ *What is alkaline activation (AA)?*

ACTIVATOR

Activating **solution**

Alkaline solution usually based on sodium (Na) or potassium (K).

- Simple (Na/K hydroxide/silicate), or
- Combined (Na/K hydroxide + Na/K silicate)

+

PERCURSOR

Solid aluminosilicate source

- Metakaolin – for very specific applications (e.g. monument restoration)
- Industrial by-products: fly ash, blast furnace slags, etc...

The percursor *dehydroxylation* is very important to transform its structure from crystalline to amorphous !

Introduction

➢ *What is alkaline activation (AA)?*

The reaction process:

1. The percursor covalent bonds Si-O and Al-O are broken due to the high pH of the solution (high OH^- concentration)

2. The metalic cations (Na or K) of the activator compensate the negative charges associated to the new change in the Al coordination with O

3. The resulting products acumulate and form a ions “soup” that originates the aglutination/nucleation process

4. An amorphous gel responsible for the material final properties is formed by the precipitation of Si and Al species

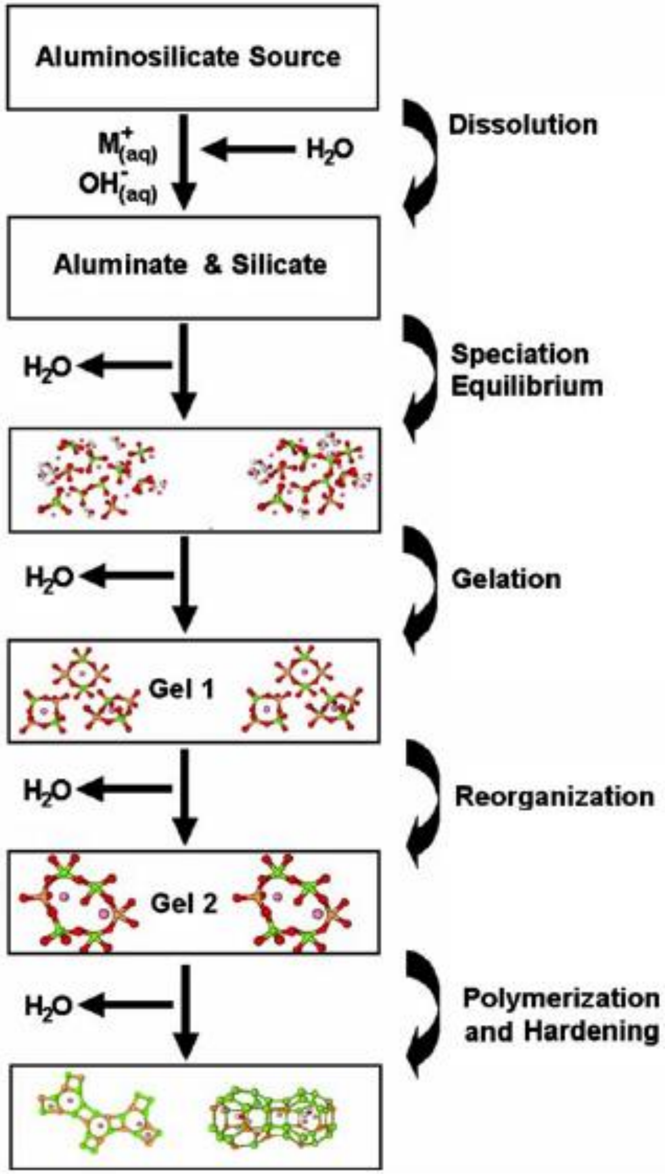

Duxson et al. (2007)

Introduction

➢ *What is alkaline activation (AA)?*

The eventual presence of Ca can have a strong influence on the formed gel (**C-S-H** ou **N-A-S-H)**, depending on its proportion in relation to Si and Al ions.

The production conditions are easier when Ca is involved which has motivated the development of hybride percursors mixed by Portland cement and wastes.

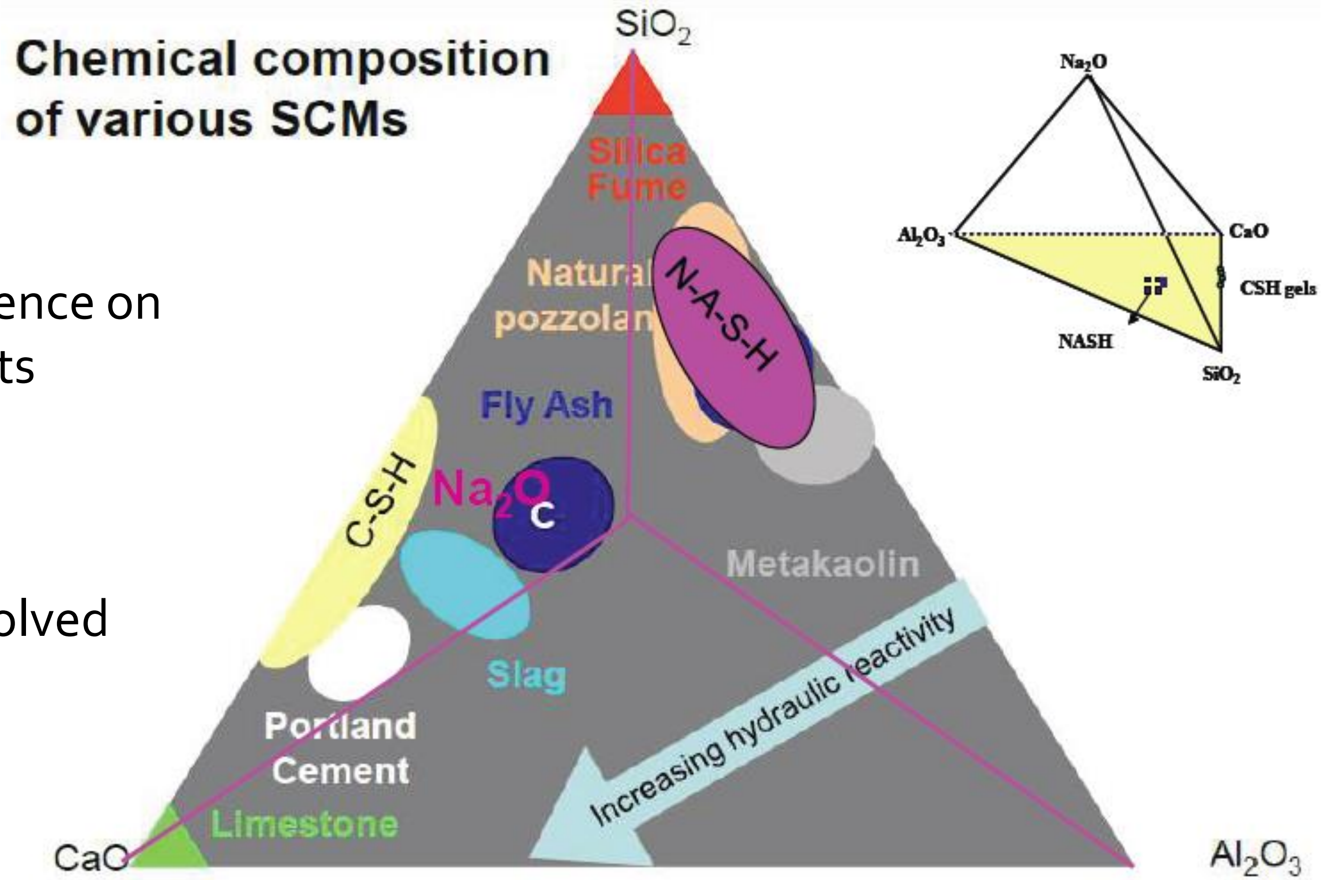

Inês García-Lodeiro (2016)

Introduction

➢ *What is alkaline activation (AA)?*

The final product is affected by the following factors:

➢ Percursor composition (ratio Si/Al)	PERCURSOR
➢ Percursor amorphous phase content	PERCURSOR
➢ Concentration of Ca ions on the solution	
➢ Activator composition	ACTIVATOR
➢ Curing time, temperature and humidity	CURING CONDITIONS

Introduction

➢ *What are the challenges of using alkali activated binders in soil stabilization*

Varying ambient temperature

Varying ambient humidity

In situ soils (Clays, sands, ...)

Characteristics of a soil stabilisation technique:

Compaction energy

Soil water content

Applications

- *Jet Grouting*



Applications

➢ *Jet Grouting*

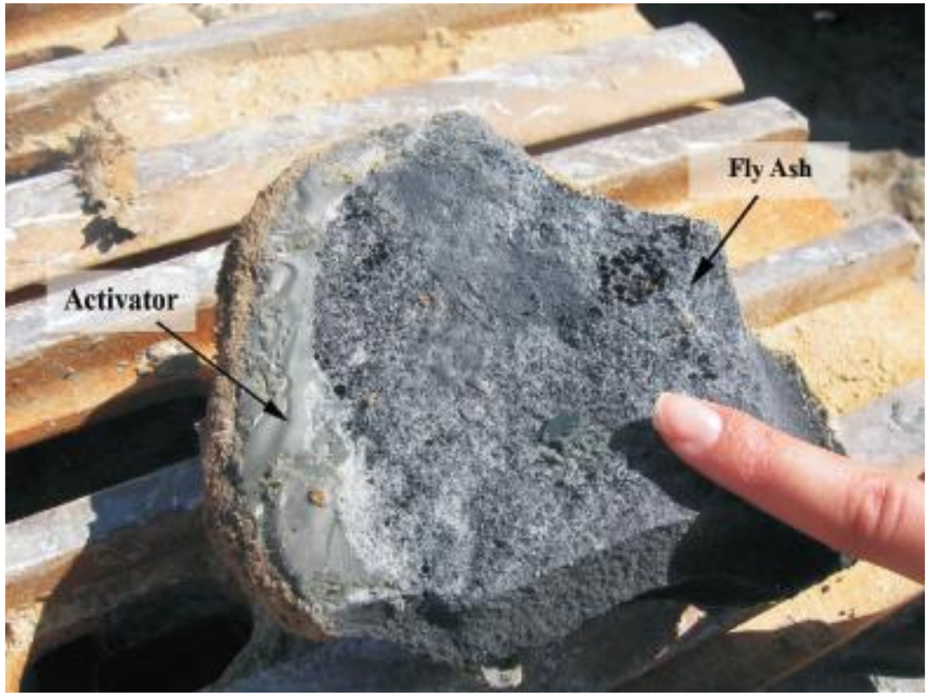

Applications

➢ *Jet Grouting*

OPC Column

AAFA Column

Applications

➢ *Jet Grouting*

90 days of curing

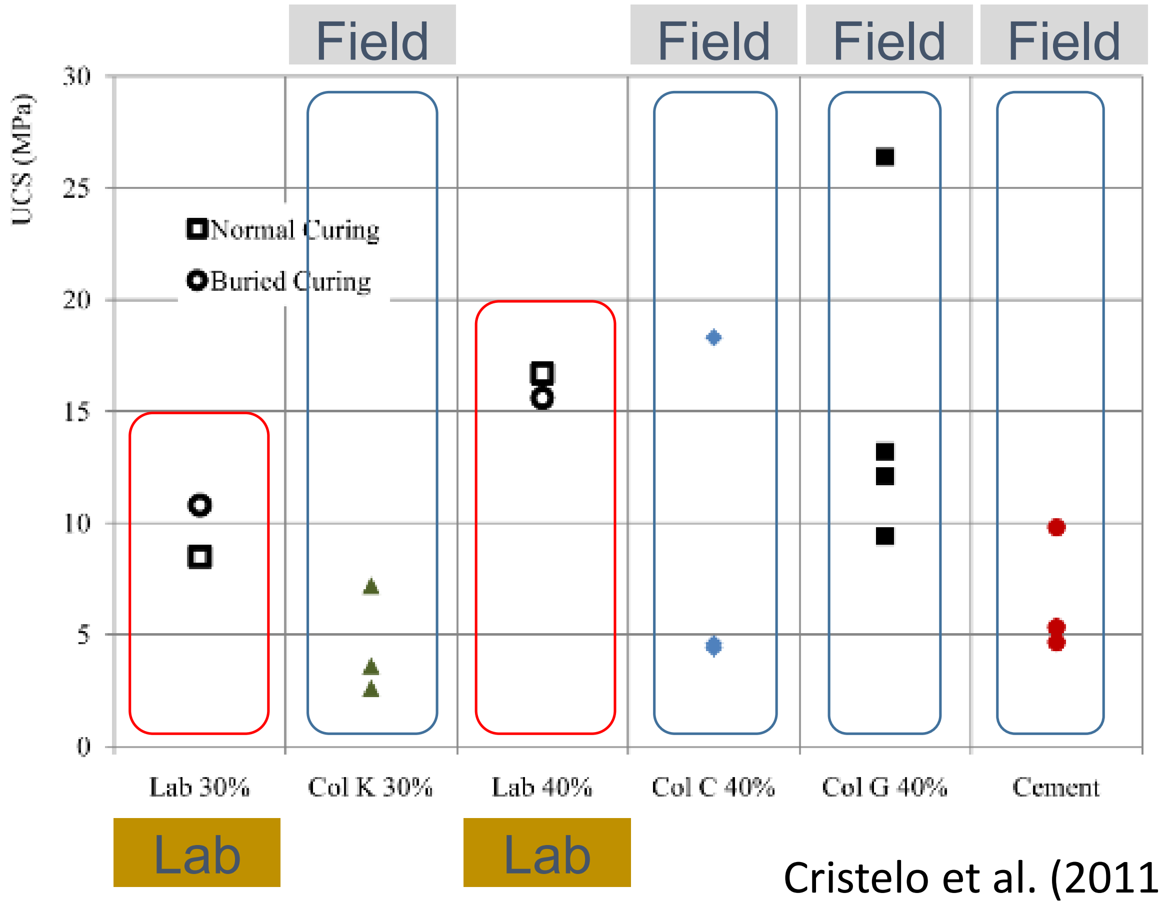

Cristelo et al. (2011)

Material	Percentage of total slurry	
	30% fly ash	40% fly ash
Sodium hydroxide	6·7	5·9
Water	13·3	11·8
Sodium silicate	40.0	35·2
Fly ash†	40·0	47·1

* This percentage refers to the grout + soil mixture.
† This percentage refers to the grout without the soil.

Applications

- *Jet Grouting*

Material	Percentage of total slurry	
	30% fly ash	40% fly ash
Sodium hydroxide	6·7	5·9
Water	13·3	11·8
Sodium silicate	40.0	35·2
Fly ash†	40·0	47·1

* This percentage refers to the grout + soil mixture.
† This percentage refers to the grout without the soil.

Laboratory

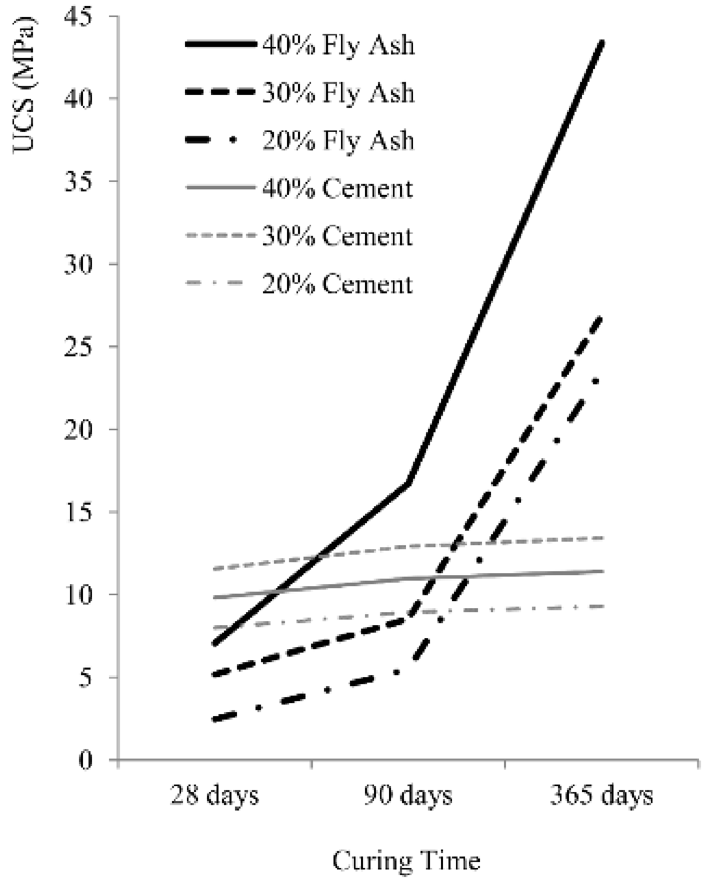

Cristelo et al. (2011)

Applications

- *Compressed earth blocks*






Applications

- *Compressed earth blocks*

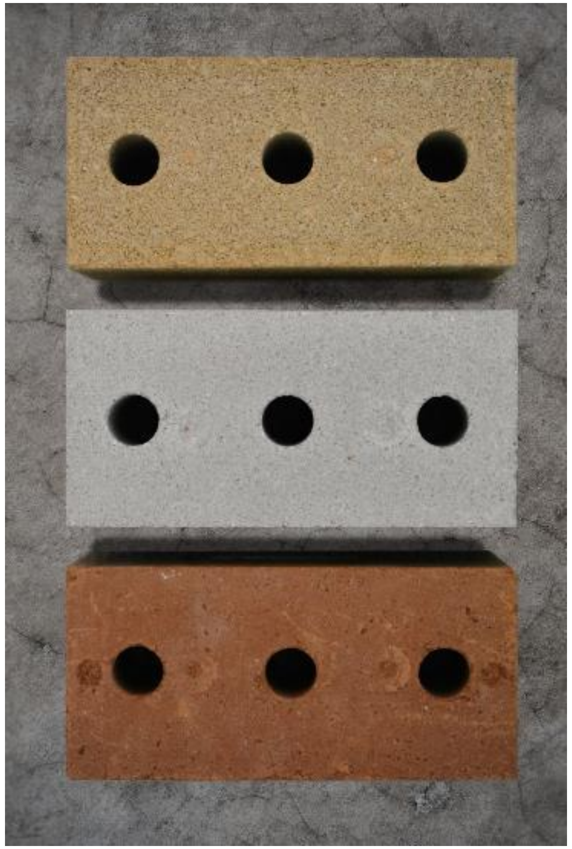

Applications

- *Compressed earth blocks*

Applications

➢ *Compressed earth blocks*

Under compression

Under three-point bending

Silva et al. (2015)

Applications

- *Compressed earth blocks*

Mixture	Soil (wt.%)	Fly ash (wt.%)	Activator/solids (wt.%)	Na_2O/fly ash (–)
SFA10	90.0	10.0	13.4	0.250
SFA15	85.0	15.0	13.7	0.170

Under compression

Mixture	γ_b (kg/m^3)	$f^d_{c,u}$ (N/mm^2)	$f^s_{c,u}$ (N/mm^2)	$f^s_{c,u}/f^d_{c,u}$
SFA10	1810 (1%)	8.8 (11%)	5.6 (10%)	0.64
SFA15	1854 (1%)	12.0 (8%)	8.0 (21%)	0.67

Unsoaked in water

Soaked in water

180 curing days

Under three-point bending

Mixture	γ_b (kg/m^3)	$f^d_{b,u}$ (N/mm^2)	$f^s_{b,u}$ (N/mm^2)	$f^s_{b,u}/f^d_{b,u}$
SFA10	1810 (1%)	1.8 (14%)	0.7 (36%)	0.40
SFA15	1854 (1%)	2.3 (11%)	1.1 (9%)	0.49

Silva et al. (2015)

Applications

➢ *Soil-stabilised bases for platform infrastructures*

ID	Ash / solids (wt.)	Na_2O / ash (wt.)	NaOH concent. (molal)	Water content (%)	Activ. content (%) [a]	Activ. / ash (wt.)	Dry unit weight (kN/m^3) [b]	SiO_2 / Na_2O (wt.) [c]
M01	0.15	-	-	11.7	-	-	18.22	-
M02	0.20	-	-	15.6	-	-	17.08	-
M03	0.25	-	-	19.5	-	-	16.04	-
M1	0.15	0.125	7.5	8.8	11.7	0.781	18.22	0.552
M2	0.20	0.125	7.5	11.7	15.6	0.781	17.08	0.552
M3	0.25	0.125	7.5	14.7	19.5	0.781	16.04	0.552

[a] For a SS/SH ratio of 0.5; [b] For a unit weight of 20 kN/m^3; [c] Quantities from the activator

Unconfined compression

Elastic stiffness evaluation with ultrassonic transducers

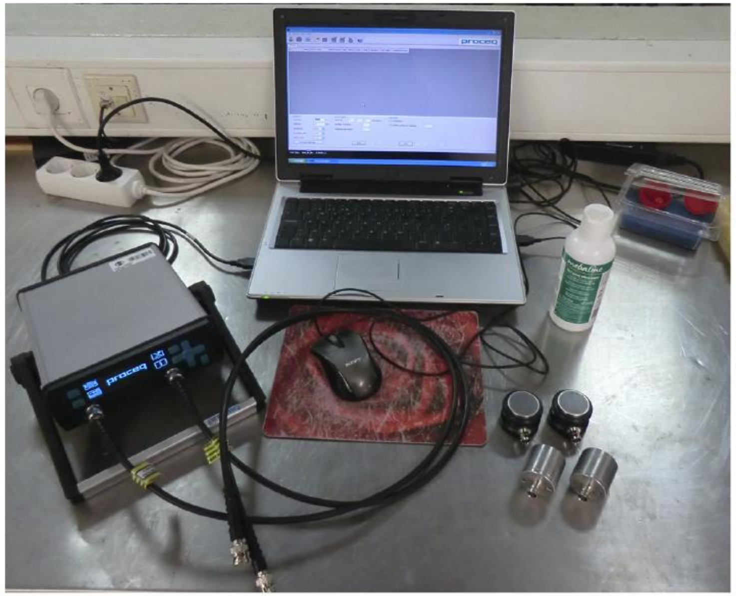

Applications

➢ *Soil-stabilised bases for platform infrastructures*

Unconfined compression

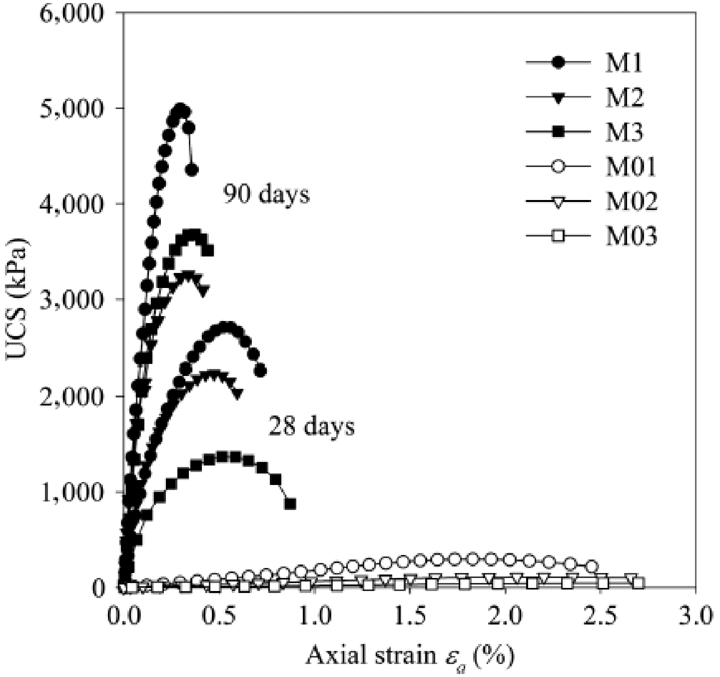

Elastic stiffness evaluation with ultrassonic transducers

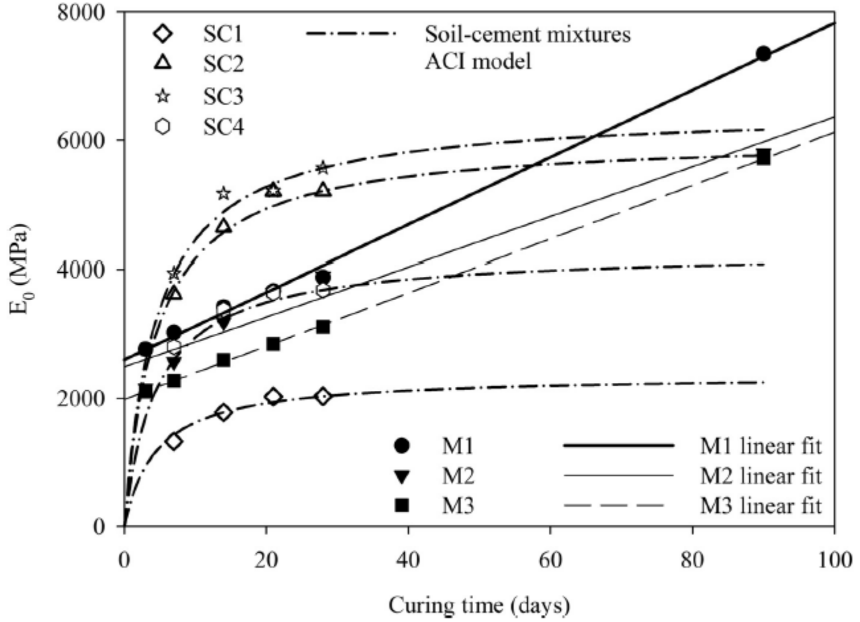

Rios et al. (2016 a e b)

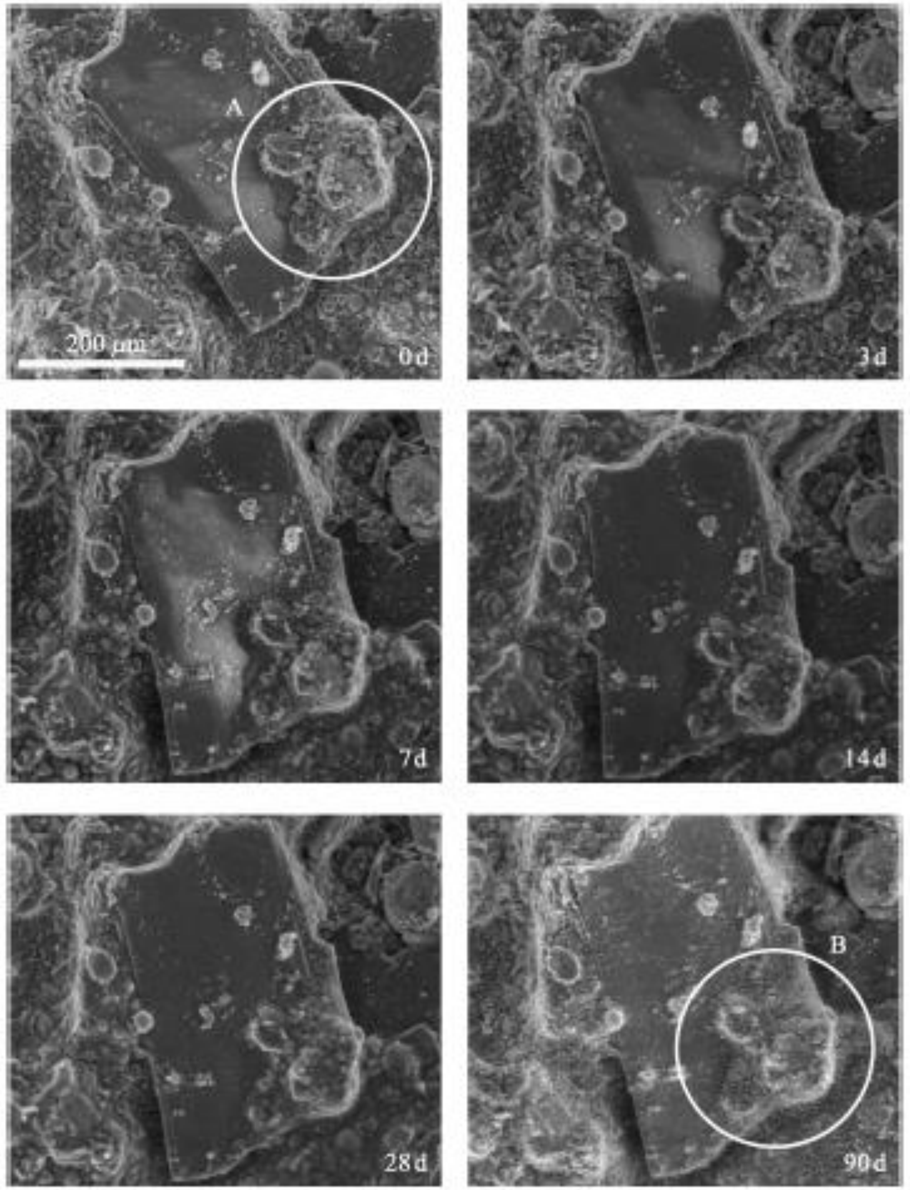

Applications

- *Soil-stabilised bases for platform infrastructures*

Applications

Depending on the application, the mixtures properties can vary with influence on:
- mixture workability and way of compaction
- very different strength values
- very different pattern of behaviour in terms of balance between mechanical and chemical response

Consistency similar to soil-stabilised

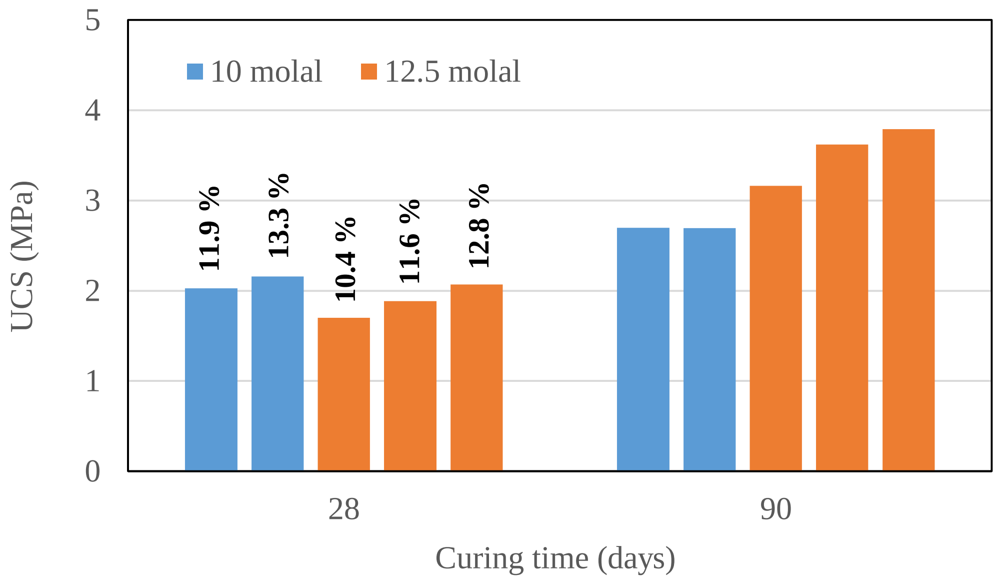

Consistency similar to fresh concrete

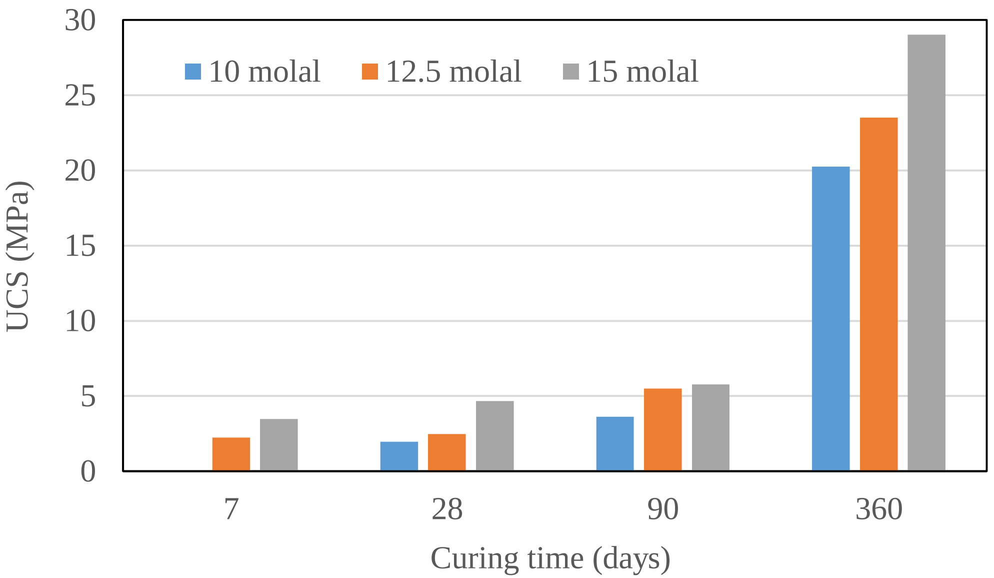

How to define the optimum compaction conditions?

➢ *The challenge*

Soil stabilised with OPC

Soil	Water	Cement

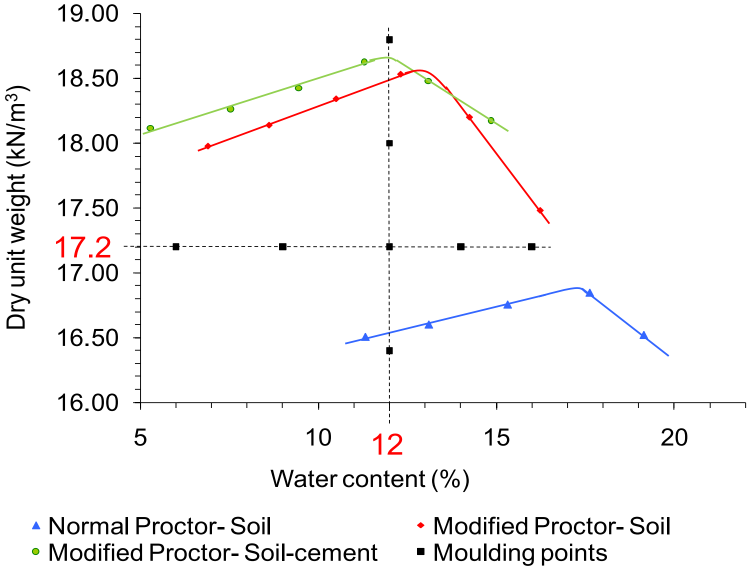

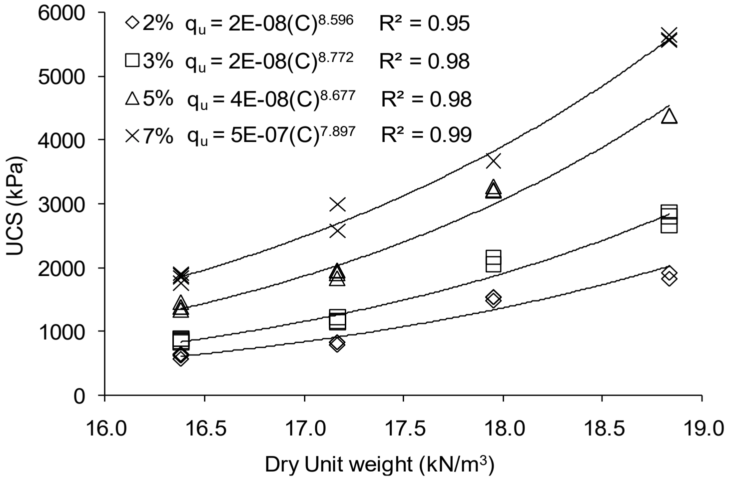

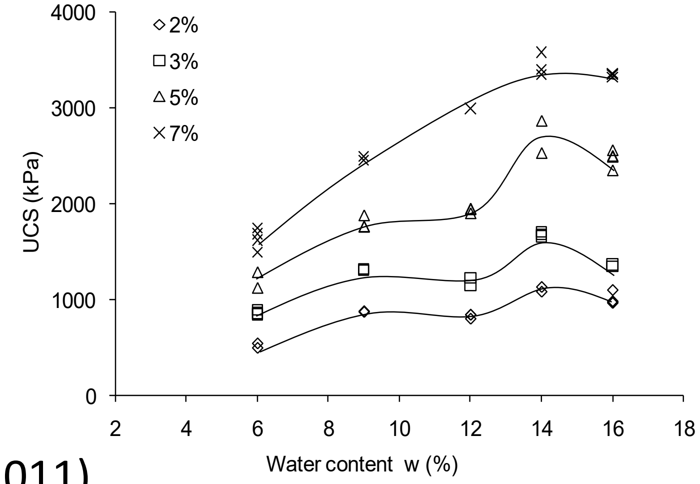

Rios (2011)

Geotechnical approach

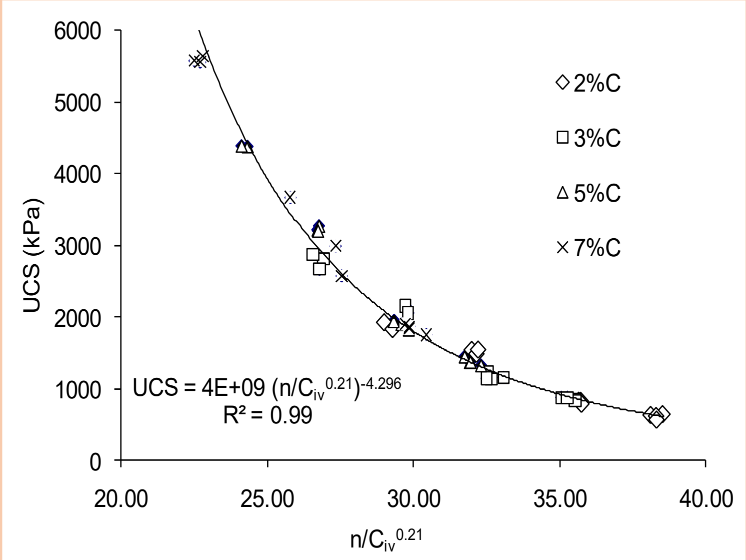

Chemical approach

Enough water to hidrate the cement

GTS (2000): w > 0,5 * C%

How to define the optimum compaction conditions?

➢ *The challenge*

Soil stabilised with AAC

Soil	Activator	Fly ash

Solids/Liquid ratio (S/L) → Mixture fluidity and workability

Water content → Viscosity of the liquid phase (mechanical) and chemical concentration of the activator

Type of alkali metal (content in Ca, Na, Si and Al) → Type of gel formed

Geotechnical approach

Chemical approach

The optimum liquid phase content, obtained by a Proctor test, will only match the ideal liquid phase, in terms of chemical reactions, by coincidence!

How to define the optimum compaction conditions?

➢ *The challenge*

Soil stabilised with AAC

Soil	Activator	Fly ash

Geotechnical approach

Proctor Test

- The Proctor tests needs to be executed with soil, fly ash and activator otherwise it will not be representative (Higher dry unit weights are obtained when the activator is used instead of water);
- But, the Proctor curve needs to be defined in terms of water content (and not liquid content), otherwise it will not be possible to compare mixtures with different activator concentrations.

ATENTION: the water content cannot be measured by the oven method !

How to define the optimum compaction conditions?

➢ *Some results*

Soil stabilised with AAC

Soil	Activator	Fly ash

Sodium hydroxide   Sodium silicate

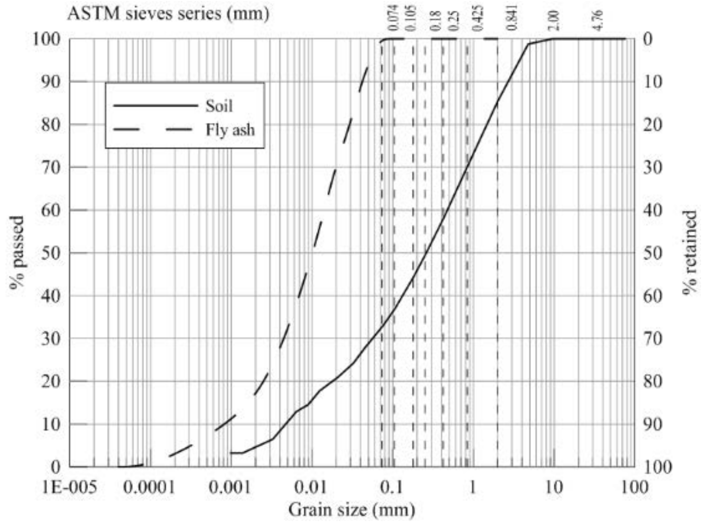

Several Proctor tests were performed:

- keeping the water content constant;
- keeping the S/L ratio constant;
- keeping the concentration of the activator constant.

A completely different pattern was found when the relation between sodium hydroxide and sodium silicate (SS/SH) changed.

How to define the optimum compaction conditions?

➢ *Some results*

Soil stabilised with AAC

Soil	Activator	Fly ash

Sodium hydroxide   Sodium silicate

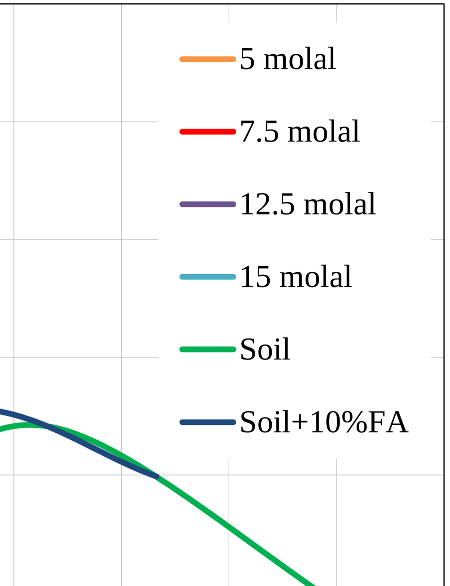

SS/SH = 0.5

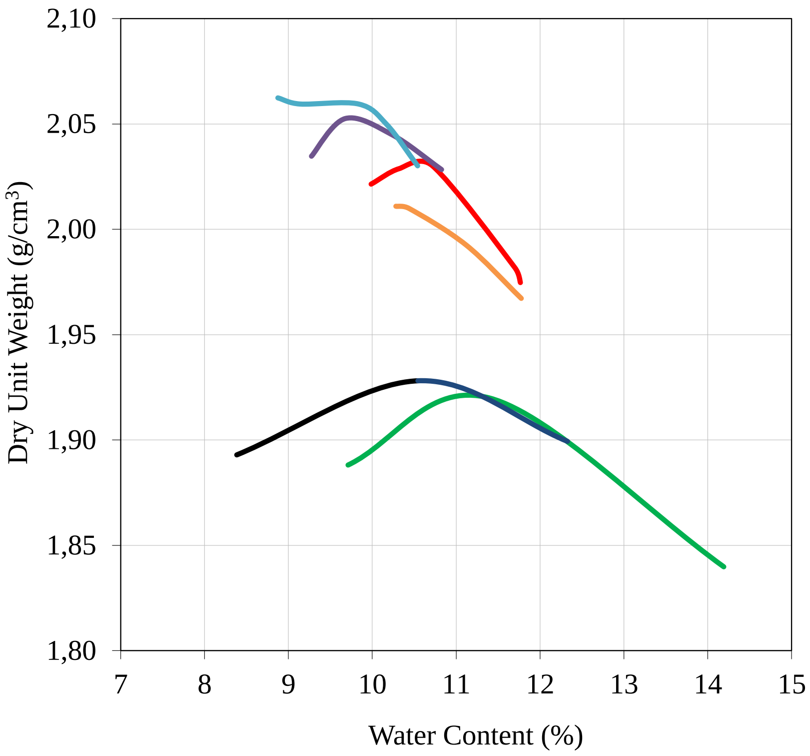

SS/SH = 1,0

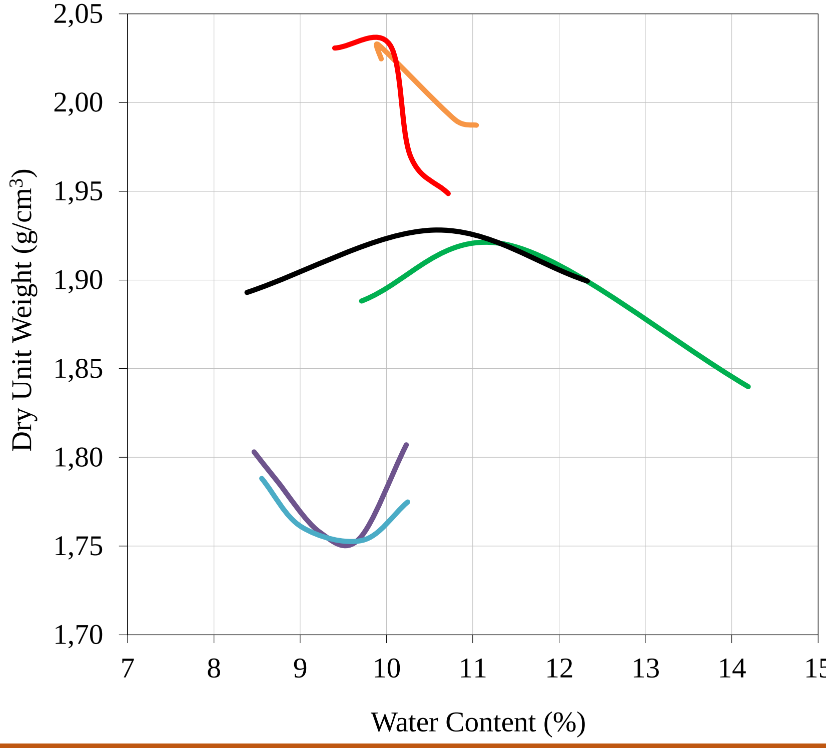

How to define the optimum compaction conditions?

➢ *Some results*

Soil stabilised with AAC

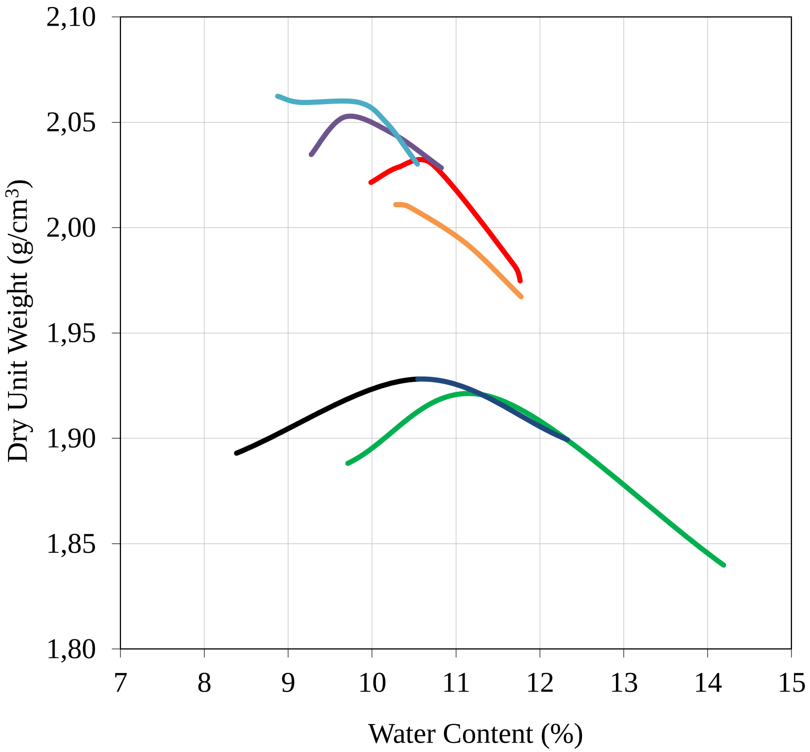

- In the first case (SS/SH=0,5), the increase of the SH concentration reduces the optimum water content. This is expected because the increase in the concentration reduces the amount of water in the mixture.

How to define the optimum compaction conditions?

➢ *Some results*

Soil stabilised with AAC

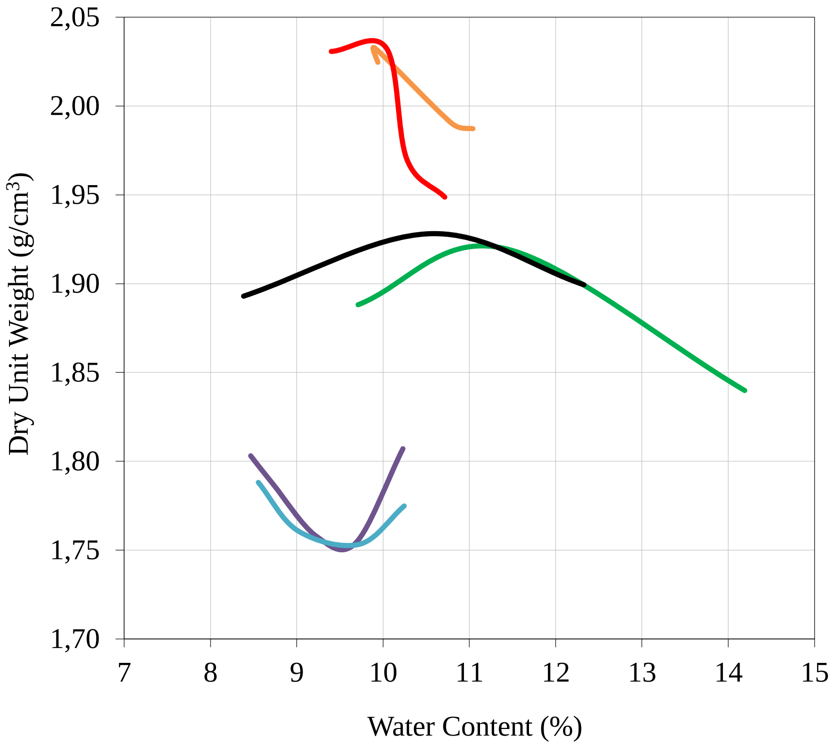

- In the first case (SS/SH=0,5), the increase of the SH concentration reduces the optimum water content. This is expected because the increase in the concentration reduces the amount of water in the mixture.
- In the second case (SS/SH=1,0), the increase in the SH concentration reduces the optimum dry unit weight. This is an indication that the viscosity dificults the mixture compaction.
- The two cases show completely different patterns, indicating that a higher amount of silicate has an important influence on the mixture viscosity and consequently on the mixture compaction.

Conclusions

- The use of alkali activated binders in soil stabilisation has proved to be a very interesting technique to replace Portland cement demonstrating high levels of strength and stiffness;
- Its applications can range from Jet grouting grouts, compressed earth blocks, or sub-base layers for soil improvement;
- The balance between the geotechnical and chemical approaches is not straightforward in these binders as a decrease in the activator concentration (which could improve the mixture workability and compaction) produces higher water content, and consequently, less effective chemical reactions between activator and fly ash.
- Further work is needed to obtain a rational methodology of mixture design as it exists for soil stabilised with Portland cement.

Further developments

- More data is necessary regarding the use of different soils, different compaction energies, and different mixture compositions
- Analysis of the influence of curing conditions (temperature and humidity variation with time)
- Effect of soil water content (the concentration activator needs to be adapted)
- Data that could relate compaction energy and mixtures ratios with strength that could lead to a rational methodology for design

References

- Cristelo, N., Glendinning, S., and Pinto, A. T. (2011). "Deep soft soil improvement by alkaline activation." Proc. ICE—Ground Improvement, 164 (2), 73–82.
- Duxson, P., A. Fernandes-Jiménez, J. L. Provis, G. C. Luckey, A. Palomo and J. S. J. van Deventer (2007). "Geopolymer technology: the current state of the art." Journal of Materials Science, 42(9), 2917-2933. http://dx.doi.org/10.1007/s10853-006-0637-z
- Rios, S. (2011). "A general framework for the geomechanical characterization of artificially cemented soil." Ph.D. thesis, Univ. of Porto, Porto, Portugal.
- Rios, S., Cristelo, C., Viana da Fonseca, A., Ferreira, C. (2016a). "Structural Performance of Alkali Activated Soil-Ash versus Soil-Cement". Journal of Materials in Civil Engineering, 28(2), http://dx.doi.org/10.1061/(ASCE)MT.1943-5533.0001398
- Rios, S., Cristelo, C., Viana da Fonseca, A., Ferreira, C. (2016b). "Small and large strain behavior of soil-geopolymer versus soil-cement". International Journal of Geomechanics, http://dx.doi.org/10.1061/(ASCE)GM.1943-5622.0000783
- Silva, R. A., E. Soares, D. V. Oliveira, T. Miranda, N. M. Cristelo and D. Leitão (2015). "Mechanical characterisation of dry-stack masonry made of CEBs stabilised with alkaline activation." Construction and Building Materials 75: 349-358. http://dx.doi.org/10.1016/j.conbuildmat.2014.11.03

Thank you for your attention!

Ground Improvement Solutions for Harbours

António Cristóvão[1], Alexandre Pinto[2],Rui Tomásio[3]

1. JET$_{SJ}$ Geotecnia, Lda, Portugal
2. JET$_{SJ}$ Geotecnia, Lda, Portugal
3. JET$_{SJ}$ Geotecnia, Lda, Portugal

1. Introduction

2. Jet Grouting

   2.1 Quay Wall Reinforcement

   2.2 Temporary Earth Retaining Walls

   2.3 Assessment of Jet Grouting Columns Diameter using Non-Destructive Methods

3. Vibro Techniques

   3.1 Vibrocompaction

   3.2 Stone columns combined with vibrocompaction

4. Main Conclusions

1. Indroduction

- Over recent years the world witnessed the construction of new port infrastructures has they play a crucial role on the development of worldwide trading and regional economic growth.

- The availability of free land together with deep water coast lines, compatible with the use of large draft vessels, is becoming increasingly hard to find.

- The construction of deep quay walls and the creation of technically demanding artificial platforms are challenging the engineering capacities.

- Seeking for inexpensive and appropriate technical solutions, capable to overcome the challenges imposed by the construction of such infrastructures, use has been made of **ground improvement solutions**. Its wide range of techniques, easily adapted to different technical scenarios and geological conditions, are considered to be an added value in most projects.


Lomé Container Terminal– Total area: 800.000 m²


Portugal
España
Spain
Lisboa
Barcelona
Marseille
Roma
Tyrrhenian Sea
Black Sea
България
Bulgaria
Ελλάς
Greece
İstanbul
Ankara
Türkiye
Turkey
İzmir
Antalya
Αθήνα
Athens
Mediterranean Sea
Algiers
Tunis
Oran
Casablanca
Morocco
Tunisia
Tripoli
Alexandria
Israel
Lebanon
Syria
Jordan
Algeria
Libya
Egypt
Western Sahara
Mauritanie
Mauritania
Nouakchott
Red Sea
Mali
Niger
Tchad
Chad
Sudan
Dakar
Sénégal
Senegal
Bamako
Niamey
Burkina Faso
Bénin
Benin
Nigeria
Conakry
Guinée
Guinea
Sierra Leone
Côte d'Ivoire
Ghana
Lagos
Lome
Liberia
Abidjan
Gulf of Guinea
Cameroun
Cameroon
République Centrafricaine
Central African Republic
South Sudan
Equatorial Guinea
Uganda
Kenya


N2
N2

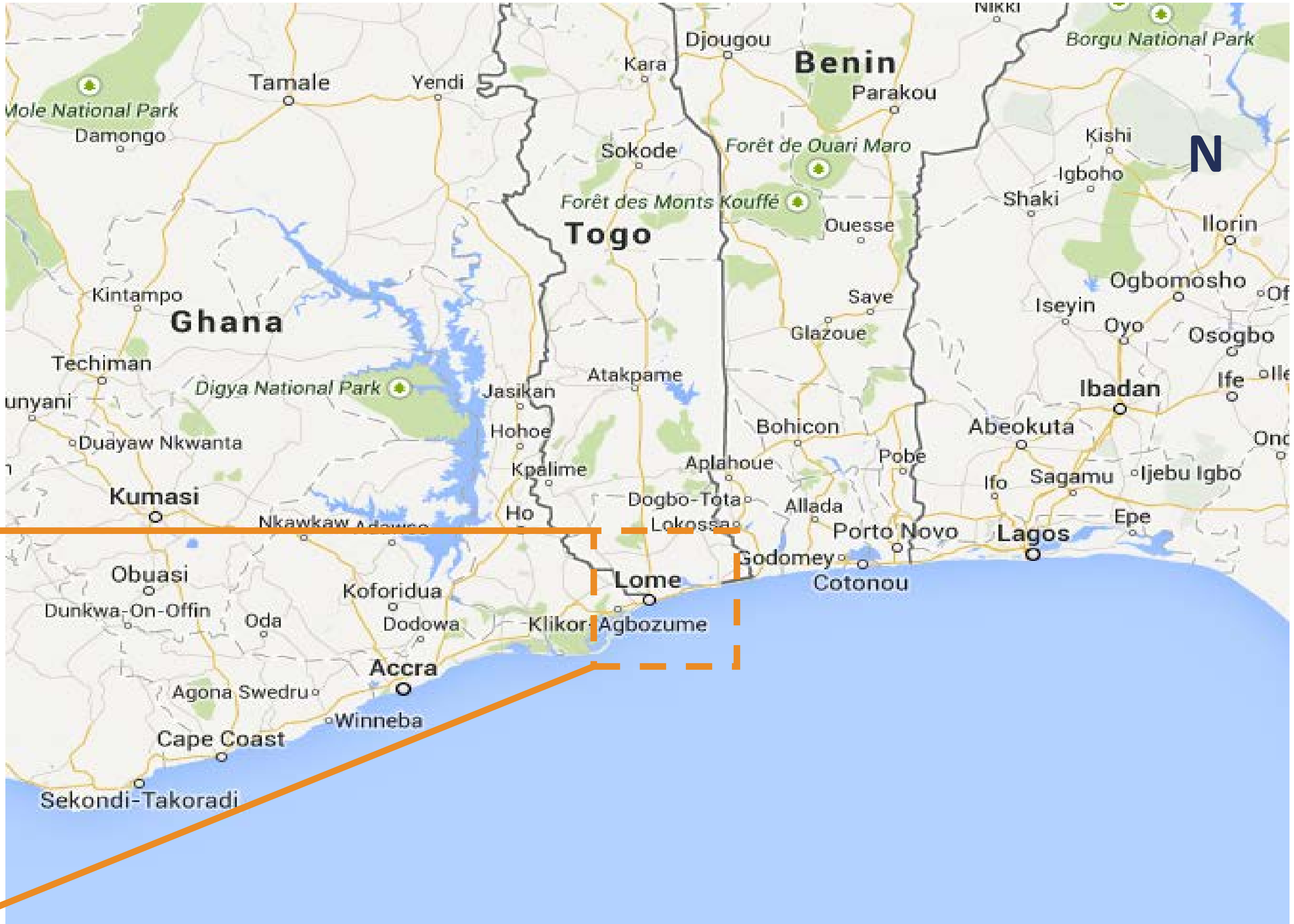
N
Nikki
Djougou
Benin
Borgu National Park
Kara
Parakou
Tamale
Yendi
Mole National Park
Damongo
Sokode
Forêt de Ouari Maro
Kishi
Igboho
Shaki
Forêt des Monts Kouffé
Togo
Ouesse
Ilorin
Ogbomosho
Kintampo
Ghana
Save
Iseyin
Oyo
Osogbo
Glazoue
Techiman
Atakpame
Ibadan
Ife
Digya National Park
Jasikan
Bohicon
Abeokuta
Hohoe
Duayaw Nkwanta
Aplahoue
Pobe
Kpalime
Ifo
Sagamu
Ijebu Igbo
Kumasi
Dogbo-Tota
Allada
Ho
Lokossa
Porto Novo
Lagos
Epe
Godomey
Obuasi
Lome
Cotonou
Koforidua
Dunkwa-On-Offin
Oda
Dodowa
Klikor
Agbozume
Accra
Agona Swedru
Winneba
Cape Coast
Sekondi-Takoradi


New Terminal Location
0m
500m
1000m

2. JET GROUTING

2.1 Quay Wall Reinforcement

Quay Wall Characteristics

- Front Quay Wall:
  - Quay wall lenght: **1.000 lm**
  - **29m deep reinforced concrete diaphragm wall**, connected to a 0.8m thick anchored dead man wall through a 45 meter long steel tie rod system (tie-rods, spaced of 1.5m (in average), anchored at level +1.0m at the front wall and +0.0m at the anchor wall)
  - Reinforced concrete wall thickness: 1.2m

- On the sea side, the crane rail is located on the front wall axis, whilst on the land side, it rests on a 1.4m wide and 1.25m high reinforced concrete beam, held by a row of 1.2 m diameter bored piles, founded at level -22.0m and spaced at a distance of 3.0m between axes.

Current Solution

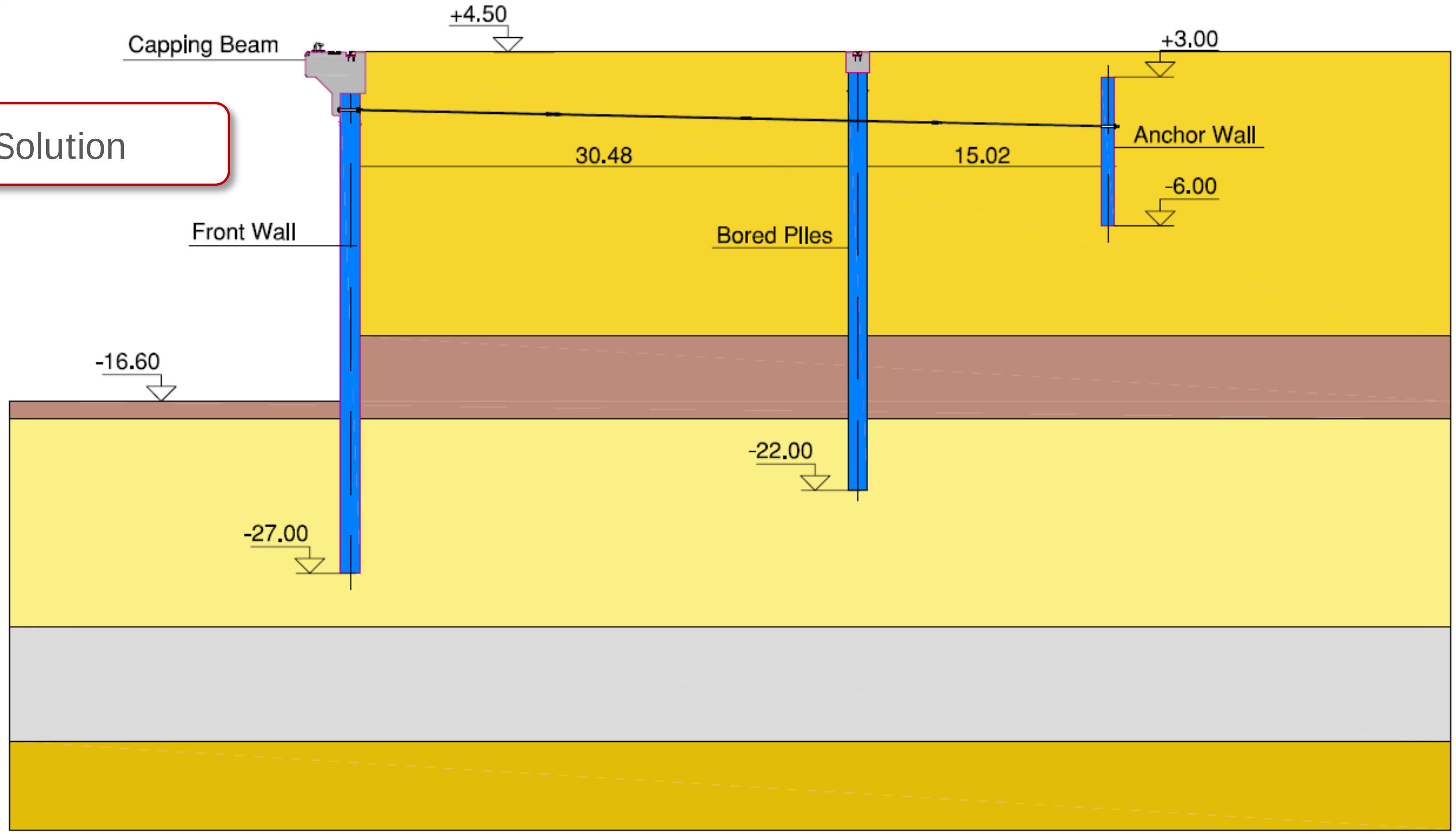

- Single supported quay wall
- The front wall is a 1,2m RC diaphragm wall
- The anchor wall is a 80cm RC diaphragm wall
- The Tie-rods length is 45m
- The land-side crane rail is supported by Ø1200mm bored piles

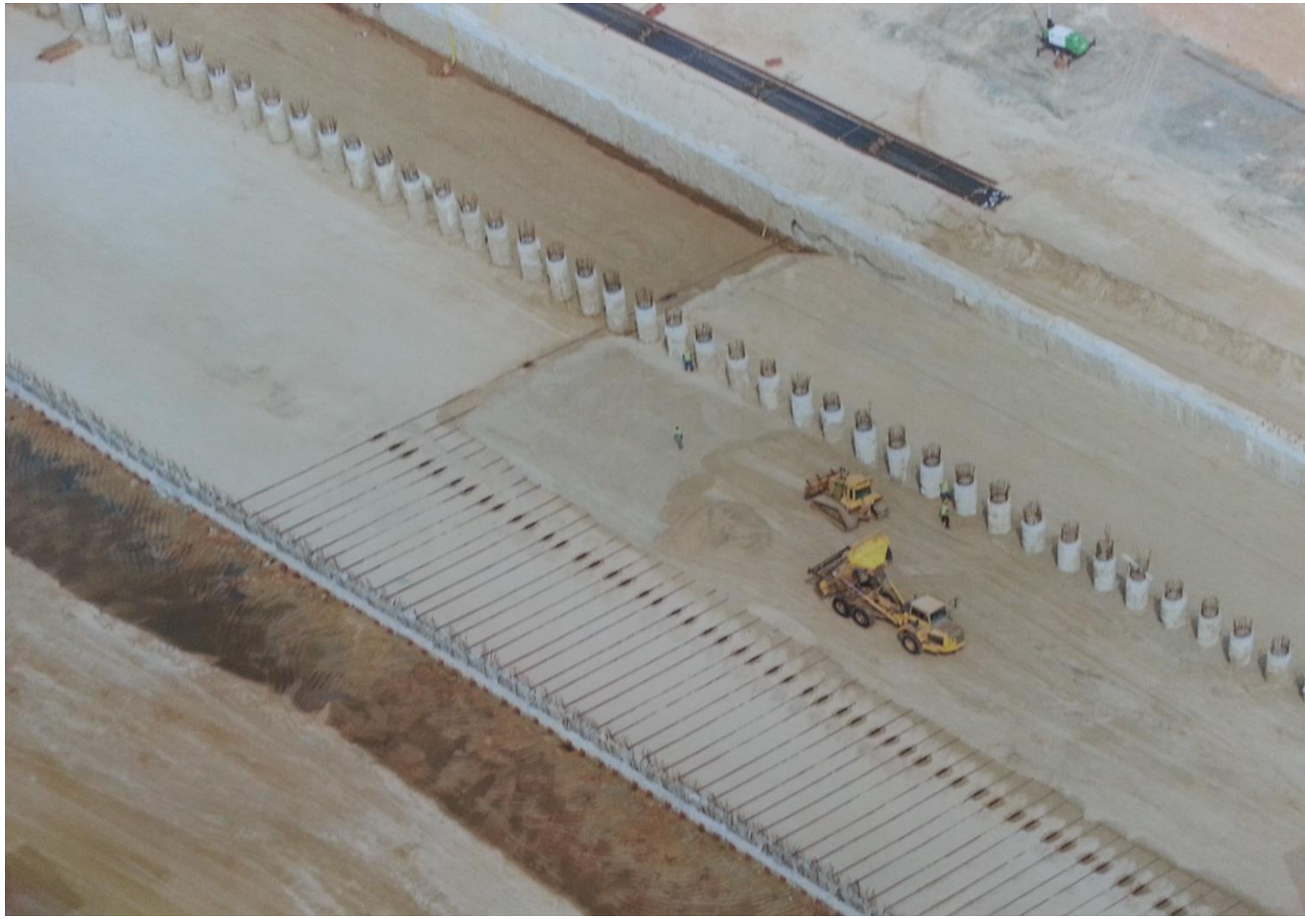

Particular Solution

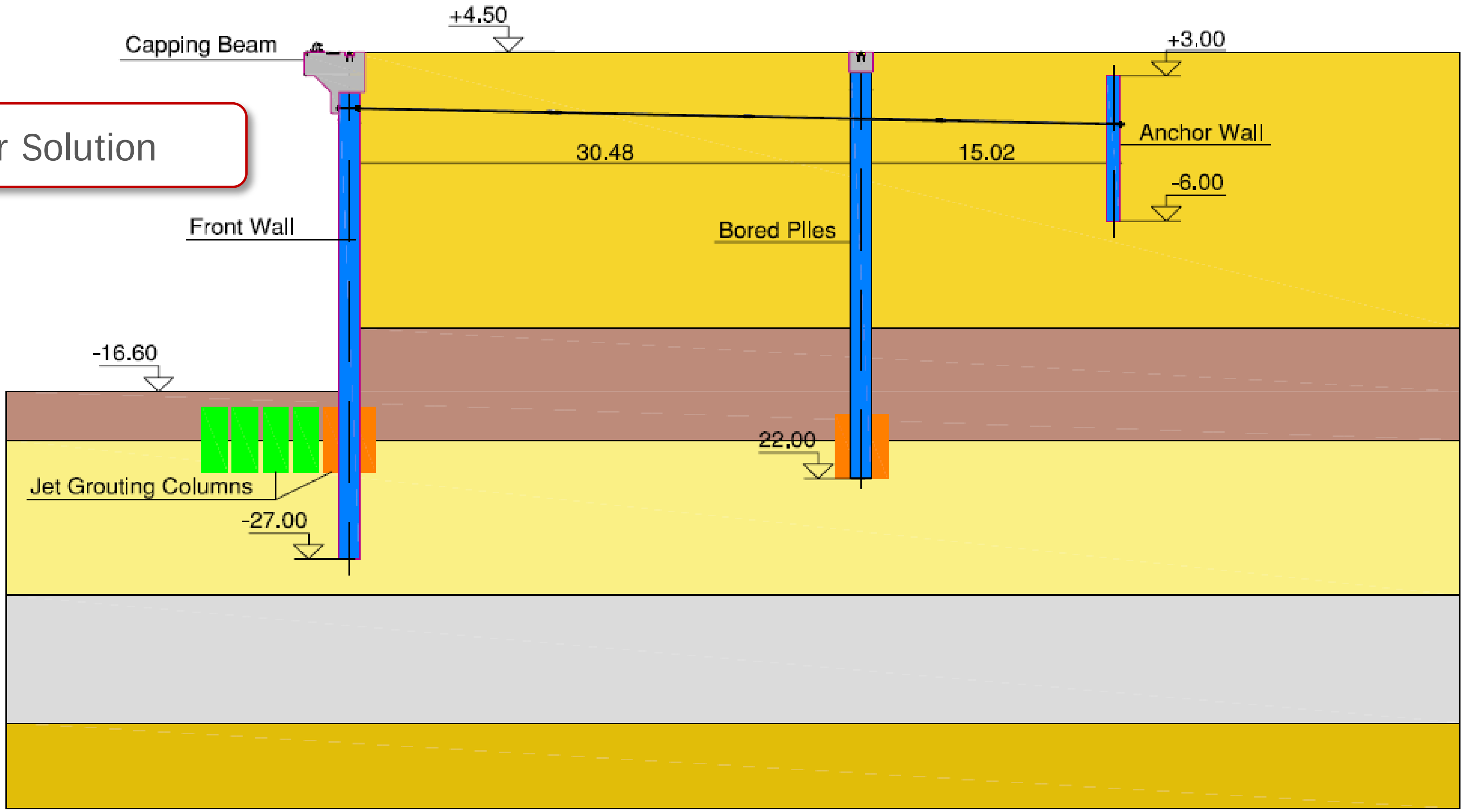

- Main differences:
  - Softer and weaker silty layer at the passive zone;
  - Soft clay layer very close to the bottom of the quay wall;
- Main problems:
  - Increase of the bending moments;
  - Reduced safety against vertical punching failure
- Adopted Solutions:
  - skin friction increase by means of secant jet grouting columns
  - increase of passive stiffness and resistance by means of a ground improvement with jet grouting columns

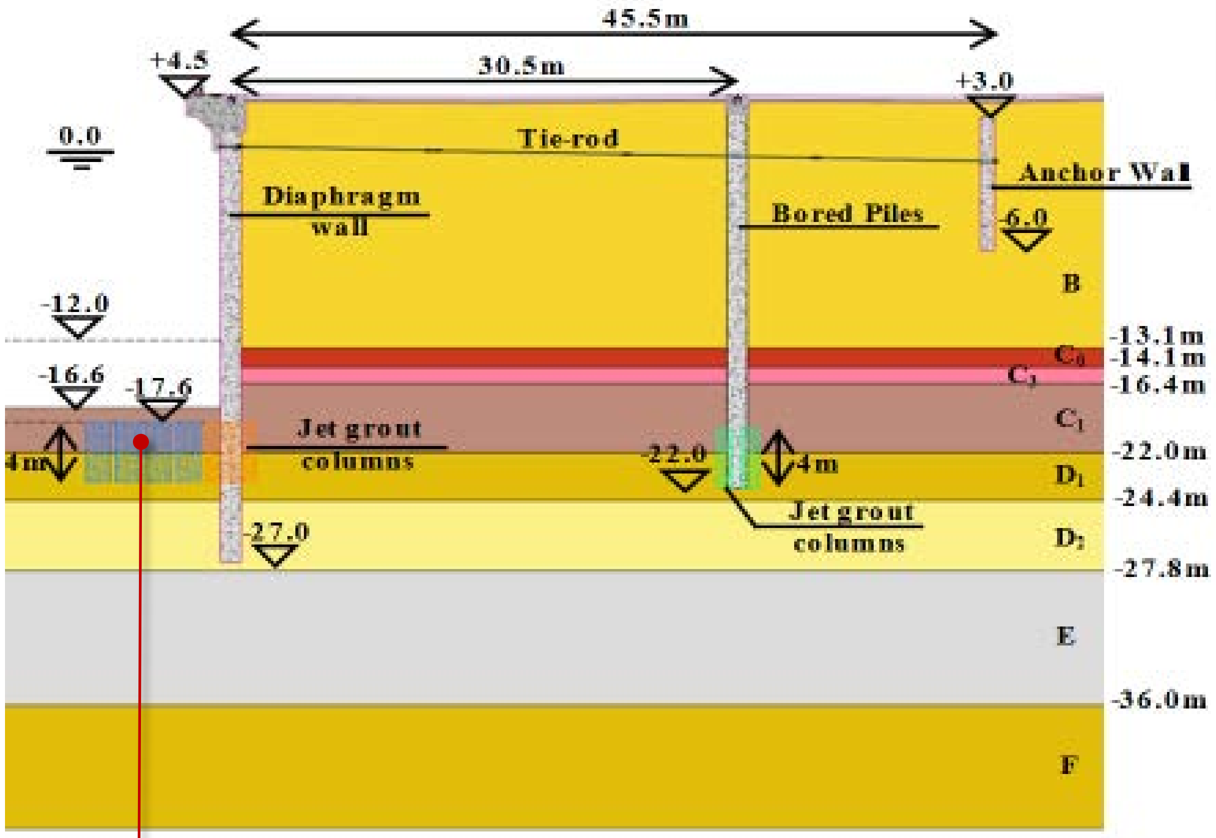

Secant Jet Grouting Columns
Φ 1.500mm at a distance of 0.80m from the wall axis, spaced 3.0m

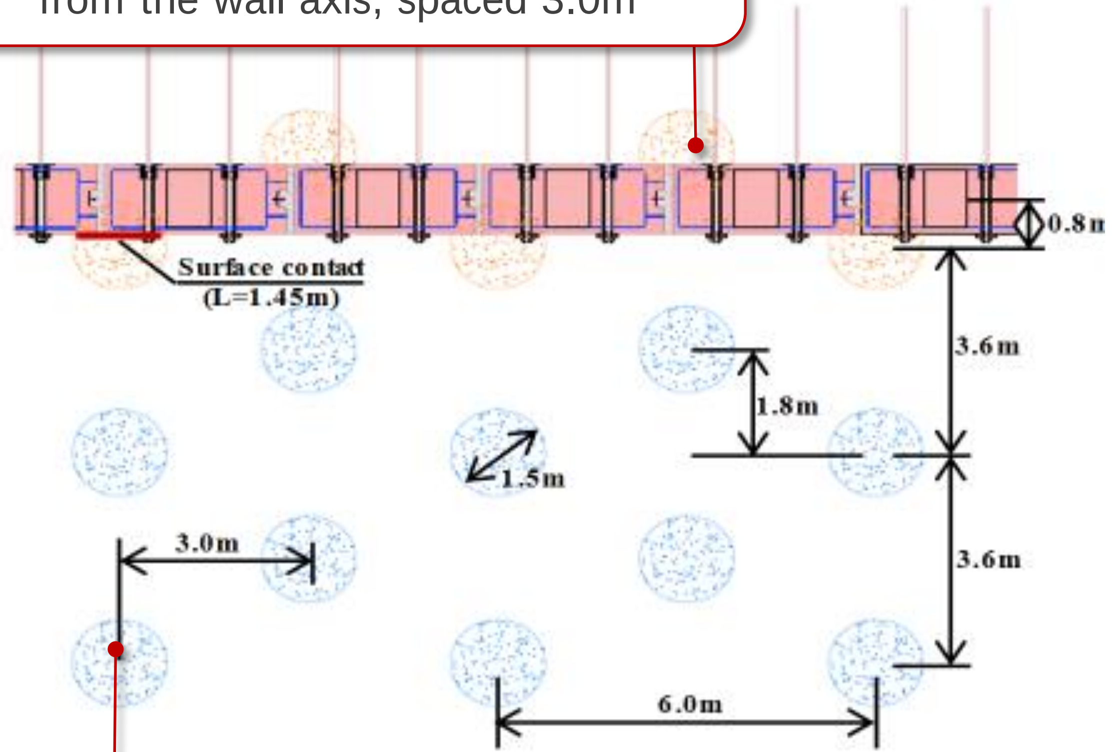

Jet Grouting Columns
Φ 1.500mm – L=4,0m
Passive zone

Jet Grouting Columns
(Passive Zone)
Triangular treatment grid spacing 3.0m x 3.0m

ULS Verification – Global Failure

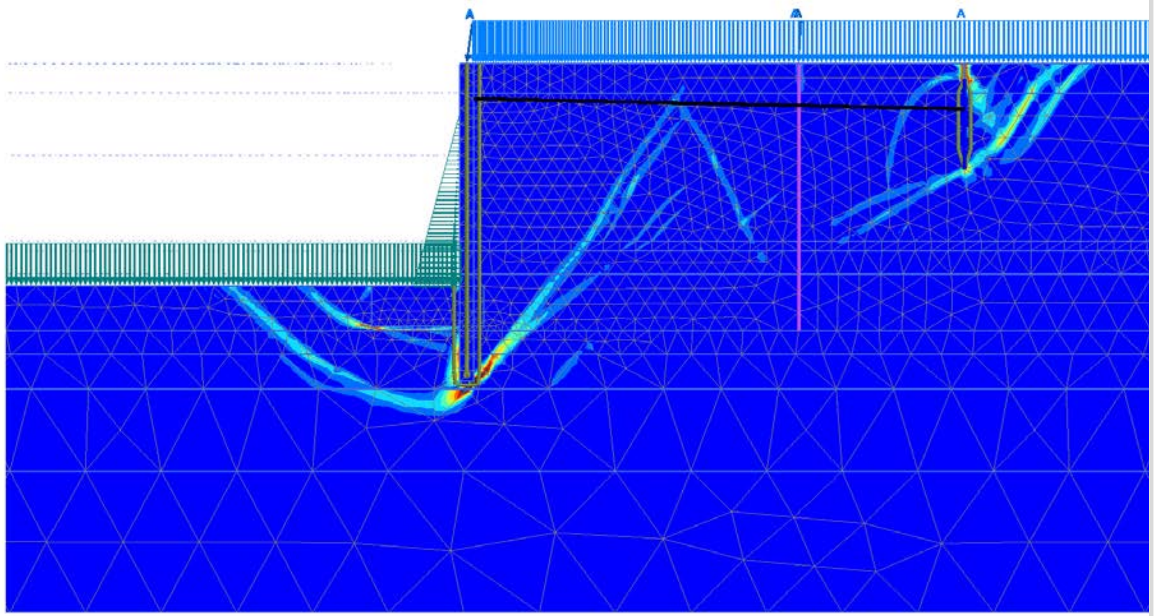

SLS Verification – Identification of the control points

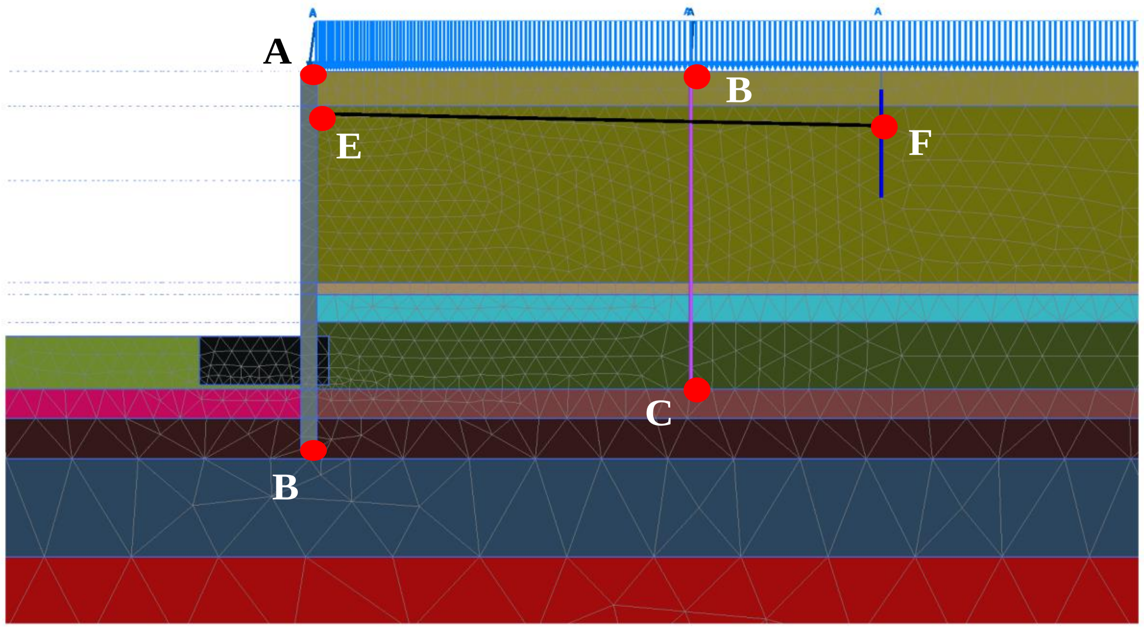

- The results of the overall stability modes, assessed by a φ'/c' reduction analysis (Plaxis 2D (Brinkgreve et al., 2014), lead to safety factors of 1.10 and 1.01 (higher than the required minimum safety factor of 1.0, according to Eurocode 7)

2.2 Temporary Earth Retaining Walls

- The versatility of jet grouting enables its use on temporary earth retaining structures, allowing overcoming earth stability problems during construction.

- The present case reports to the construction of jet grouting walls, in the transition zone between a new quay wall and an existent breakwater.

- Two different solutions were executed according to the excavation geometry and the main constraints observed at the site.

- **SOLUTION 1 – Jet grouting gravity wall**:
  - 1.5m diameter jet grouting columns, spaced at 1.2m, center to center;
  - Use was made of 14.0m to 15.0m long jet grout columns to support the container storage platform and the slope stability in the breakwater area.

- **SOLUTION 2 – Junction of the quay wall with the existing breakwater**
  - The jet grouting wall was formed by two rows of 1.5m diameter jet grouting columns.
  - The wall stability was partially ensured by buttresses composed by 1.5m diameter jet grouting columns, spaced of 2.4m. Each buttress was constituted by 9 perpendicular jet grouting columns.

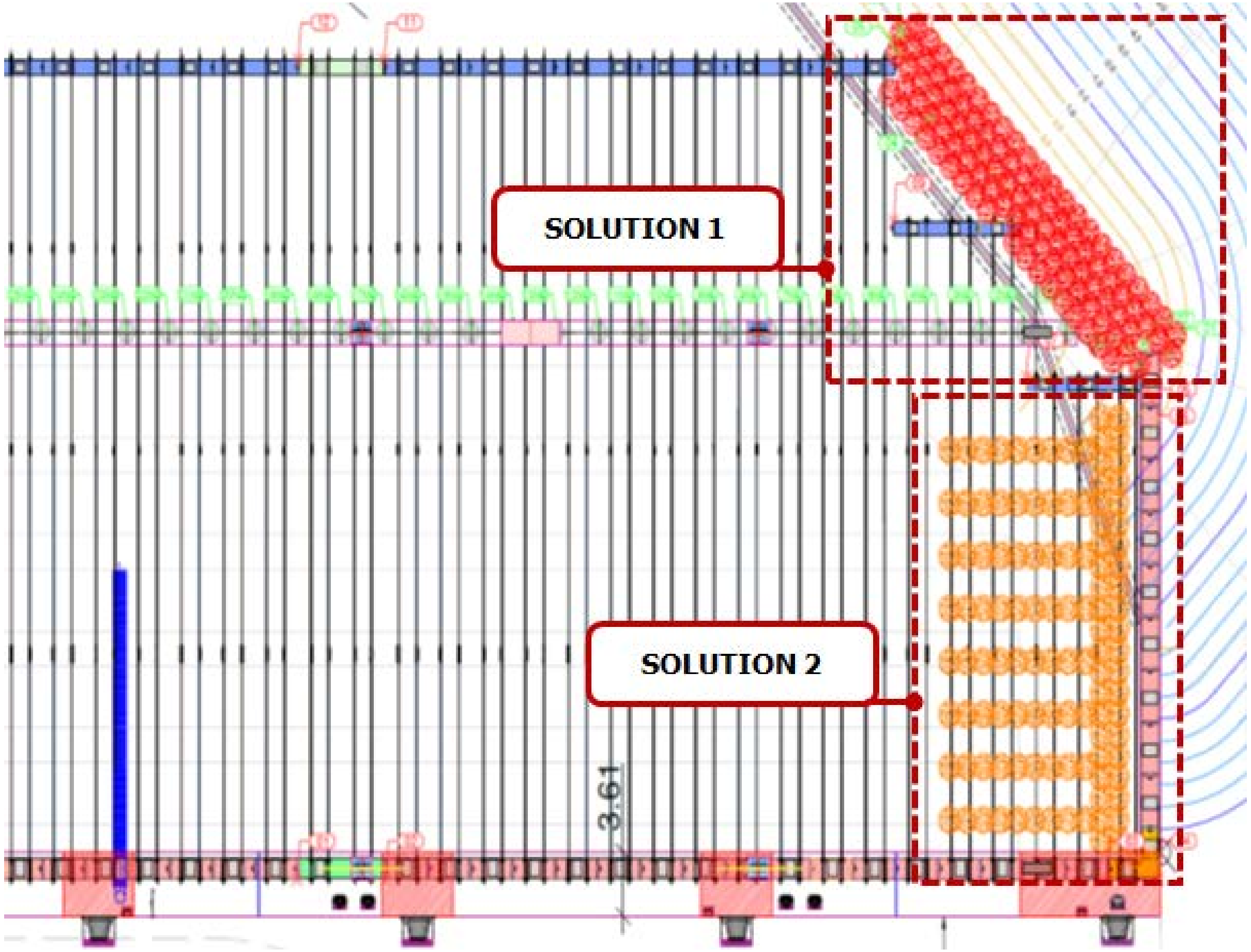
SOLUTION 1
SOLUTION 2
3.61

2.3 Assessment of Jet grouting Columns Diameter using Non-Destructive Methods

What is the real jet grouting columns diameter over depth??
Do they meet the design requirements??

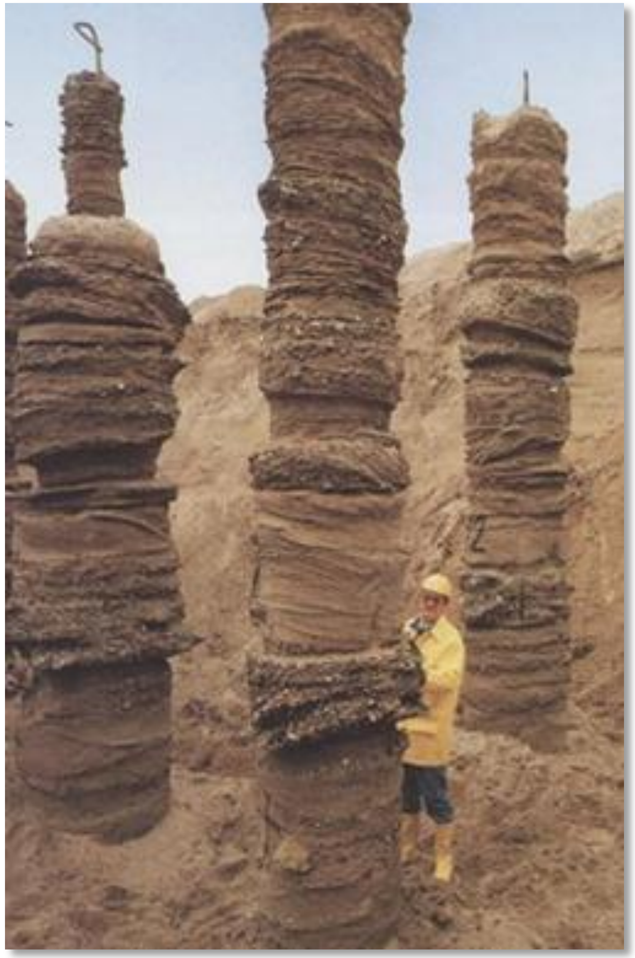

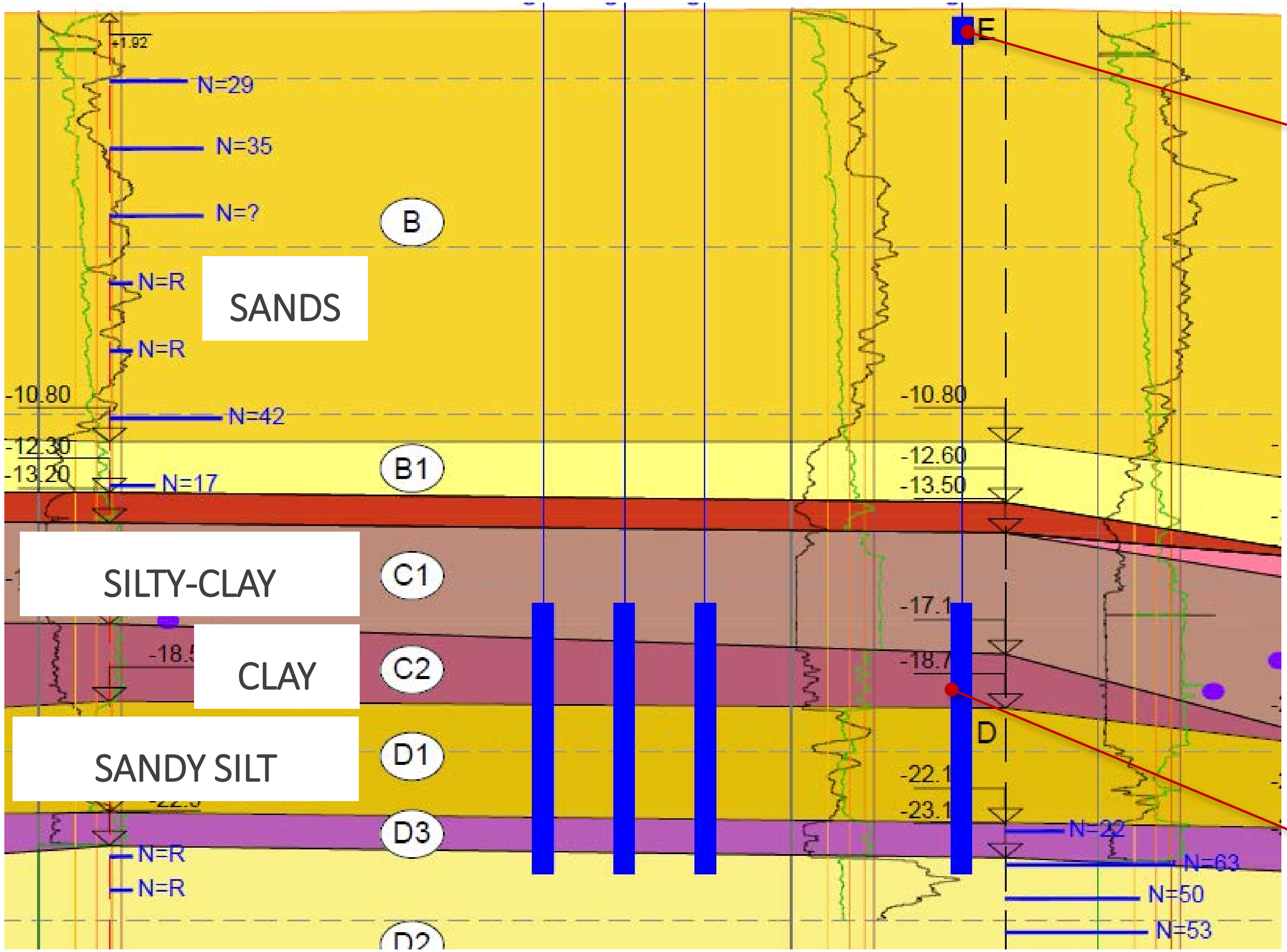

JG TEST **column E**
(depth: 1.0m - 5.0m)
L=4.0m

GEOLOGICAL / GEOTECHNICAL PROFILE

TEST COLUMNS

JG TEST **column D**
(depth. 20.1m - 28.1m)
L=8.0m

JET GROUTING – EXECUTION PARAMETERS

	Injector		Fluid Press.	Air Press.	Flow rate	Progress speed	Rotation	Dosage of grout	Gouted volume	Cement rate
	n.	DN mm	bar	bar	l/min	Sec/4 cm	rpm	A/C	l/ml	Kg/ml
Drilling	2	4-4.5	240	10-12	355	2,4	35	-	-	-
Water Jet	2	4-4.5	350	14	425	12	4.05	-	-	-
Grounting	2	4-4.5	415	10	365	15	7	0,74	2281	2237

Quality Control / Quality Assurance

Destructive Methods (tradicional):

- Extraction of soil-cement samples, collected by coring;

Non-Destructive Methods

- Electric resistivity tests(“electric cilinder” - CYLJET®);
- Seismic cross hole tests.

Destructive Methods (core drillings)

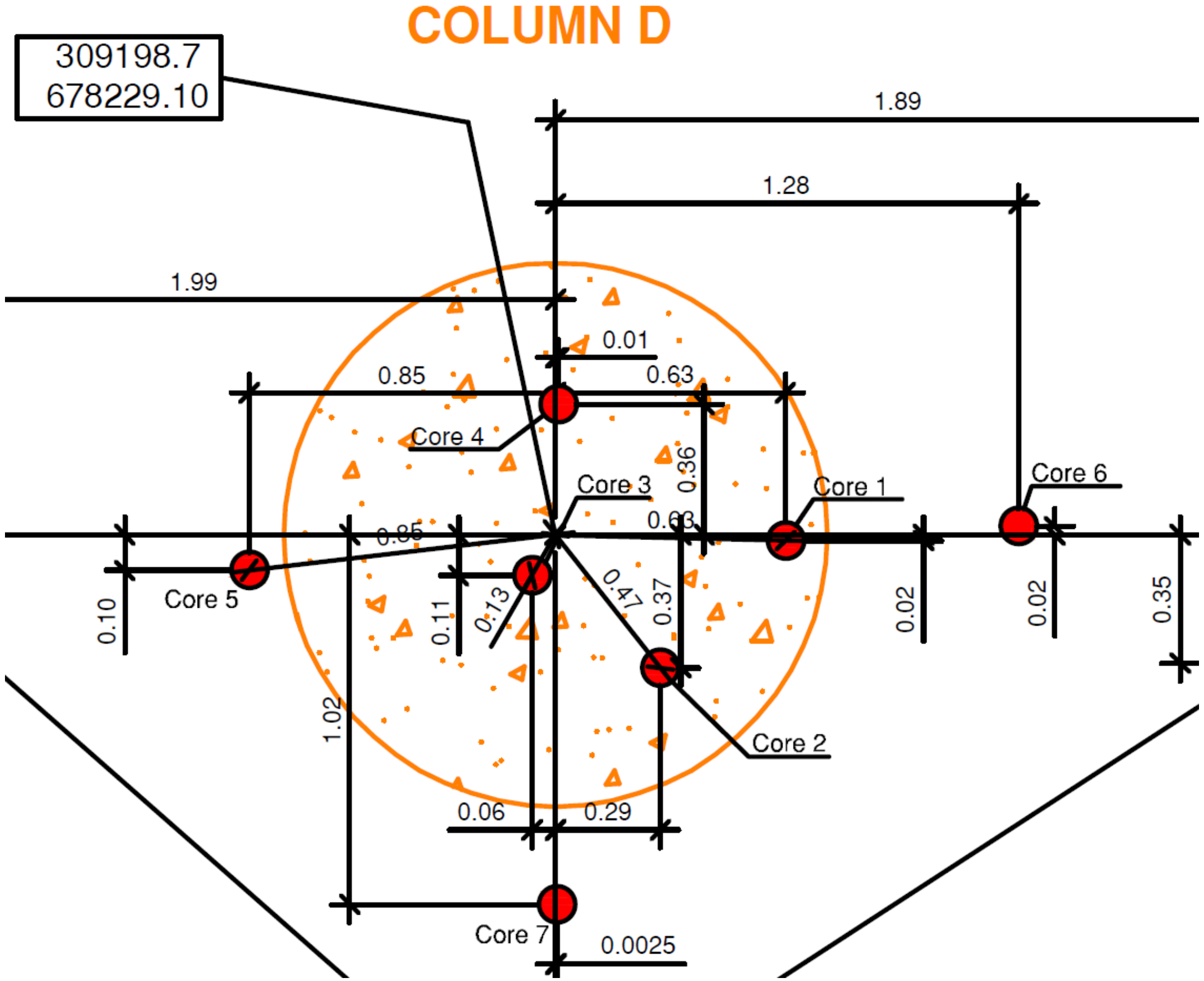

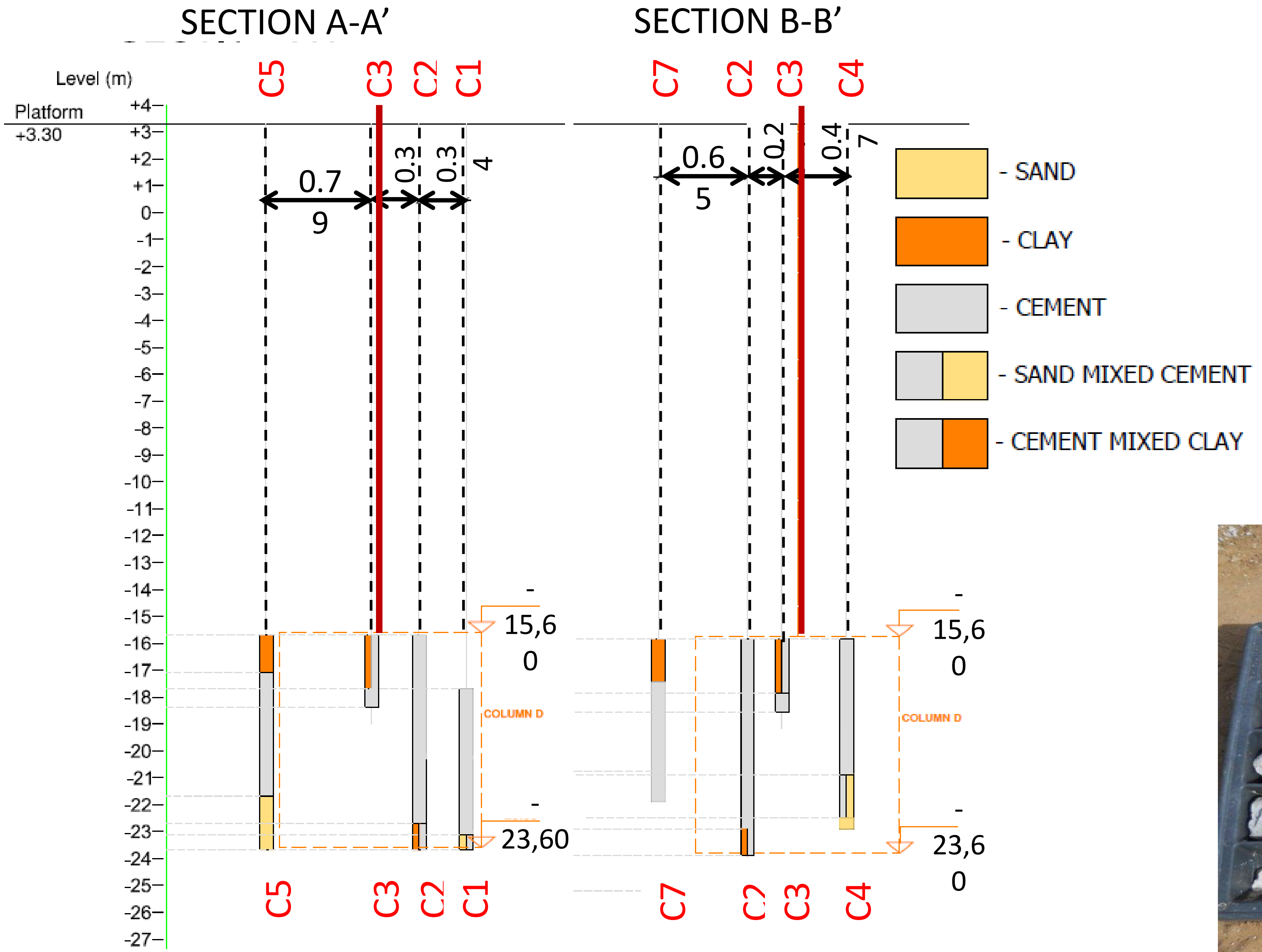
SECTION A-A'
SECTION B-B'
Level (m)
Platform
+3.30
C5
C3
C2
C1
C7
C4
0.7
9
0.3
0.3
4
0.6
5
0.2
0.4
7
-15,60
-23,60
-15,6
0
-23,6
0
COLUMN D
- SAND
- CLAY
- CEMENT
- SAND MIXED CEMENT
- CEMENT MIXED CLAY

Destructive Methods (extraction of soil-cement samples, collected by coring):

- Main inconvinients:
  - Costs and schedules:
    1. Core drillings are costly and time consuming
    2. The coring process and the quality of the samples requires that the composed soil-cement material is sufficiently hardened (specially in clays)
  - Execution:
    1. The quality of the samples is often compromized (dificult interpretation of the results);
    2. Drilling deviations (namely, in columns executed at considerable depths – TIGOR device is highly recomended).
  - Main limitations :
    1. Results are limited to the singular point where the drilling was undertaken (distance to the column axis);
    2. Reliable results require that a great number of cores are extrated.

Examples of soil-cement samples collected by coring
What are the conclusions regarding the column diameter?

Non-Destructive Methods (seismic cross hole and electric resisitivity tests):

- Main Advantages:
  - **Costs and schedules**:
    1. Tests are very economic (by comparison with core samples extration);
    2. The tests can (must be) undertaken imediatly after the jet grouting column is executed;
    3. The data is easily processed, leading to a quick obtention of the results.
  - **Execution:**
    1. The installation of measuring devices is simple and easy to control;
  - **Results:**
    1. Assessement of the complete jet grouting columns diameter over their entire lenght;
    2. Accuracy of the results (+/- 10% on the calculated diameter using the resistivity method – electric cylinder)

Electric Resistivity Test – Electric Cylinder CYLJET®:

- Assessement of the *in situ* soil resistivity – calibration borehole;

- Once the jet grouting column is completed, a PVC slotted casing in driven down the column centreline, while the column is still in fresh. An electric cylinder cable is then inserted to measure the resistivity in the surrounding medium.

- The PVC casing must be fulfilled with water or other substance providing good electrical contact between the electrodes and the surrounding ground. In case of CYLJET® application, a cable with 32 electrodes, spaced of 0.30m is used

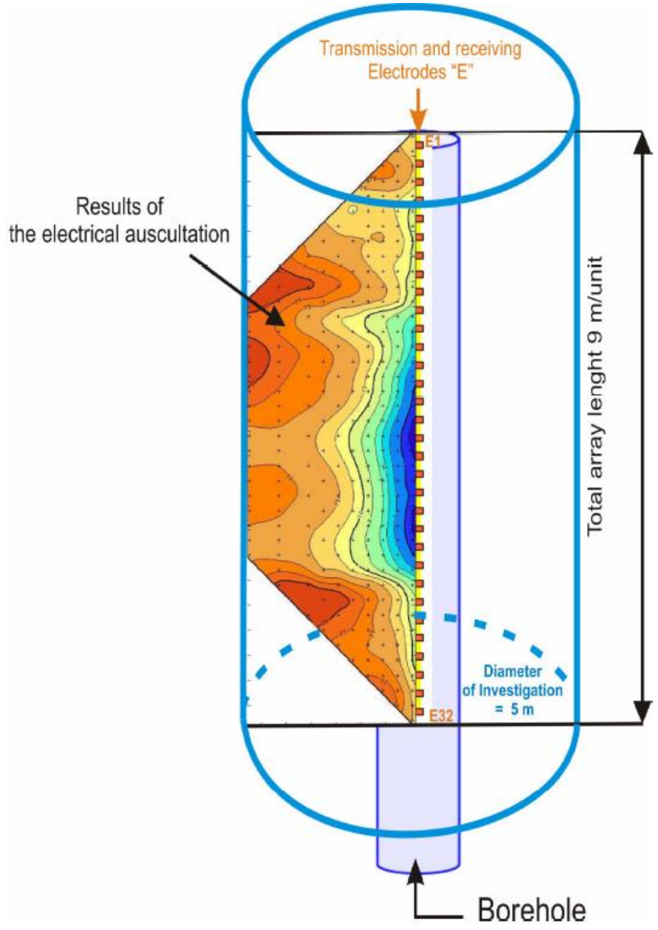

Electric Resistivity Test – Electric Cylinder CYLJET®:

- New assessment of the soil electric resistivity (after the jet grouting column is executed);
- Resistivities comparison (before and after the jet grouting column is executed):
  - Natural Soil – low conductivity (dezens of ohm-m);
  - Jet grouting (fresh) – high conductivity (a few ohm-m).

Remmark : The lower the resistivity, the more easily the material allows the passage of an electrical load.

- The electric cylindrical test (CYLJET®) provides a resistivity pseudo section in a **3 to 5 meters diameter cylinder of ground** (depending on ground resistivity).

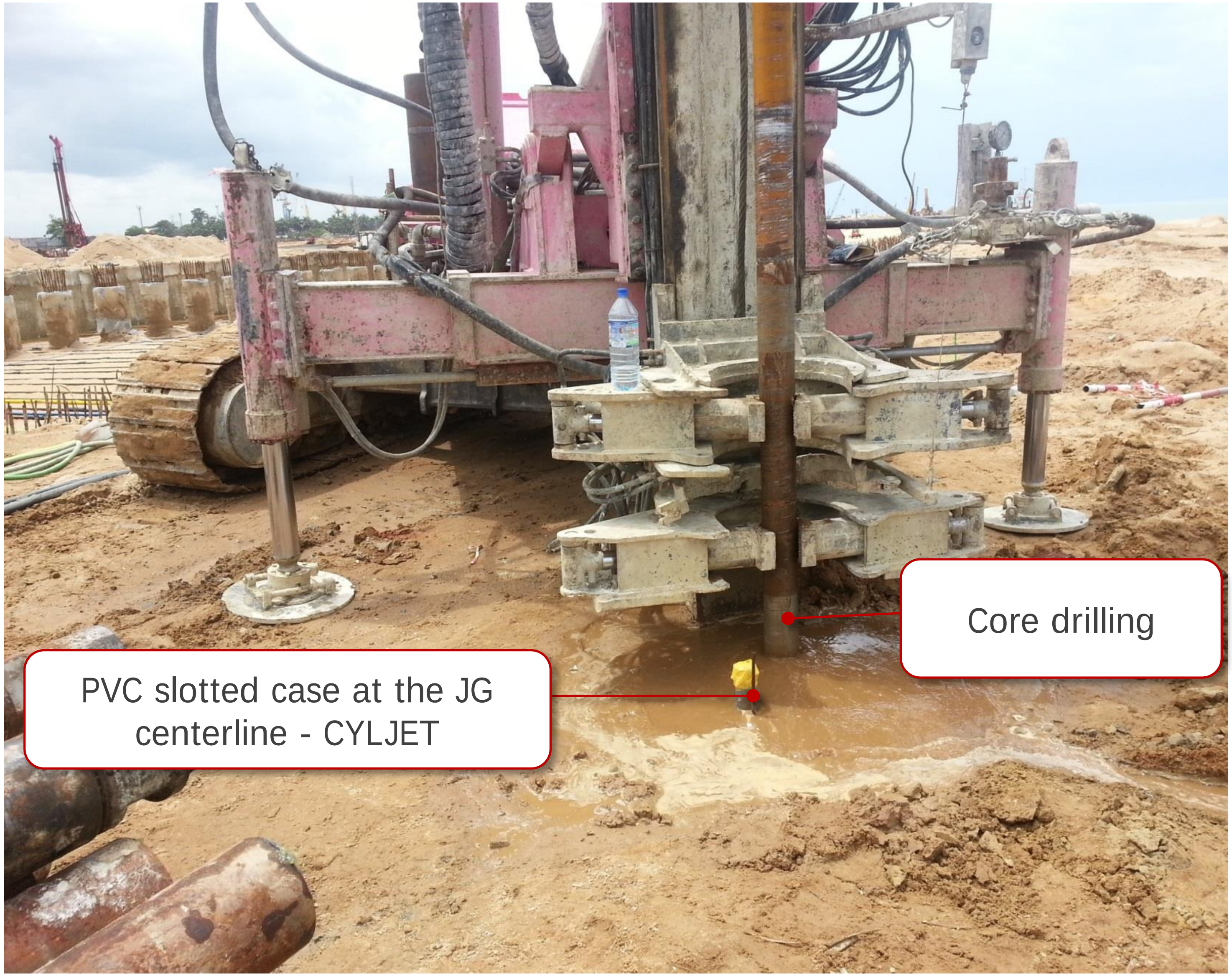
Core drilling
PVC slotted case at the JG centerline - CYLJET

Summary of results – JET GROUTING TEST COLUMN D

Destructive Methods (soil-cement material colection):

- Core drillings at a maximum distance of 0.79m from the column axis – minimum JG column diameter 1.500mm was reached.

Non-Destructive Method - Electric Resistivity - CYLJET®:

- Minimum JG column diameter: 1.500mm.
- Maximum JG column diameter: 1.700mm

JG COLUMN D
(Depth. 20.1m to 28.1m)
L=8.0m

Non-Destructive Method Seismic Cross Hole

- Average JG column diameter: 1.750mm.

Seismic Cross Hole

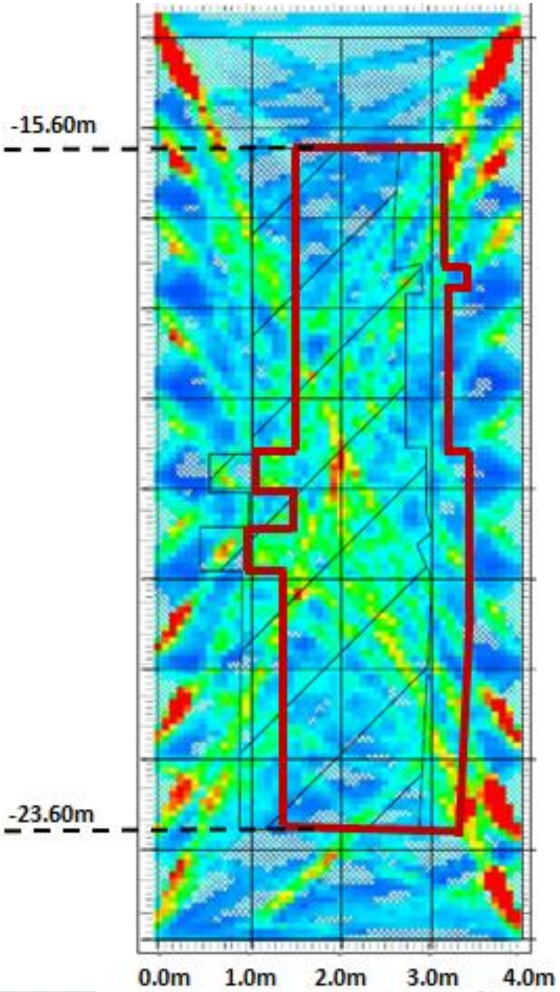

JG COLUMN D
(Depth. 20.1m to 28.1m)
L=8.0m

Seismic Cross-hole Column D
Date: 7/07/2014
Shot spacing: 1 meters
Number of channels: 2
Number of mesurements: 470
Type of wave: S
Hole deep: 27 meters
Max. definition: 2.5 cm.
Promedium diameter: 1.75
Weight of Inyection: 7.57

Electric Cylinder - CYLJET®

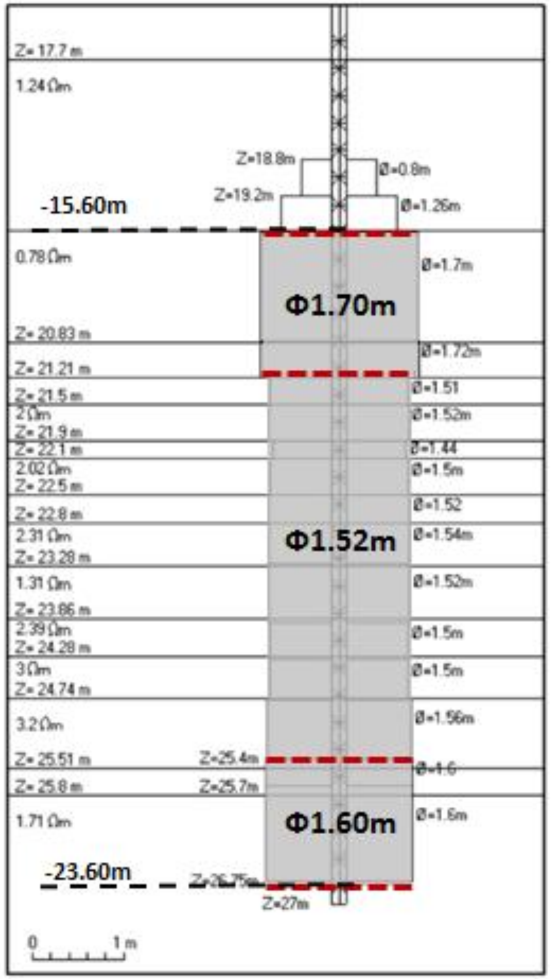

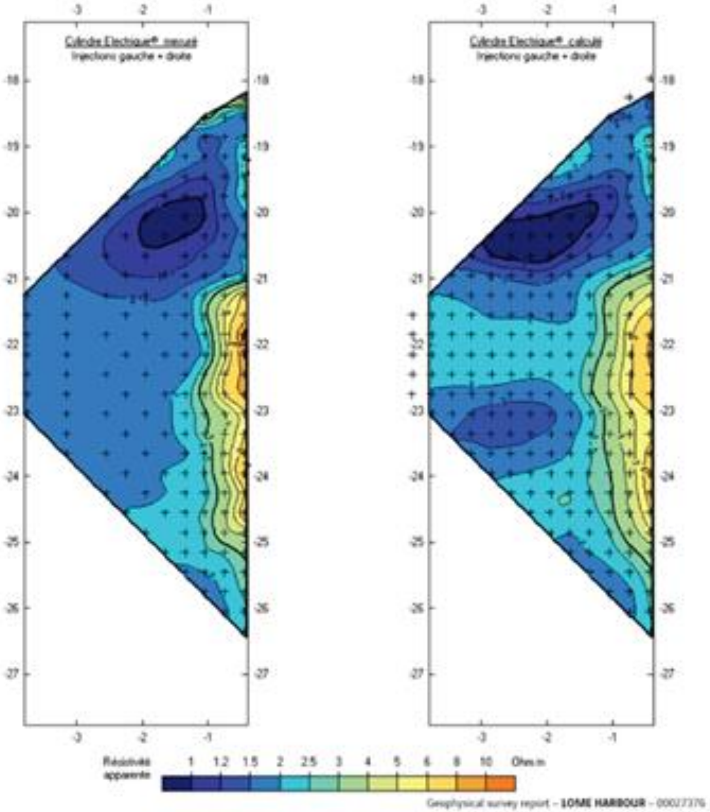

Confirmation Electric Resistivity Test Results – SURFICIAL JET GROUTING TEST COLUMN E

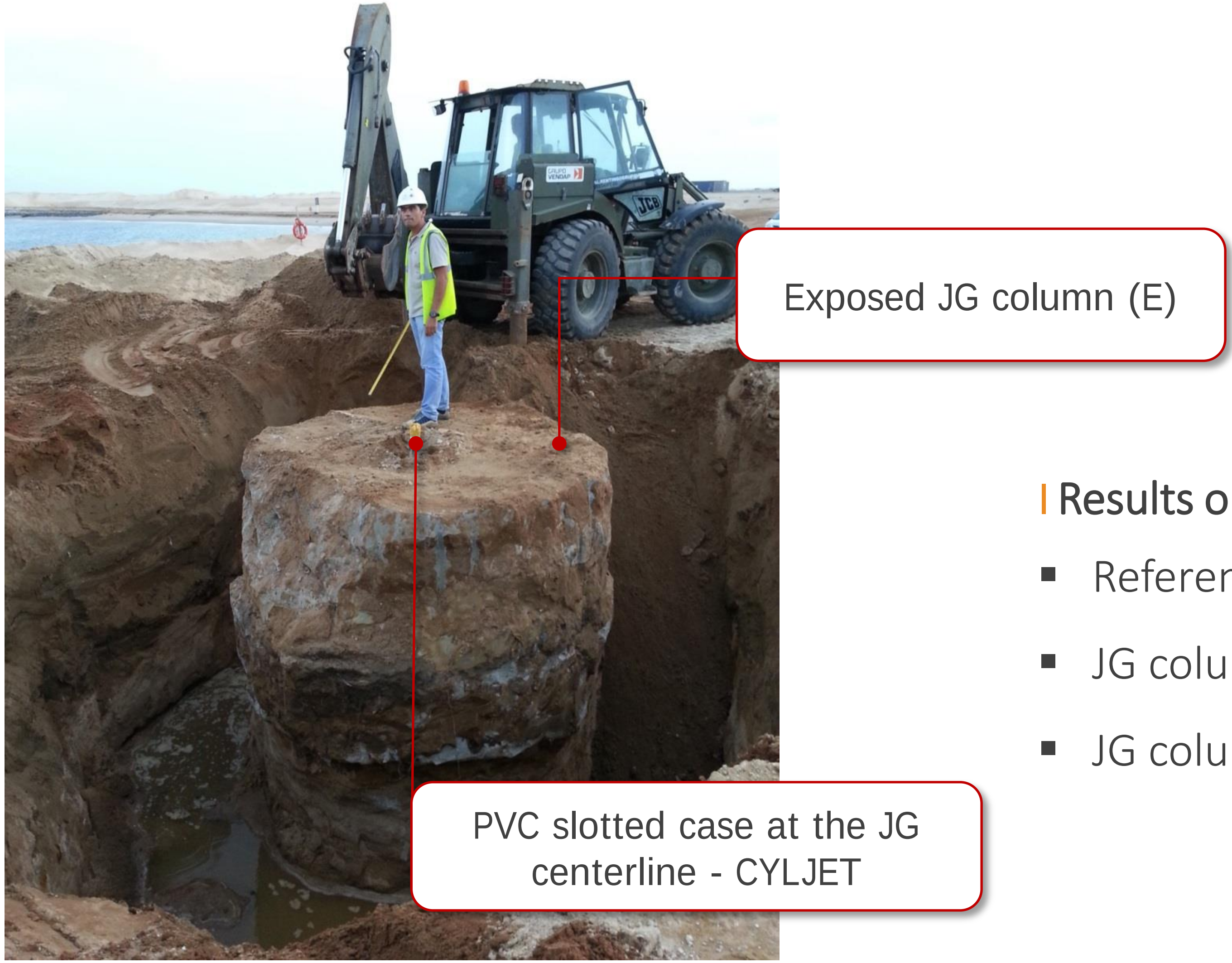

JG COLUMN E
(depth. 1.0m to 5.0m)
L=4.0m

Results obtained by direct measuring

- Reference JG column depth: 3.10m (level -0.60m)
- JG column perimeter: 7.30m
- JG column diameter: **2.32m**

Electric Cylinder - CYLJET®

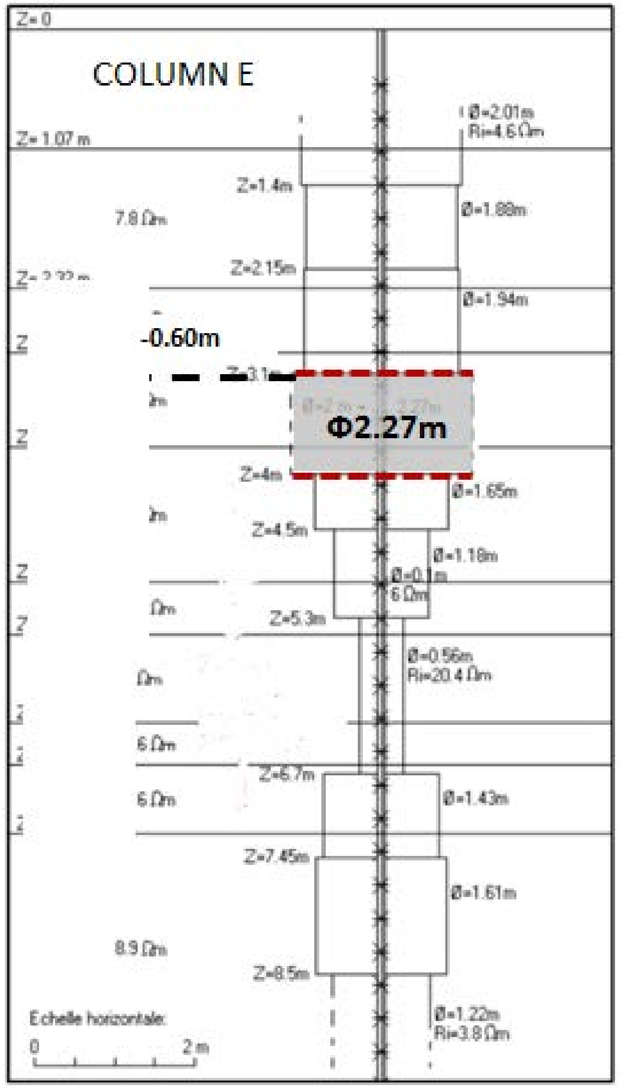

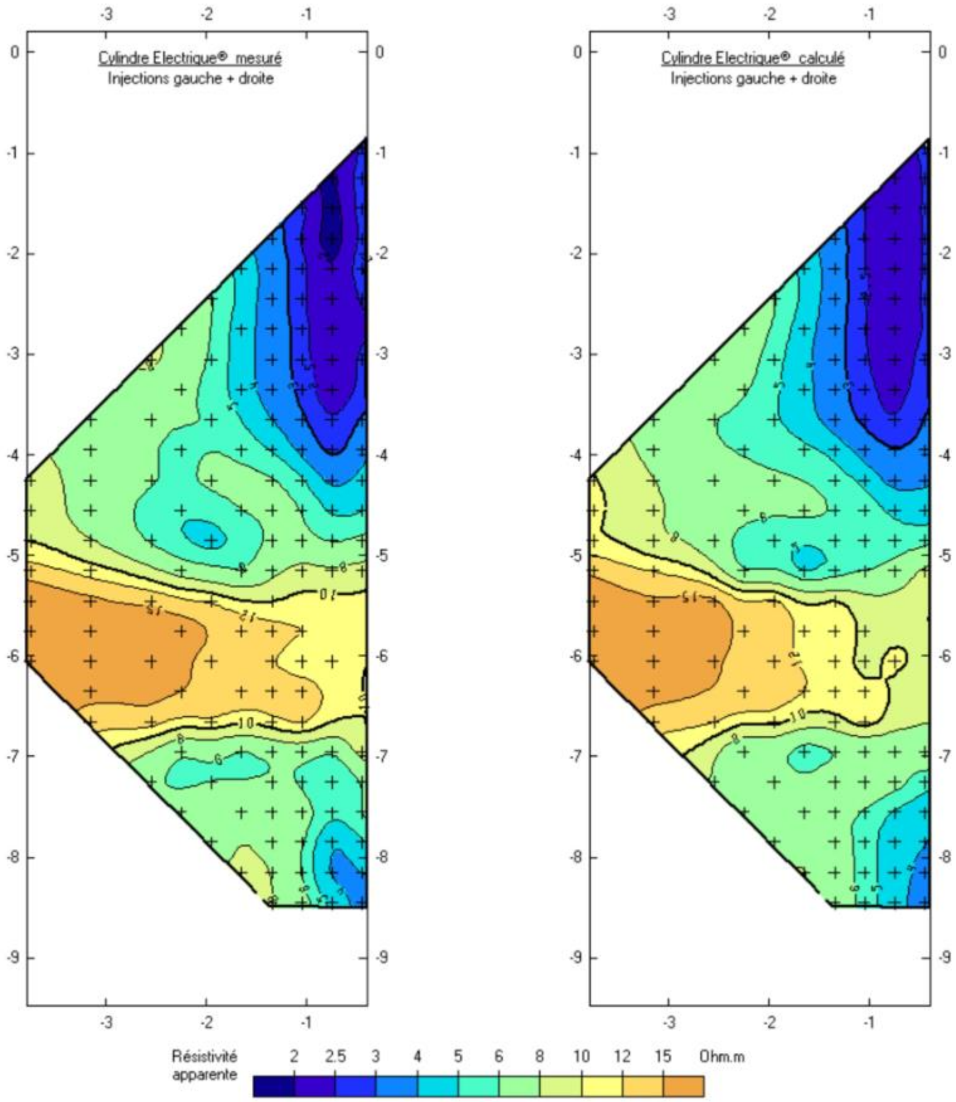

JG COLUMN E
(depth. 1.0m to 5.0m)
L=4.0m

Results

- Real: 2.32m
- CYLJET: **2.27m**
- Error: 2.2%

2. VIBRO TECHNIQUES

3.1 Vibrocompaction

Site characteristics

- Terminal area: 800.000m^2
- Port platform: **3.50m high landfill** (to form a base for the concrete pavement slab)
- Service load: **70 kPa**

Objectives

- Achievement of a minimum relative density of **ID>70%** in all the upper frictional soil layers ("medium dense to loose" sands - found to be at a maximum depth of 12m to 15m);
- Reduce the magnitude of the horizontal earth pressure imposed on the 1000m long quay wall (by increasing the soil internal friction angle).

Main Challenges

- Definition of the terminal areas where the ground improvement was necessary (and compatible with the vibrocompaction process):
  - Determine the soils with a relative density ID<70%;
  - Evaluate the soils characteristics and their compatibility with the use of vibrocompaction;
  - Define the execution parameters (required treatment grid spacing of the compaction probe);
  - Cost optimization.

3.1.1 Assessement of ground improvement areas

Preliminary stage (grain size distribution analysis) :

- Identification of soils with a fine content FC <10% - *Degen (1997)*
- Qualititive soil classification based on an "acceptability parameter" (SN) - *Brown (1977*)

Execution stage:

- Soil Classification using CPT results: "Soil Behaviour type Index" (Ic) - *Robertson (2010)*
- Evaluation of "soil compactibility" - *Massarch (1994)*

(analysis undertaken based on 85 CPT results and 81 boreholes with SPT)

SOIL BEHAVIOUR TYPE INDEX" (IC) - *Robertson (2010)*

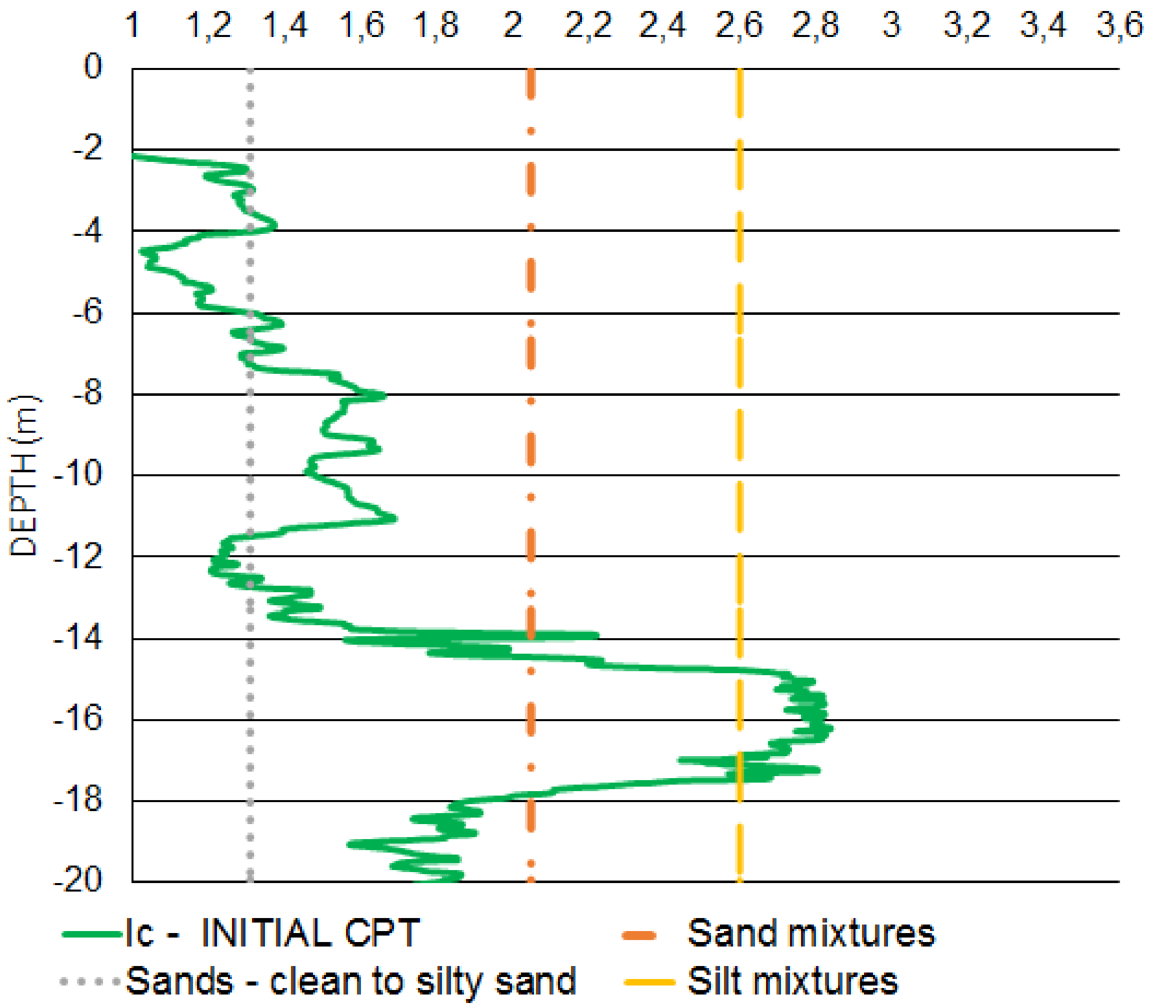

SOIL COMPACTIBILITY - Massarch (1994)

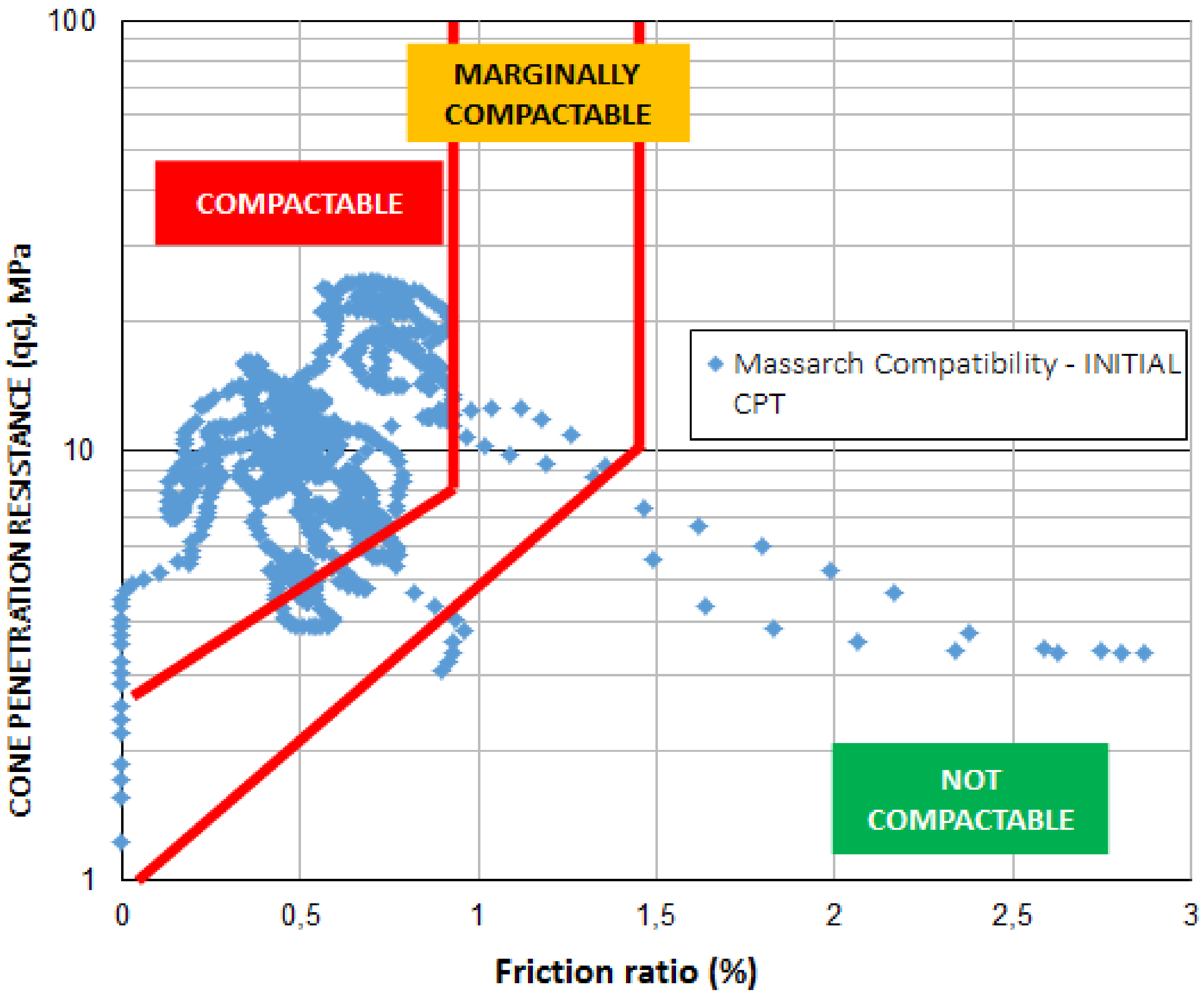

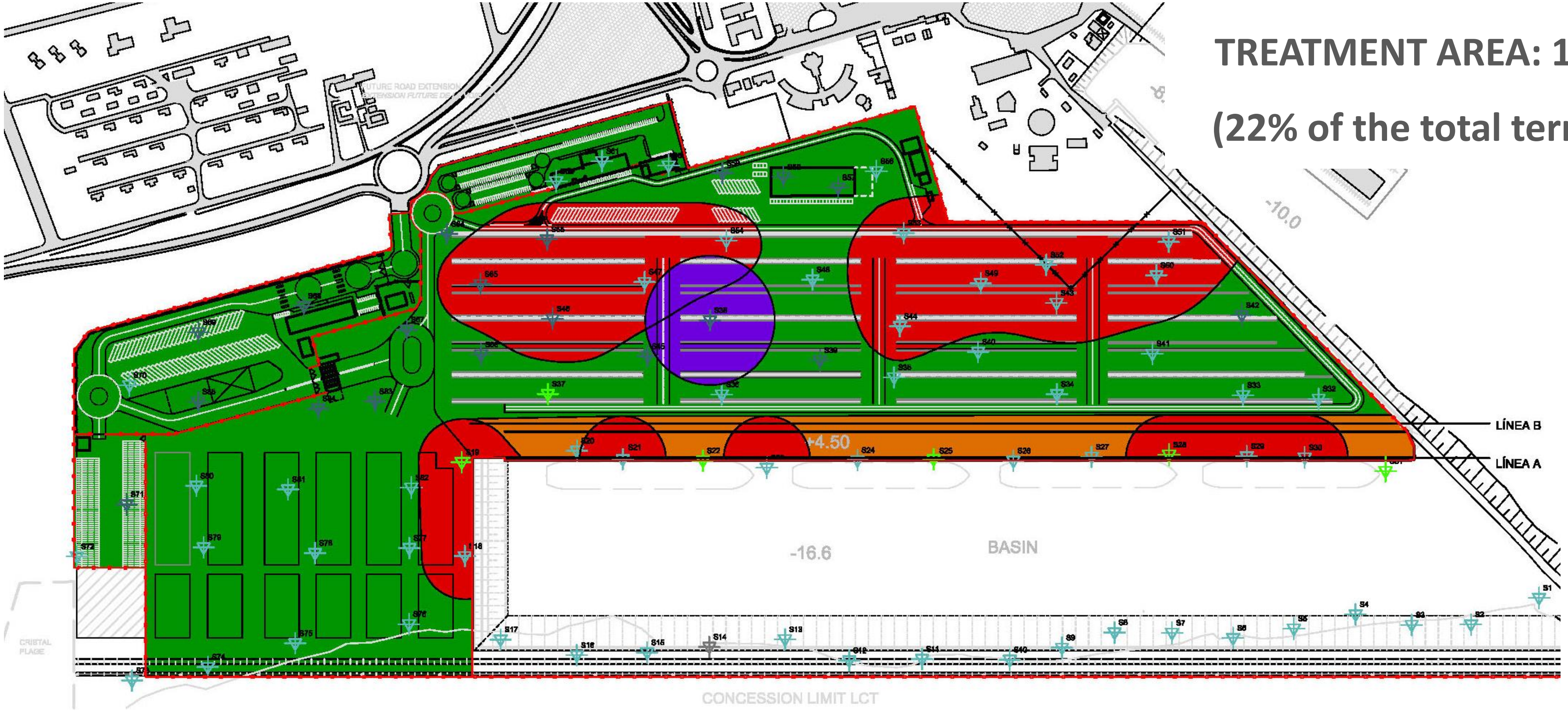

TREATMENT AREA: 176.000 m2

(22% of the total terminal area)

VIBROCOMPACTION NOT REQUIRED

COMPACTABLE ZONE

MARGINALLY COMPACTABLE

3.1.2 Relative Density Results

Preliminary Field Tests

- Define the required treatment grid spacing of the compaction probe to achieve a minimum relative density **ID<70%** in all the upper frictional soils.

- Soil relative density was determined according to the **Jamiolkowski et al. (2001)** formulation (relative density can be directly determined as a function of the cone penetration resistance (q_c) and soil vertical effective stress).

- Trials were performed in 9 field tests (FT1 to FT9) distributed at several locations of the terminal area.

Field Tests **FT1 to FT4**:

- **6** triangular treatment pattern grids with spacings of 3.30m; 3.50m; 3.70m; 3.90m, 4.10m and 4.30m;
- 58 compaction probe points (at depths varying from 12m to 15m);

Field Tests **FT5 to FT9**:

- **3** triangular treatment pattern grids with spacings of 3.30m; 3.50m and 3.70m

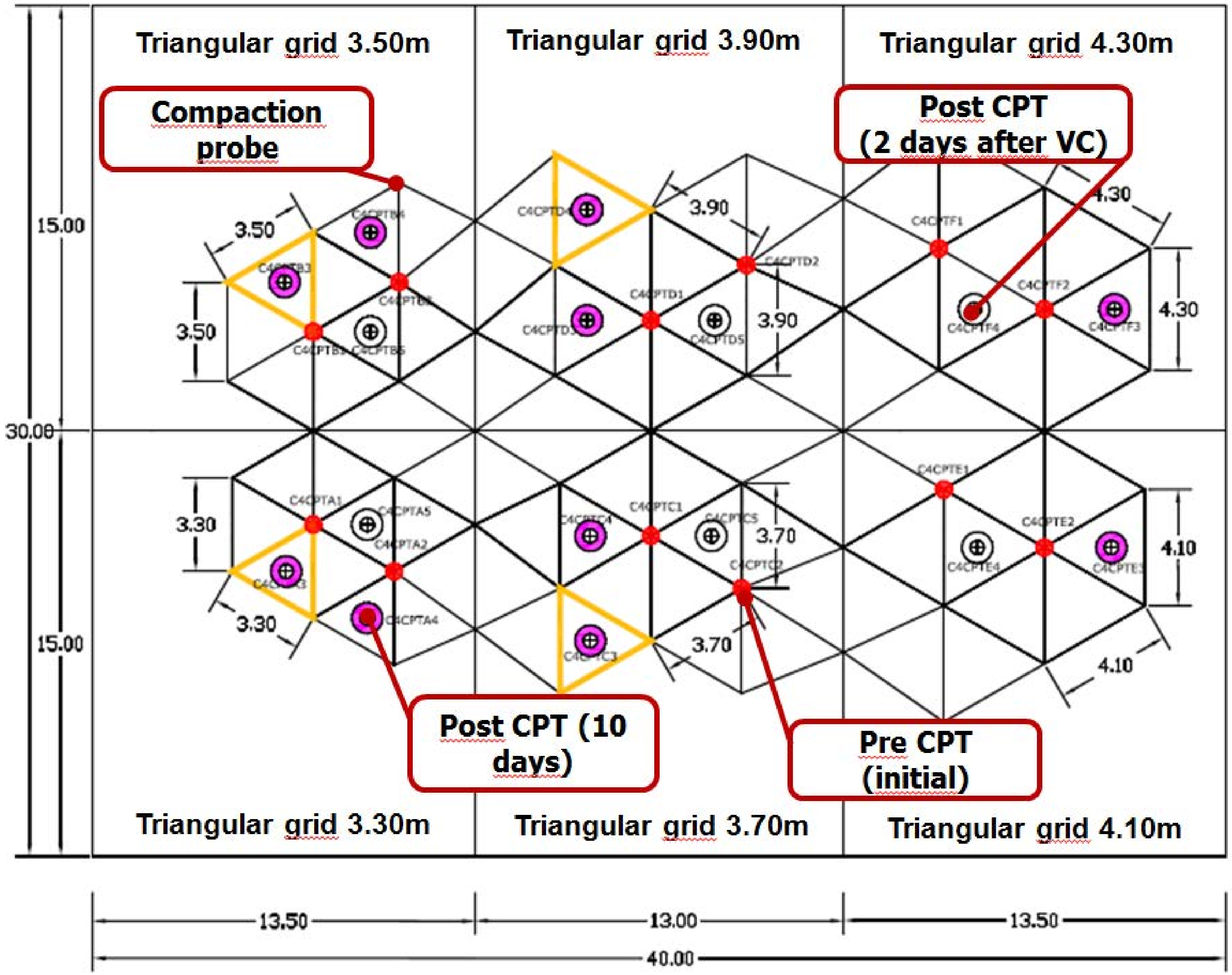
Triangular grid 3.50m
Triangular grid 3.90m
Triangular grid 4.30m
Compaction probe
Post CPT (2 days after VC)
Post CPT (10 days)
Pre CPT (initial)
Triangular grid 3.30m
Triangular grid 3.70m
Triangular grid 4.10m
15.00
30.00
15.00
13.50
13.00
13.50
40.00

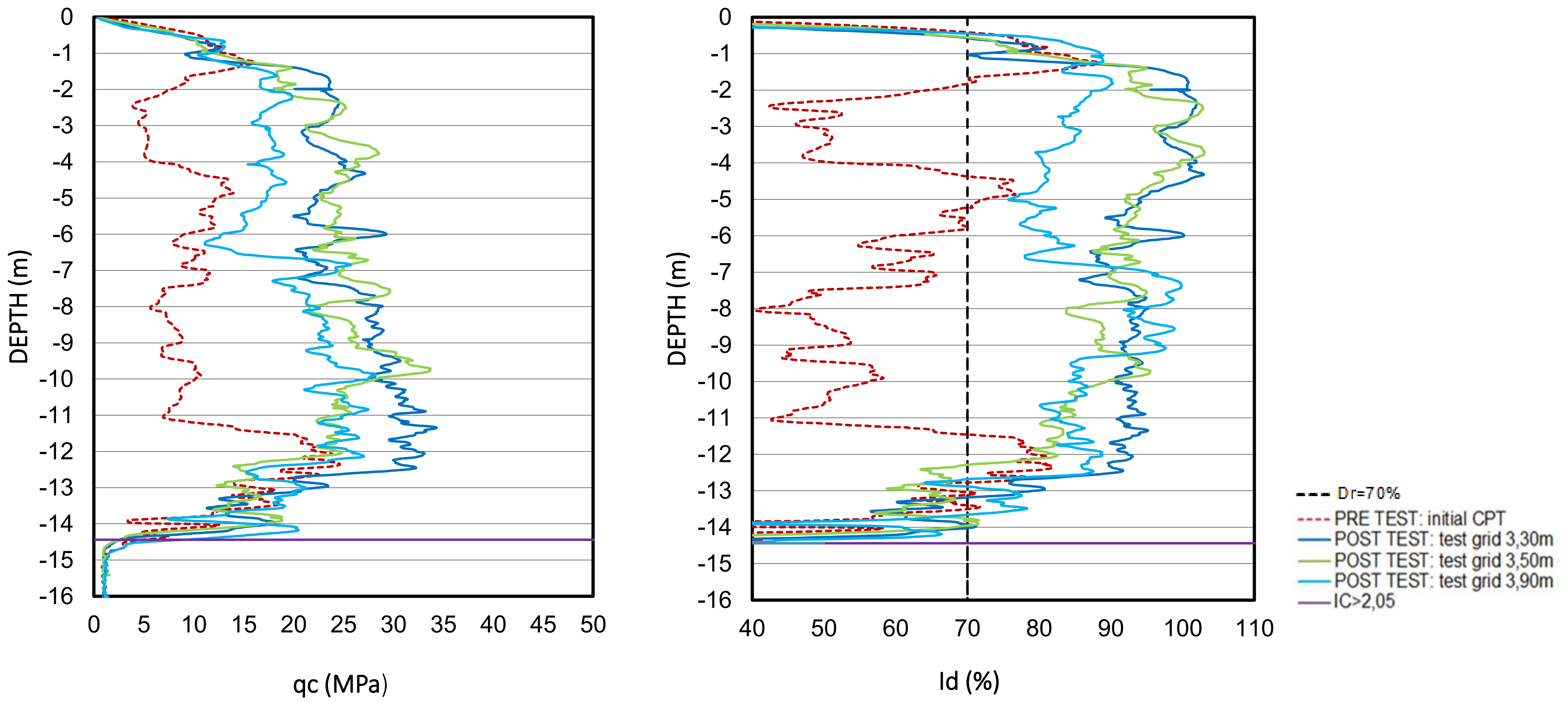
DEPTH (m)
qc (MPa)
Id (%)
Dr=70%
PRE TEST: initial CPT
POST TEST: test grid 3,30m
POST TEST: test grid 3,50m
POST TEST: test grid 3,90m
IC>2,05

TIME EFFECT AFTER VIBROCOMPACTION

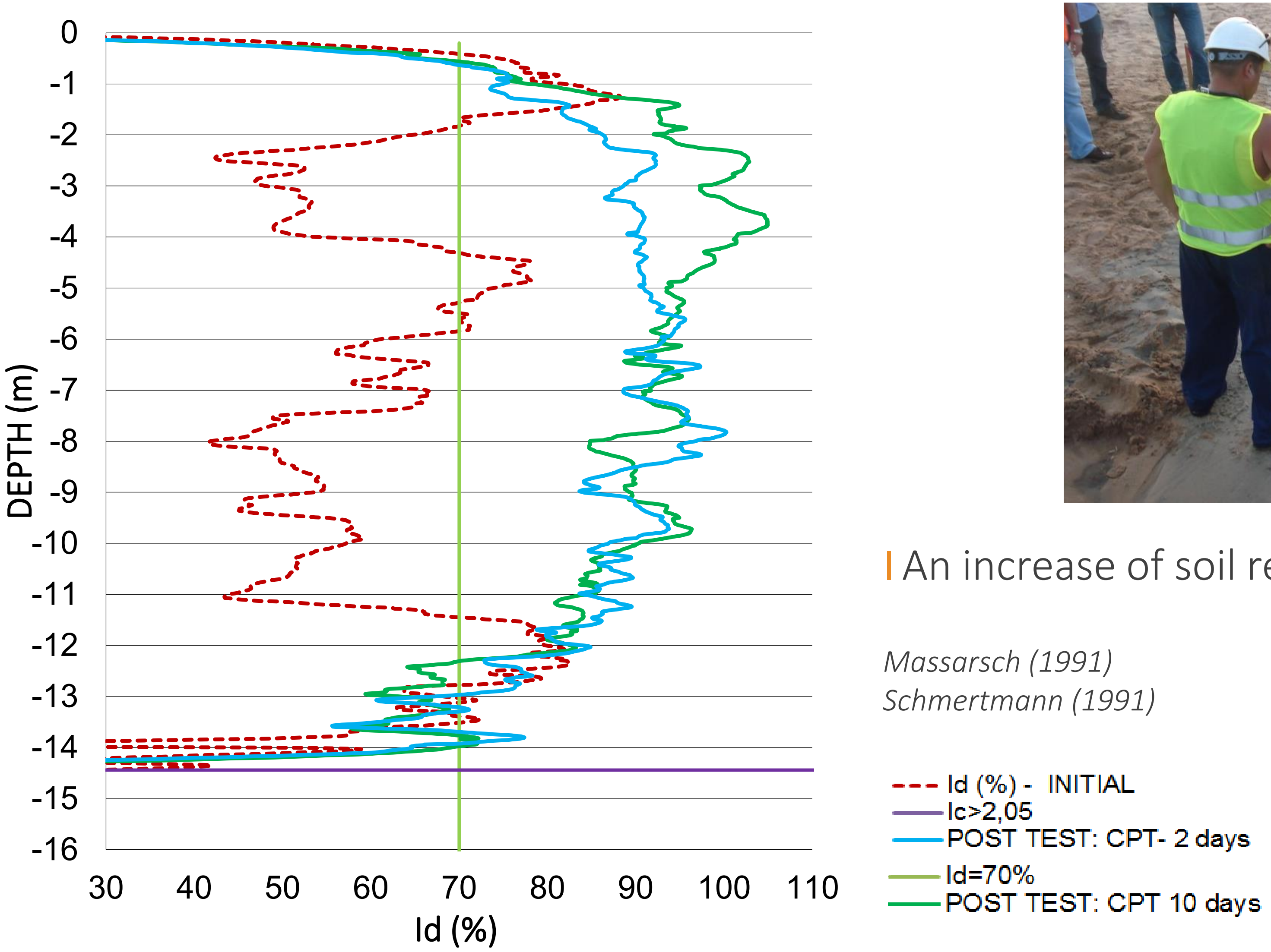

- An increase of soil relative density over time has been observed

Massarsch (1991)
Schmertmann (1991)

3.1.3 Limitations of Vbrocompaction Treatment

Particular case of Field Test **FT3** :

- Characterized by the presence of dense sands, typically with cone resistance values **25 <qc < 30 MPa;**
- Ground improvement efficiency was assessed based on field test results (triangular grid spacing of 3.30m and 4.30m);
- Evaluation of ground improvement behaviour over time (2 and 10 days after vibrocompaction has been completed).

3.30m TRIANGULAR GRID SPACING

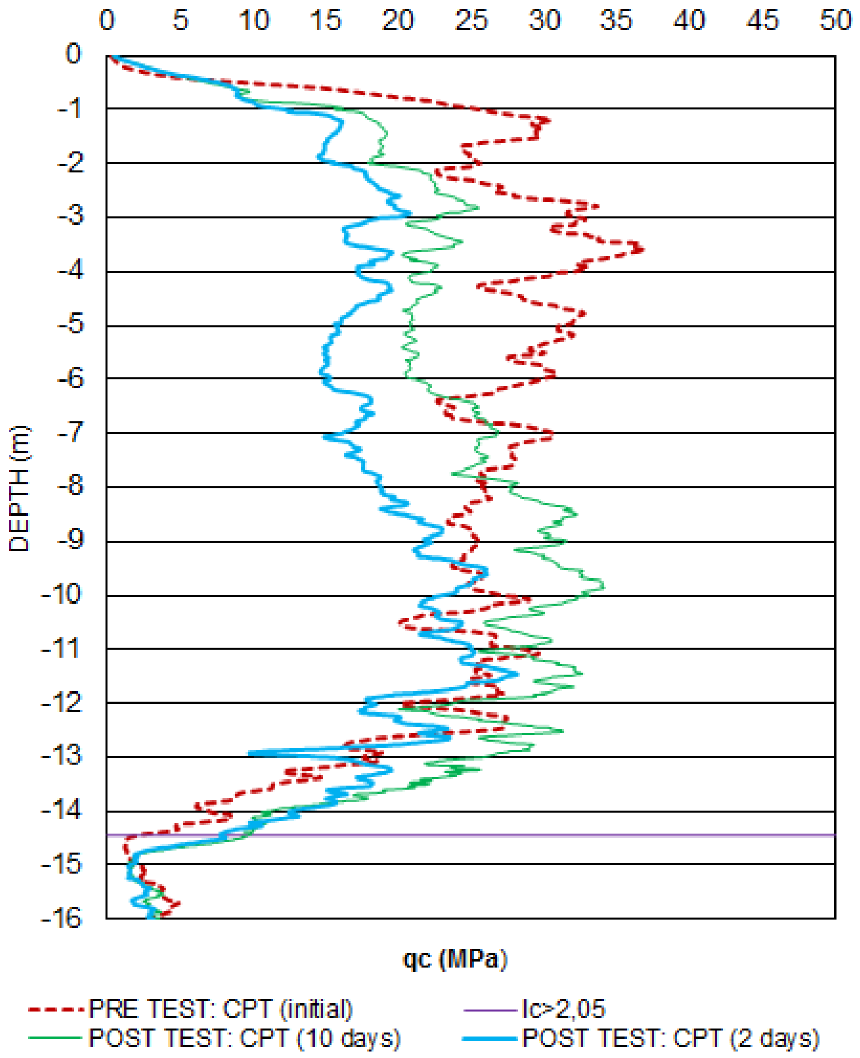

4.30m TRIANGULAR GRID SPACING

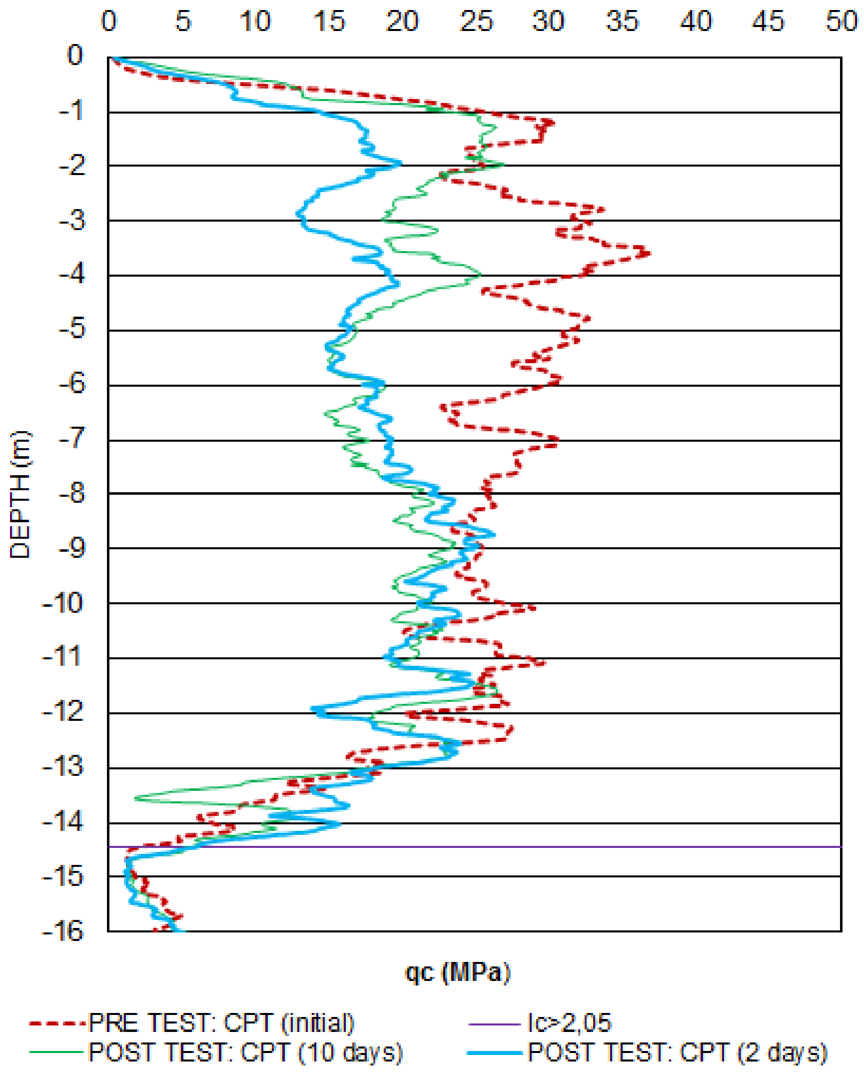

3.1.4 Assessment of Soil Contamination by Washed Clay

- One of the concerns raised during the work related to the maximum depth that should be reached by the vibroflot, as there was the possibility that the disaggregation of the clay, caused by the high impact energy of the vibroflot water jet, might reduce the effectiveness of the ground treatment;

- The base of the granular soils (sands) was found at a depth of approximately 14.50m. Underneath the sandy soil layer (>14,50m) a clay layer has been detected;

- In order to check if contamination of the upper sand layers by the washing in of clay had an impact on the vibrocompaction process, additional field tests were performed:
  - <u>TEST 1</u>: The vibroflot was taken down to a depth of **15.5m** (**penetrating 1.0m in the clay layer**);
  - <u>TEST 2</u>: The vibroflot did not reach the clay layer, stopping at a depth of **14.50m**

- Note: No washing of the hole was undertaken.

3.50m TRIANGULAR GRID SPACING

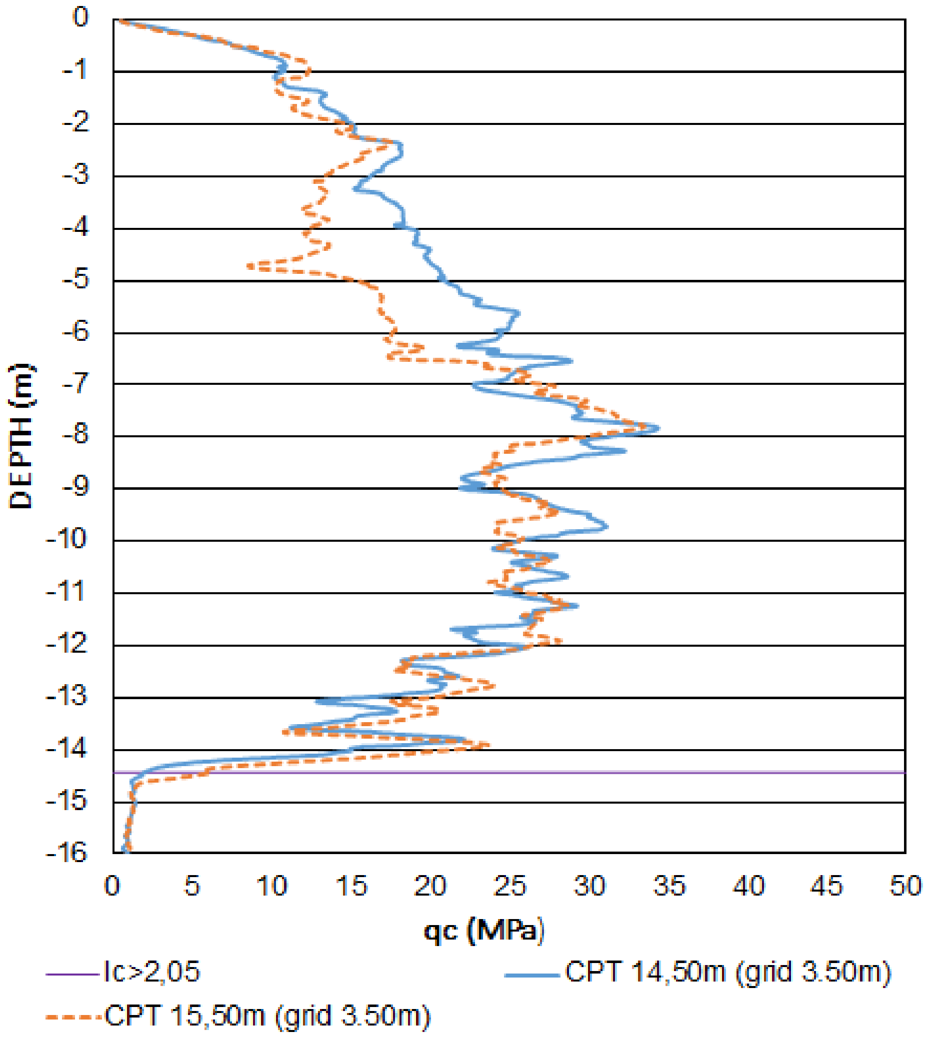

3.70m TRIANGULAR GRID SPACING

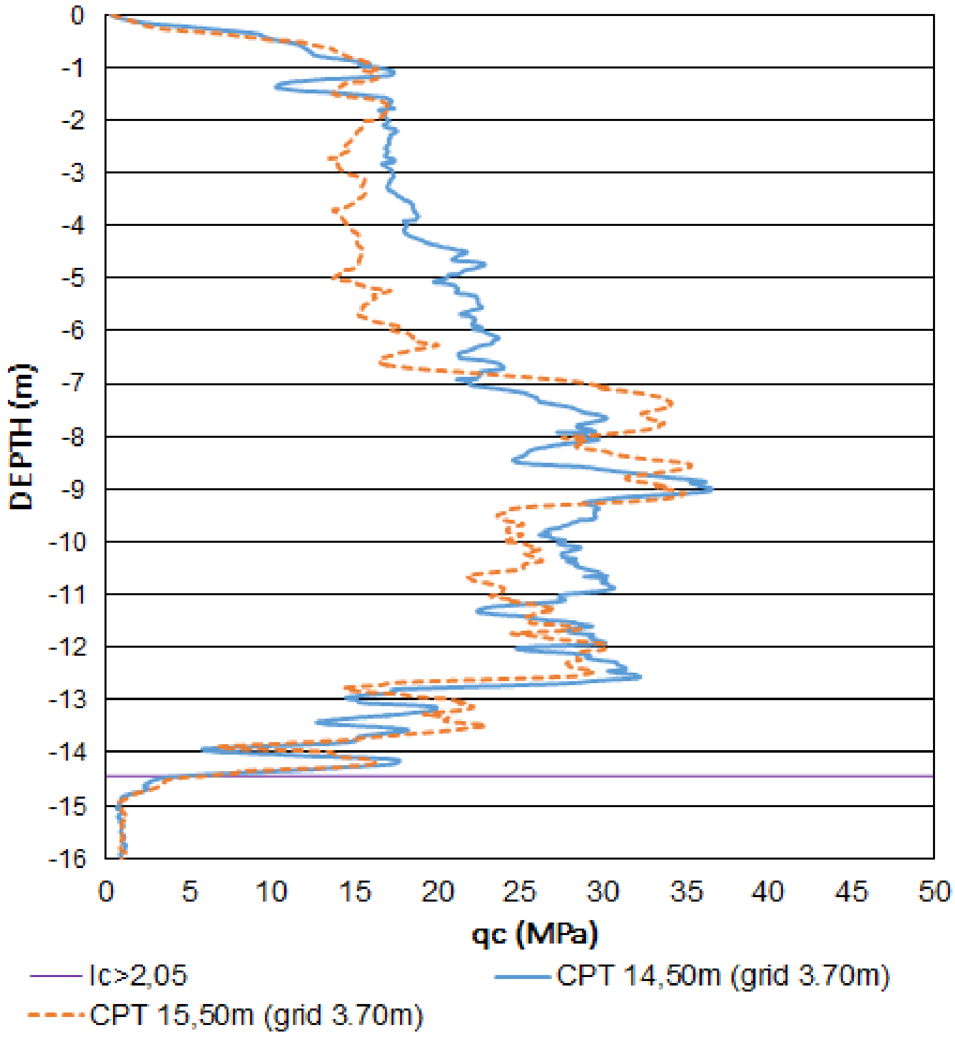

3.1.5 The use of DPSH on Relative Density Assessment

- A malfunction with the CPT equipment prevented its use for the required vibrocompaction quality control assessment;

- As there was an immediate need to proceed with the vibrocompaction works, an alternative method for relative density assessment was required.
The alternative relied on the **DPSH** (*deep probe super heavy*) equipment available at the site;

- The use of DPSH for relative density assessment required a validation procedure. For the purpose, correlations between the CPT cone resistance (qc) and the DPSH blow count (NDPSH) were undertaken.

(in total, 24 CPT's and 6 DPSH's were used to determine a reliable correlation between test types)

Using the results obtained and taking into consideration the variation of soil conditions with depth, it was possible to determine the following correlations between the CPT equivalent cone resistance (q_{ceq}) and number of blows (N_{DPSH}) of the DPSH.

Depth 0,0m to 2,0m: $$q_{ceq} = 5{,}8 \times N_{DPSH} \times \sigma'_{v0}{}^{-0{,}5}$$

Depth 2,0m to 12,0m: $$q_{ceq} = 8{,}5 \times N_{DPSH} \times \sigma'_{v0}{}^{-0{,}5}$$

Depth 12,0m to 14,0m: $$q_{ceq} = 5{,}6 \times N_{DPSH} \times \sigma'_{v0}{}^{-0{,}5}$$

Knowing the equivalent equivalent cone resistance (q_{ceq}) , derived from the correlations, the soil relative density after vibrocompaction was determined - *Jamiolkowski et al. (2001) formulation*.

CORRELATION q_c (CPT) vs q_{eq} (DPSH)

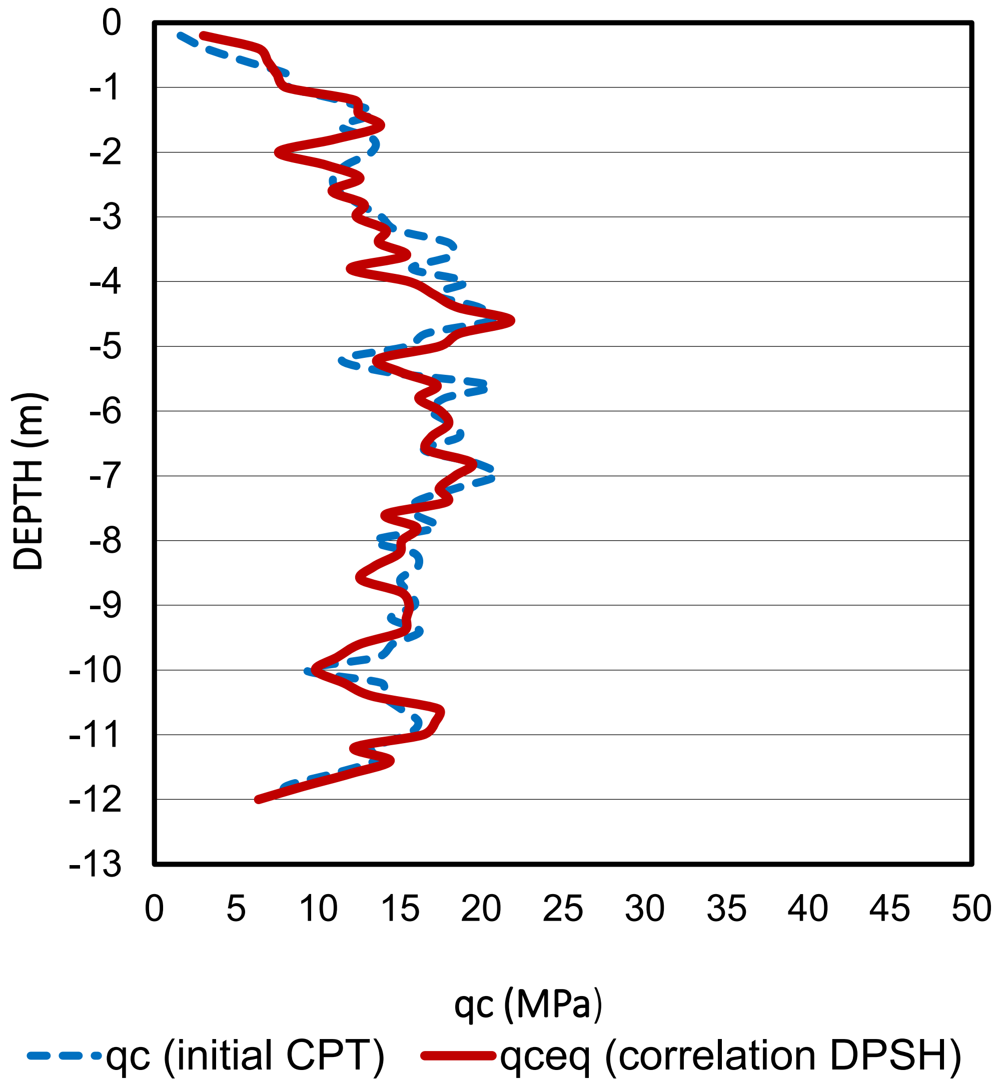

RELATIVE DENSITY - CORRELATION qc (CPT) vs q_{eq} (DPSH)

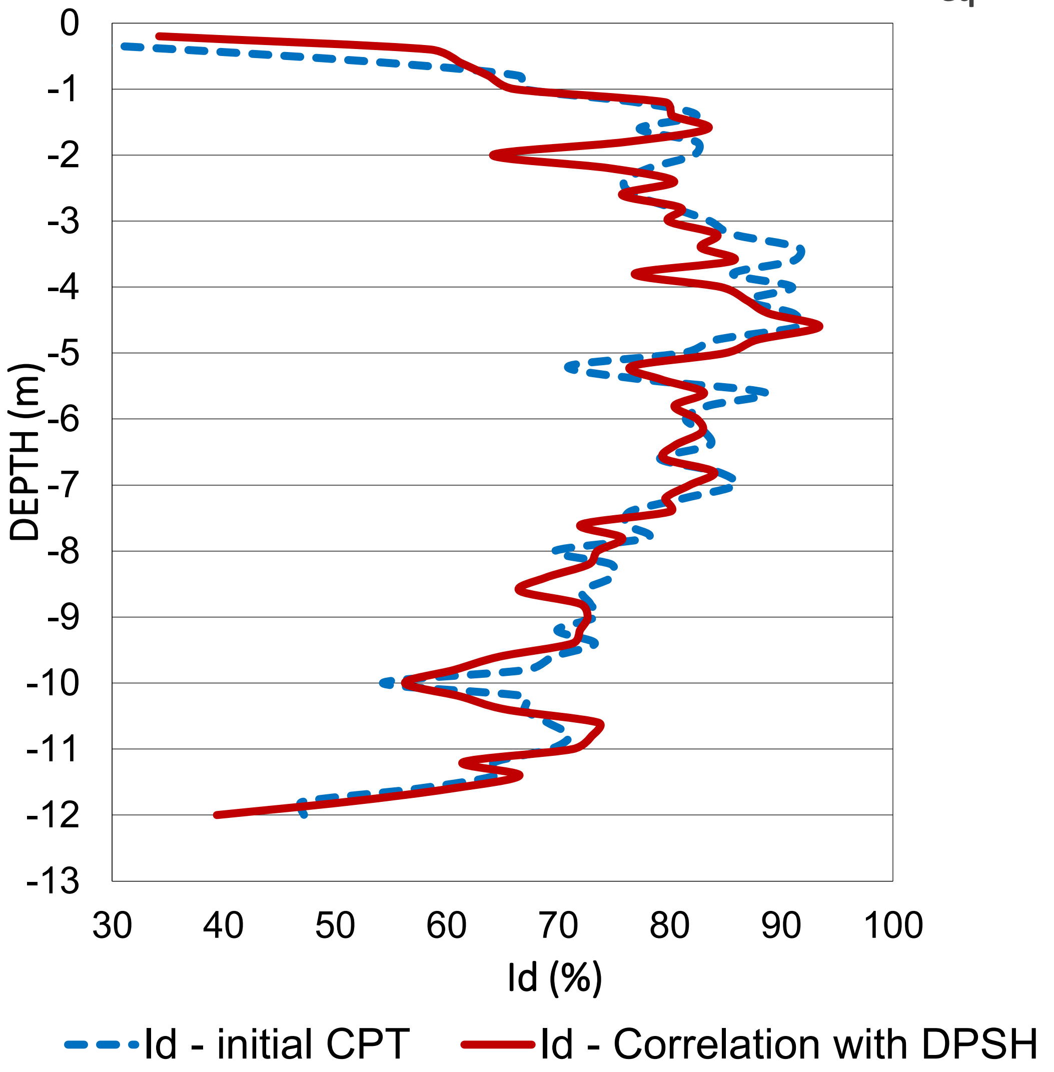

3.2 Stone Columns Combined with Vibrocompaction

- The presence of a **6.0m thick clayey silty layer**, found at a depth of 12.0m on a singular area of the container storage platform, determined the application of vibroreplacement (**stone columns**) to reduce long term settlements;

- Combined solution: stone columns were built from 19.0m to 11.0m depth and vibrocompaction treatment was following executed until ground surface.;

- As stone columns and vibrocompaction can be executed using the same equipment (top-feed wet system), both types of treatment were performed on the same borehole.

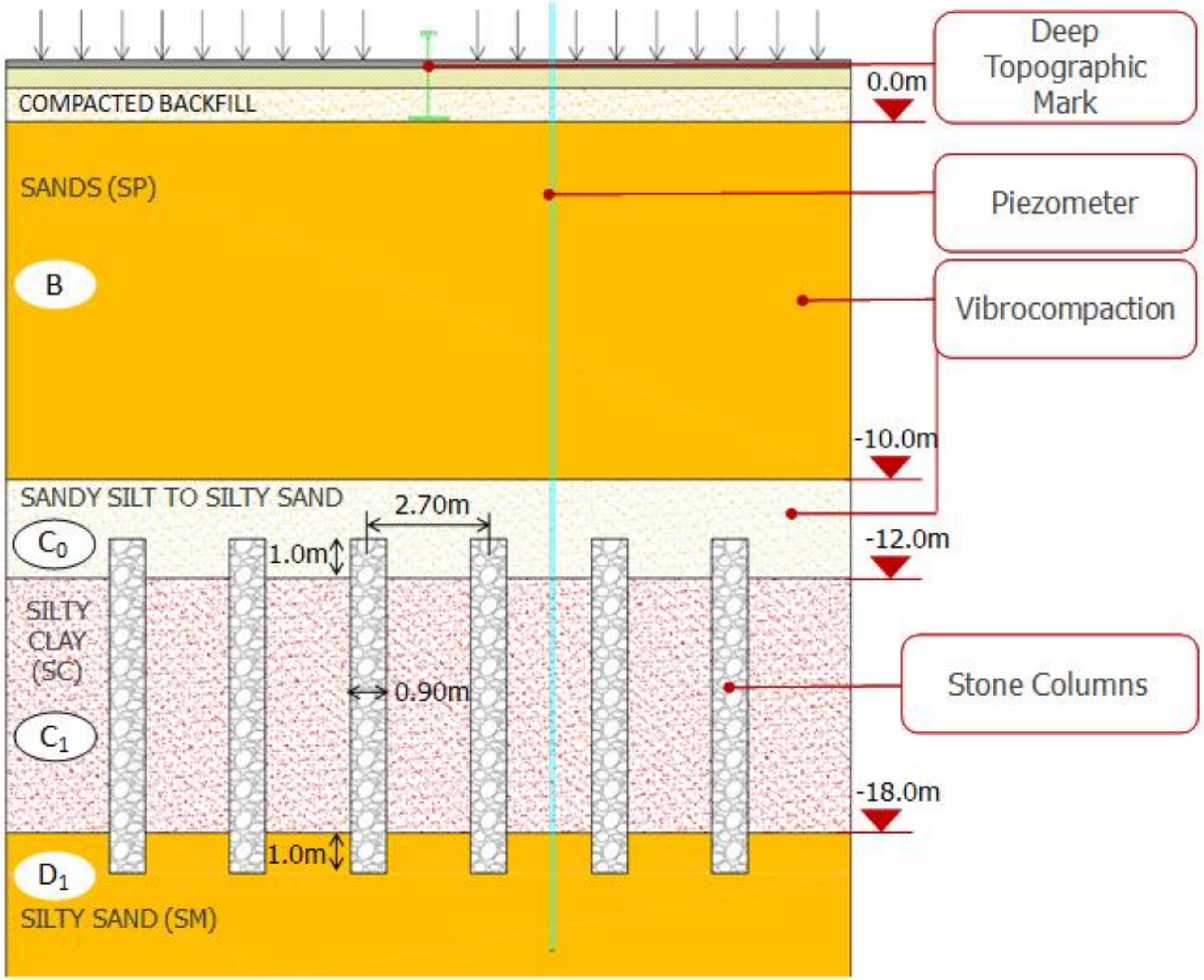

- Ground improvement treatment area :10.700m^2
- Stone columns:
  - Average diameter: 0.90m
  - Square regular grid pattern of 2.70m
  - Area replacement ratio (ARR): 8.7 %

- Estimated settlements of **0.15m** were assessed according to *Priebe (1995)*, leading to an improvement factor of **1.73**;

- Due to its large diameter and high permeability, stone columns are compared to large diameter drains. Taking advantage of these characteristics it was possible to reduce and anticipate part of the immediate settlements by a **consolidation process**.

- Consolidation - *Balaam and Booker (1981)*
  - A 3.50m high temporary embankment was placed over the entire treatment area;
  - Time for consolidation: **2 months** for a degree of consolidation **U = 90%** - *Balaam and Booker (1981)*

- After the required period for consolidation, residual settlements of **5.5 cm** were observed at the site.

MAIN CONCLUSIONS

- To be well succeeded, both jet grouting and vibro techniques require an **exhaustive geological-geotechnical** campaign, carried out before and during the works, as well as **appropriate field trials**.

- Jet grout columns were found to be an added value to increase the **overall quay wall stability** as well as the **wall bearing capacity**.

- Jet grouting proved to be an useful technique to build temporary earth retaining structures, especially at zones intersecting existing jetties (specially when at the presence of existing rockfills).

- The **electric cylinder** method provides accurate results, making of it a **valid method** to estimate the jet grout columns diameter.

MAIN CONCLUSIONS

- Using **vibrocompaction** it was possible to increase the soil relative density, typically corresponding to behaviour soil type index behaviour (Ic) of between **1.31 and 2.05.** No evident improvement was observed in soils with a behaviour soil type index (Ic) higher than 2.05.

- It has been confirmed that the **soil relative density tends to increase along the time** when soils are submitted to vibrocompaction.

- Careful use of vibrocompaction shall be observed when at the presence of **dense sands**, typically with CPT cone resistance values varying from 25 to 30MPa, as a decrease of soil initial stiffness/density may be expected.

- During vibrocompaction works, **any contact with underlying clay layers may lead to soil contamination** due to washed in clay material, precluding the achievement of higher relative density results.

MAIN CONCLUSIONS

- The use of DPSH testing was found to be a good instrument for vibrocompaction quality control assessment, however, calibration with CPT data performed at the site shall always be undertaken.

- The use of stone columns in combination with vibrocompaction has proved to be an optimized and cost effective ground improvement solution, enabling improving simultaneously clay layers positioned underneath granular and compactable soils.

JET SJ

THE GROUND IS OUR CHALENGE

Thank you for your attention

www.jetsj.com
info@jetsj.com

ACKNOWLEDGEMENTS

Somague Engenharia
cyes
vipp LAVORI SPECIALI srl
SOLDATA
geozone

The Advantages of advanced quality control methods during PVD installation and heavy Rapid Impact Compaction

Jan-Willem Vink[1], Jeroen Dijkstra[2]

1. *Cofra bv, The Netherlands*
2. *Cofra bv, The Netherlands*

Cofra

Index

1. Introduction
2. Quality control for vertical drain projects
3. Quality control for heavy rapid impact projects
4. Conclusion

Quality Control

- Why? Registration of the basic parameters to
  - provide proof that the work has been performed as designed
  - Use the data for design and optimization purposes
  - Gain insight in the soil conditions
  - Gain insight in production and overall progress

- There is no standard quality control method for the industry.
  - Every contractor has their own system
  - Requirements differ per project

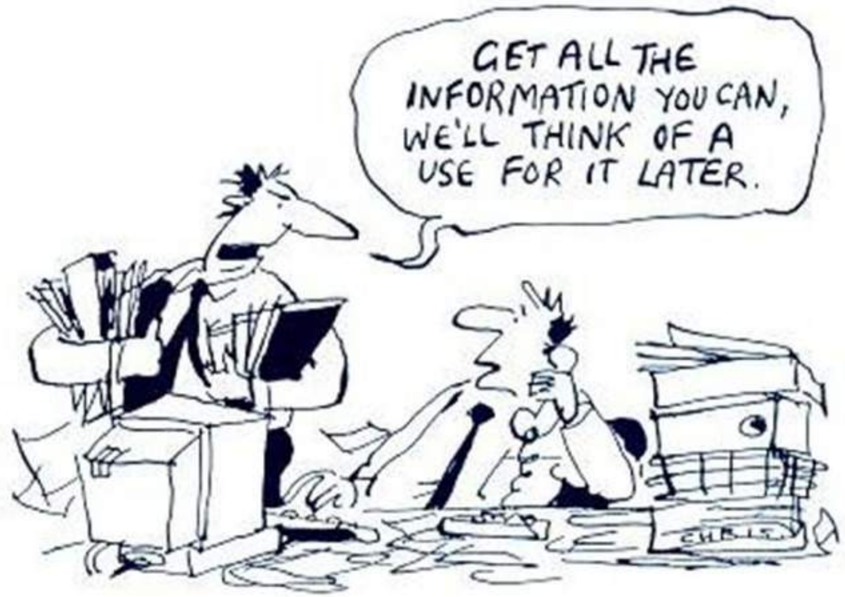

Index

Work method Vertical Drain

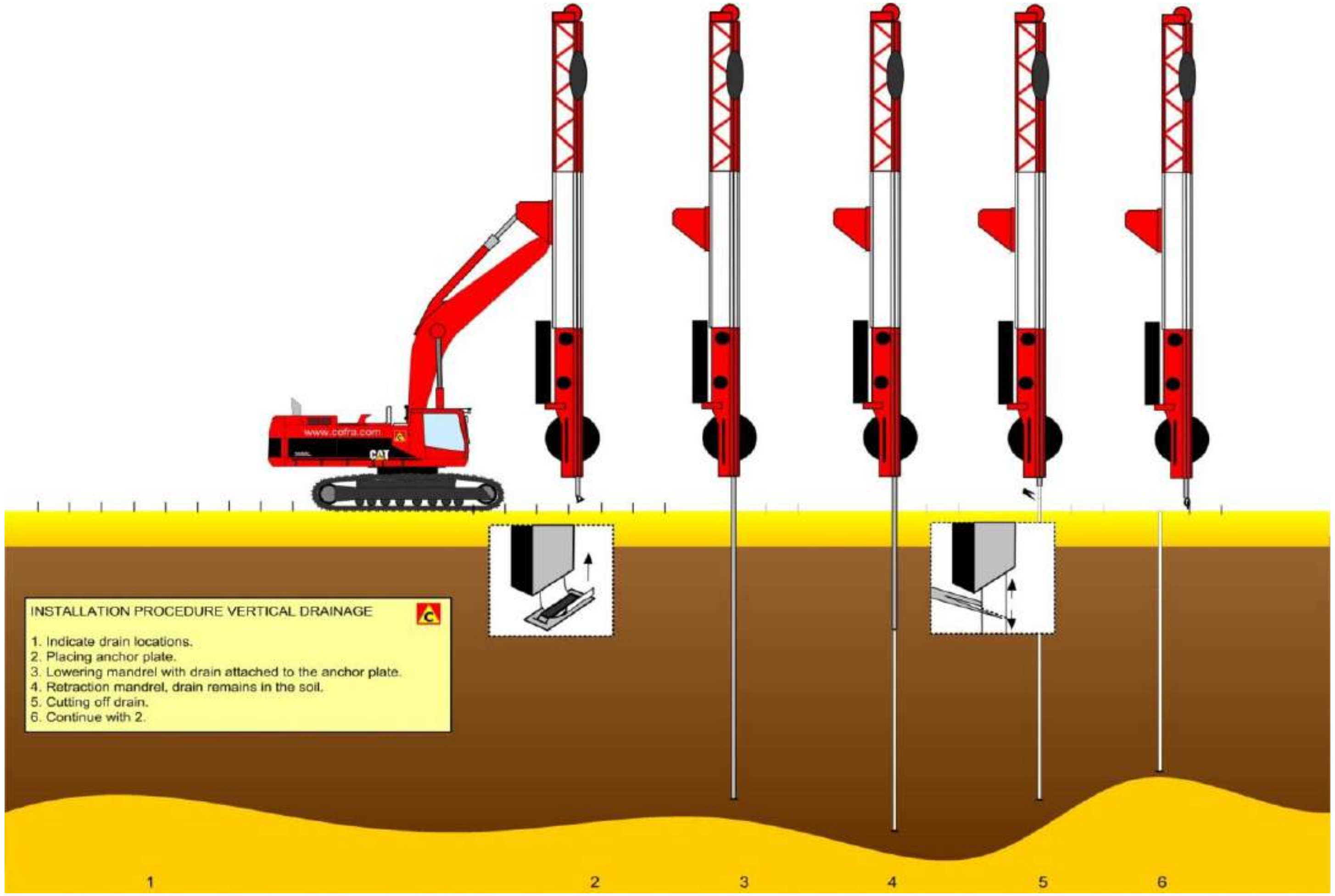

Vertical Drain equipment

General Quality control for vertical drain projects

- During PVD installation several parameters are logged
  - ID
  - Date and time
  - Base unit
  - Installation depth
  - Push force at selected intervals

Advanced Quality control for vertical drain projects

- During PVD installation several parameters are logged
    - ID
    - Date and time
    - Base unit
    - Installation depth
    - Push force at selected intervals
- The latest development is the use of GPS based logging and positioning
- The registered data can be of advantage to both the contractor as well as the designer / site engineer

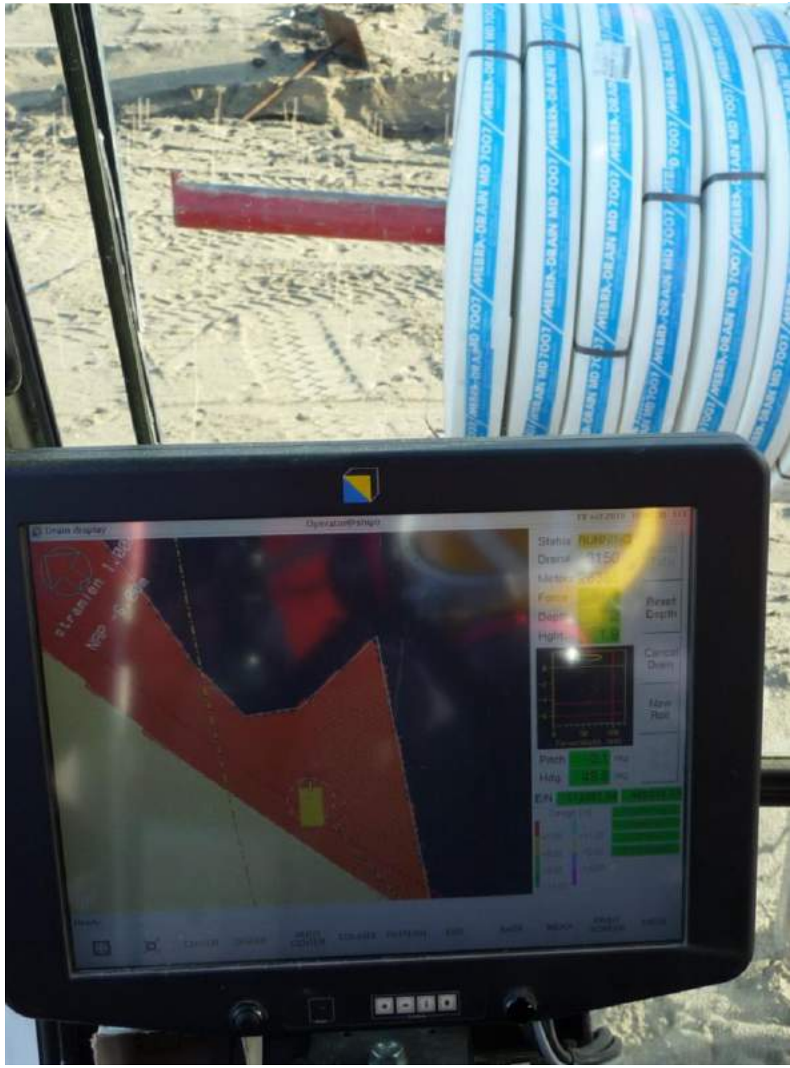

Advantages general

During Installation

- Autocad drawing
    - Location of underground infrastructure can be shown to the operator
    - Depth map / Installation on chart datum level / automatic stop
    - No positions required on the field
- Increase safety by being able to detect weak spots in platform during installation

Accuracy

Advantages general

After installation

- Exact position of each drain
    - Location monitoring equipment
    - Predrilling locations when refusals are encountered
    - Total force graph at each drain location (x-ref)
- Leads to a high standard of Quality Assurance

Advantages for Engineers

What can we do with the data

- Depth map of the installation data
  - Where is the hard layer?
  - Is the design followed?

Advantages for Engineers

What can we do with the data

- Depth map of the installation data
    - Where is the hard layer?
    - Is the design followed?
    - Are there differences from the initial design and SI?
    - Do we need to place additional settlement markers?

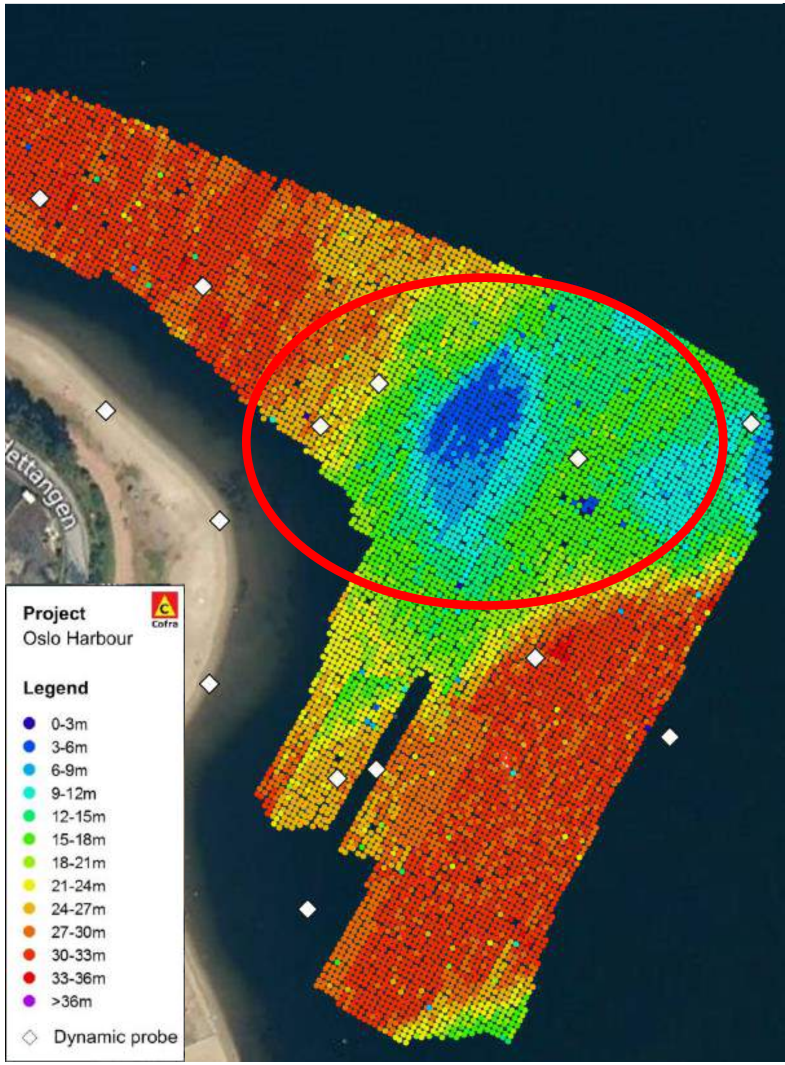

Advantages for Engineers

What can we do with the data:

- Depth map of the installation data
    - Where is the hard layer?
    - Is the design followed?
    - Are there differences from the initial design and SI?
    - Do we need to place additional settlement markers?
- Push force at specific depths
    - Mapping sand lenses

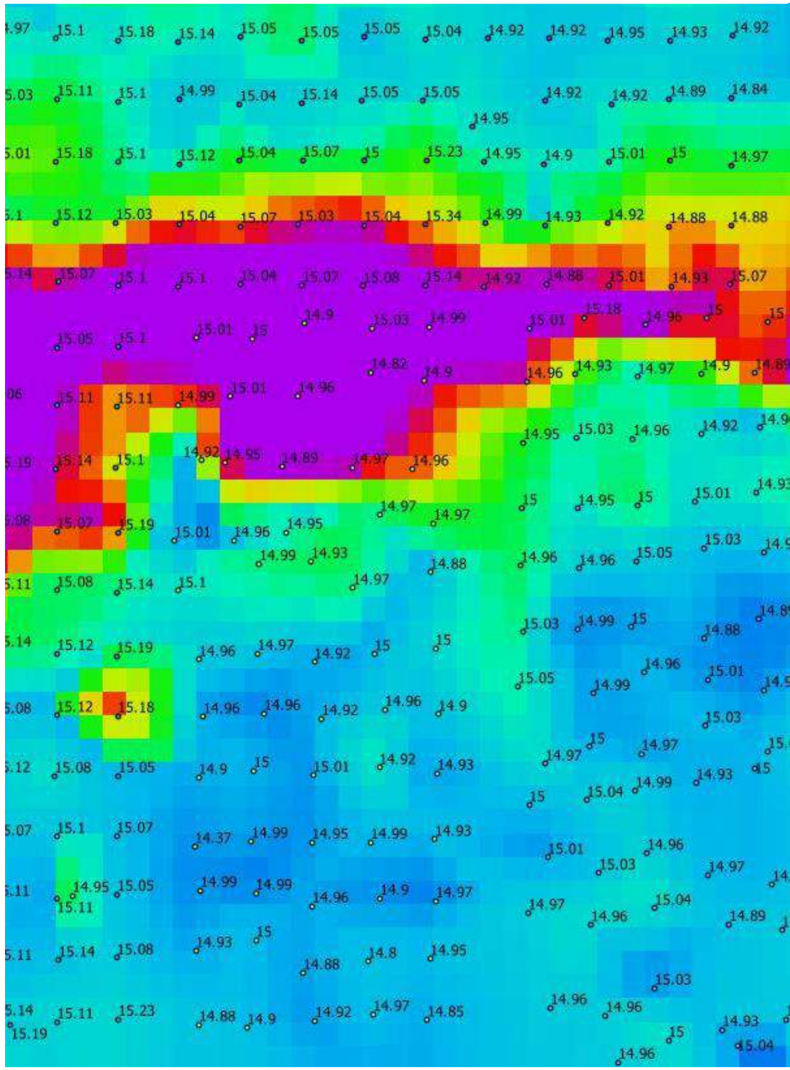

Push Force

Push force is the total force on the mandrel measured by oil pressure

Influenced by several factors

- Tip resistance
- Friction of mandrel
- Friction inside mast
- Pretension
- Speed of installation

Should be used as an indication

- Delineation between sand and soft material is possible
- Delineation between peat and soft clay not possible

DGPS – push force at specific depth

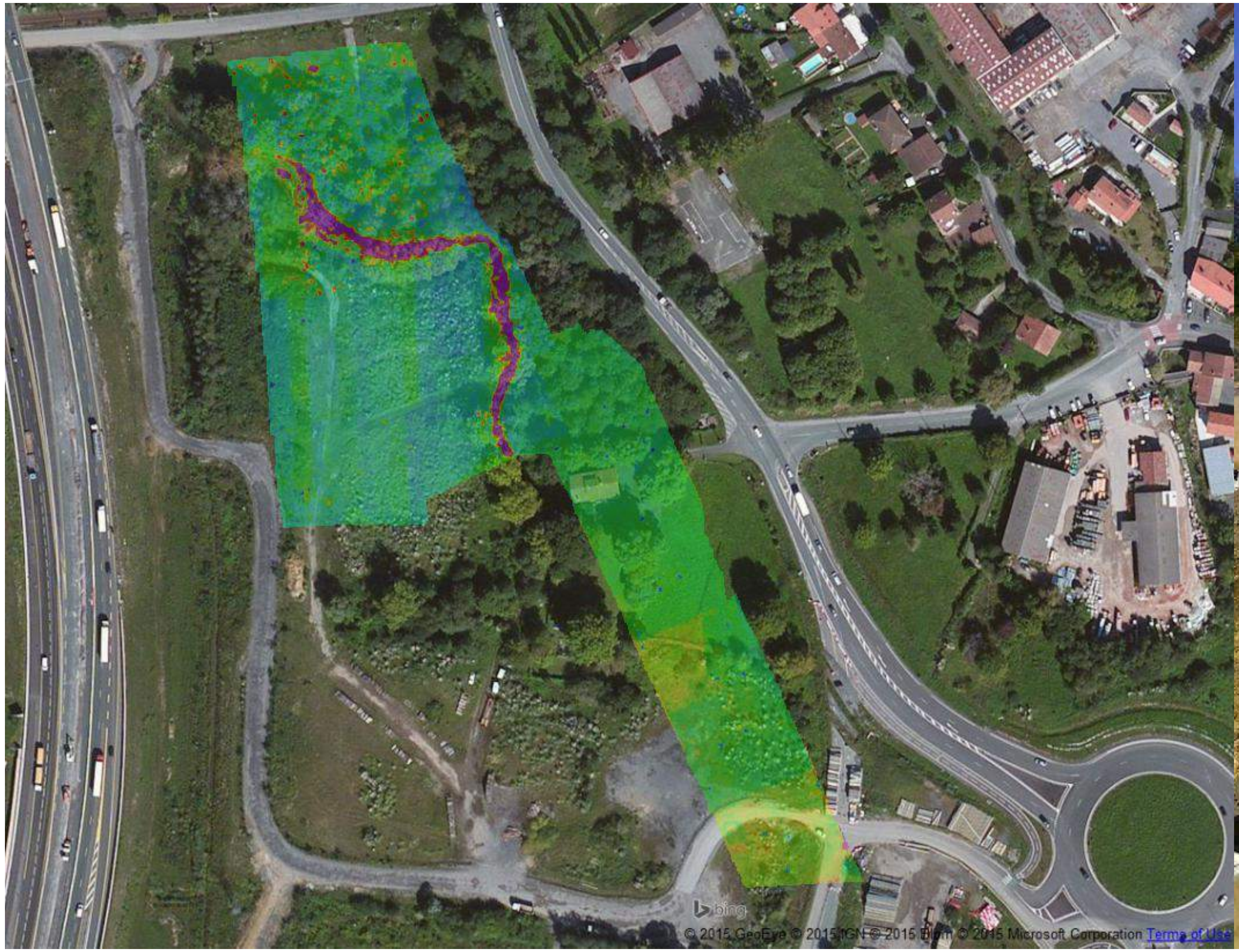

DGPS – push force at specific depth

DGPS – push force at specific depth

DGPS – push force at specific depth

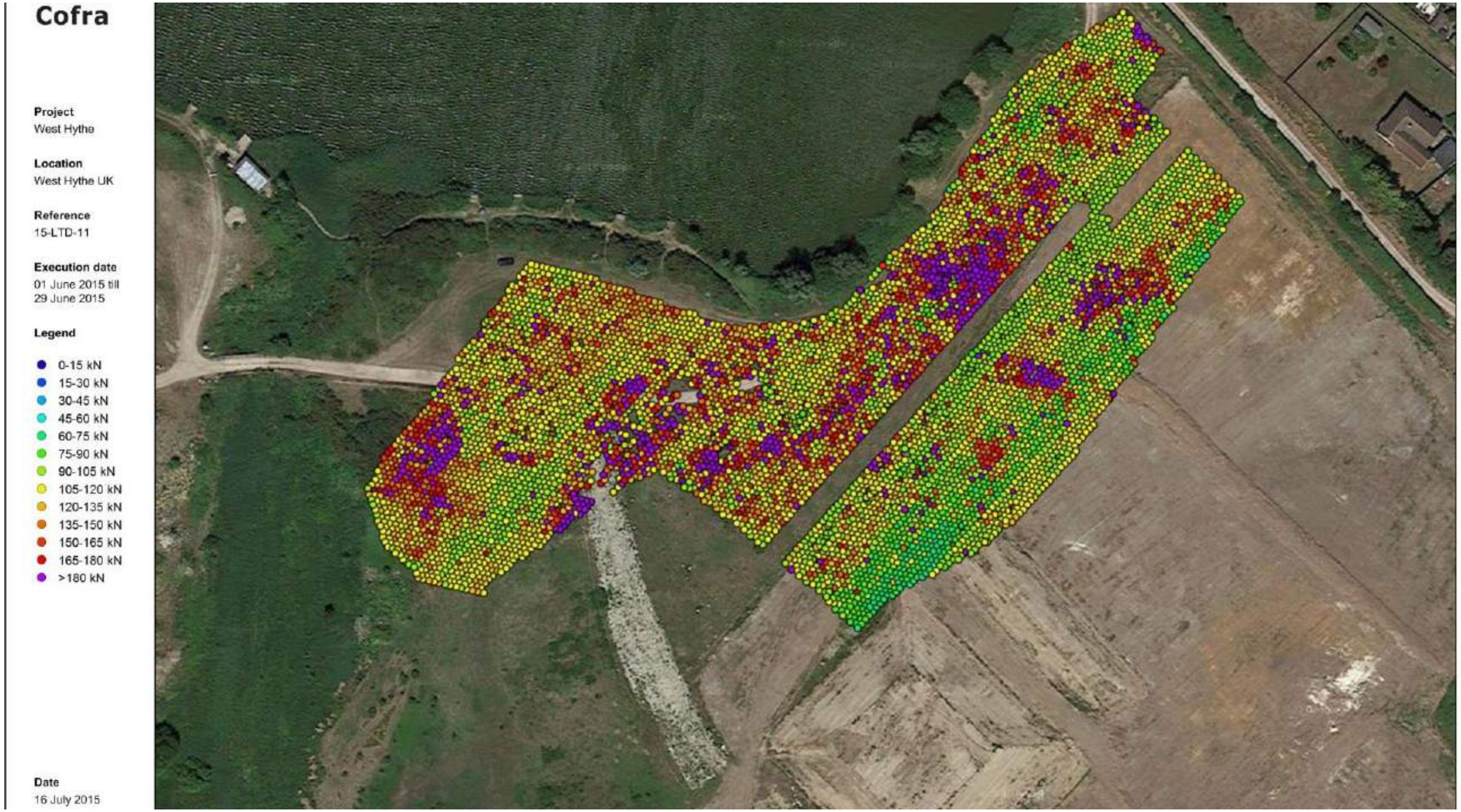

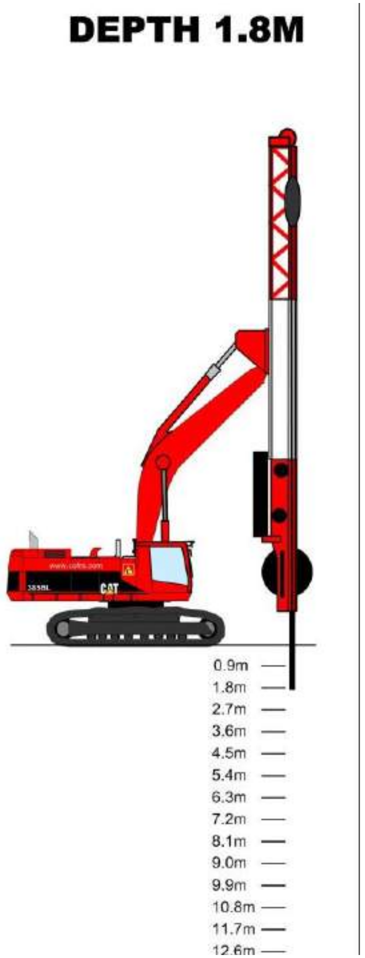

DGPS – push force at specific depth

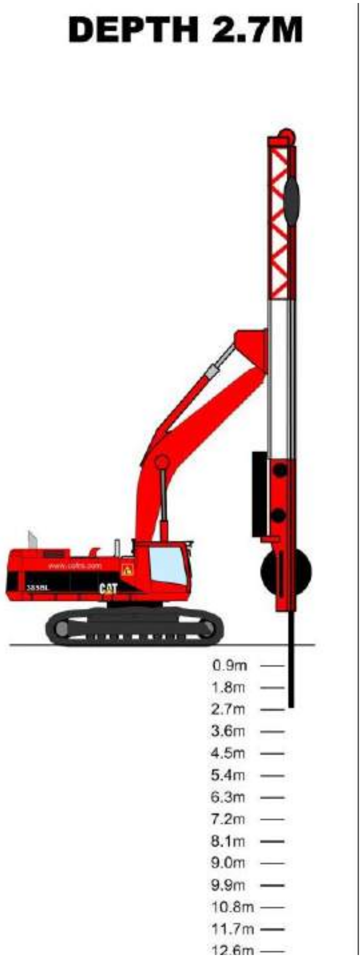

DGPS – push force at specific depth

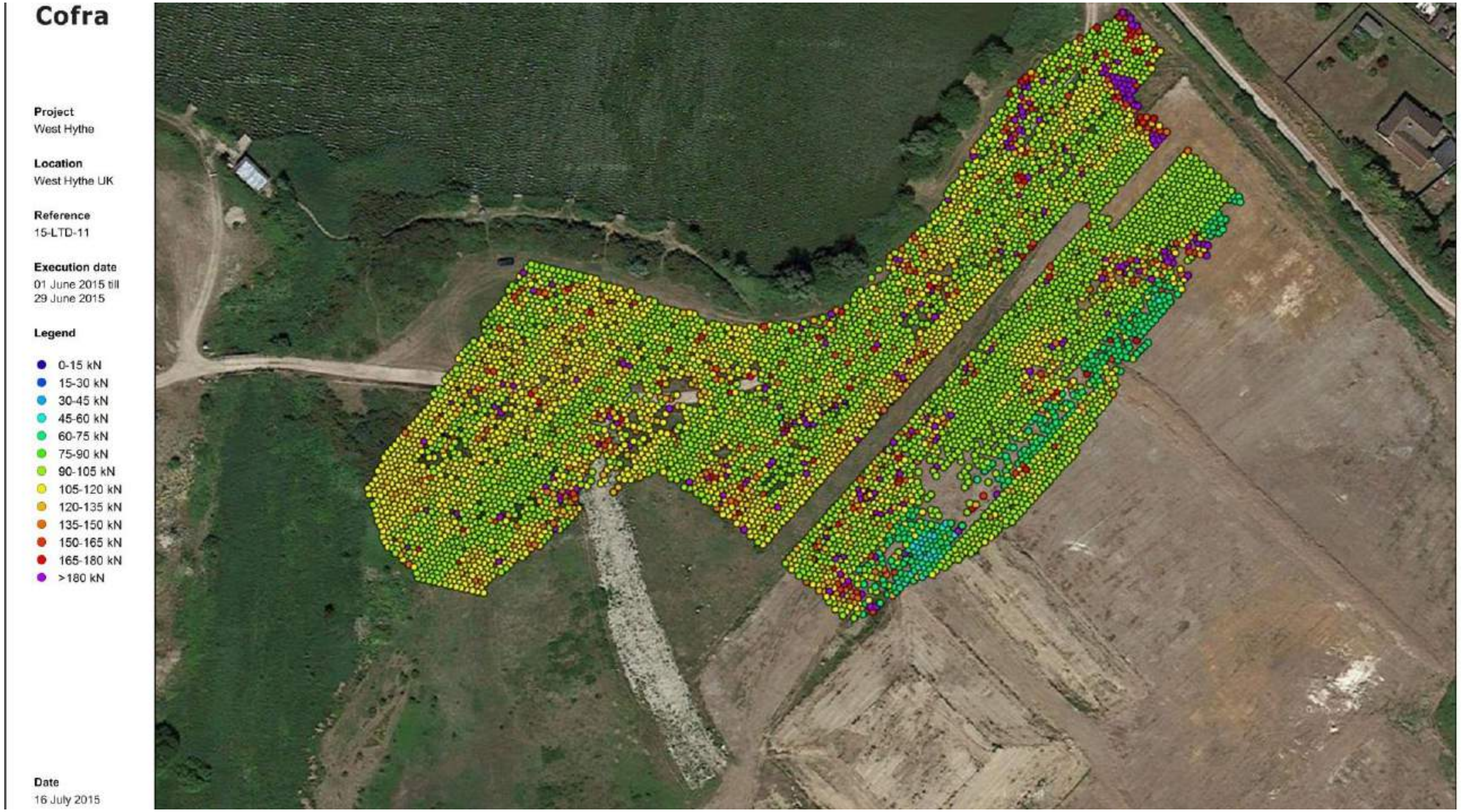

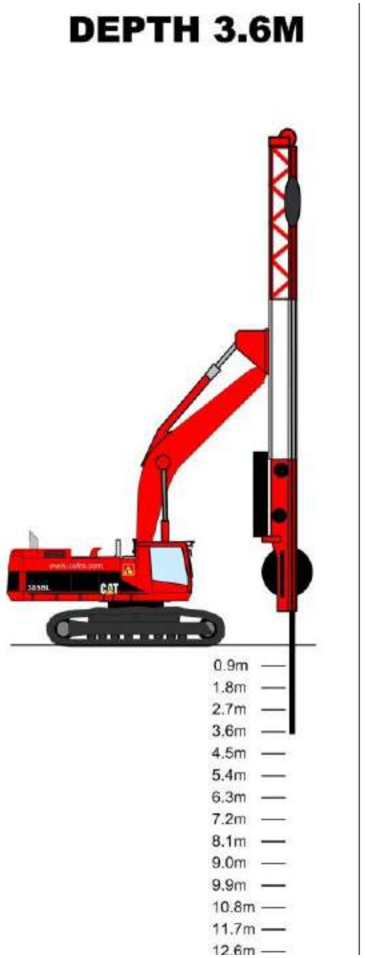

DGPS – push force at specific depth

DGPS – push force at specific depth

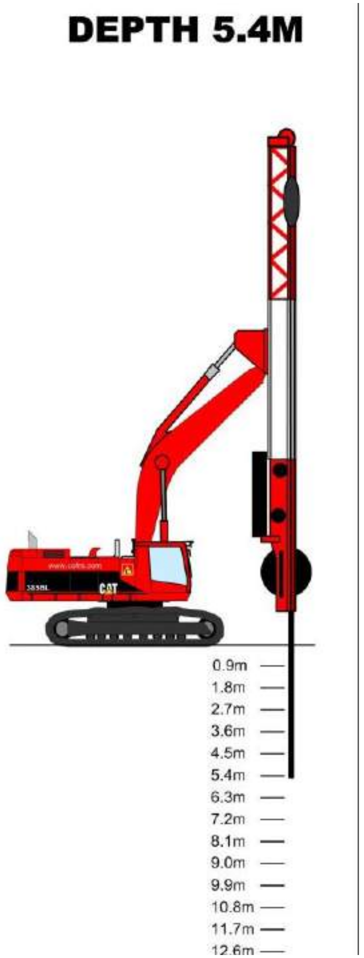

DGPS – push force at specific depth

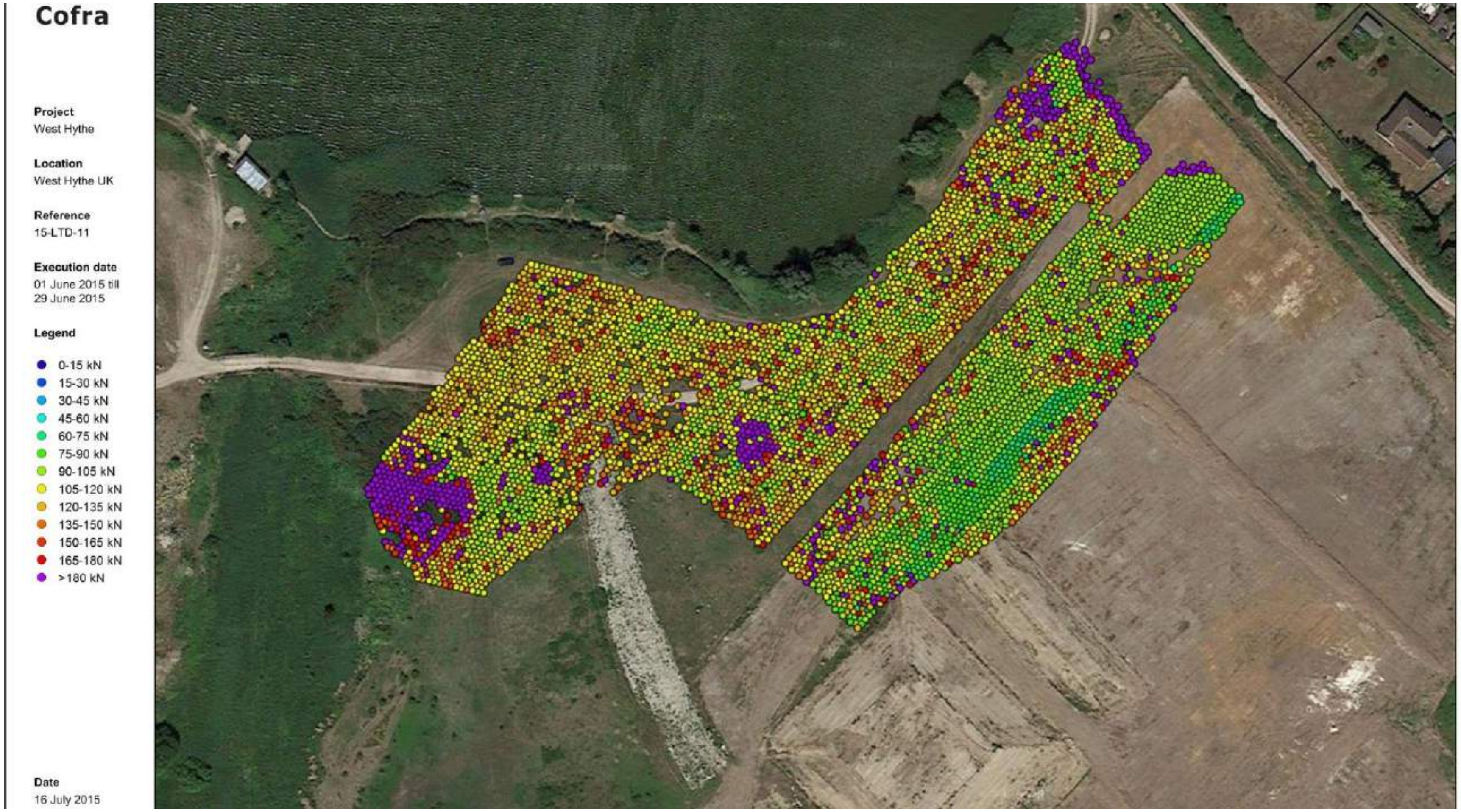

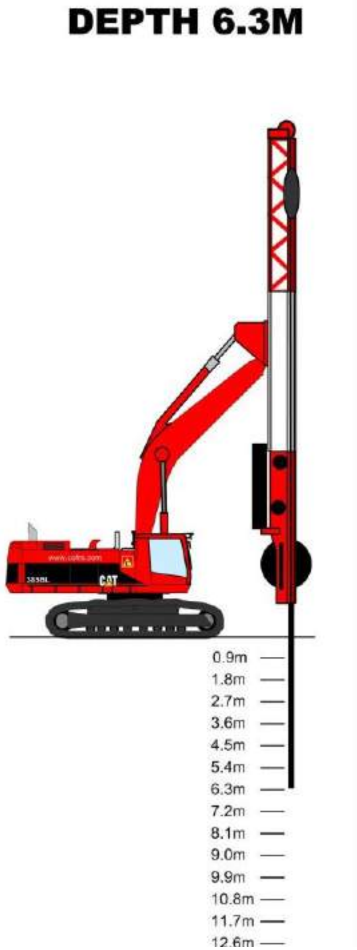

DGPS – push force at specific depth

DGPS – push force at specific depth

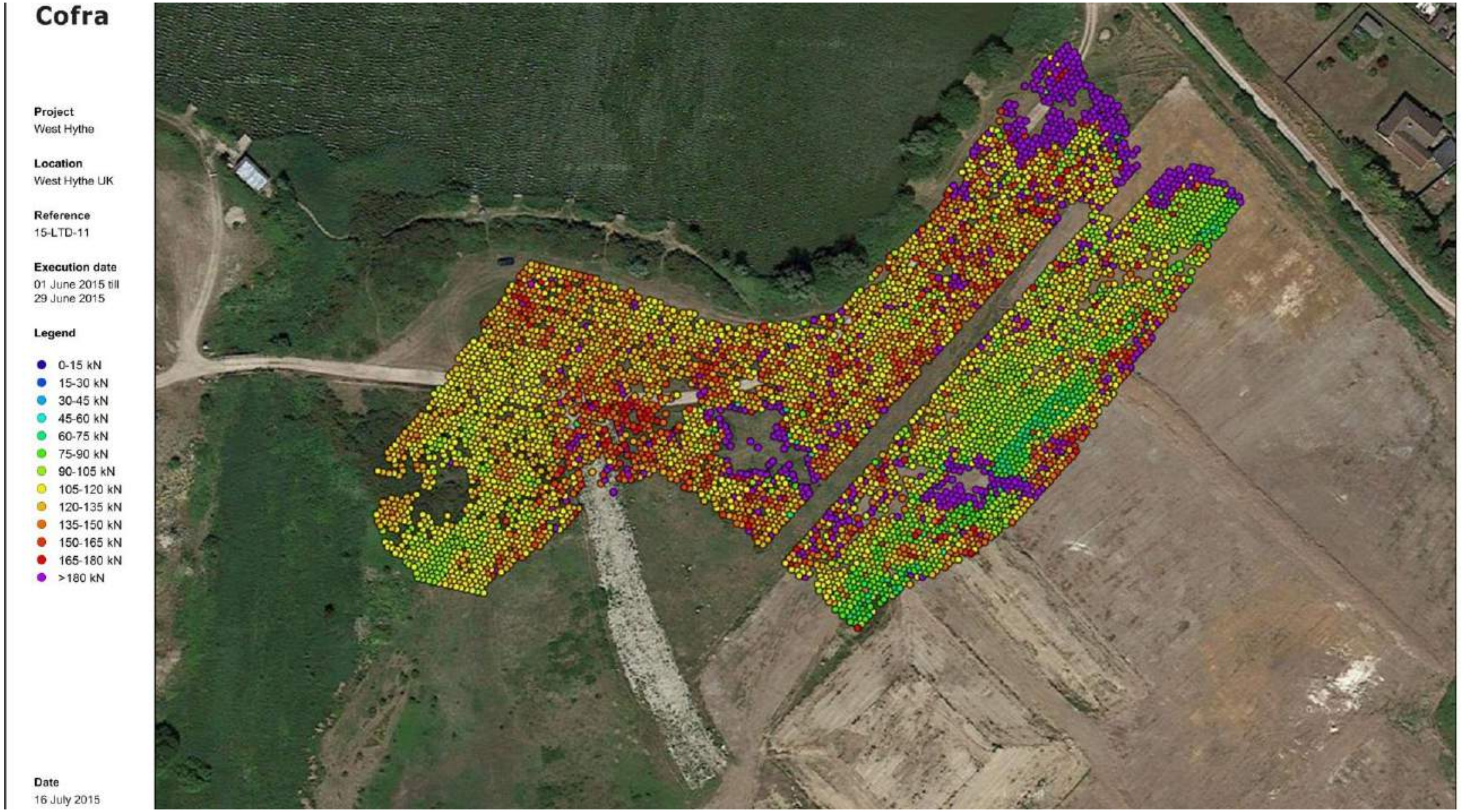

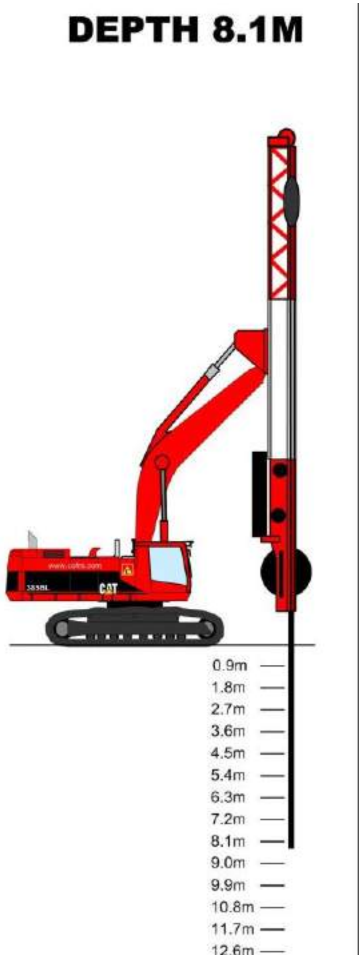

DGPS – push force at specific depth

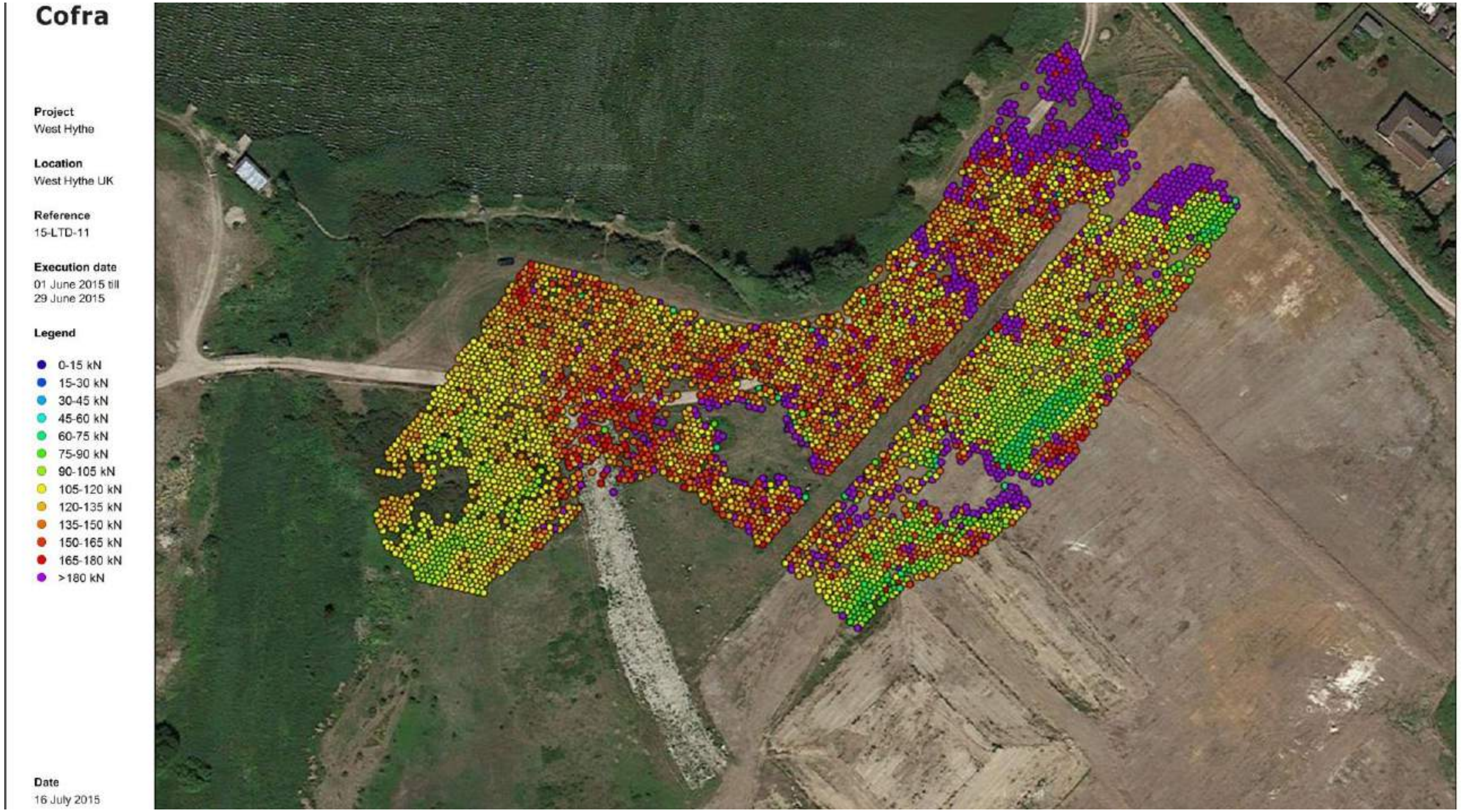

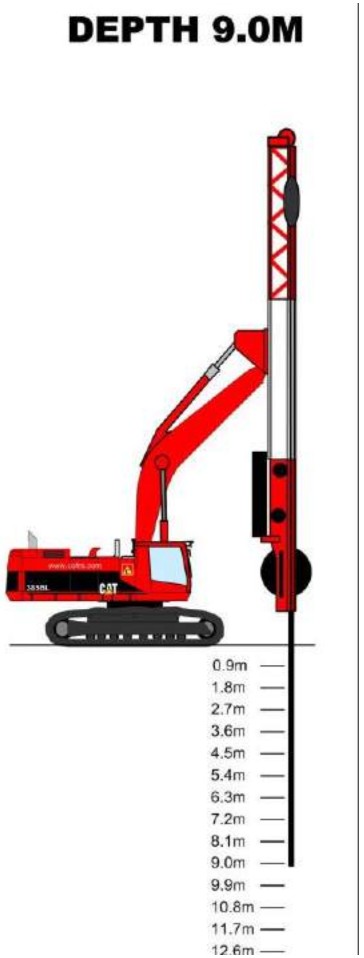

DGPS – push force at specific depth

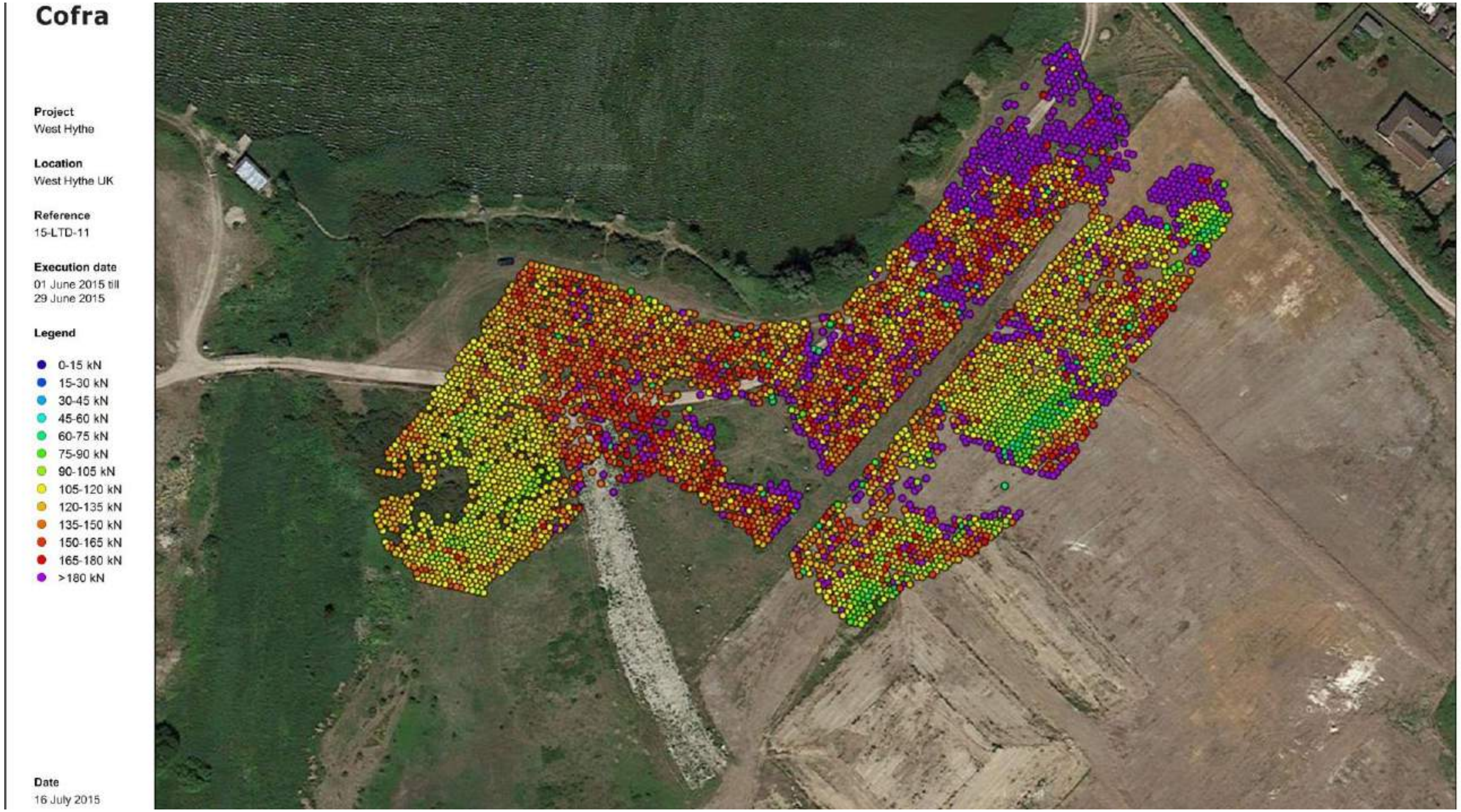

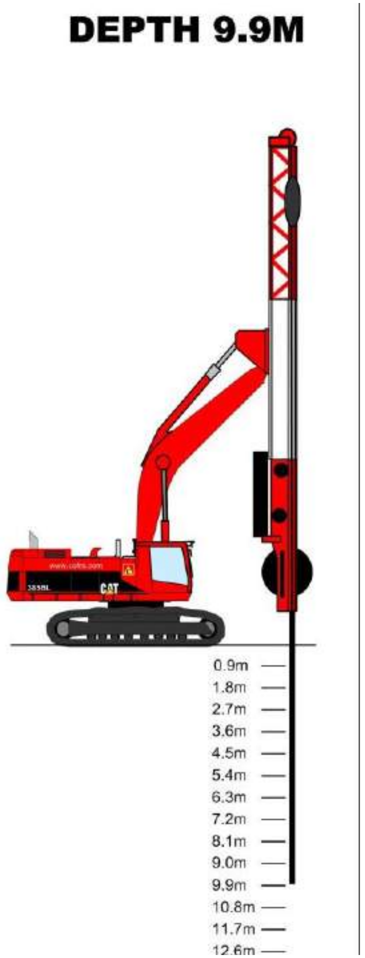

DGPS – push force at specific depth

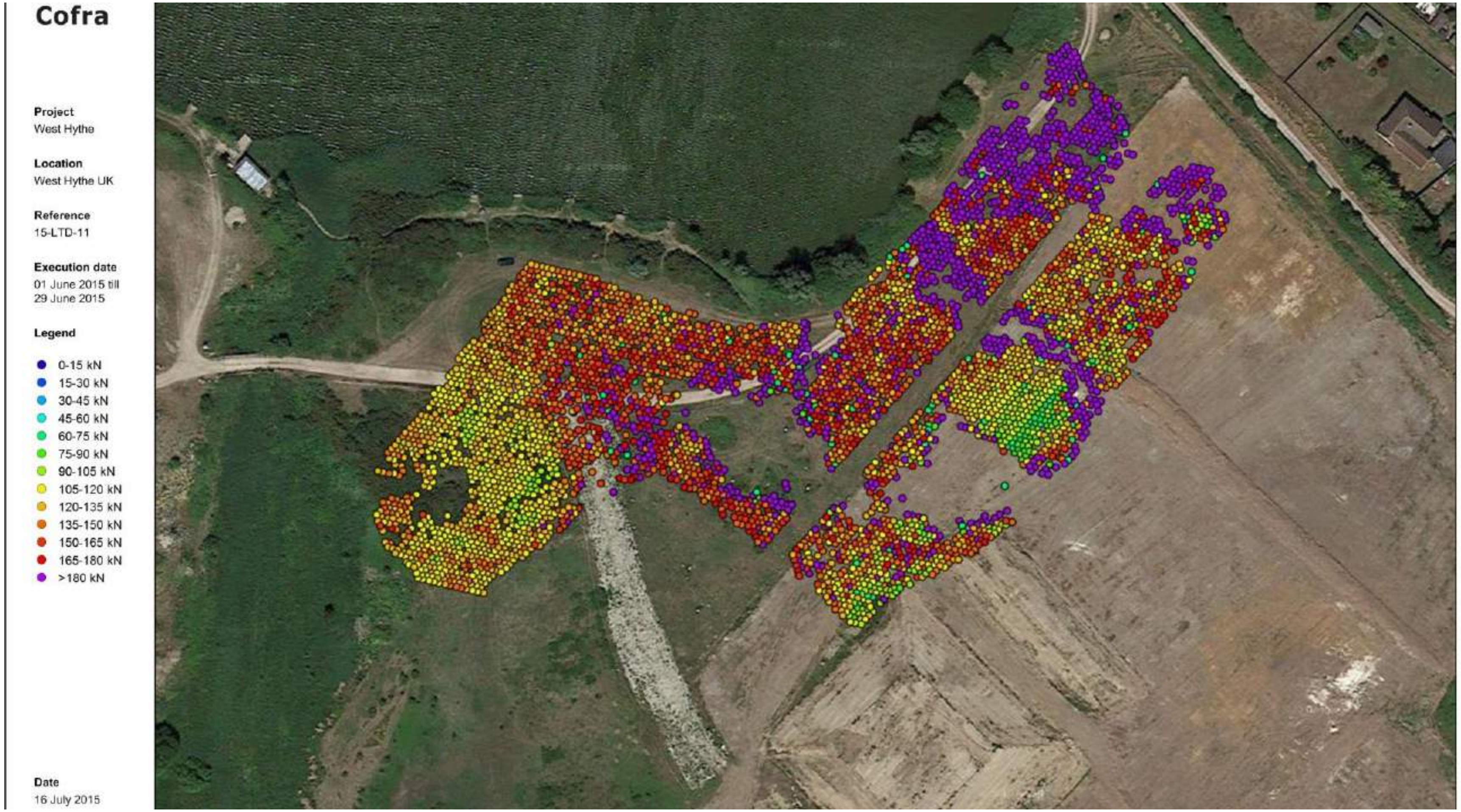

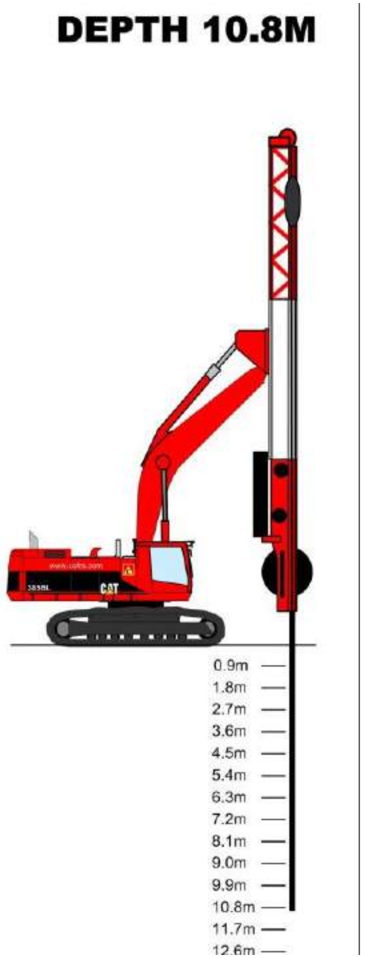

DGPS – push force at specific depth

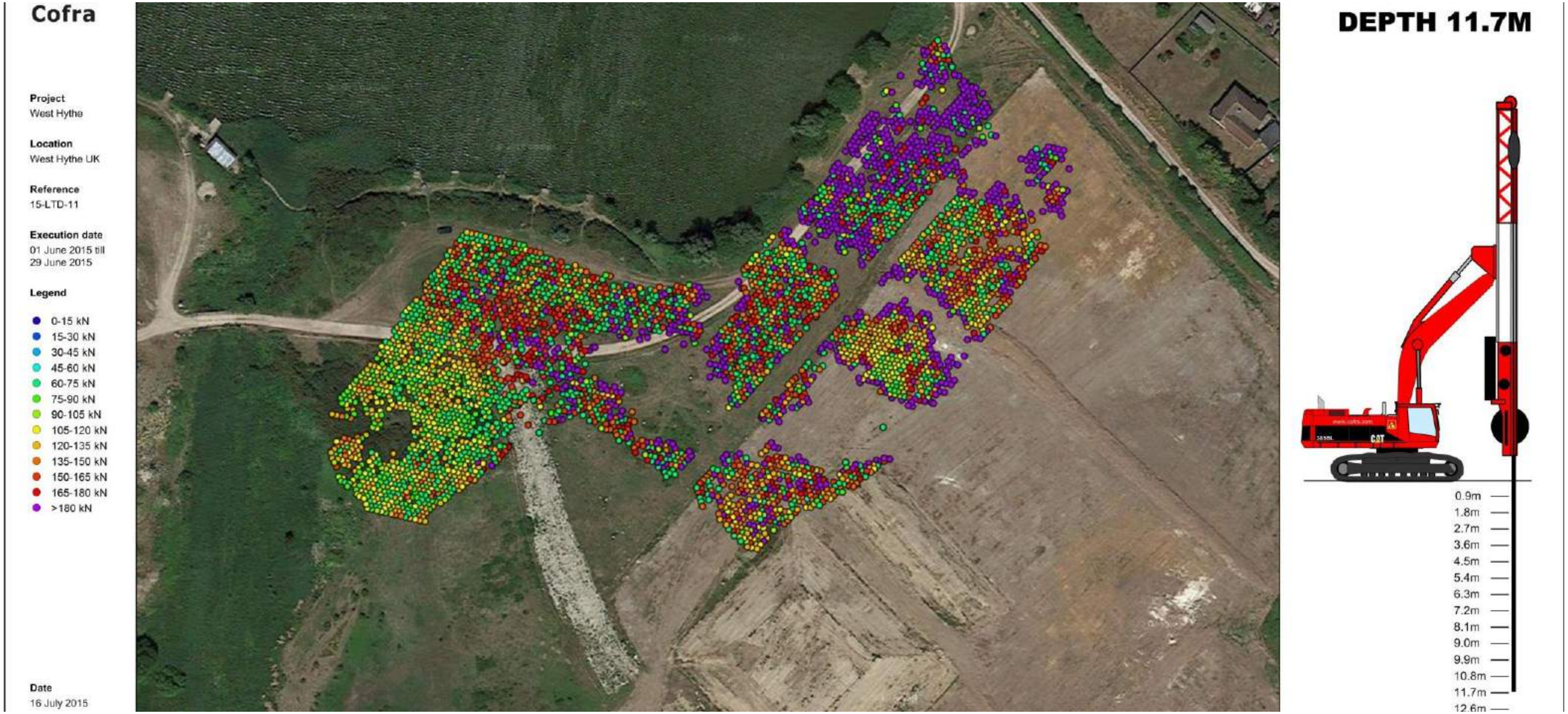

DGPS – push force at specific depth

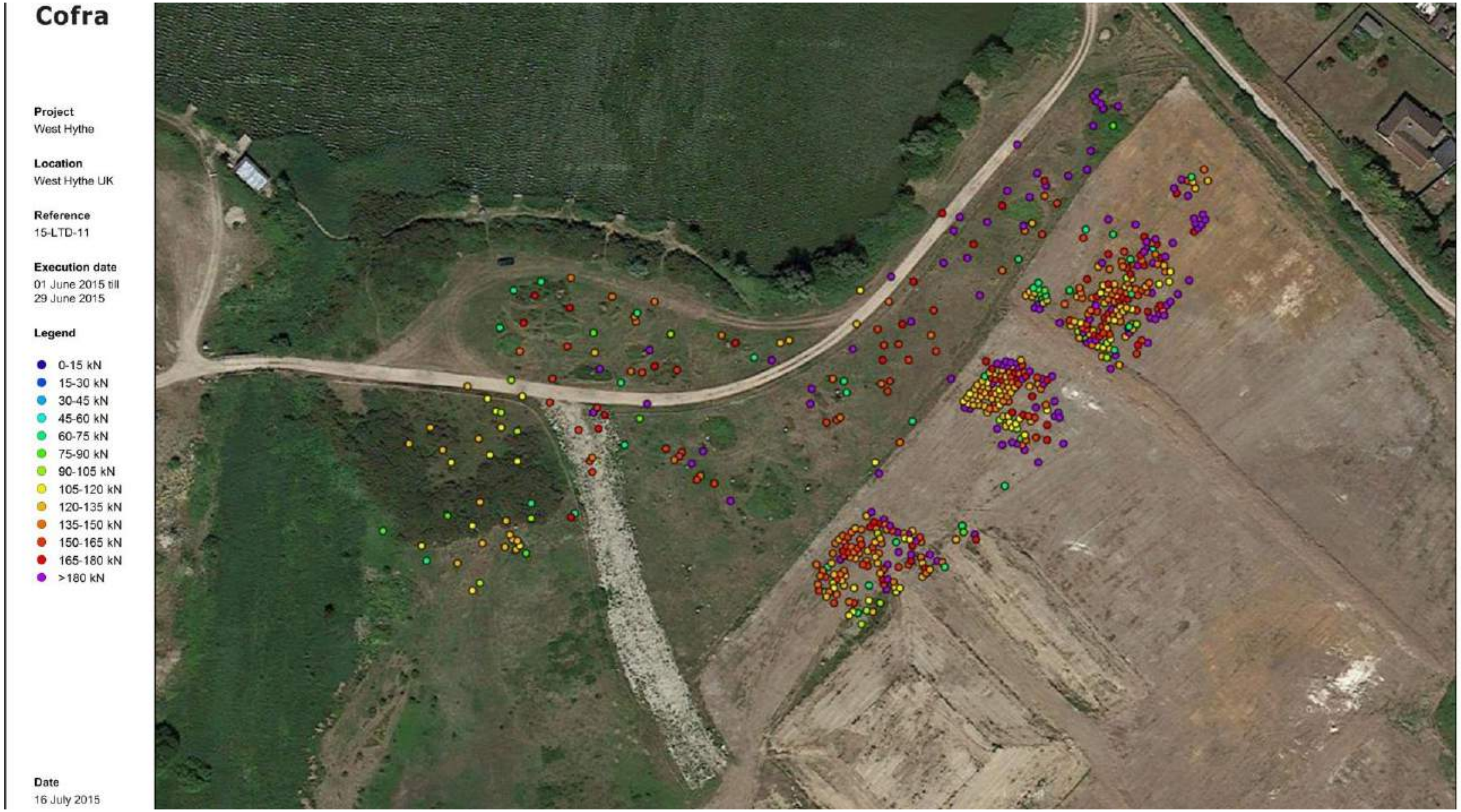

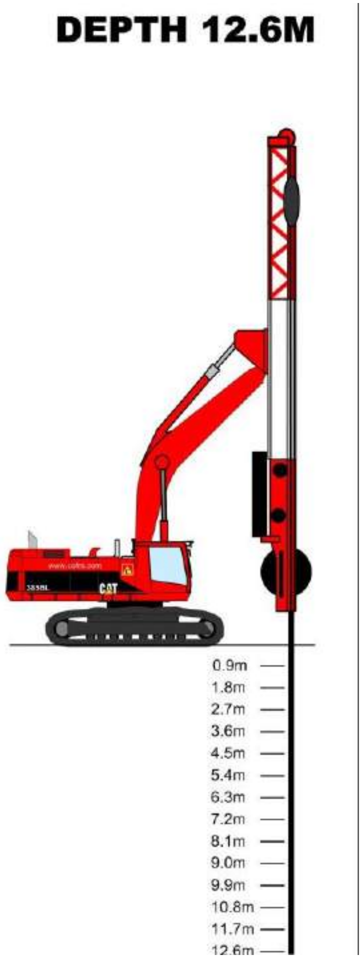

Advantages for Engineers

What can we do with the data:

- Depth map of the installation data
    - Where is the hard layer?
    - Is the design followed?
    - Are there differences from the initial design and SI?
    - Do we need to place additional settlement markers?
- Push force at specific depths
    - Mapping sand lenses
- Cross section of push force
    - Geological profiling

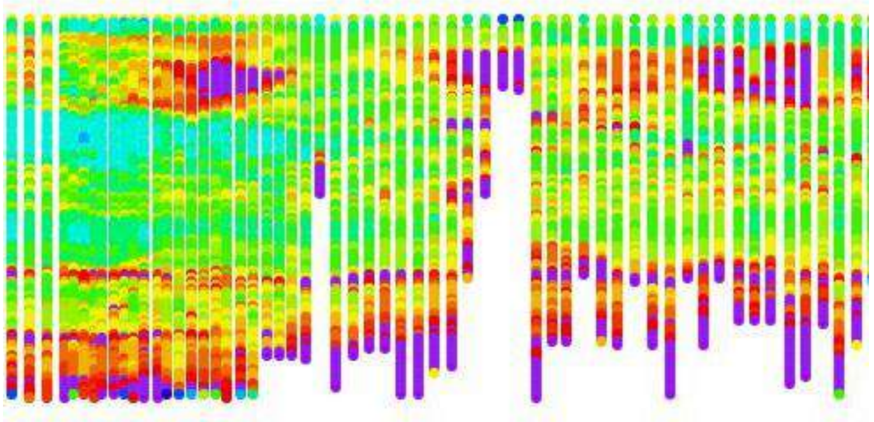

Profiling

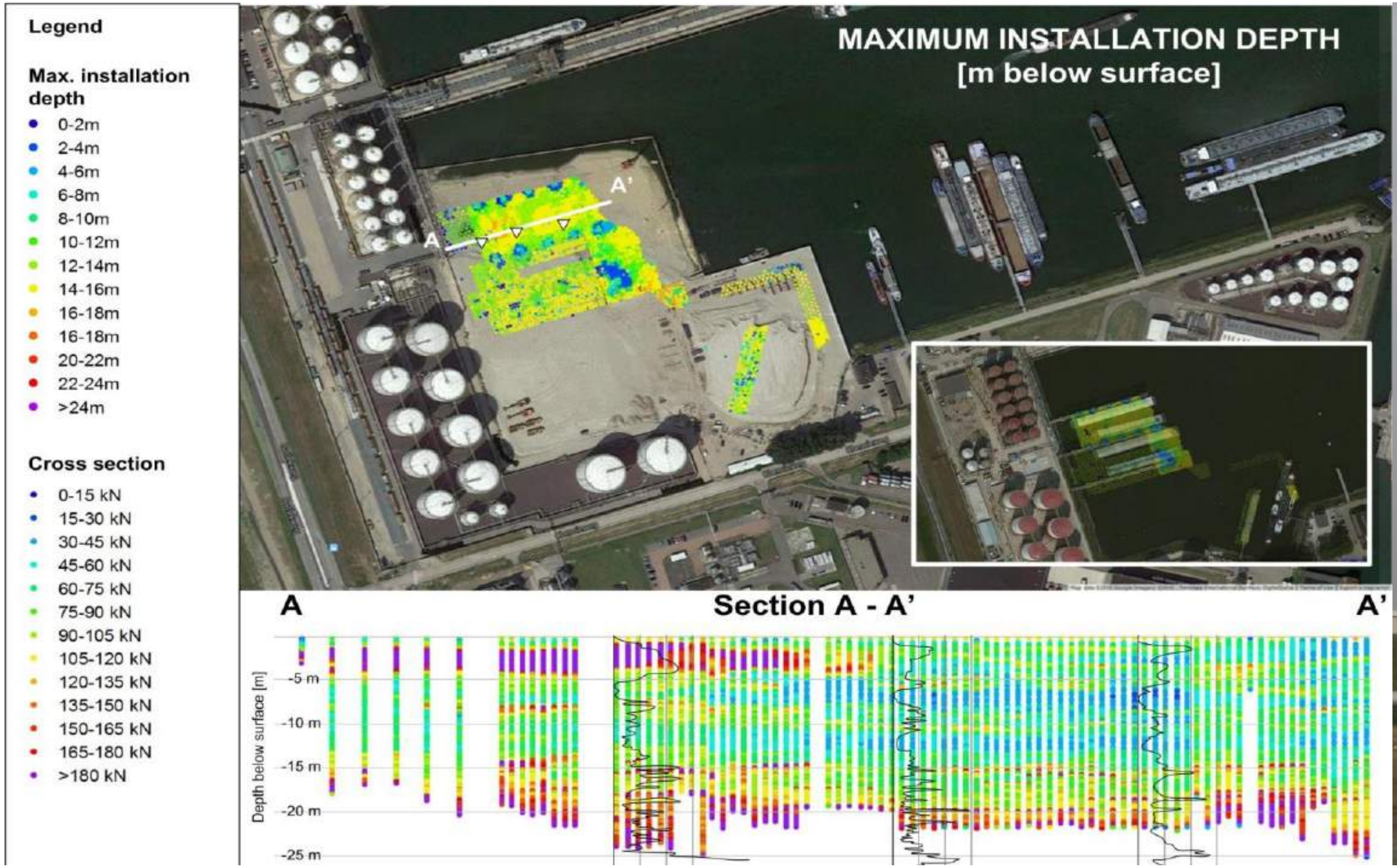
Legend
Max. installation depth
0-2m
2-4m
4-6m
6-8m
8-10m
10-12m
12-14m
14-16m
16-18m
16-18m
20-22m
22-24m
>24m
Cross section
0-15 kN
15-30 kN
30-45 kN
45-60 kN
60-75 kN
75-90 kN
90-105 kN
105-120 kN
120-135 kN
135-150 kN
150-165 kN
165-180 kN
>180 kN
MAXIMUM INSTALLATION DEPTH
[m below surface]
A
A'
Section A - A'
Depth below surface [m]
-5 m
-10 m
-15 m
-20 m
-25 m

Profiling

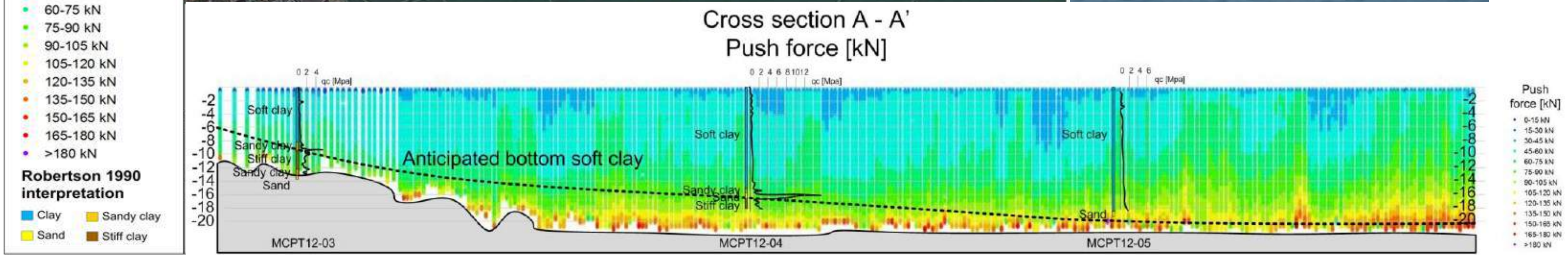
Legend
Max. installation depth
0-2m
2-4m
4-6m
6-8m
8-10m
10-12m
12-14m
14-16m
16-18m
16-18m
20-22m
22-24m
>24m
CPT
Cross section
0-15 kN
15-30 kN
30-45 kN
45-60 kN
60-75 kN
75-90 kN
90-105 kN
105-120 kN
120-135 kN
135-150 kN
150-165 kN
165-180 kN
>180 kN
Robertson 1990 interpretation
Clay
Sandy clay
Sand
Stiff clay
MAXIMUM INSTALLATION DEPTH
[m below seabed]
A
A'
Cross section A - A'
Push force [kN]
Soft clay
Sandy clay
Stiff clay
Sandy clay
Sand
Anticipated bottom soft clay
Sandy clay
Sand
Stiff clay
Sand
MCPT12-03
MCPT12-04
MCPT12-05
Push force [kN]

Optimization?

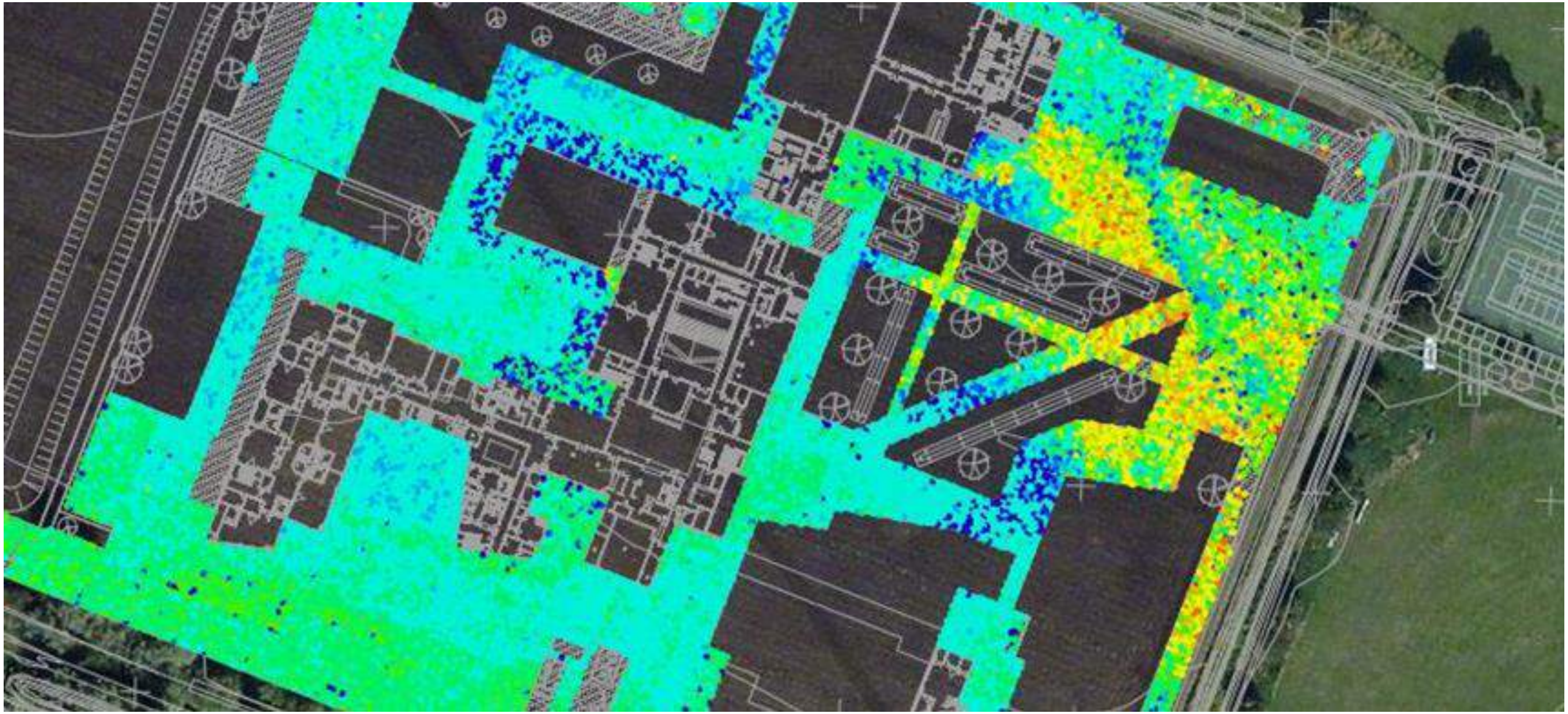

Index

1. Introduction
2. Quality control for vertical drain projects
3. Quality control for heavy rapid impact projects
4. Conclusion

Rapid Impact Compaction (CDC)

- Surface compaction technique
- 7 to 16 ton hammers
- 40 blows per minute, 1.2m fall height – compaction of a location less than 2 minutes
- Different foot diameters available to accommodate for soil conditions
- Depth of influence depending on requirements
- Generally between 6 and 8 meters (10m also observed)
- 16 ton results come close to dynamic compaction results

Work Method

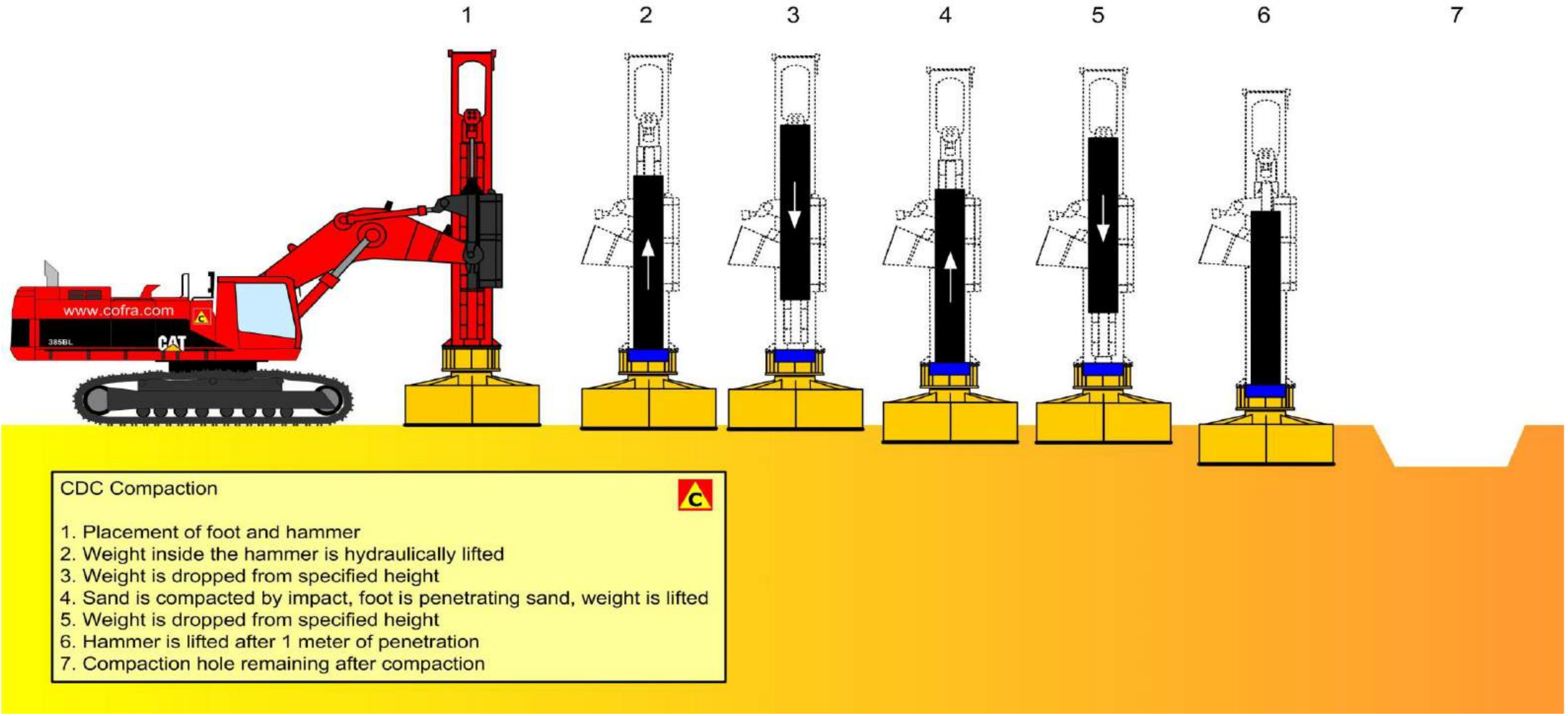
1
2
3
4
5
6
7
www.cofra.com
CAT
CDC Compaction
1. Placement of foot and hammer
2. Weight inside the hammer is hydraulically lifted
3. Weight is dropped from specified height
4. Sand is compacted by impact, foot is penetrating sand, weight is lifted
5. Weight is dropped from specified height
6. Hammer is lifted after 1 meter of penetration
7. Compaction hole remaining after compaction

Work Method

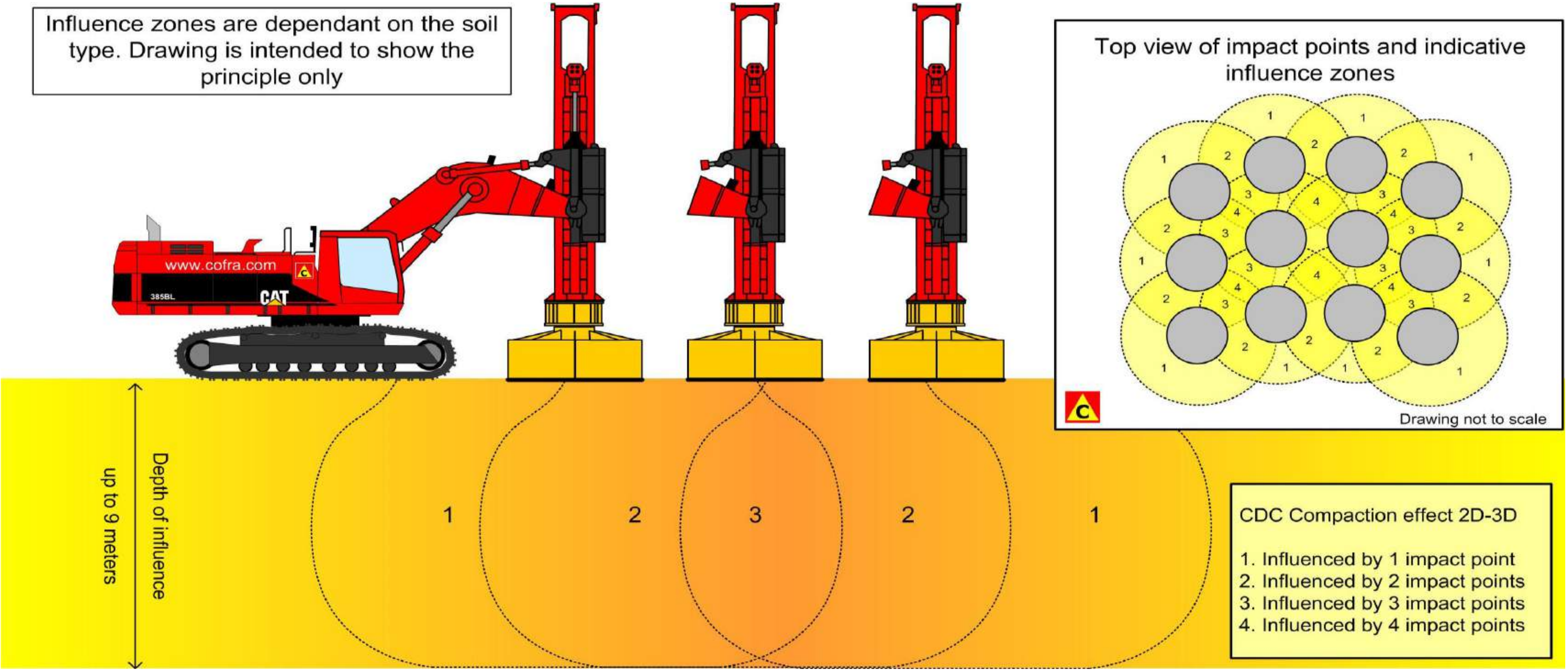
Influence zones are dependant on the soil type. Drawing is intended to show the principle only
Top view of impact points and indicative influence zones
Drawing not to scale
www.cofra.com
385BL
CAT
Depth of influence
up to 9 meters
1
2
3
2
1
CDC Compaction effect 2D-3D
1. Influenced by 1 impact point
2. Influenced by 2 impact points
3. Influenced by 3 impact points
4. Influenced by 4 impact points

Work Method

General Advantages

During Installation

- Each compaction location is shown to the operator
- No positions required on the field
- Single local spots can be compacted

General Advantages

During Installation

- Each compaction location is shown to the operator
- No positions required on the field
- Single local spots can be compacted
- Homogeneous subsoil after compaction

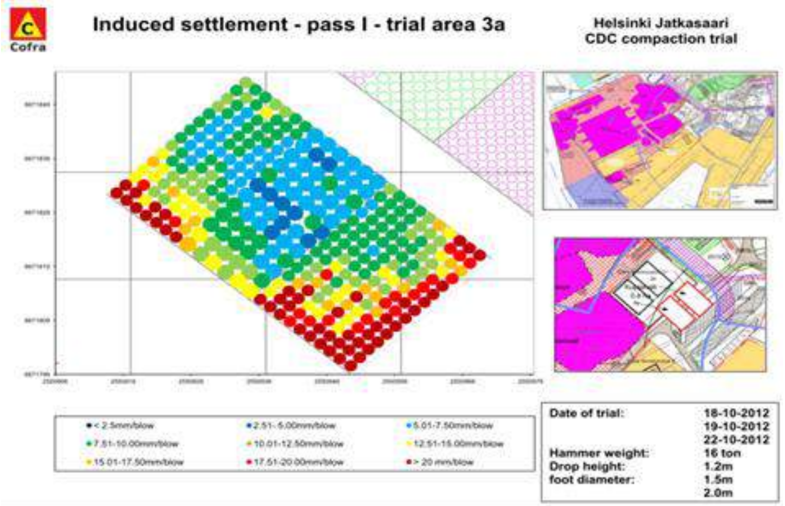

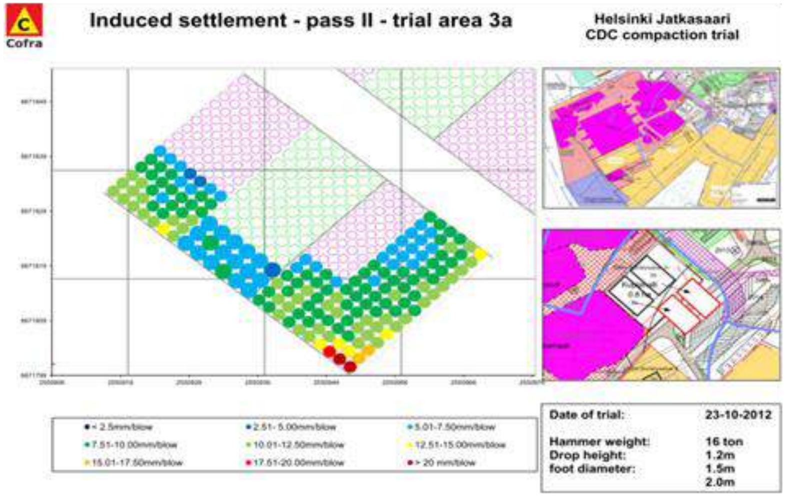

Advantages General

After installation

- Exact position of compaction location
- Settlement profile at each compaction location (x-ref)
- Better Quality Assurance
- Mapping of non compliant soil / clayey sections

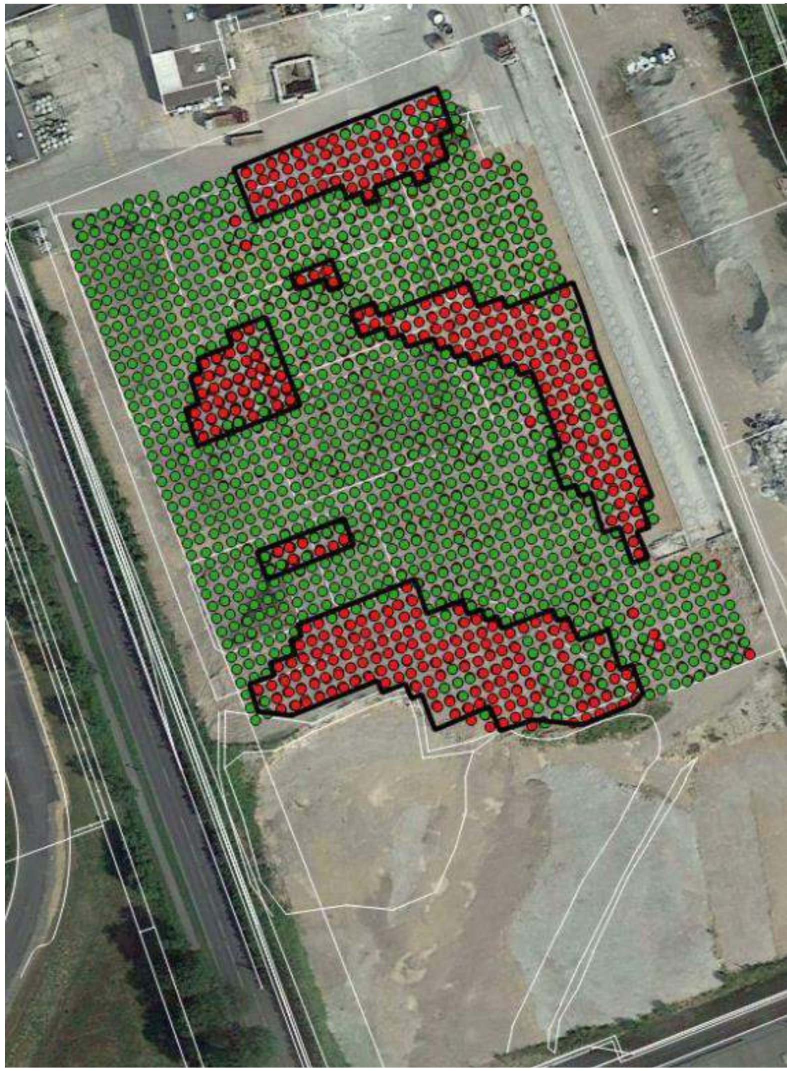

Advantages for the Engineer

- Site specific correlation between induced settlement and site investigation results

- Stop criterion is determined during trial and used during compaction

- After compaction logger data is assessed for requirement of additional pass

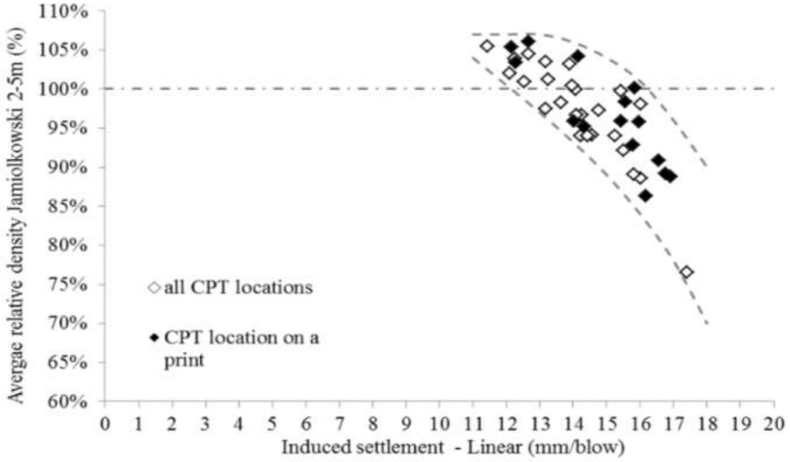

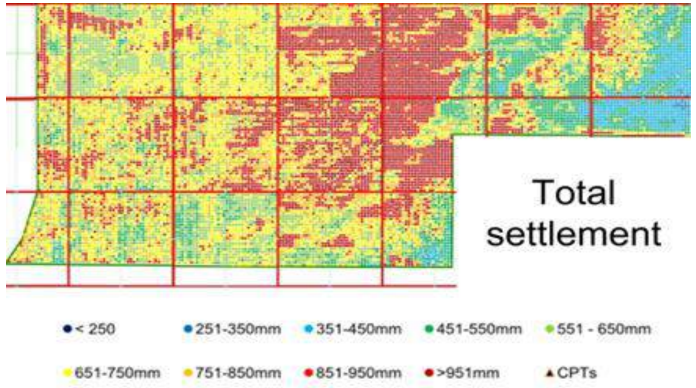

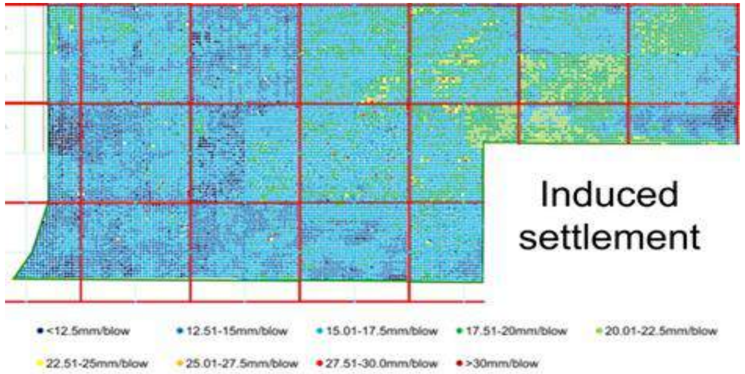

Compaction - Amsterdam

SAA-ONE – Total Settlement

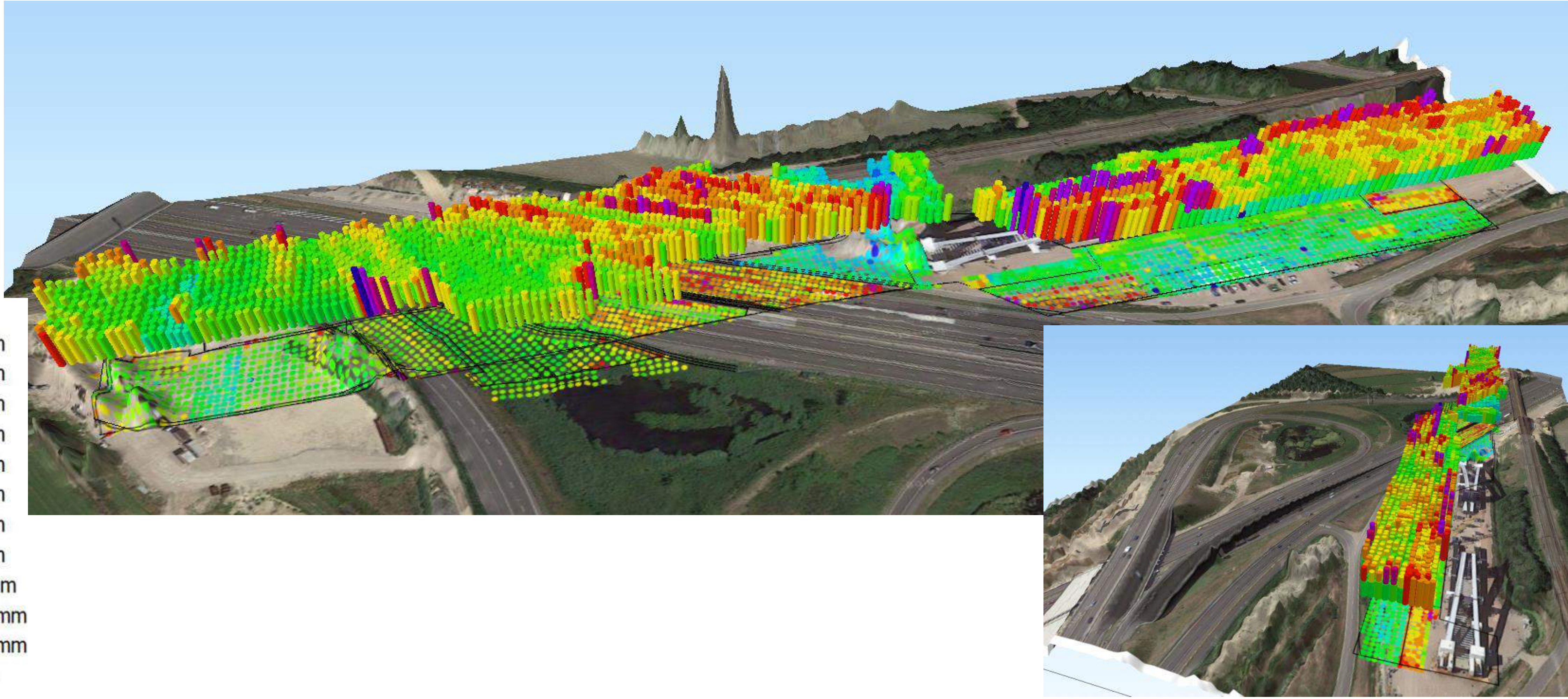

- 0-100mm
- 100-200mm
- 200-300mm
- 300-400mm
- 400-500mm
- 500-600mm
- 600-700mm
- 700-800mm
- 800-900mm
- 900-1000mm
- 1000-1100mm
- 1100-1200mm
- >1200mm

Index

Conclusion for PVD

- Major advantages over traditional logging
- Makes installation on chart datum levels possible
- Makes normally not used data accessible and easily traceable
- Gives the engineer far more information about the subsoil
- Data can be used to
  - Optimize monitoring
  - Optimize surcharge
  - Reduce geotechnical risks
  - Improve quality

Conclusion for CDC Compaction

- Highly controllable compaction
- Client is updated at regular intervals on progress in easy to understand images
- System can be used to homogenize terrains / map soft sections
- Reaction (E-Modulus) of the soil can be predicted

Thank you for your attention

Rigid Inclusions,
a Ground Reinforcement Solution rather than a Ground Improvement Solution

Baldomiro Xavier

Teixeira Duarte Engenharia e Construções SA

INDEX

THE BASICS

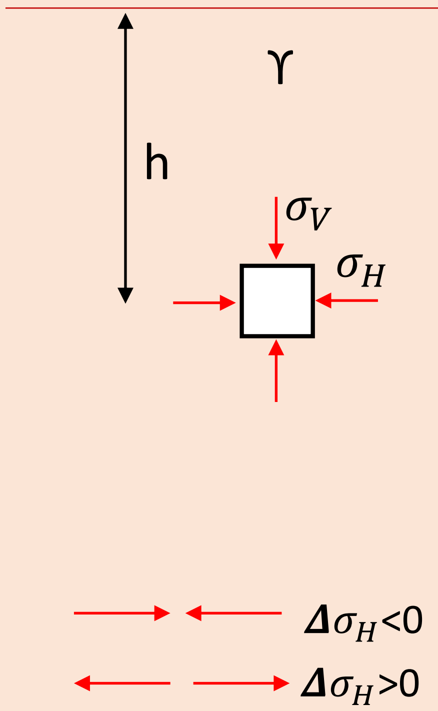

$\sigma_v = \gamma\, h$ $\sigma_h = k\, \sigma_v$

K

K_a K_0 K_p

$K_a = 1 / k_p$

If a soil feels like water

$K_a = K_0 = K_p = 1$ $\Delta\sigma_H = 0$

IDEAS FROM THE KITCHEN 1

IDEAS FROM THE KITCHEN 2

STRUCTURAL REHABILITATION OF AN ACCUMULATION TANK – MADEIRA

STRUCTURAL REHABILITATION OF AN ACCUMULATION TANK – MADEIRA

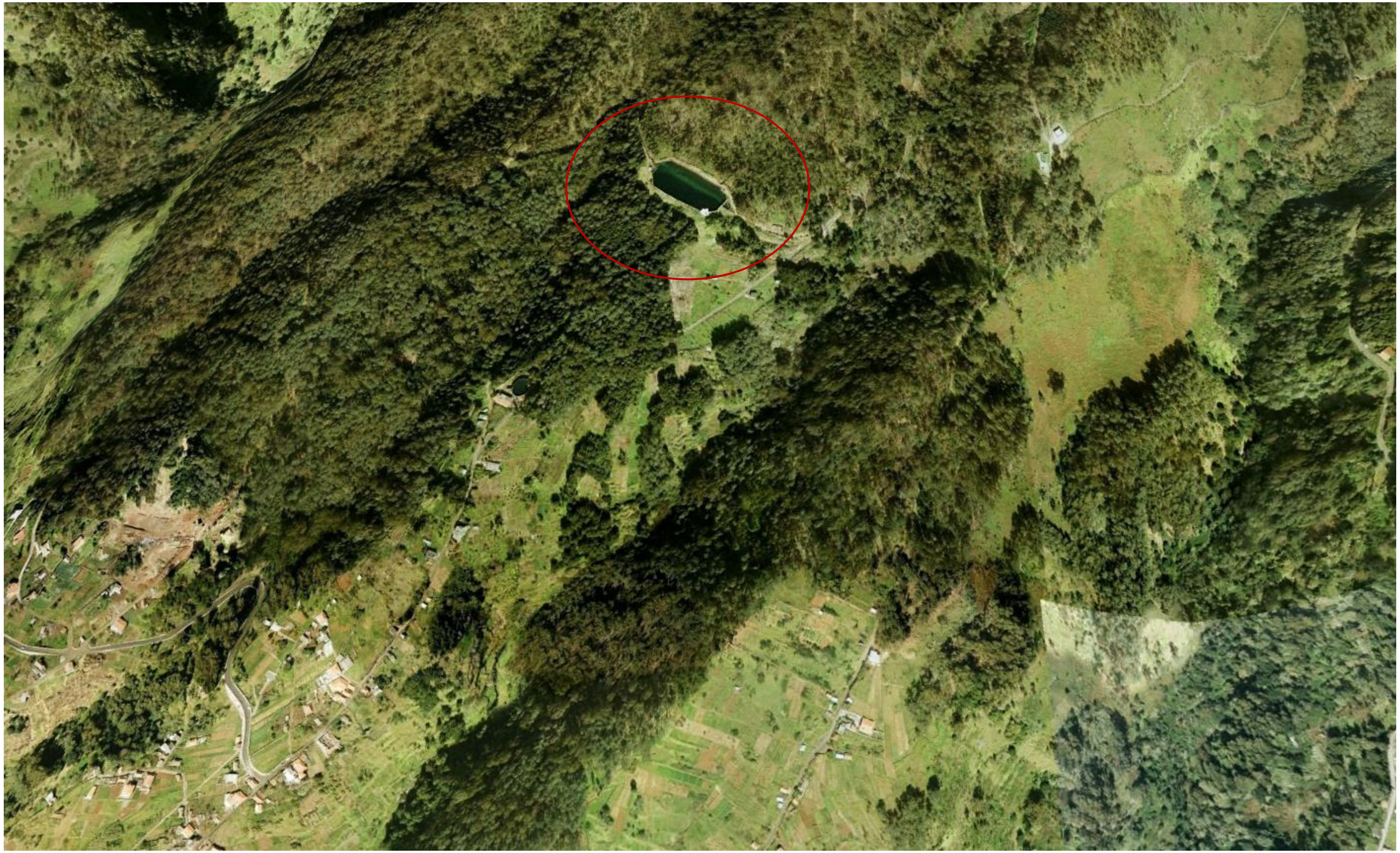

STRUCTURAL REHABILITATION OF AN ACCUMULATION TANK – MADEIRA

EXISTING SITUATION

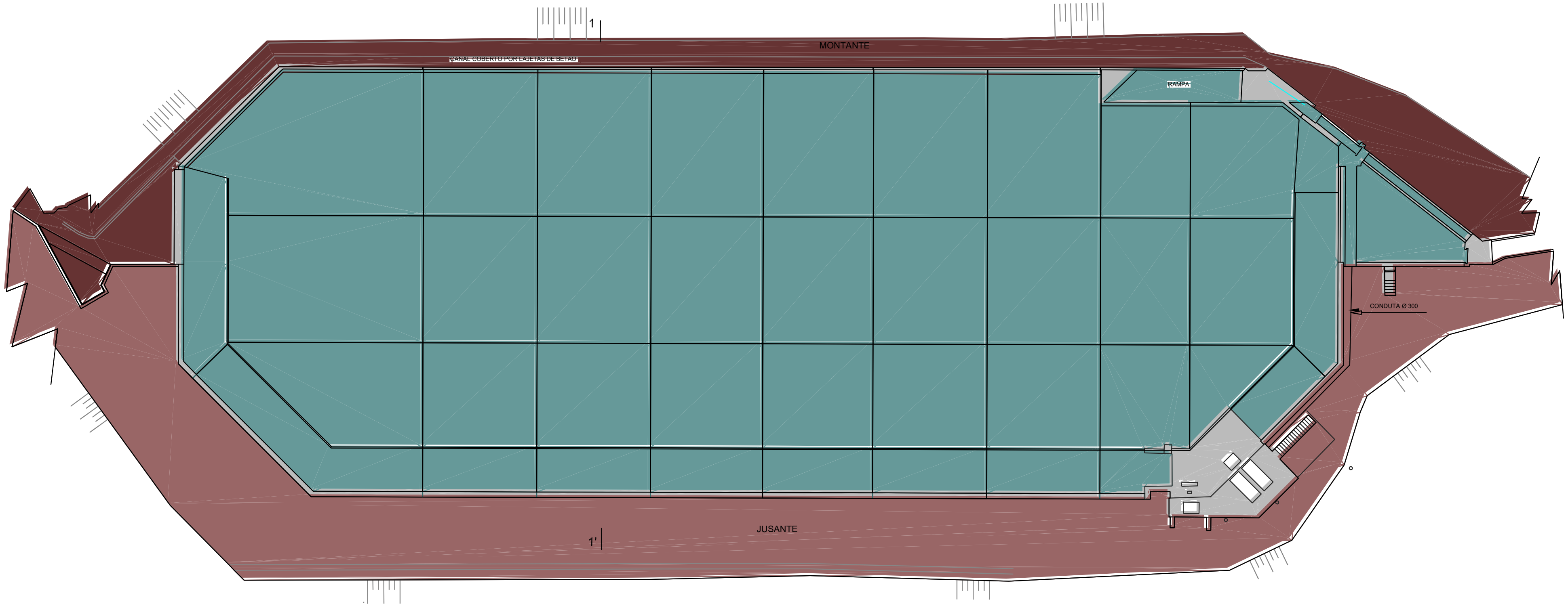

STRUCTURAL REHABILITATION OF AN ACCUMULATION TANK – MADEIRA

EXISTING SITUATION – SECTION

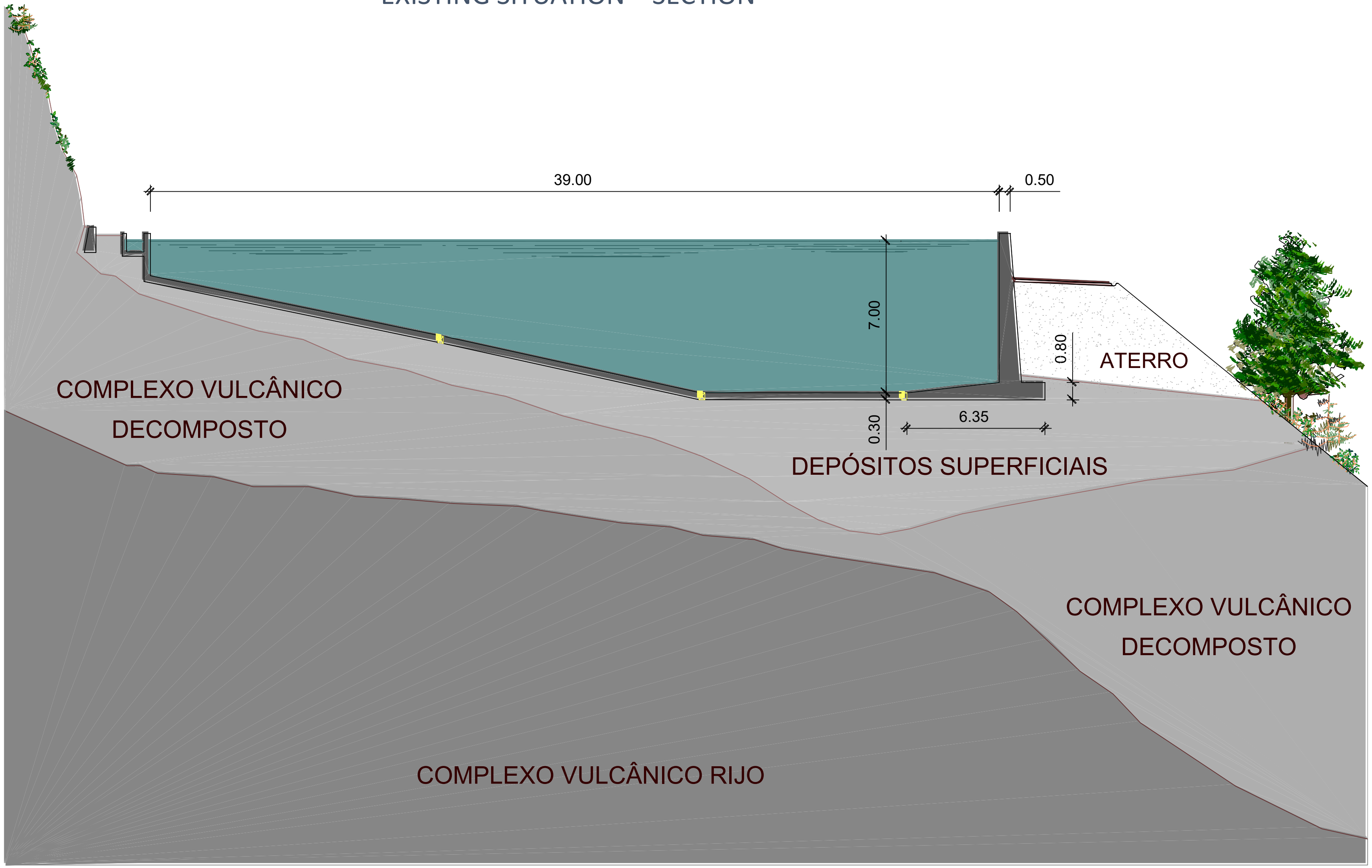

CENTRAL HIDROELÉCTRICA DE INVERNO DA CALHETA
CÂMARA DE ACUMULAÇÃO

SITUAÇÃO DETECTADA

STRUCTURAL REHABILITATION OF AN ACCUMULATION TANK – MADEIRA

EXISTING SITUATION – CROSS SECTION

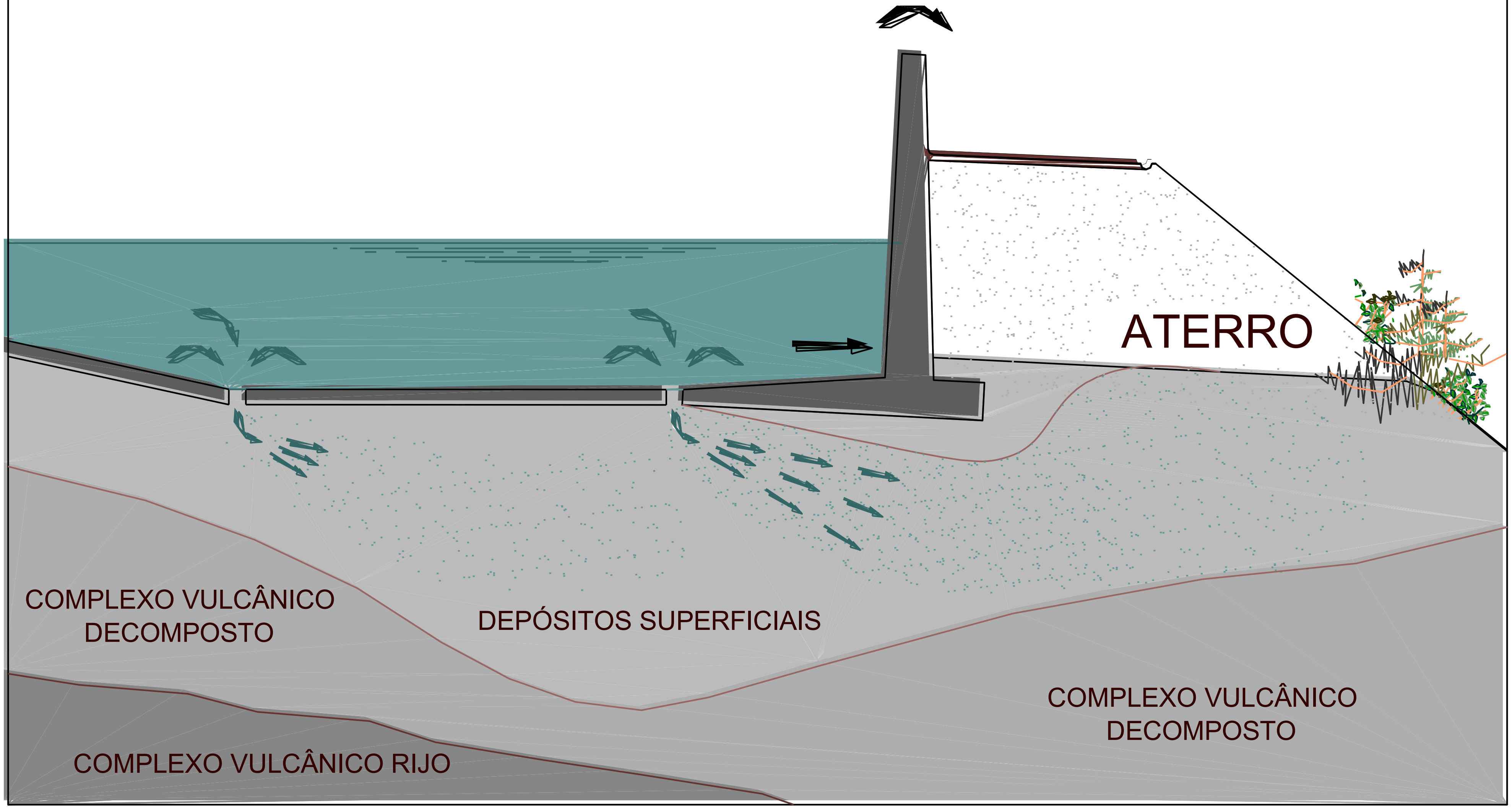

STRUCTURAL REHABILITATION OF AN ACCUMULATION TANK – MADEIRA

CROSS SECTION: SOLUTION WITH MICROPILES

PRIMEIRA SOLUÇÃO DE REFORÇO ESTRUTURAL
MICROESTACAS INCLINADAS ENCASTRADAS NO COMPLEXO VULCÂNICO RIJO

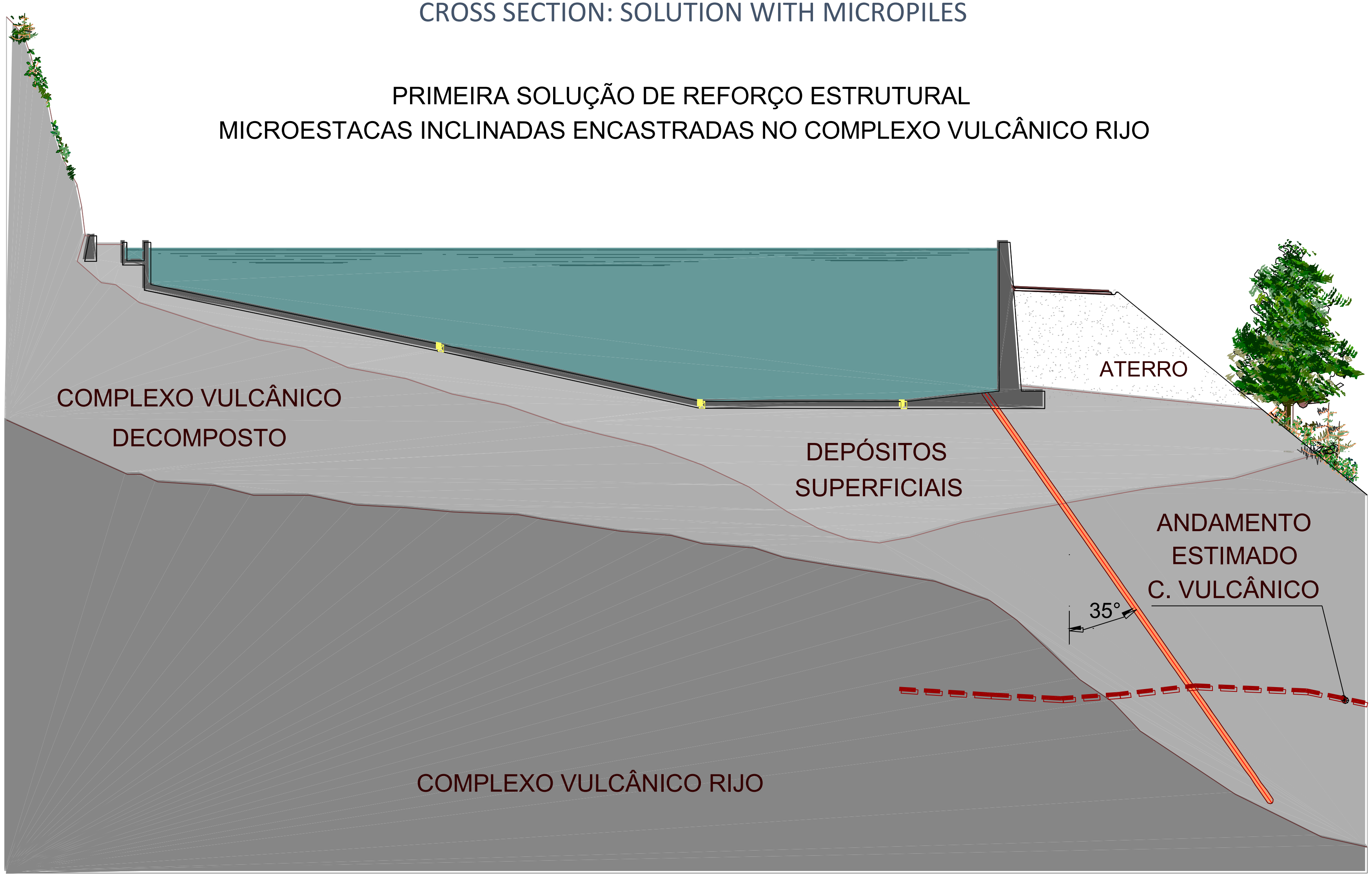

STRUCTURAL REHABILITATION OF AN ACCUMULATION TANK – MADEIRA

THE EQUILIBRIUM

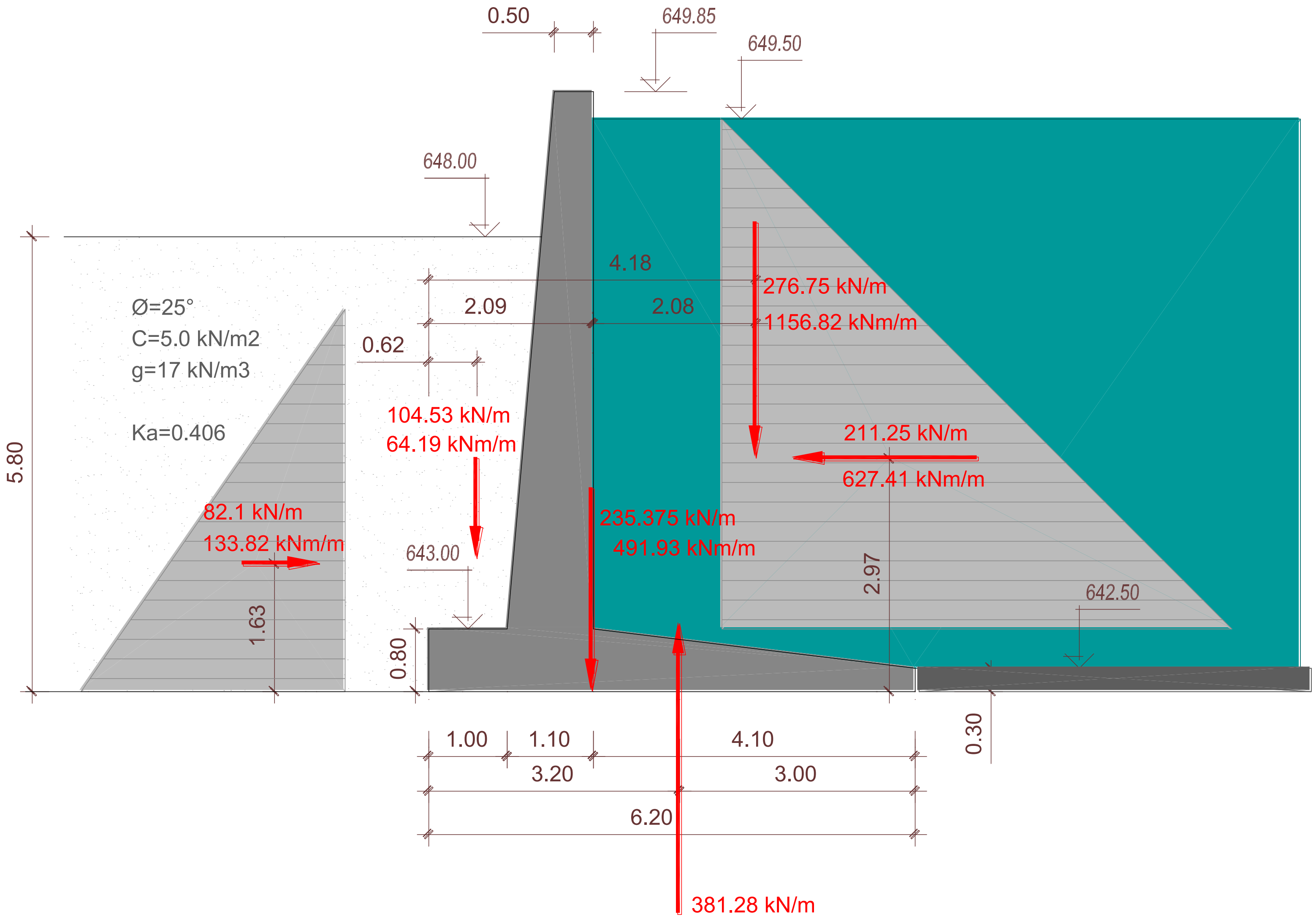

STRUCTURAL REHABILITATION OF AN ACCUMULATION TANK – MADEIRA

FOUNDATION REFURBISHMENT - JET GROUTING COLUMNS

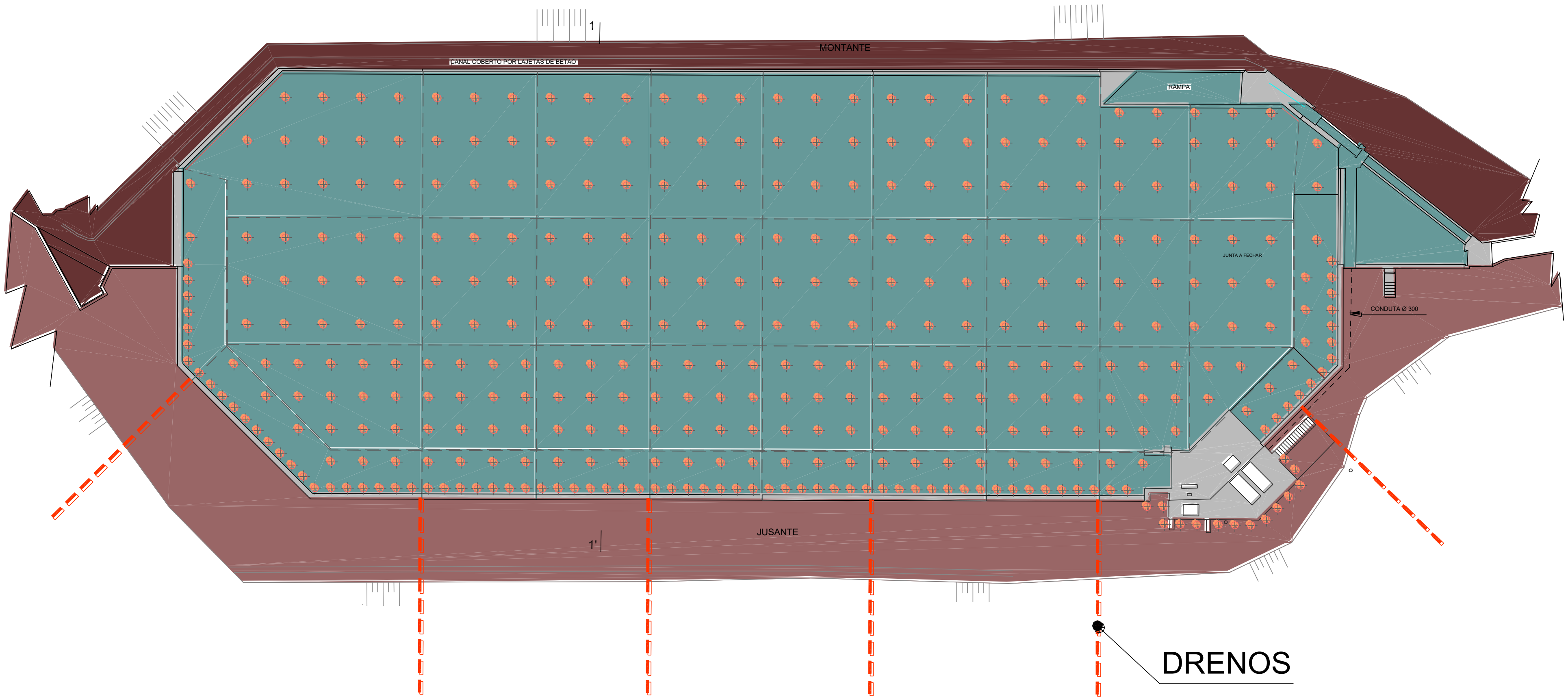

STRUCTURAL REHABILITATION OF AN ACCUMULATION TANK – MADEIRA

FOUNDATION REFURBISHMENT - JET GROUTING COLUMNS

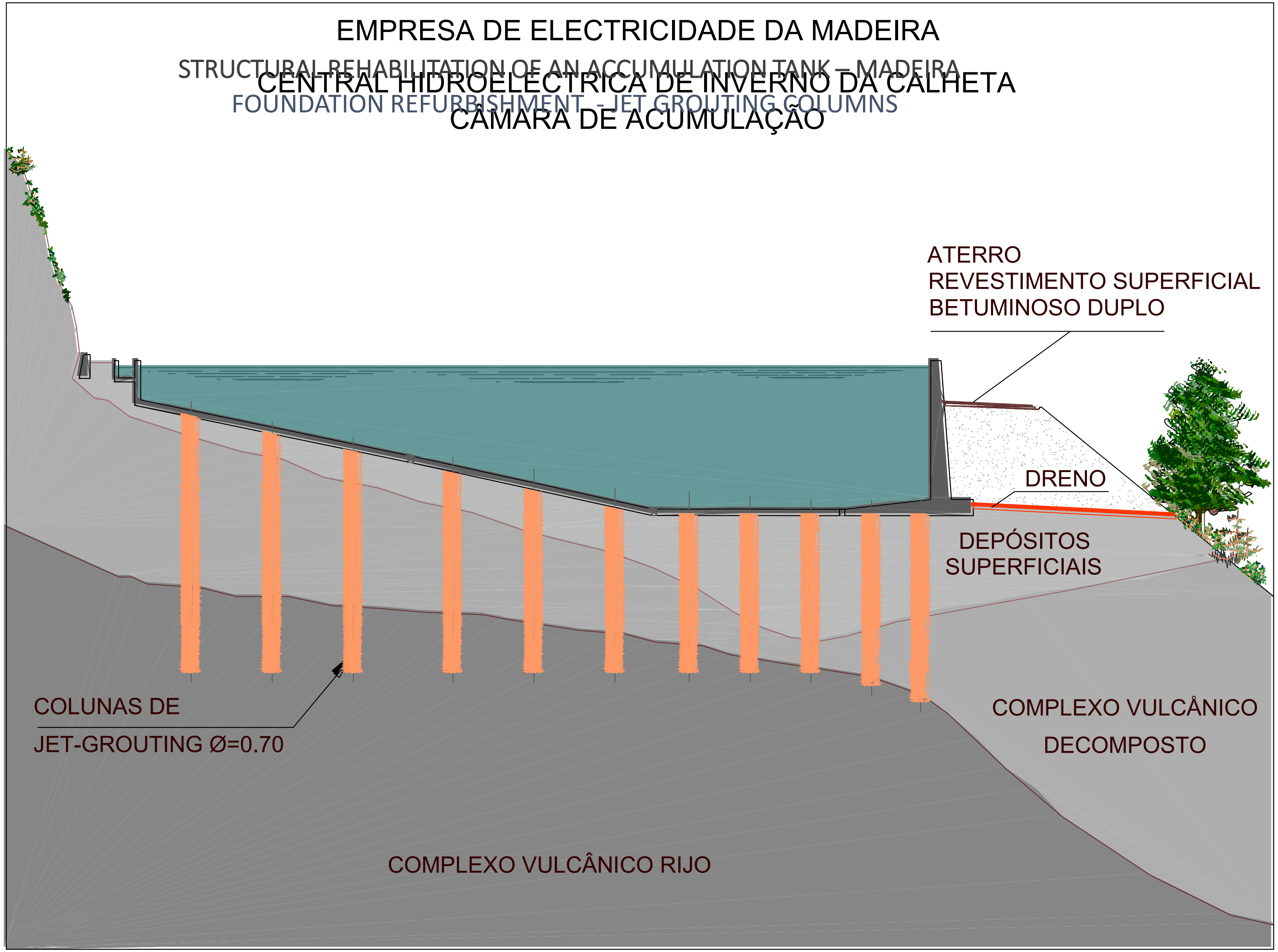

STRUCTURAL REHABILITATION OF AN ACCUMULATION TANK – MADEIRA

TESTING PHASE

STRUCTURAL REHABILITATION OF AN ACCUMULATION TANK – MADEIRA

TESTING PHASE

STRUCTURAL REHABILITATION OF AN ACCUMULATION TANK – MADEIRA

NEARBY SLOPE AND BYPASS CANAL

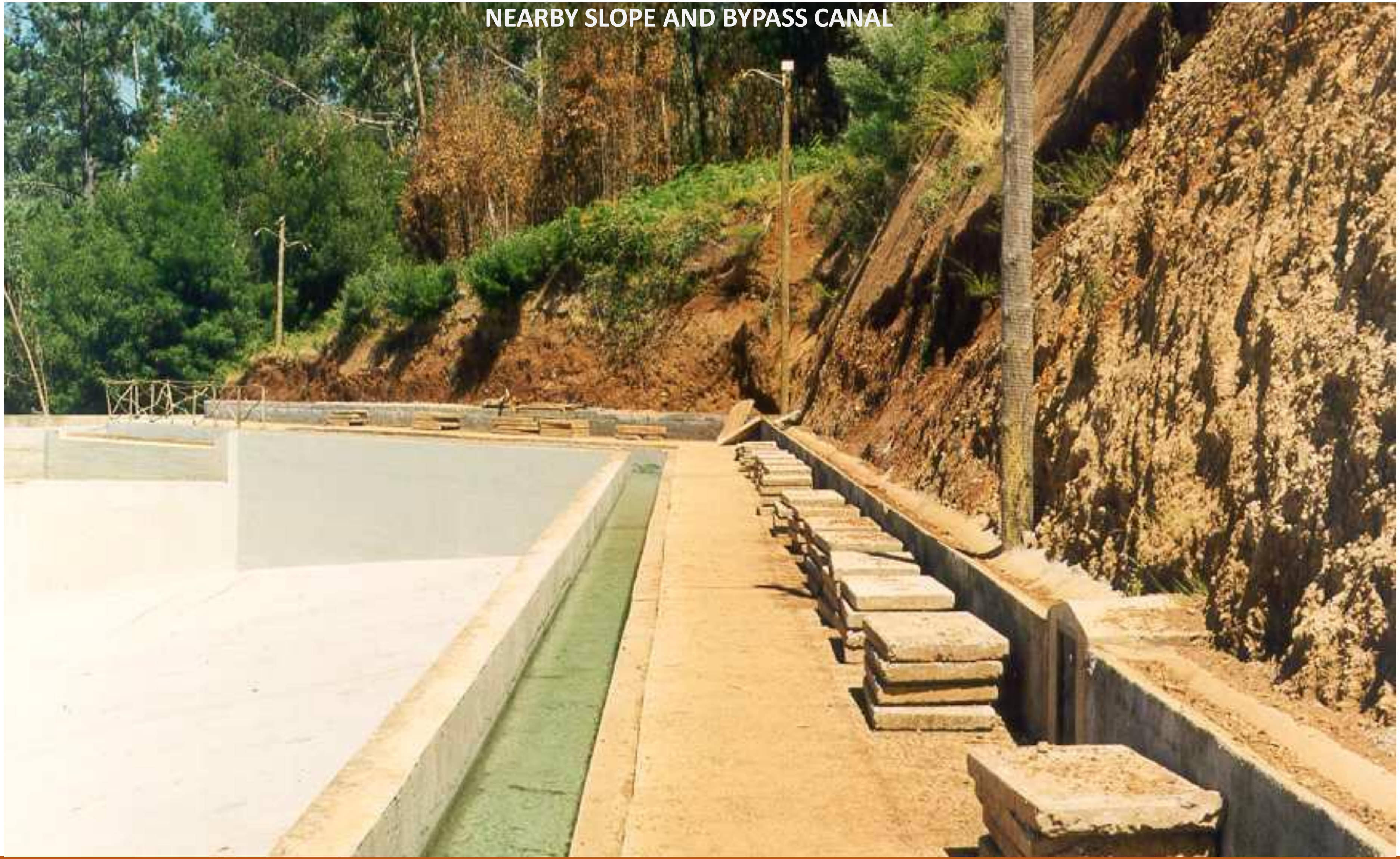

STRUCTURAL REHABILITATION OF AN ACCUMULATION TANK – MADEIRA

STRUCTURAL REHABILITATION OF AN ACCUMULATION TANK – MADEIRA

STRUCTURAL REHABILITATION OF AN ACCUMULATION TANK – MADEIRA

ALREADY IN OPERATION

SANTARÉM SEWAGE TREATMENT PLANT

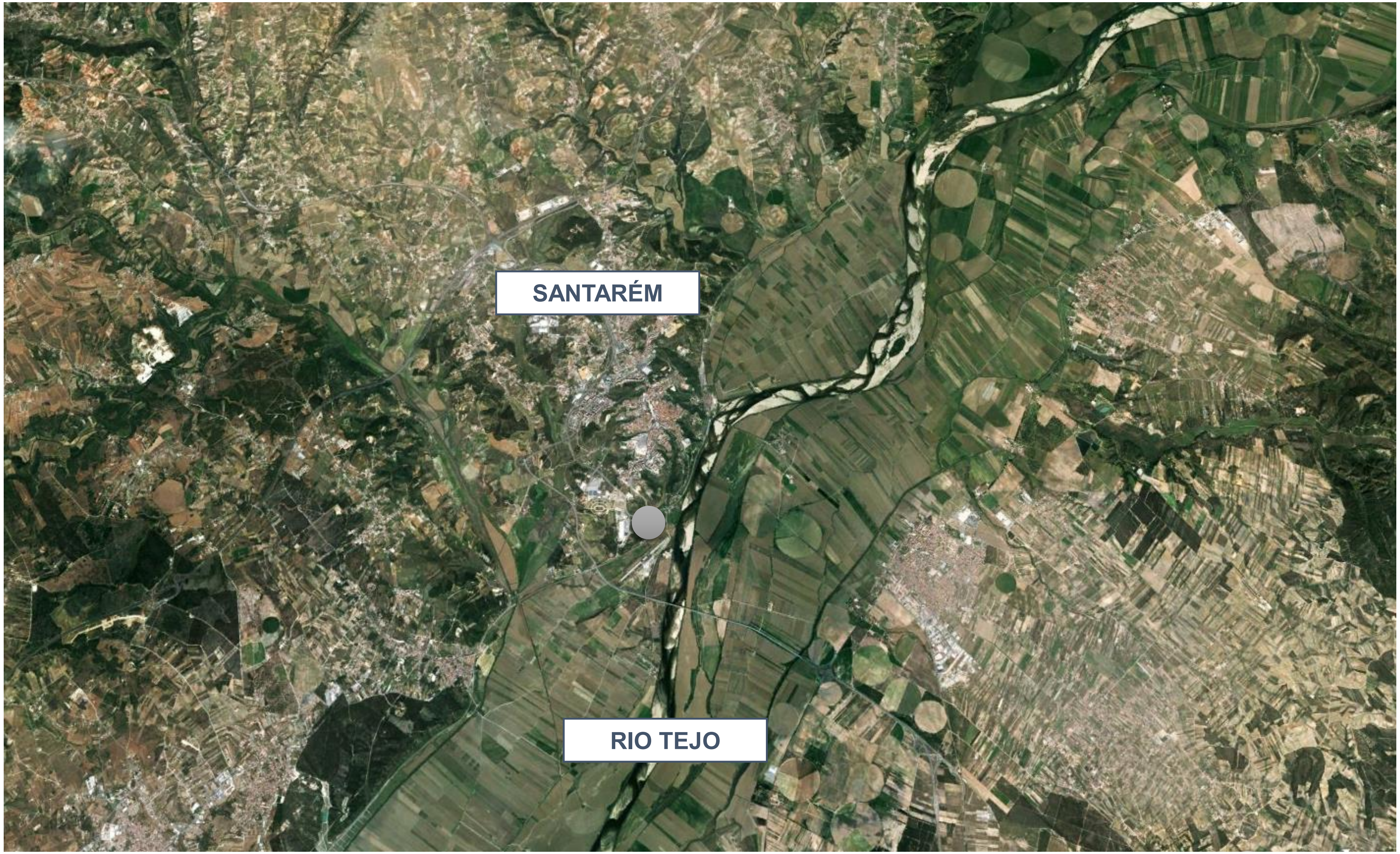

SANTARÉM SEWAGE TREATMENT PLANT

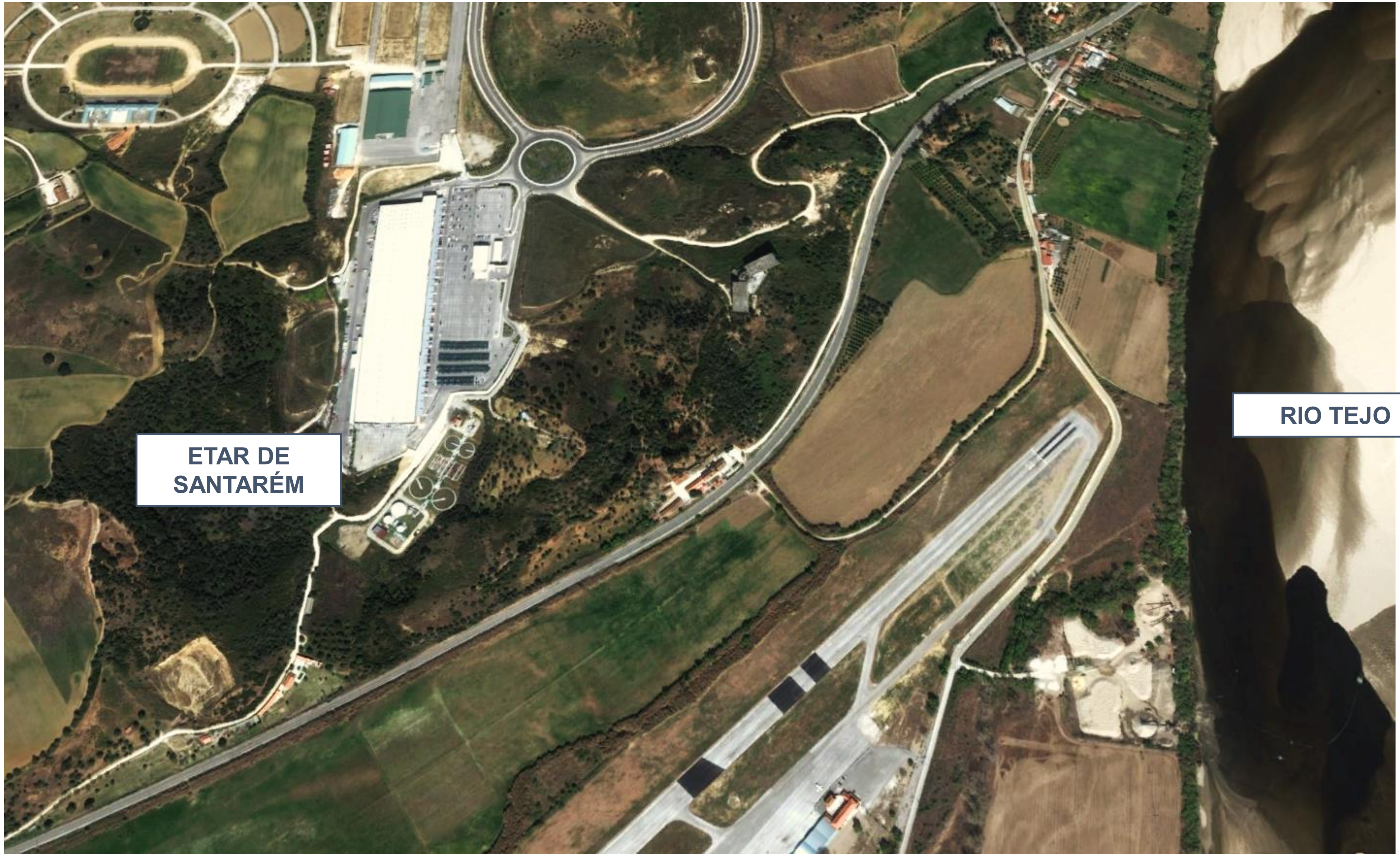

SANTARÉM SEWAGE TREATMENT PLANT

SANTARÉM SEWAGE TREATMENT PLANT

SANTARÉM SEWAGE TREATMENT PLANT

SANTARÉM SEWAGE TREATMENT PLANT

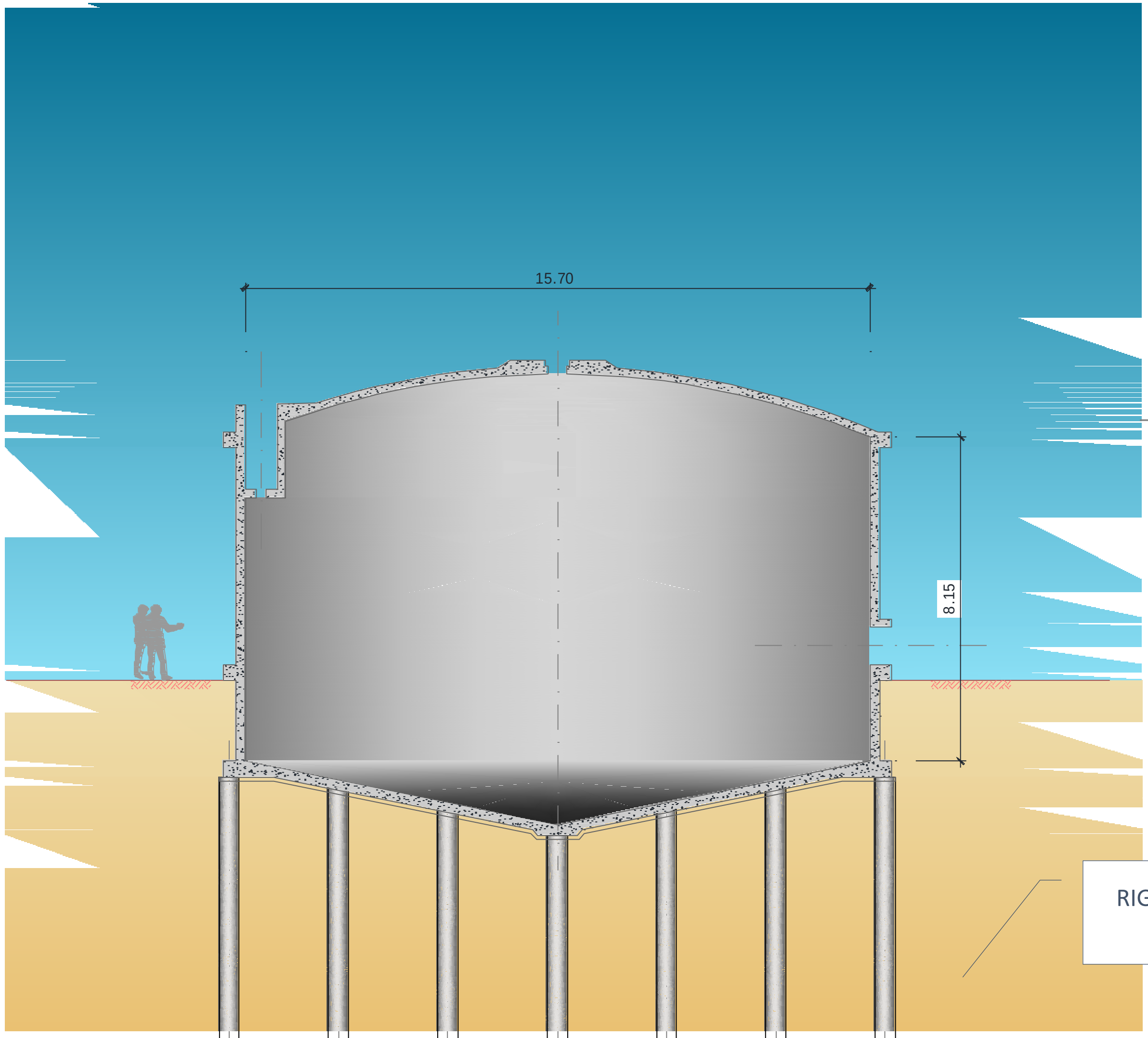

RIGID INCLUSIONS
ϕ=500 mm

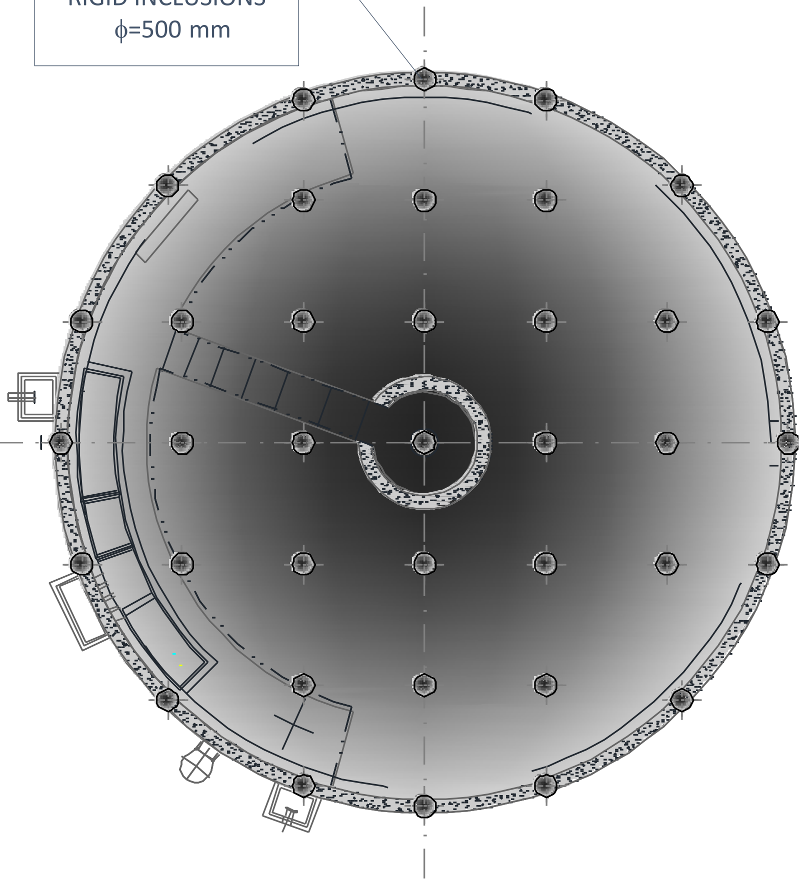

RIGID INCLUSIONS
ϕ=500 mm

SANTARÉM SEWAGE TREATMENT PLANT

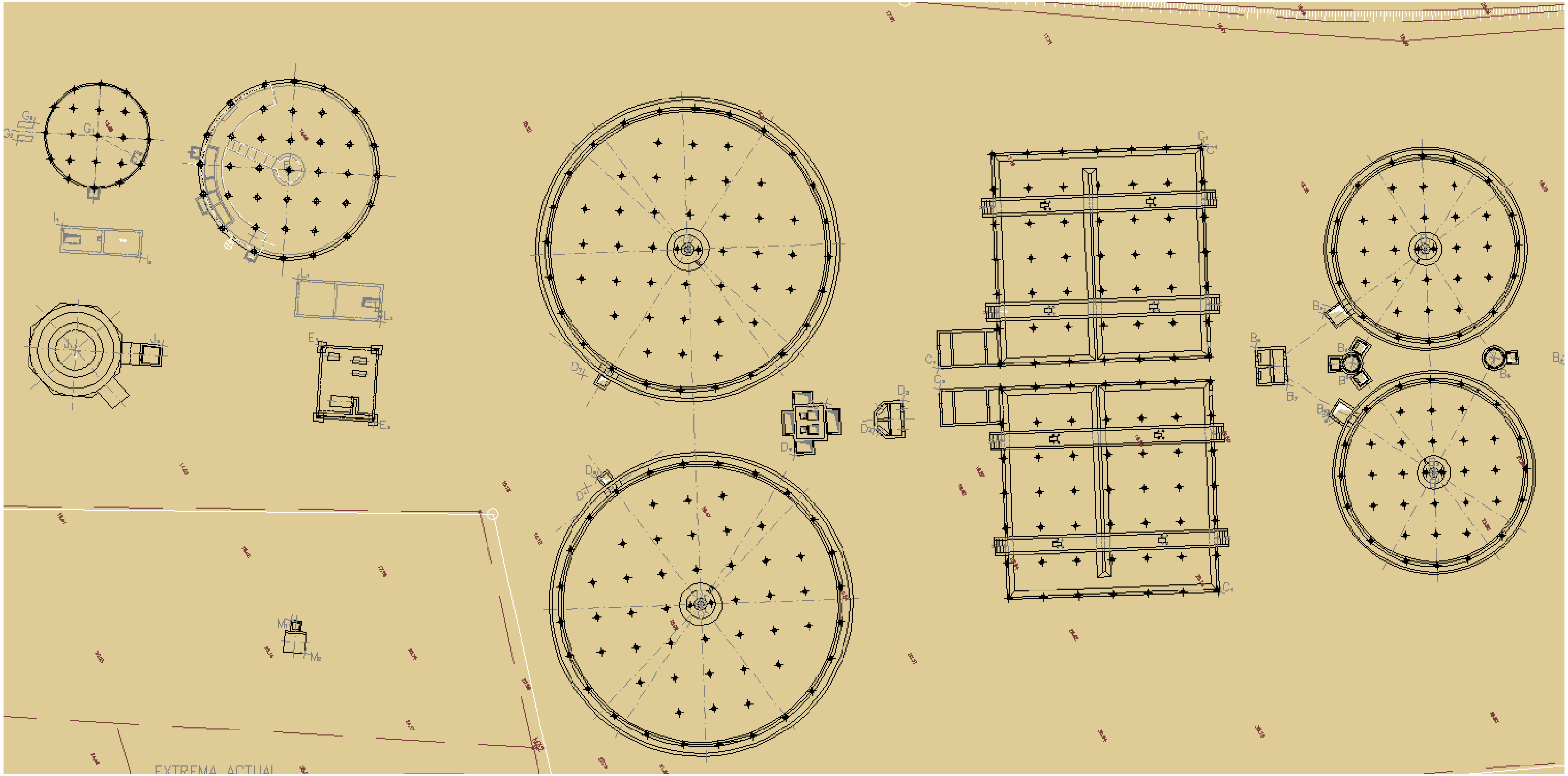

ESCOM TOWERS - LUANDA

ESCOM TOWERS - LUANDA

ESCOM TOWERS - LUANDA

ESCOM TOWERS - LUANDA

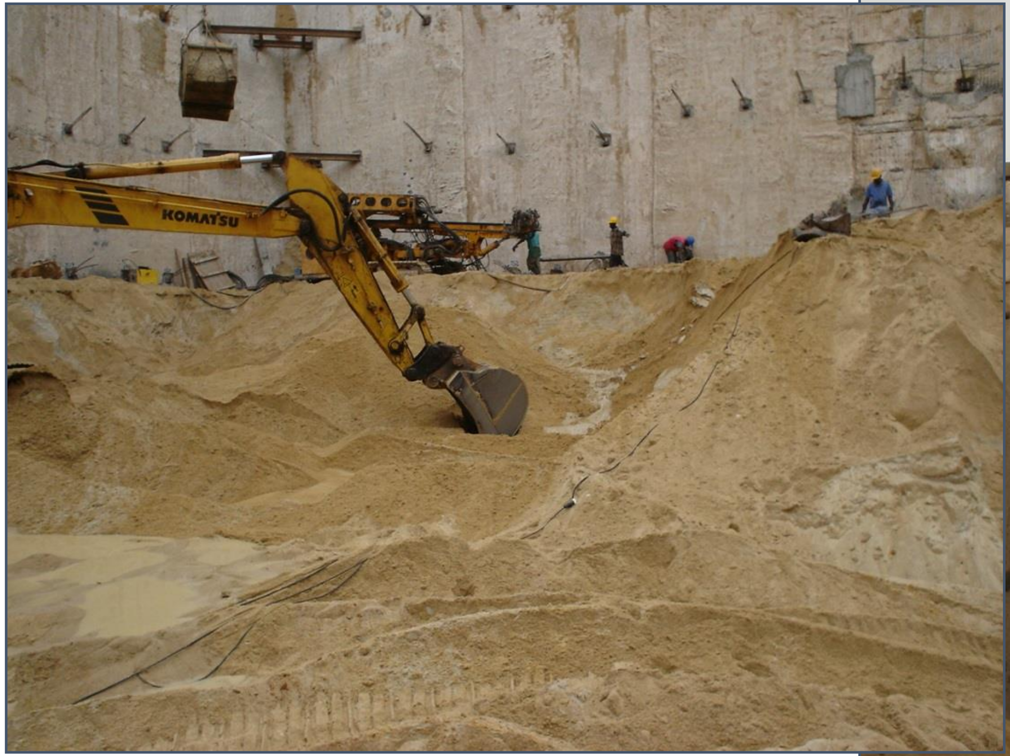

ESCOM TOWERS - LUANDA

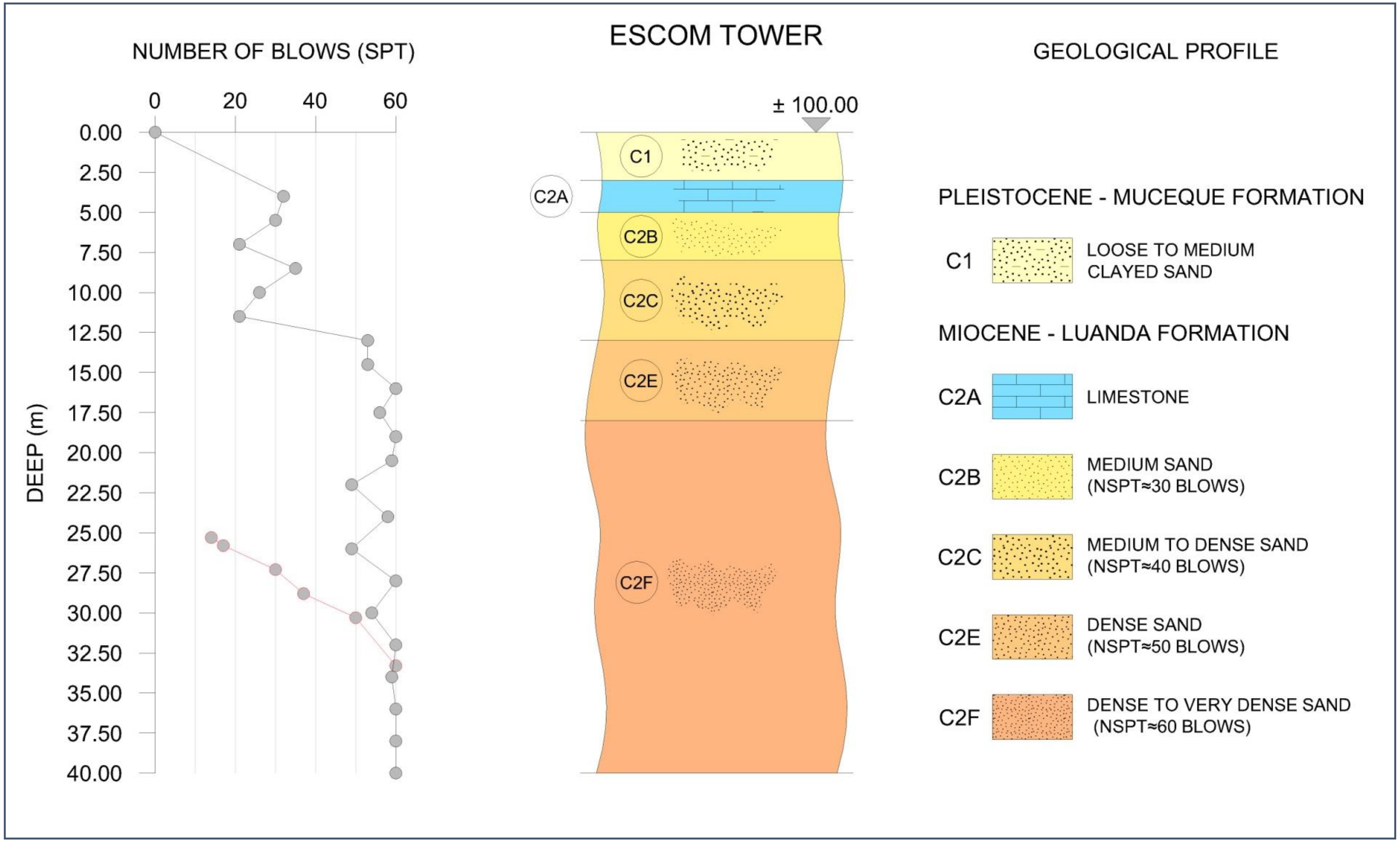

ESCOM TOWERS - LUANDA

Settlements prediction by Timoshenko & Goodier (1951)

$$\Delta H = q_0 \cdot B' \cdot \frac{1-\upsilon^2}{E_S} \cdot m \cdot I_S \cdot I_F$$

$$I_S = \left(I_1 + \frac{1-2\mu}{1-\mu} I_2 \right)$$

$$I_1 = \frac{1}{\pi}\left[M \cdot \ln \frac{\left(1+\sqrt{M^2+1}\right)\sqrt{M^2+N^2}}{M\left(1+\sqrt{M^2+N^2+1}\right)} + \ln \frac{\left(M+\sqrt{M^2+1}\right)\sqrt{1+N^2}}{M+\sqrt{M^2+N^2+1}} \right]$$

$$I_2 = \frac{N}{2\pi} \arctan\left(\frac{M}{N\sqrt{M^2+N^2+1}} \right) \quad (\text{arctan em radianos})$$

em que : $N = \frac{H}{B'}$ e $M = \frac{L'}{B'}$, com

$L' = \frac{L}{2}$ para o centro; $L' = L$ para o canto

$B' = \frac{B}{2}$ para o centro; $B' = B$ para o canto

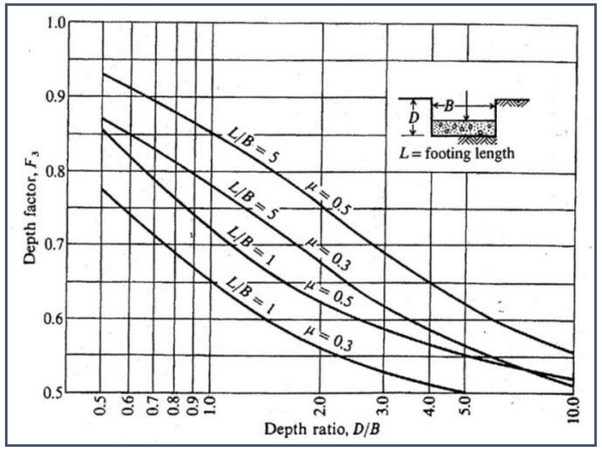

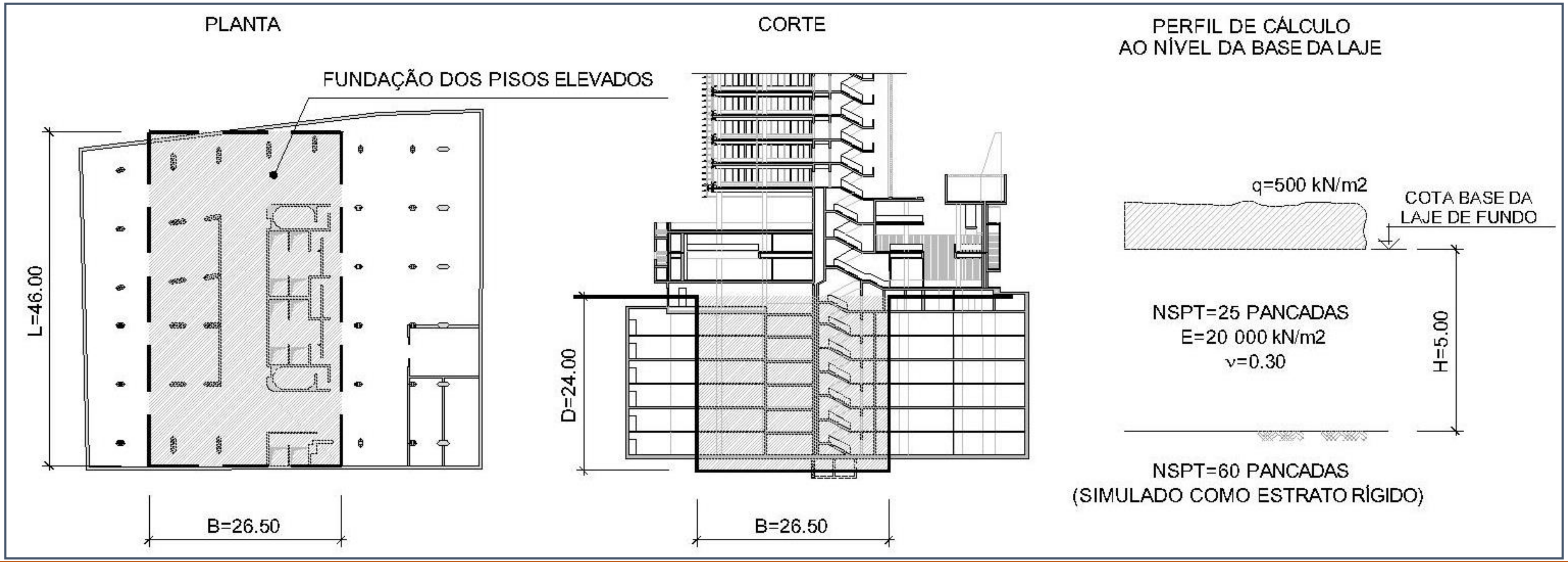

ESCOM TOWERS - LUANDA

PLATE LOAD TEST

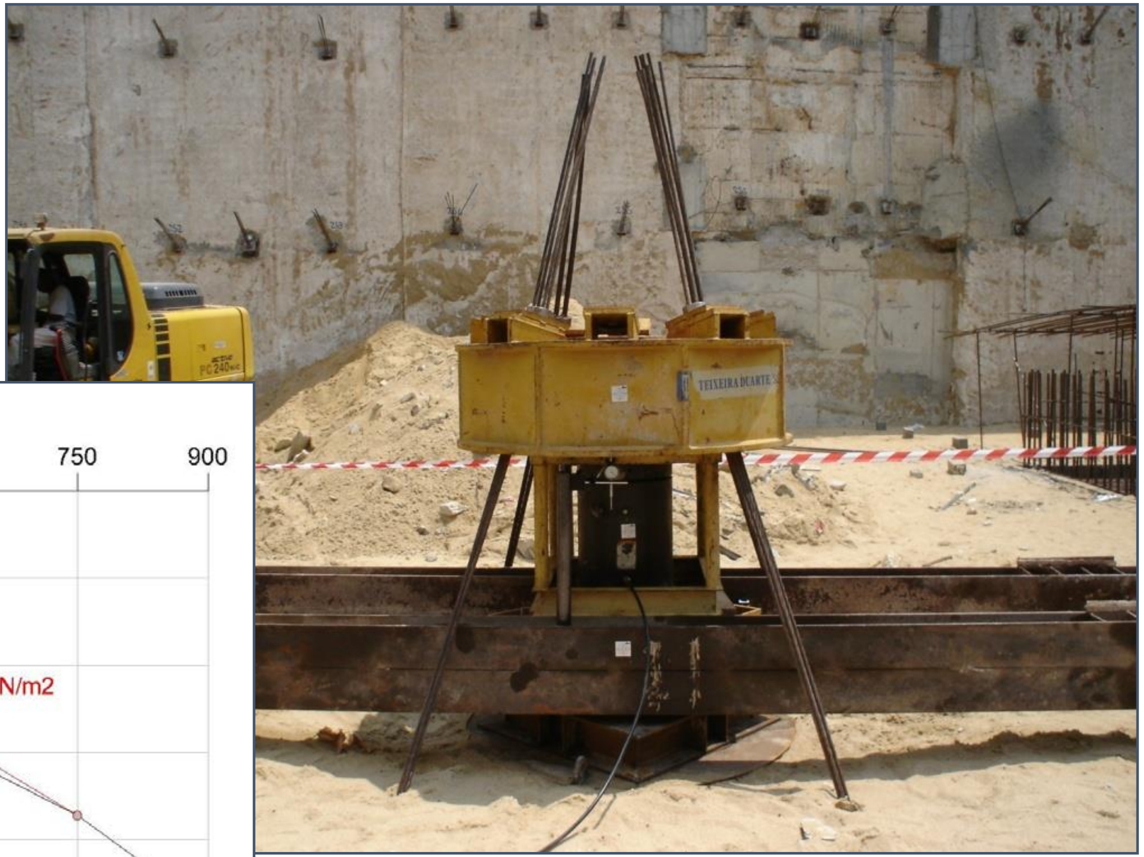

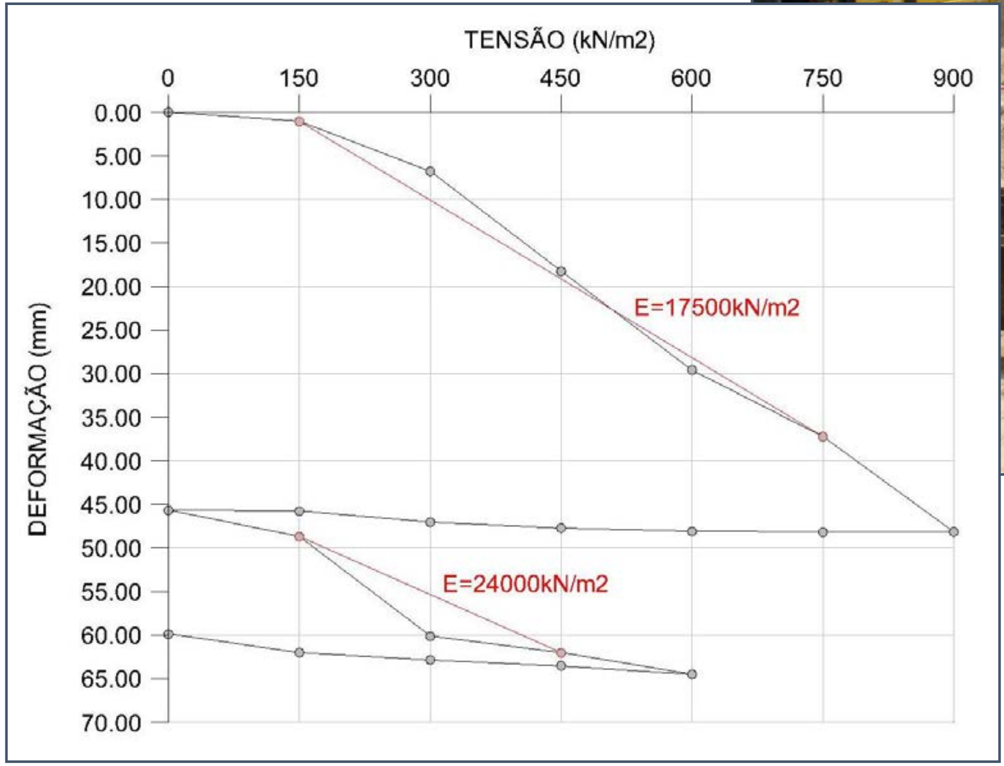

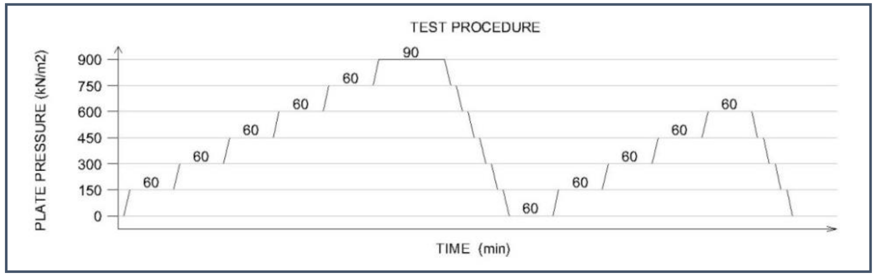

ESCOM TOWERS - LUANDA

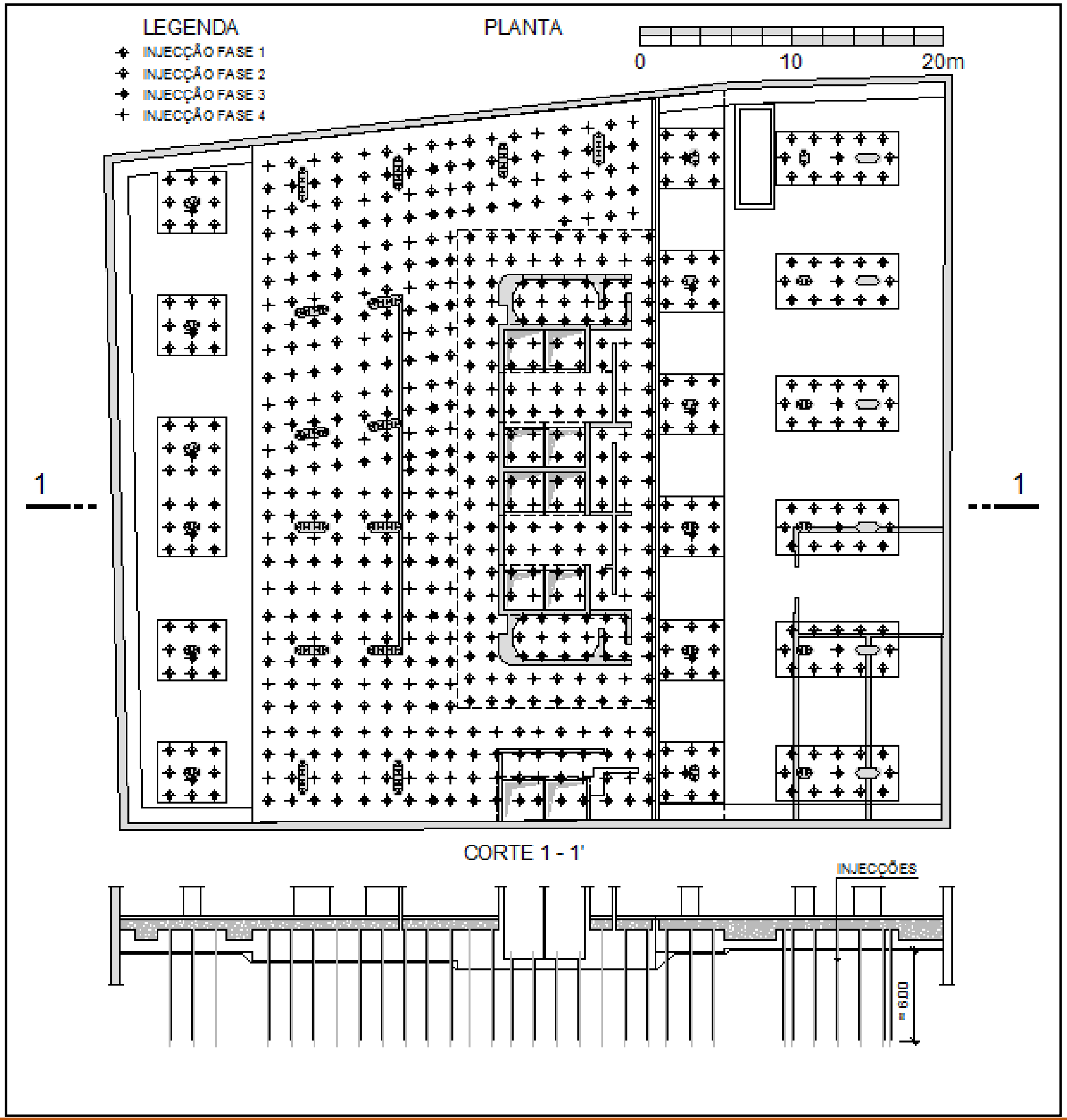

ESCOM TOWERS - LUANDA

ESCOM TOWERS - LUANDA

ESCOM TOWERS - LUANDA

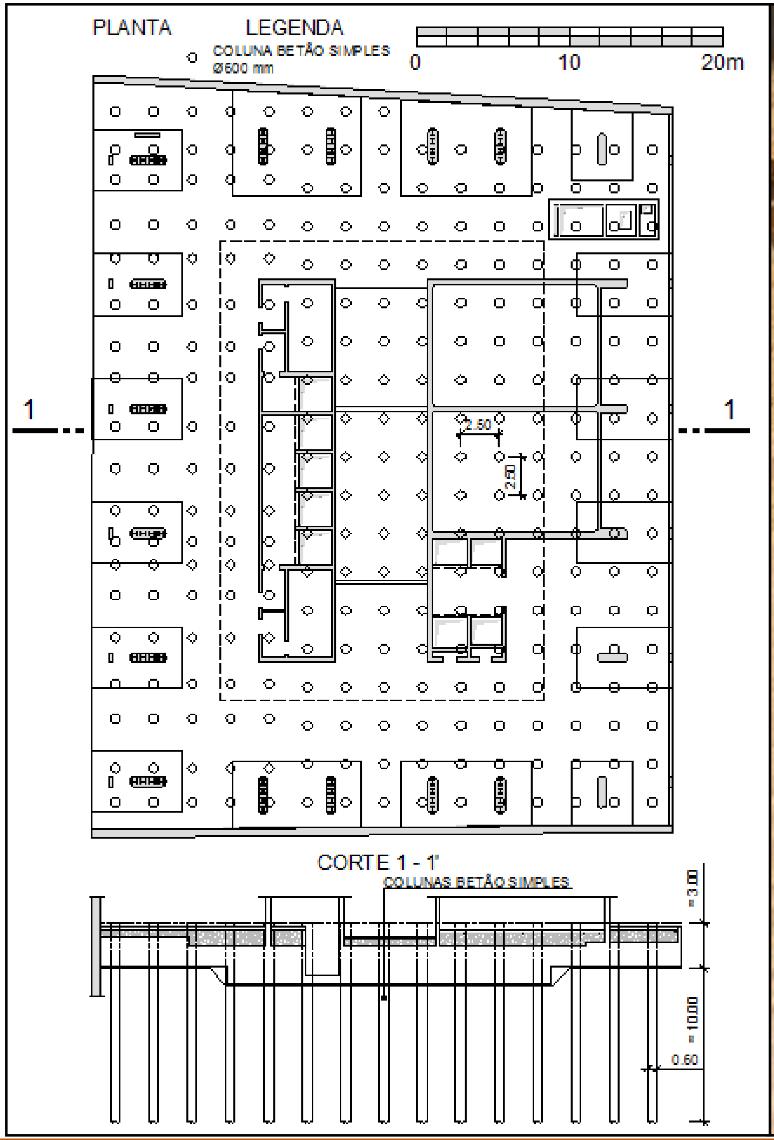

ESCOM TOWERS - LUANDA

SOIL IMPROVEMENT WITH RIGID INCLUSIONS

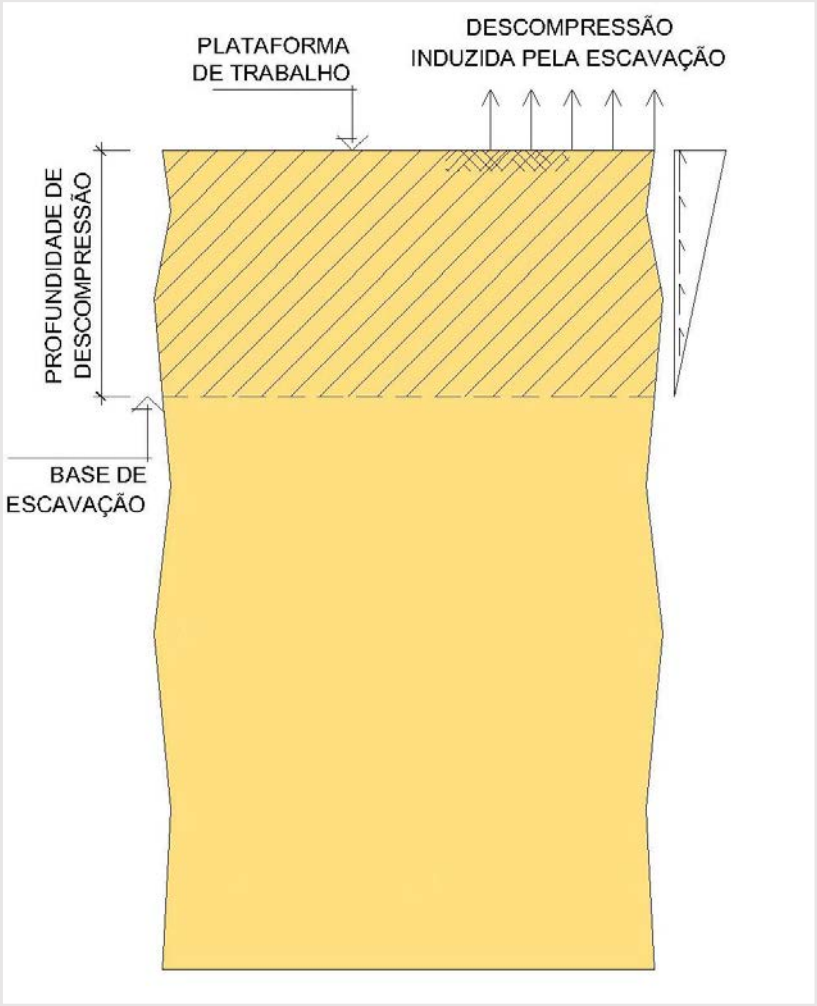

ESCOM TOWERS - LUANDA

SOIL IMPROVEMENT WITH RIGID INCLUSIONS

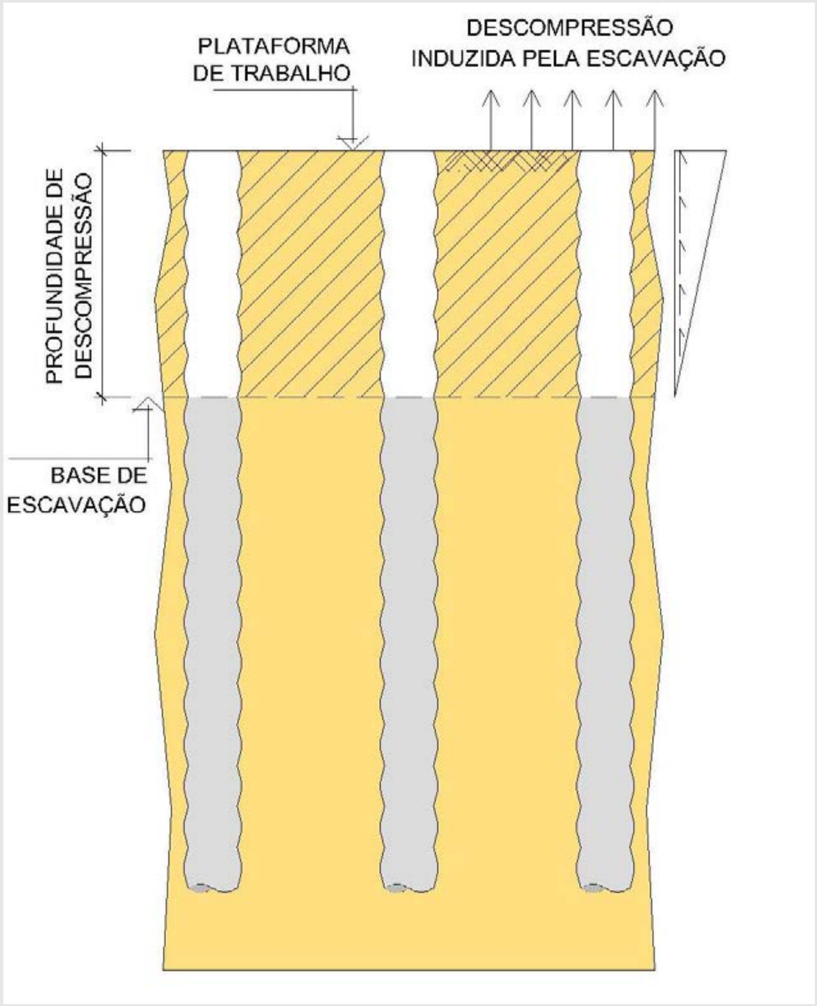

ESCOM TOWERS - LUANDA

SOIL IMPROVEMENT WITH RIGID INCLUSIONS

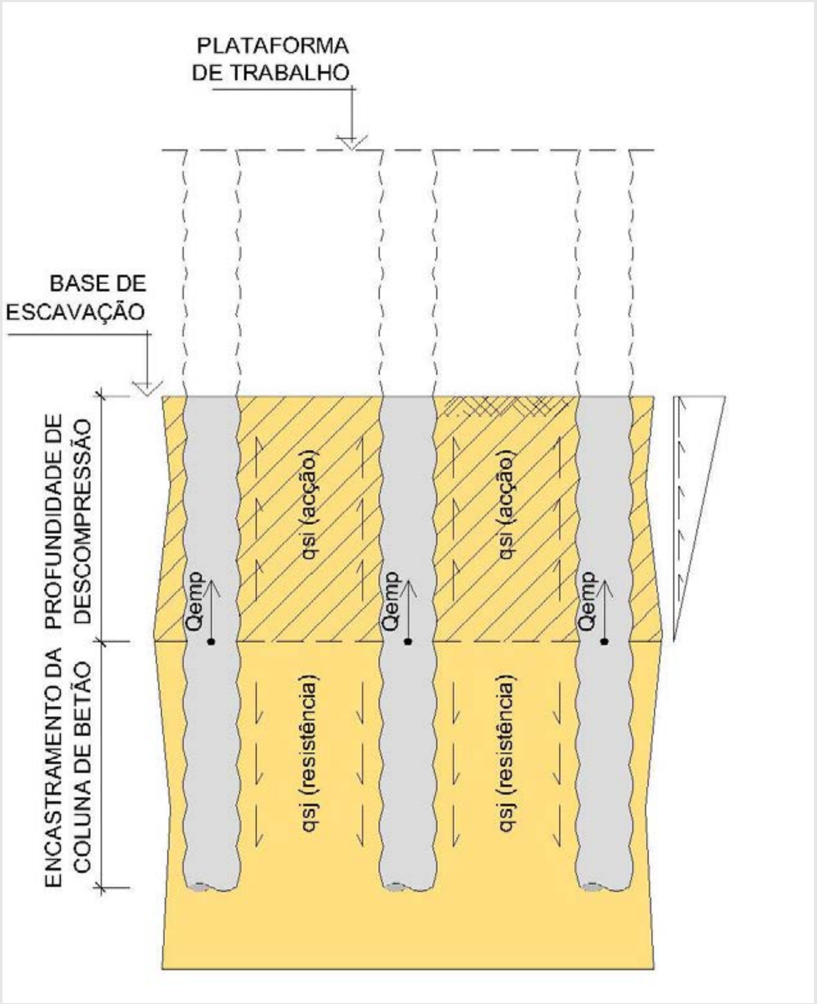

ESCOM TOWERS - LUANDA

ESCOM TOWERS - LUANDA

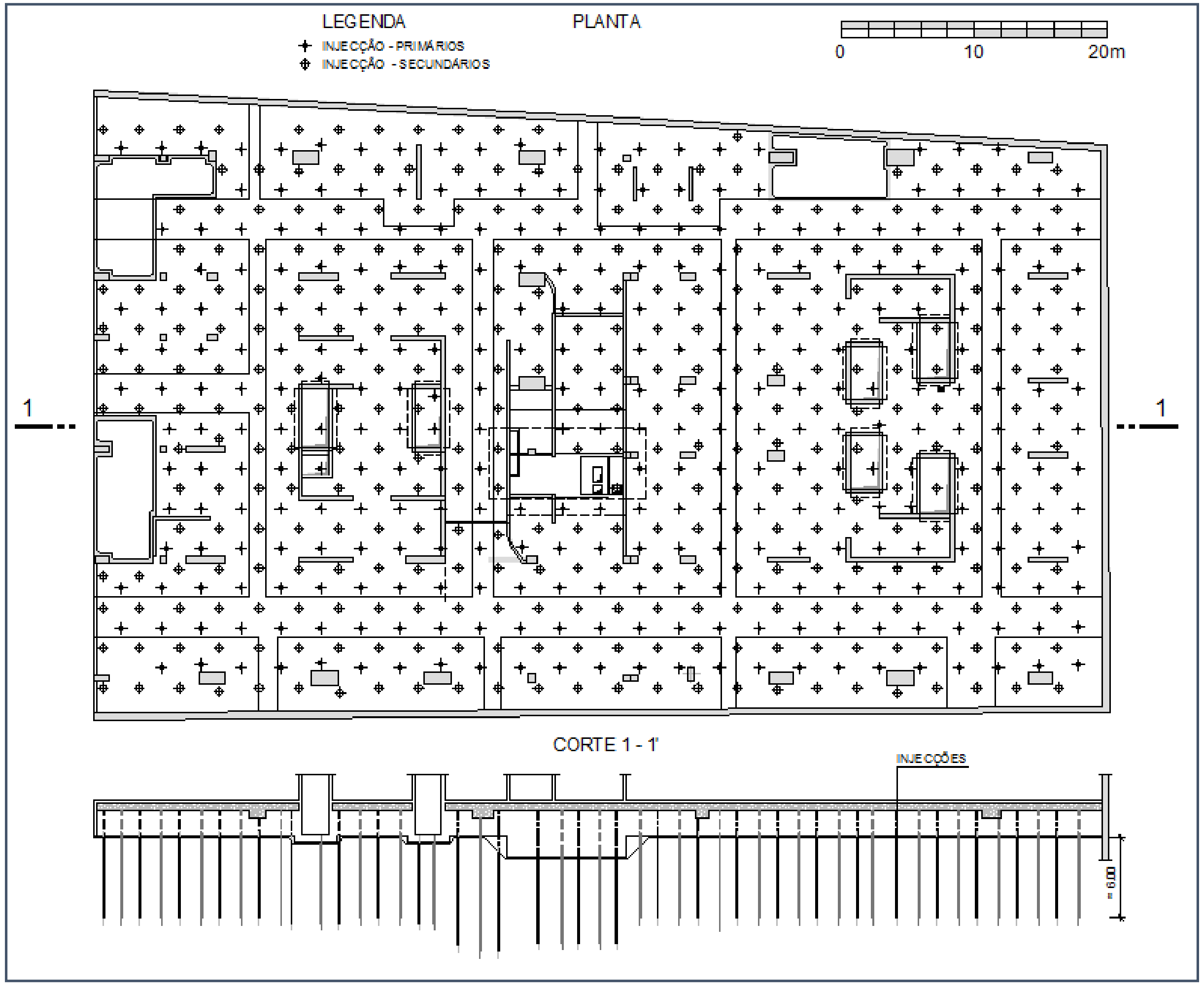

ESCOM TOWERS - LUANDA

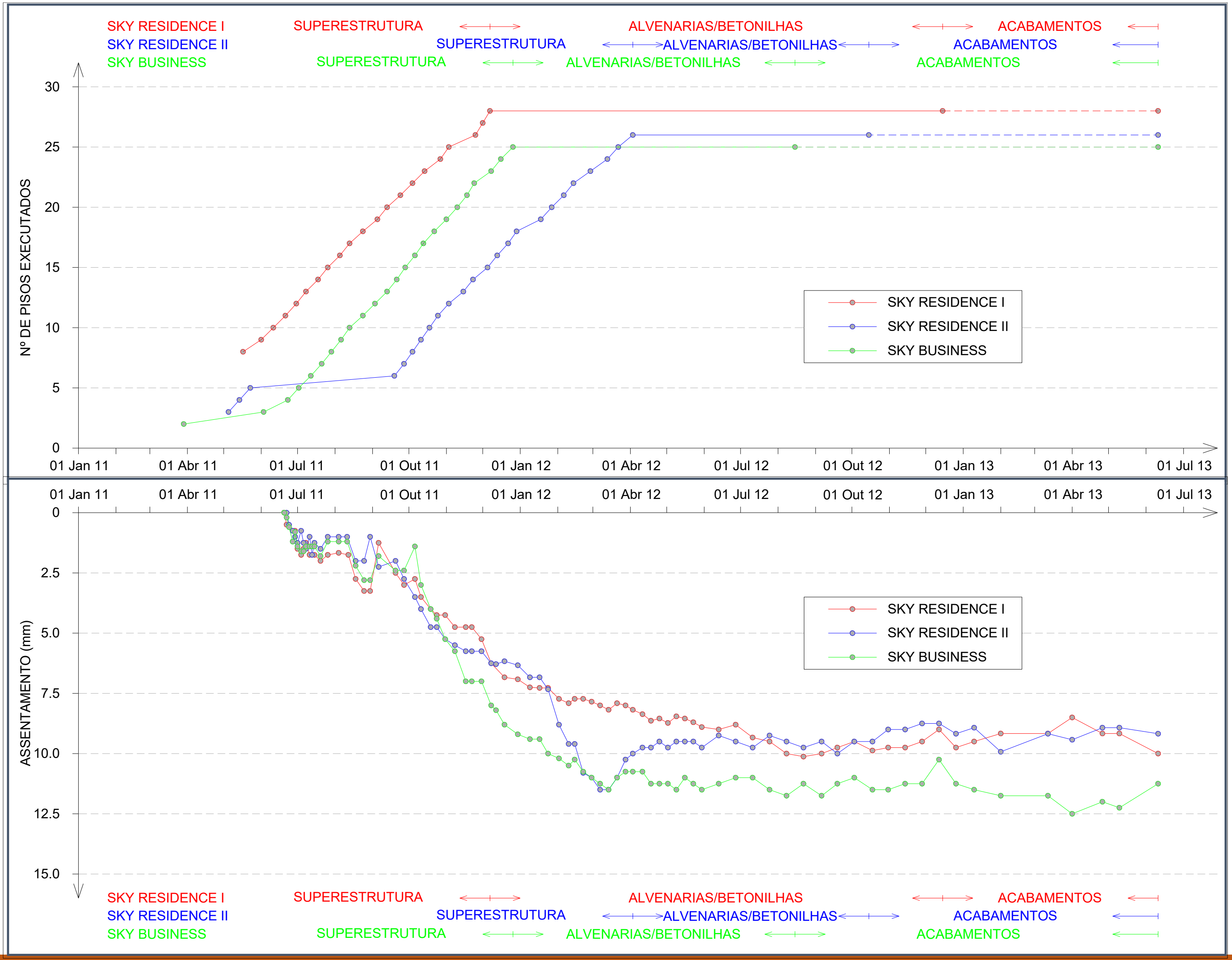

MARAVILHA BUILDING - LUANDA

MARAVILHA BUILDING - LUANDA

MARAVILHA BUILDING - LUANDA

DEEP EXCAVATIONS - IMPLEMENTATION OF NEW TECHNOLOGIES

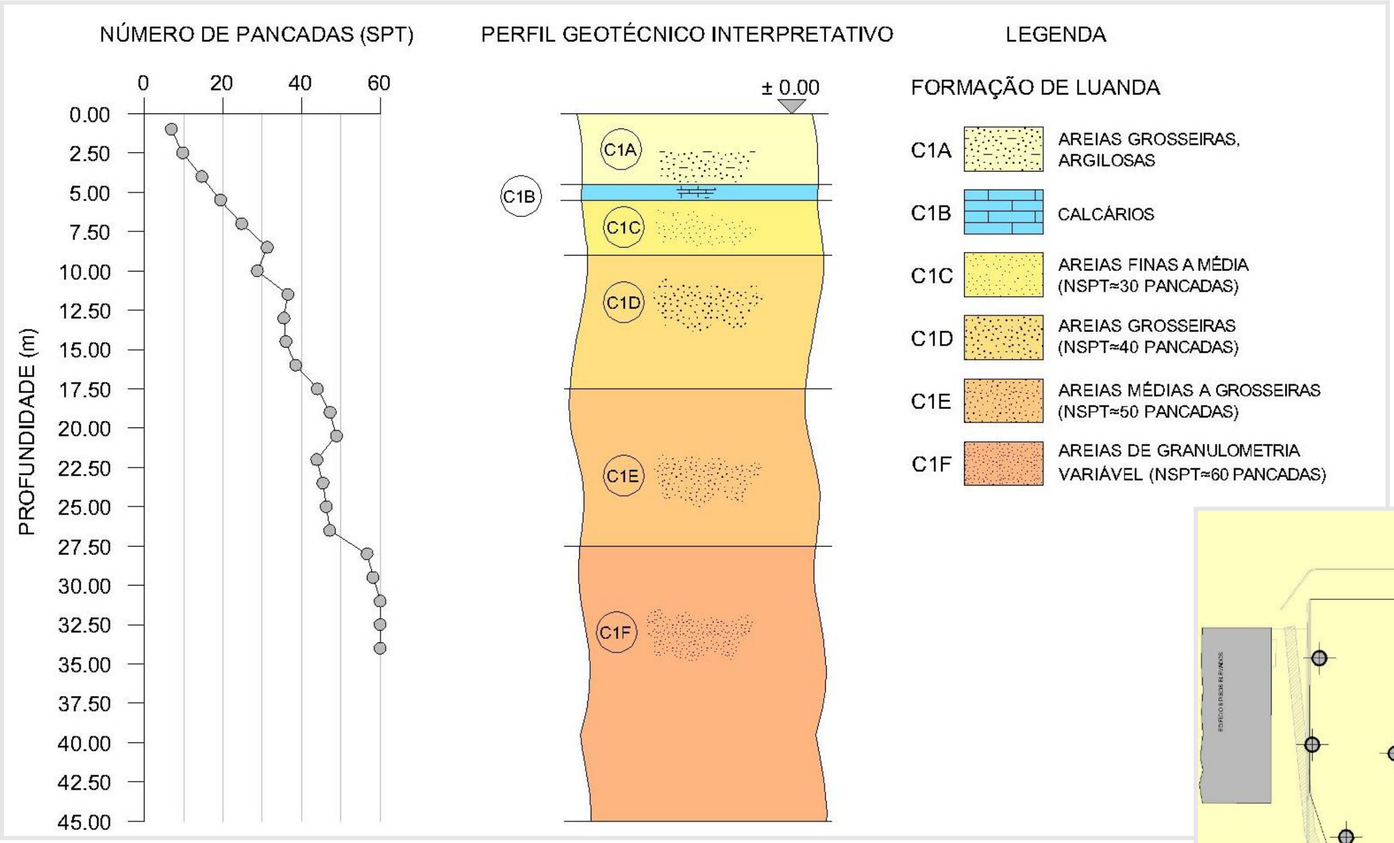

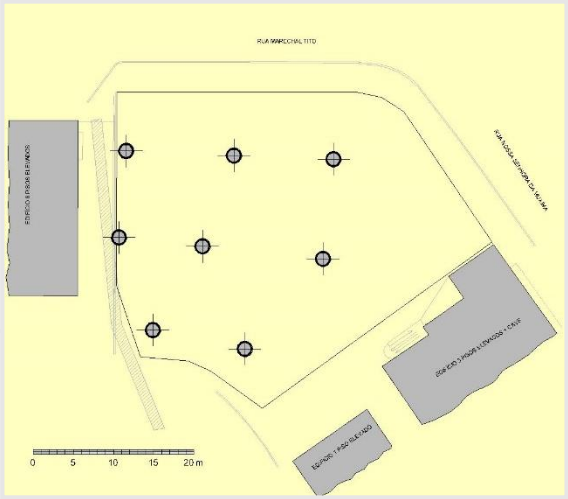

Initial Site Investigations Results (level +0.00)

SOIL IMPROVEMENT WITH RIGID INCLUSIONS

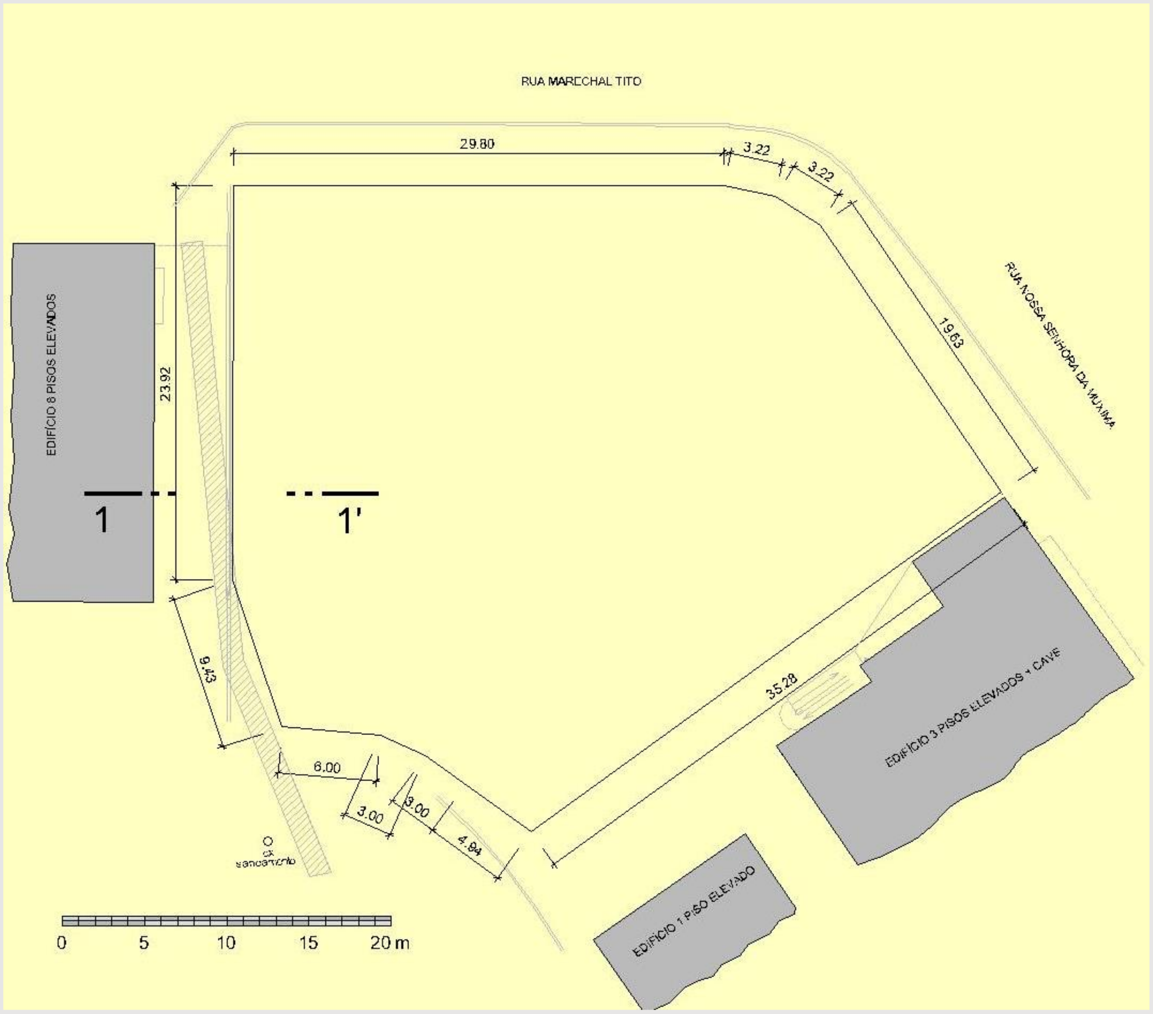

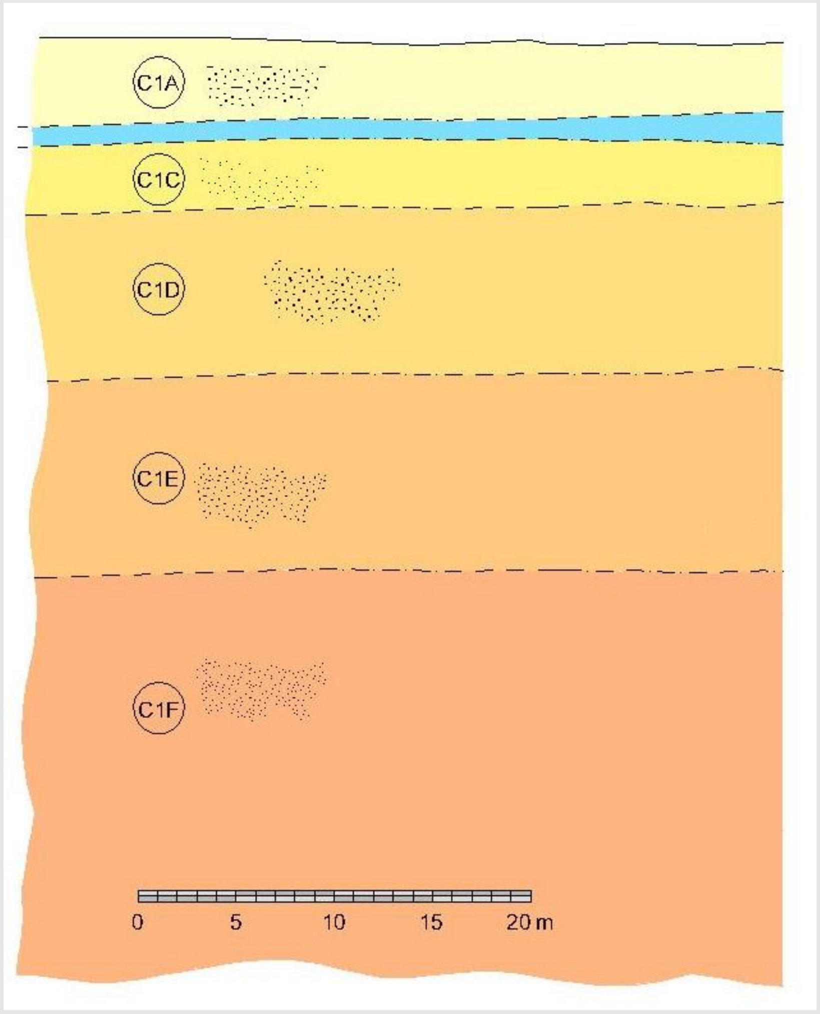

MARAVILHA BUILDING - LUANDA

SOIL IMPROVEMENT WITH RIGID INCLUSIONS

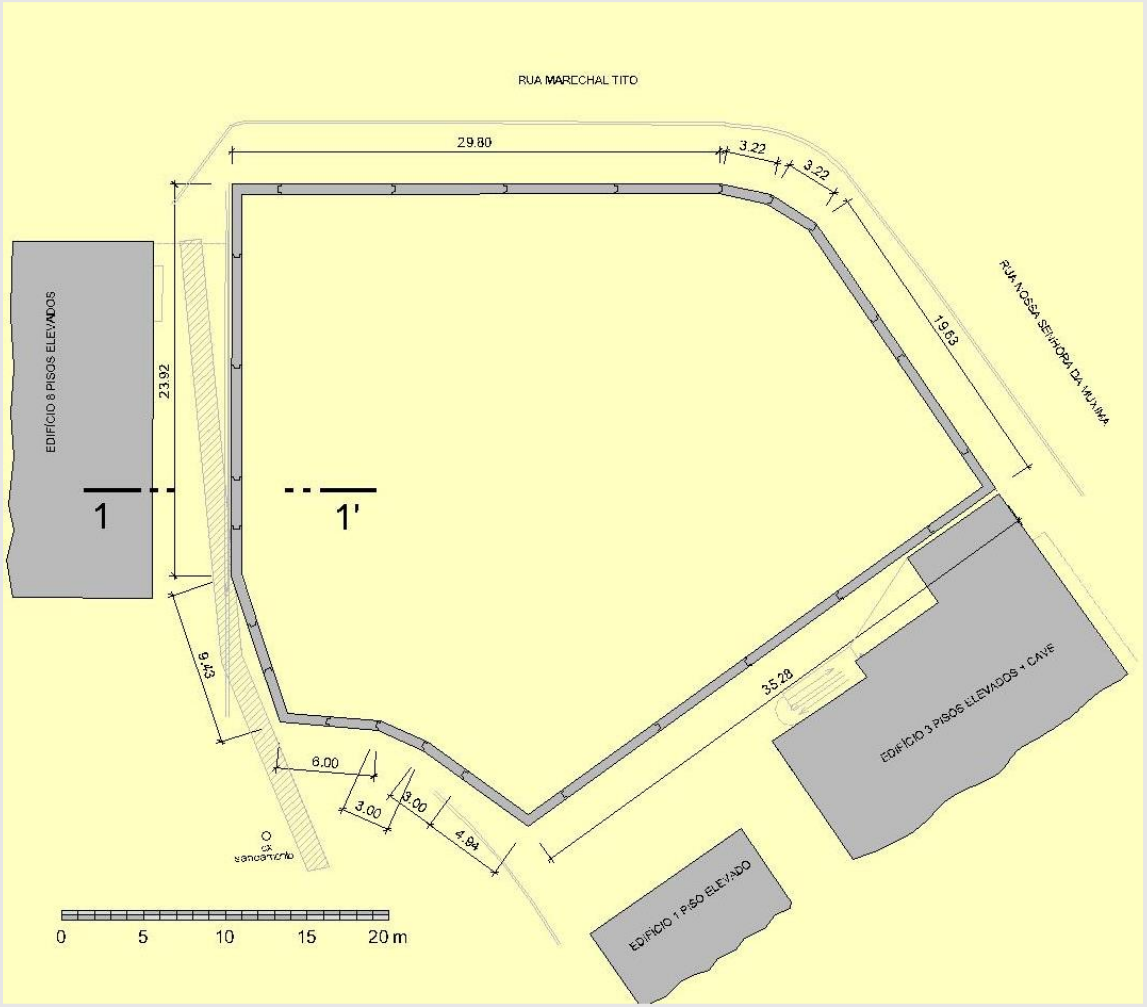

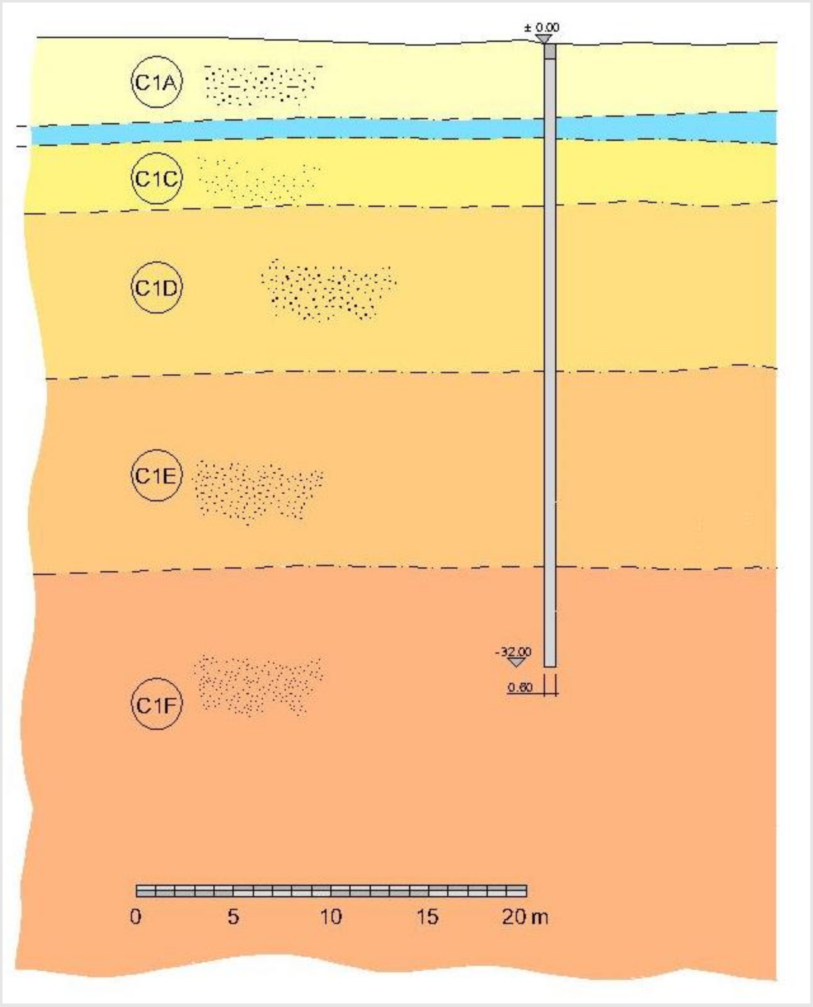

MARAVILHA BUILDING - LUANDA

SOIL IMPROVEMENT WITH RIGID INCLUSIONS

MARAVILHA BUILDING - LUANDA

SOIL IMPROVEMENT WITH RIGID INCLUSIONS

MARAVILHA BUILDING - LUANDA

SOIL IMPROVEMENT WITH RIGID INCLUSIONS

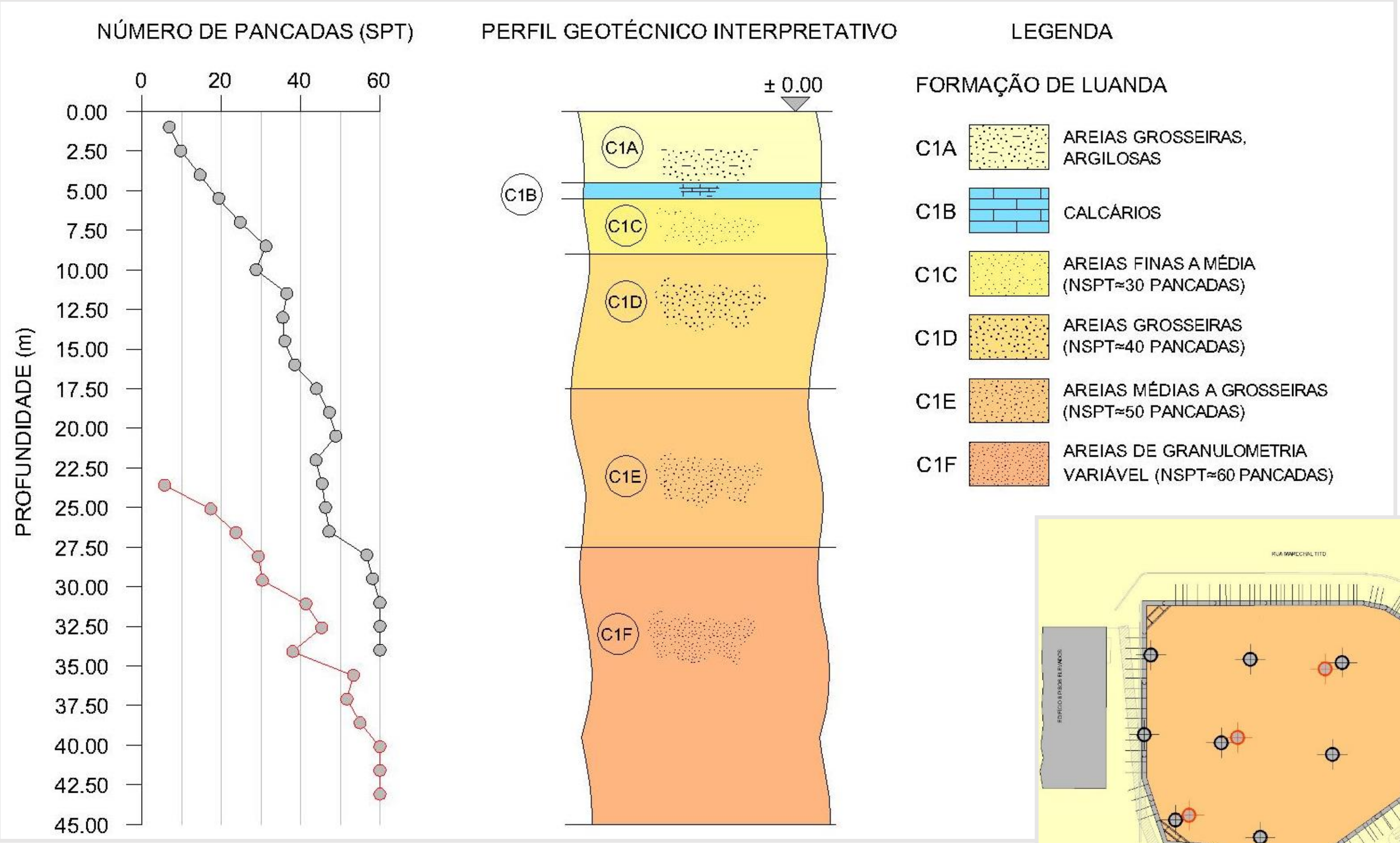

2nd Site Investigations Results (Level -23.00)

MARAVILHA BUILDING - LUANDA

SOIL IMPROVEMENT WITH RIGID INCLUSIONS

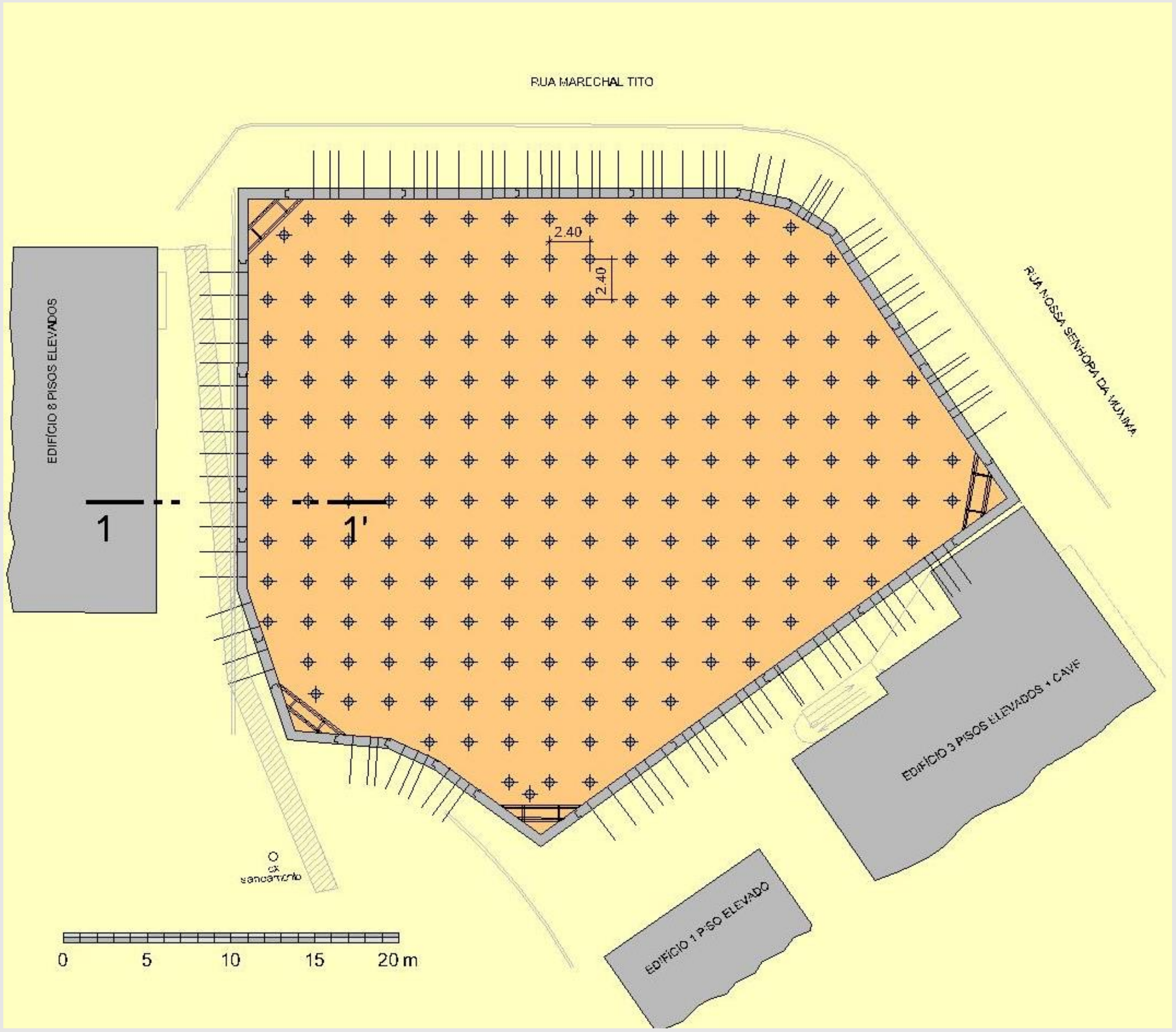

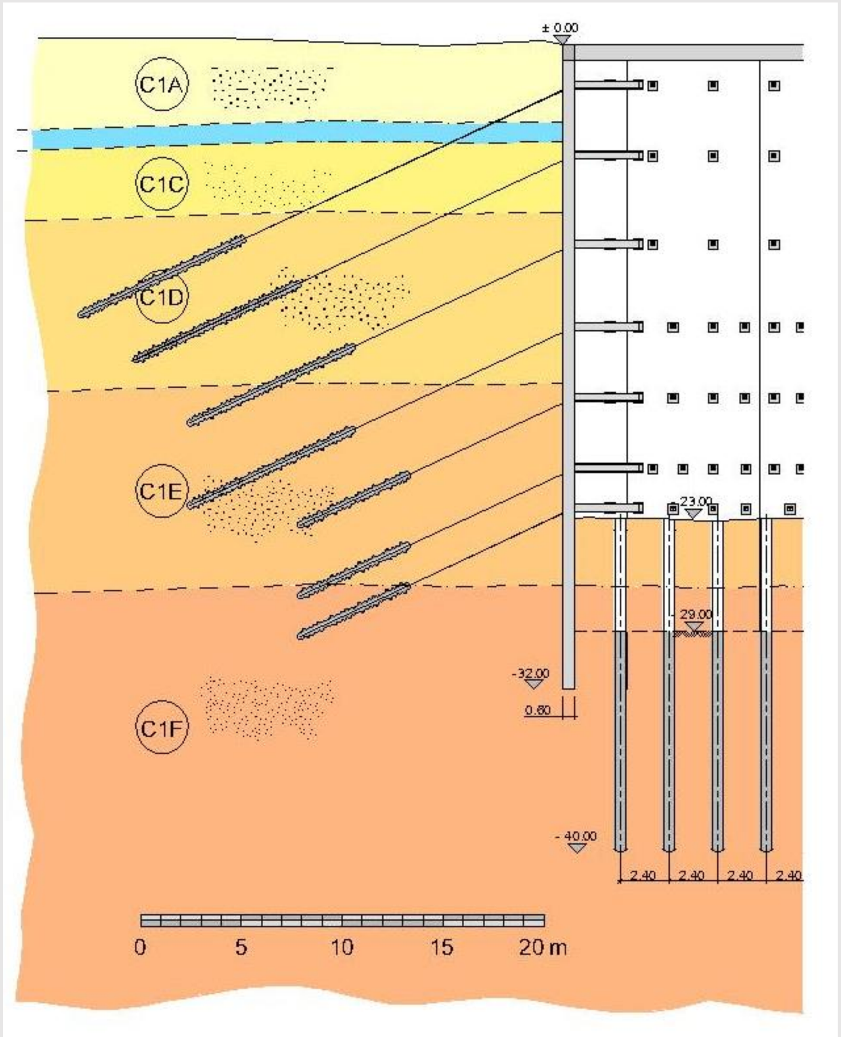

MARAVILHA BUILDING - LUANDA

SOIL IMPROVEMENT WITH RIGID INCLUSIONS

MARAVILHA BUILDING - LUANDA

SOIL IMPROVEMENT WITH RIGID INCLUSIONS

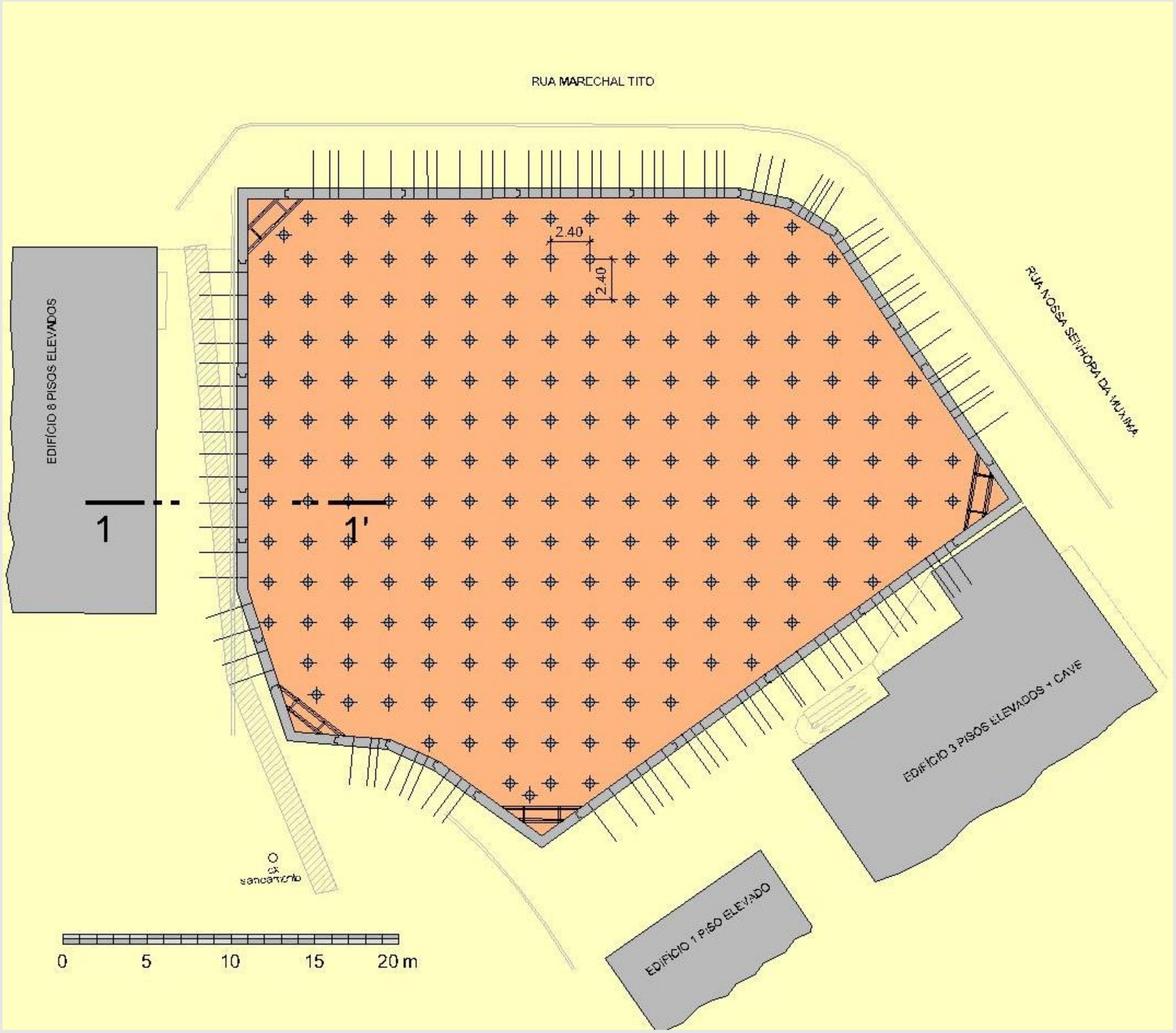

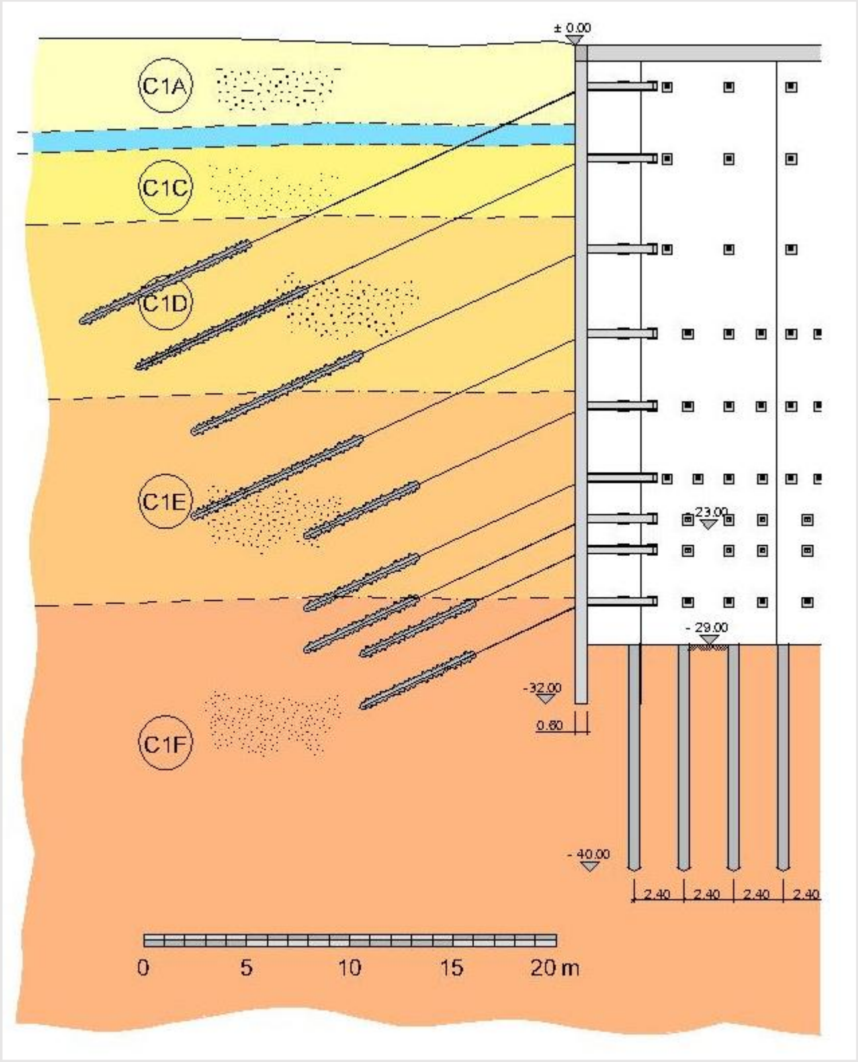

MARAVILHA BUILDING - LUANDA

SOIL IMPROVEMENT WITH RIGID INCLUSIONS

MARAVILHA BUILDING - LUANDA

SOIL IMPROVEMENT WITH RIGID INCLUSIONS

MARAVILHA BUILDING - LUANDA

SOIL IMPROVEMENT WITH RIGID INCLUSIONS

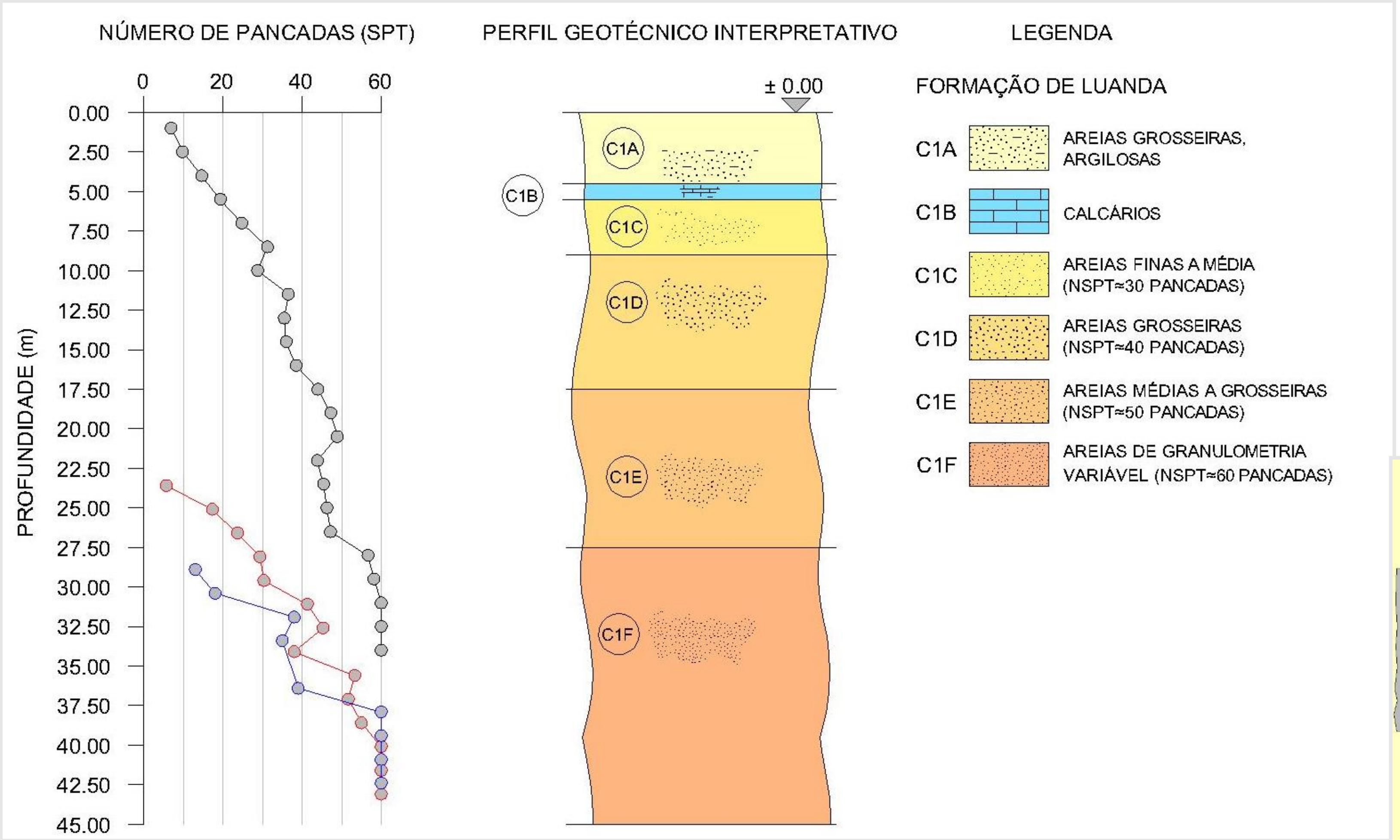

3th Site Investigations Results (Level -29.00)